CORROSION BEHAVIOR OF REINFORCED CONCRETE BRIDGE DECKS UNDER LABORATORY AND FIELD CONDITIONS

By

HASAN AL-NAWADI

A dissertation submitted to the

School of Graduate Studies

Rutgers, The State University of New Jersey

in partial fulfillment of the requirements

for the degree of

Doctor of Philosophy

Graduate Program in Civil and Environmental Engineering

Written under the direction of

Hani H. Nassif, PhD., P.E.

and approved by

_____

_____

_____

_____

New Brunswick, New Jersey

January 2019

ABSTRACT OF THE DISSERTATION

CORROSION BEHAVIOR OF REINFORCED CONCRETE BRIDGE DECKS UNDER LABORATORY AND FIELD CONDITIONS

By HASAN AL-NAWADI

Dissertation Director:

Hani Nassif, PhD., P.E.

Reinforced concrete is one of the most efficient building materials widely used across the world, however, corrosion of its embedded steel reinforcement is the most aggressive rival to its durability. Corrosion becomes more aggressive in the presence of cracks, which makes the ingress of chloride ions from deicing salts into concrete bridge decks more critical, leading to an annual cost of about 8.3 billion for mitigation and rehabilitation of bridge decks in the United States of America.

The research consists of two components: laboratory testing and field monitoring. The laboratory testing is aimed at evaluating the effects of cracks and crack sealants in concrete specimens on the corrosion process using ASTM G109, and correlation of bridge deck service life and long-term predictions with field performance. The laboratory-based experimental program includes the use of various small-scale specimens as well as deck slabs to study the effect of various parameters such as crack width and depth as well as the efficiency of the crack sealants. Five types of steel reinforcement (Black, Duplex stainless, Galvanized, MMFX, and Epoxy-Coated), two types of concrete classes (class A and HPC),

and two Sodium chloride concentrations (3% and 15%) were used. Additionally, four crack patterns, two different crack sealants, and two types of sensors (2000 silver-silver chloride electrode and multi element probes MEPs) were also used. On the other hand, the field work used corrosion sensors for 20 years to maintain the structural health monitoring (SHM) and data collection of two existing bridges, GSP 84.1 and 159.7.

After three years of exposure to diluted as well as severe sodium chloride solutions, laboratory results show that concrete specimens with Duplex Stainless and MMFX steel rebars had an excellent corrosion resistance in comparison with Epoxy-coated rebars. Moreover, the crack depth has more influence than the crack width for all specimens. When the cracks are sealed using the T-70 MX crack sealant, it showed a remarkable efficiency in comparison with Seal Krete sealant. Additionally, results from the field monitoring of the two bridge decks show that Galvanized Steel rebars underwent noticeable corrosion activity in comparison with the Stainless Steel deck. Moreover, data collected from laboratory tests and field performance is used to validate results from simulation model to correlate service life predictions from accelerated laboratory-based tests.

DEDICATION

I dedicate my dissertation work to my father, Snedeh Jawad, who has continually supported my endeavors through thick and thin during my life. I also dedicate my dissertation to my academic advisor, Dr. Hani Nassif, who has been my continual support through all my years at Rutgers University.

ACKNOWLEDGEMENTS

First of all, I would like to thank my almighty ALLAH for granting me the power and ability to be able to live and achieve my goals. A special thanks and appreciation go to my advisor Dr. Hani Nassif for guiding me through this research. By all means, he has been an integral part of my life in the United States. I have been so fortunate to have been one of his students. Honestly, he has been a true friend I could turn to anytime for advice. Somehow it seems inadequate to say, "thank you," but it is so sincere and comes from the bottom of my heart.

My deep appreciation goes to Rutgers University for having me throughout all these years. Huge thanks must be sent to my lovely country, Iraq, for granting me the HCED scholarship. My sincere acknowledgement is expressed to Dr. Husam Najm, Dr. Hao Wang, and Dr. David W. Coit for being valuable members on my dissertation committee and for providing effective responses to my questions. Also, great thanks and appreciation go to Dr. Graziano Fiorillo for the significant contribution and help on the service life modeling program.

I want to thank New Jersey Highways Authority (NJHA) for making it easy to access the field, collect data, and provide the details of the two GSP bridges, 84.1 and 159.7. This is gratefully acknowledged. I would like to thank Dr. Mike Mota, Dr. Salem Faza, Transpo Industries, inc for supplying some steel rebars and crack sealant.

I also want to thank my colleagues at Rutgers University, Dr. Adi Abu-Obeidah, Dr. Na Chaekuk, Dr. Abdulemam Abu-saibia, Giuseppe Liberti, Greg Brewer, Eli Hadad, Anderw Habib, Merelle AlKataish, Syprain Nyaberi, Christopher Sholy, Dongjin Gao, Jonathan Rodregues, Emily Pooley, Kirollos

Gadalla, Daniel Okechukwu, Dalexander Gonzales, Andrew Shahata, Sophia Pastore, Harold Castaneda, Chan Yang, Justinian Grant, Reid Holland, Jaipartap Singh Rano, Joe Subrevi, Joe Hilmi, Zaina Hamdan, Alin HM, Albert HM, John Khoori, Mohammed Alseaedy, , and others for their friendship and support throughout the years.

My appreciation is extended to the departmental staff, Gina Cullari, Linda Szary, and to my other Rutgers Faculty and staff, Alexandria Bachmann, Barbara Sirman, Harvey Waterman, Paula Henry, Nancy Sheasley and Kate Baker.

Contents

List of Tables

List of Figures

List of Symbols

A^0	3.937×10^{-9} inch
Class A	Ordinary concrete
HPC	High Performance Concrete
LPR	Linear Polarization Resistance Method
ΔG	Change in Gibb's free energy
ΔH	Change in enthalpy
T	Temperature
ΔW	Change in additional external work
ΔS	Change in entropy
I corr	Corrosion density
NACE	National Association of Corrosion Engineers
Q	Charge / ion transfer
E	Electrochemical potential difference
N	Number of electrons transferred in the reaction
F	Faraday's constant (96,500 C/mol)
CMS	Silver-Silver corrosion sensor
V2000	
MEP	Multi-Element Prop
ASTM	American society of testing and materials
Tc	Transversal Crack

Lc	Longitudinal crack
SFR	steel fiber reinforcing
RCPT	Rapid Chloride Permeability Test
SRT	Surface resistivity Test
BS	Black steel (conventional steel rebars)
EC	Epoxy Coated steel rebars
SS	Duplex 2205 (318) Stainless steel rebars
GS	Hot Dip Galvanized Steel.
MMFX	Chrome X 9000 MMFX rebars, Martensitic Microcomposite Formable Steel (MMFX).
W/C	Water/Cement Ratio
WR	Water Reducer Admixture
SP	Super plasticizer
AEA	Air entraining Agent
HRWRA	High Range Water Reducer Admixture
HMWM	High Molecular Weight Methacrylate
T70	Concrete sealant-HMWM
T70-∥	Corrosion activities parallel to crack sealed with T-70
T70-⊥	Corrosion activities perpendicular to crack sealed with T-70
SK	Crack sealant-Acrylic
SK-∥	Corrosion activities parallel to crack sealed with SK
SK-⊥	Corrosion activities perpendicular to crack sealed with SK
$N_a C_l$	Sodium Chloride

ACI	American Concrete Institute
SME	Static Modulus of Elasticity
mpy	Mils per year
V	Corrosion potential (Volt)
mV	Milli-Volt
A	Corrosion current (Ampere)
µA	Micro Ampere
Tlife	Service life of structure
Ti	Time to corrosion initiation
d	Cover thickness
D	Chloride diffusion coefficient
Ccr	Critical chloride concentration at the rebar- concrete interface.
C0	Surface chloride concentration, and
Ci	Initial chloride concentration
t_{crack}	Time to first cracking
DET	Level of deterioration
Td	Time of the first repair
PDF	Probability density function

1. Chapter One

Introduction

1-1 Problem Statement

Corrosion is one of the most vital factors that significantly influences concrete durability. Where corrosion considers the most aggressive rival that attacks the durability and structural stability of concrete [Bavarian and Reiner 2003]. The concrete type has an important part on the corrosion process, and the high performance concrete (HPC) is one of the concrete types that significantly affected by the corrosion process. Continuously, concrete becomes more vulnerable to corrode in the presence of cracks. Where cracks make the ingress of sever materials such as chloride ion, carbon dioxide, and acidic solutions within the concrete mass faster. It is very important and timely to study the corrosion process and its effects of the reinforced concrete members because the maintenance of corrosion costs a lot of resources and efforts.

In the same direction, current research stands for studying the relationship between the crack width and/ or depth and the corrosion process; also, it aims to find out the service life of reinforced bridge decks of concrete class A and high performance concrete (HPC). In addition, this research tries to correlate the relation between the lab acceleration-based studies with the field performance in terms of chloride content and the associated corrosion potentials.

1-2 Annual Cost of Corrosion

The importance of studying corrosion comes from the annual rehabilitation cost of the infrastructures categories. Corrosion is one of the most aggressive factors that diminish the structure reliability and stability. The annual rehabilitation cost of corrosion is about 8.3 billion just for the highway bridges in the United States of America [NACE 2018].

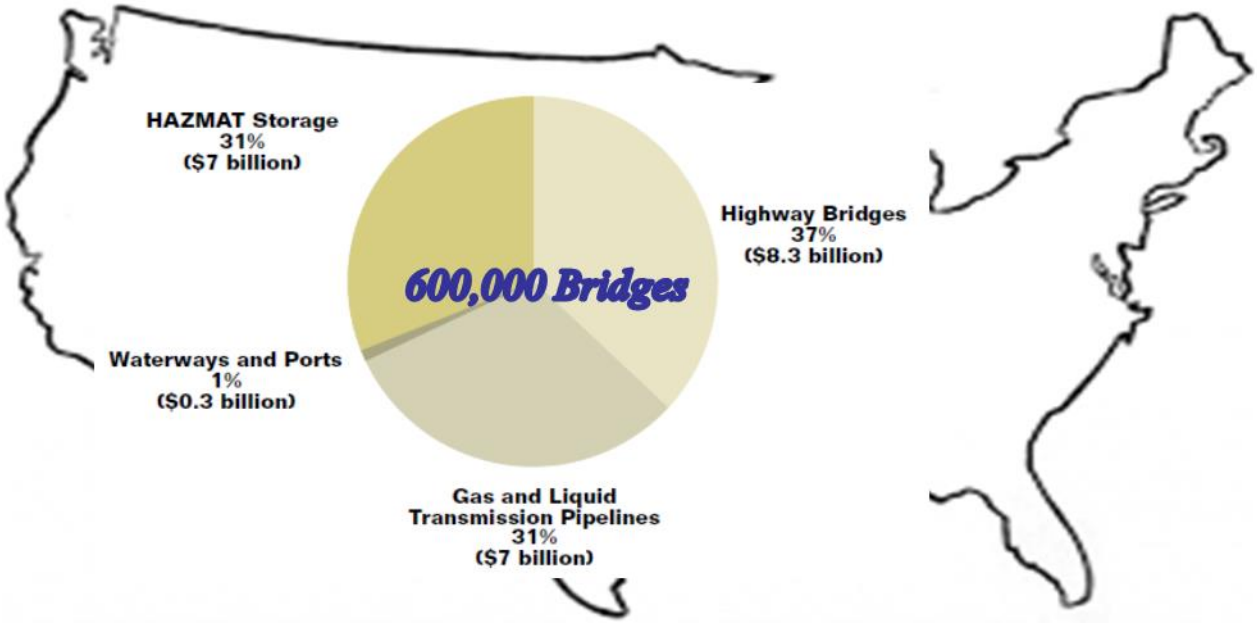

Figure 1–1 Annual Corrosion Mitigation and rehabilitation Cost [https://www.nace.org/uploadedFiles/Publications/ccsupp.pdf].

1-2 Research Methodology

As mentioned earlier, this research is aiming to compute the reinforced concrete bridge decks service life through studying the effects of cracks on the corrosion process of concrete. Also, it tries to simulate the actual field condition with the lab performance to correlate their relations. Basically, this research consists of the following major aspects.

i- Laboratory Studies on the Crack Effects of Corrosion Process of Reinforced Concrete Members by Using ASTM G-109

The aim of this part is finding out the influence of the crack depth and/ or width and the electrochemical process of corrosion. In this part the influences of the Sodium Chloride profiles on the corrosion initiation and progress of concrete class A and high performance concrete (HPC) is studied. Also, the effects of steel reinforcement types such as conventional steel (Black Steel), Duplex Stainless Steel, Chrome X-9000 MMFX rebars (Martensitic Microcomposite Formable Steel), Hot Dip Galvanized steel, and Epoxy-coated steel rebars are investigated. Two concentrations of Sodium chloride, 3% and 15% are used through this part of research.

ii- Bridge Deck Service Life Corrosion Model

This part predicts the service life of the reinforced concrete bridge decks by correlating the laboratory-based accelerated corrosion and the field performance of steel rebars (Epoxy coated, Duplex stainless steel, and MMFX) of HPC bridge decks exposed to 15% of NaCl.

iii- The Crack-Sealant Performance

This part intends to investigate the performance of two different types of concrete sealants and compares their efficiency. Herein the two types of crack sealant products are T-70 MX and Seal Krete -SK. These products are applied to the top surface of the cracked concrete of prism and slab samples, which are exposed to 15% of chloride solution. The

behavior of the two products of crack sealing are studied on both directions, longitudinal and transverse. Figure (1-2) summarizes the main parameters included in this research.

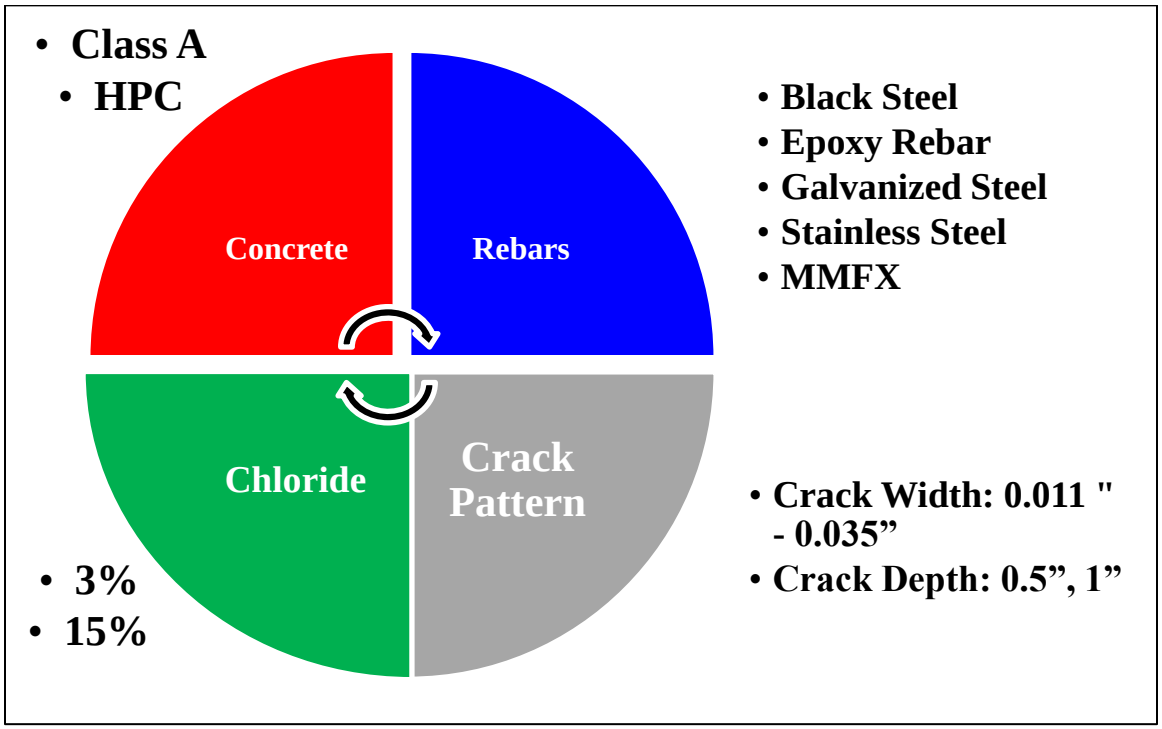

Figure 1–2 Main Parameters of the Research

1-4 Research Strategy

The research strategy implies investigating the service life of reinforced bridge decks essentially in the presence of cracks. Accordingly, the strategy of this research includes two work parts (laboratory and field work), two types of samples (prisms and slabs), two concentrations of Sodium chloride (3 and 15%), four types of crack pattern, five types of

steel reinforcing rebars, two types of concrete sealers. The following measurements and tests are considered to maintain the corrosion phenomena through this research:

i. Macro cell Corrosion-ASTM G 109 (included potentials and currents).
ii. Potentials, currents, and concrete resistivity of the field work which includes the two existing bridges (GSP Bridge 84.1 and GSP Bridge 157.9.
iii. Corrosion current density (for the field work).
iv. Chloride ion concentrations of the threshold and progress of corrosion.
v. The Bridge deck service life.
vi. Corrosion map (for slabs only).

1-5 Research Importance and contribution

The current research is intended to contribute and help to:

i. Find out the correlation between the crack patterns (width and/ or depth) and the corrosion activities in both longitudinal and transverse directions.
ii. The effect of concrete quality on corrosion process.
iii. Study the effects of steel reinforcement (Black Steel, Epoxy Coated, Stainless Steel, Galvanized Steel, and MMFX) on the corrosion process.
iv. Provide better understanding of predicting the service life of reinforced concrete bridge decks in the State of New Jersey.
v. The influences of dilated (3%) and high concentrated (15%) Sodium chloride on the corrosion progress.
vi. The performance of crack sealant.

1-6 Corrosion Mitigation Strategy

Corrosion of reinforcing steel is the main cause of concrete structures deterioration
When steel corrodes, the Rust occupies a greater volume which creates tensile stresses in the concrete which can cause cracking, spalling and delamination. This can be minimized by:

i. increasing the ingress/travel time by Increasing concrete cover or Utilizing low permeable concrete such as high performance concrete (HPC).
ii. Reduce rate of corrosion by using less corrosive rebars for example Stainless Steel.

1-7 Research Structure

This study consists of six main chapters. Chapter one includes a general information about the corrosion process and the importance and methodology of the research. Chapter two provides a review for the related research and studies that deal with the electrochemical process of corrosion, corrosion parameters, corrosion models, and standard and experimental tests of corrosion. While Chapter three contains the experimental study. This implies the properties and specifications of the used materials, standard tests, equipment, etc. Continually, Chapter four covers the results and discussion of the laboratory results. In Chapter five, the field work and its results are presented.

Chapter six reviews the most recent corrosion models and predicts the service life model of the reinforced concrete bridge decks by using a probabilistic model and Monti

Carlo simulation. The future recommendations of the entire research are summarized in this Chapter too.

2. Chapter Two

Literature Review

2-1 General

The previous research and studies relating to the electrochemical process of corrosion, corrosion parameters, and standard and experimental tests of corrosion are reviewed in this chapter. Herein, I want to refer to an important issue: There are more than one standard or experimental test of corrosion, and each method has different results and different approaches. In the same direction, the tests consequences, chloride concentrations, molds sizes and shapes, measuring equipment, and result analysis differ from one study to another. The following is a review of the relevant research and studies.

2-2 The Sequence of Corrosion

"When reinforced concrete structures are subjected to aggressive medias such as chloride ions, carbon dioxide, and acidic solutions, their steel rebars start to corrode. The sever ions start to ingress within the concrete cover and try to reach to the steel reinforcement. The steel reinforcement is attributed by a thin layer (approximately 1000 A^0) of its oxide ($Fe_2\ O_3$)" [Zdenek P. Bazant 1979]. As long as this layer resists the ingress of aggressive ions, the steel reinforcement will be in active condition, and no corrosion occurs. When these ions destroy this layer, the corrosion takes place. There are additional factors that might control the corrosion process such as PH, mass transfer and diffusivities of ions and molecules as Oxygen, and ferric hydroxide, and pore water viscosity. In

particular, PH has a unique influence, where the corrosion could not happen if the PH is 12.5 or higher as shown in figure (2-1) below. This is not always correct; if we look at the Pourbaix diagram figure (2-2) below, obviously we could see the corrosion might exist even though PH is high like 13 because the soluble ferrite will form in the pore water.

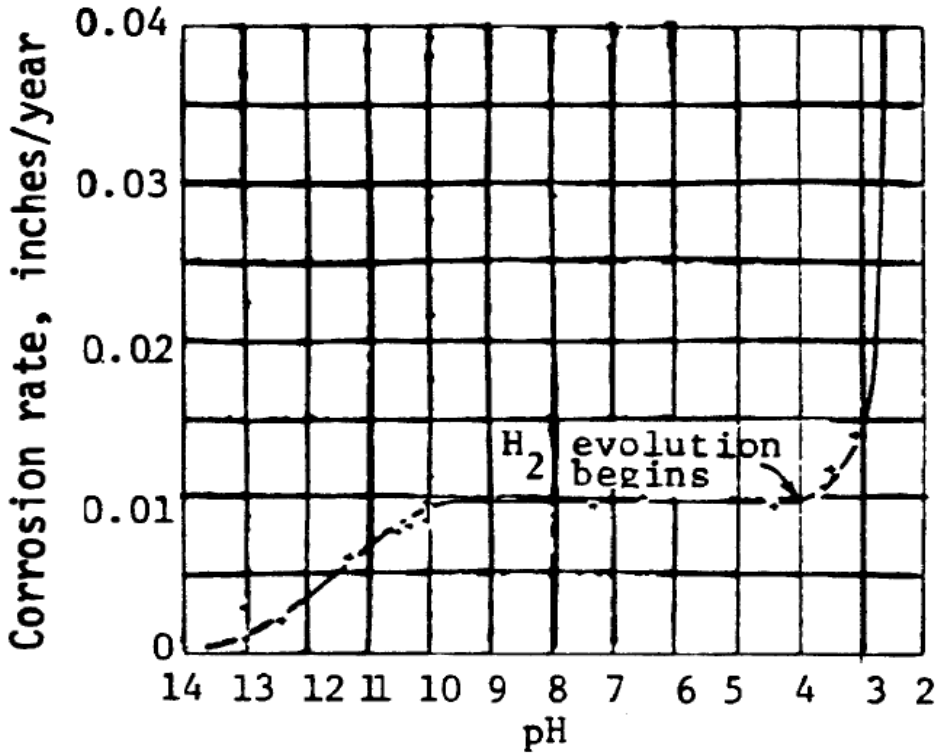

Figure 2–1The Effect of PH in the Corrosion Rate

[Zdenek P. Bazant 1979]

2-3 Electrochemical Process of Corrosion.

In general, there are three theories of chloride ion effects on corrosion phenomena [ACI 222R 1996].

1- The Oxide Film Theory: the chloride attacks the steel rebars through the protection layer defects.

2- The Adsorption Theory: the chloride ion, in competition with hydroxyl ion, OH, adsorbed by the metal surface. So, the chloride ion promotes the hydration of the metal ions and thus facilitates the dissolution of the metal ions.

3- The Transitory Complex Theory: a soluble complex of ion chloride forms due to the reaction with ferrous ion. Continuously, this complex ion diffuses away to destroy protection layer of Fe (OH) 2.

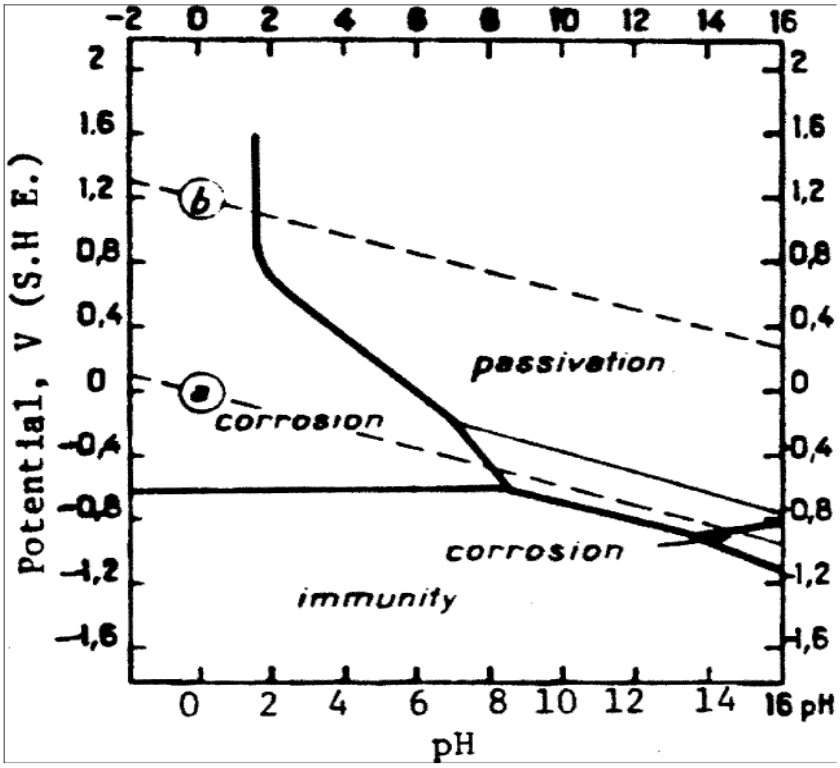

Figure 2–2 Pourbaix Diagram

[Zdenek P. Bazant 1979]

2-4 Mechanism of Corrosion.

The corrosion of steel rebars in reinforced concrete members is an electrochemical process that consists of two stages [P. Bazant 1979, ACI 222R 1996]. First is corrosion threshold, the time that is required to initiate the corrosion (from the ingress of chloride or

carbon dioxide through the concrete cover until the break down of the passive layer of reinforcing steel). Second is the corrosion rate development until the full deterioration of steel reinforcement. There are two important phases for ion diffusivity [P. Bazant 1979]. Diffusion interval stands for the time required for the chloride ion to reach the aforementioned chloride threshold value at the reinforcement level which can be determined by the diffusion process of the chloride ion through concrete, following Fick's Second Law of Diffusion (Weyers, Prowell, and Springkel 1993; Gaal, van der Veen, and Djorai 2001) equasion (2-1) and (2-2) below.

$$J = -D(\frac{Dd}{Dz}) \qquad \text{Eq.(2-1)}$$

$$\frac{Dc}{dt} = -\frac{d}{dz} = -d/dD(\frac{Dc}{Dz}) \qquad \text{Eq.(2-2)}$$

Progressive phase:

This refers to the interval of the corrosion start point until the collapse of stell rebars. As the chloride ion reaches the surface of rebar, the steel reinforcement dissolves in the pore water of concrete giving up two electrons forming cations with positive charge ions. This sub-interval is called "oxidation process" which occurs in the anodic side of corrosion circuit.

$$Fe \rightarrow Fe^{2+} + 2e^{-} \qquad \text{Eq.(2-3)}$$

Where:

Fe: iron

$Fe^{2+:}$ ferrous-ion.

and $2e^{-}$: two free electrons.

On the other side of corrosion circuit, cathodic area, the presence of the water molecules, oxygen, and the two free electrons are consumed to form negative hydroxide ions. This sub-interval is called “reduction process. ”

$$4e^- + 2H_2O + O_2 \rightarrow 4OH^- \qquad \text{Eq.(2-4)}$$

Where:

O_2 is oxygen

H_2O is water, and

OH^- is a hydroxyl ion.

As the anodic and cathodic react on each other, the ferric hydroxyde forms,

$$Fe^{2+} + 2OH^- \rightarrow Fe(OH)_2 \qquad \text{Eq.(2-5)}$$

An additional oxidation is needed to form ferric hydroxyde,

$$4Fe(OH)_2 + O_2 + 2H_2O \rightarrow 4Fe(OH)_3 \qquad \text{Eq.(2-6)}$$

Finally the ferric oxide, FeO_3, rust, forms as a result to dehydration of ferric hydroxyde,

$$2Fe(OH)_3 \rightarrow Fe_2O_3.H_2O + 2H_2O \qquad \text{Eq.(2-7)}$$

The electrochemical process of corrosion is illustrated in figure (2-3) below.

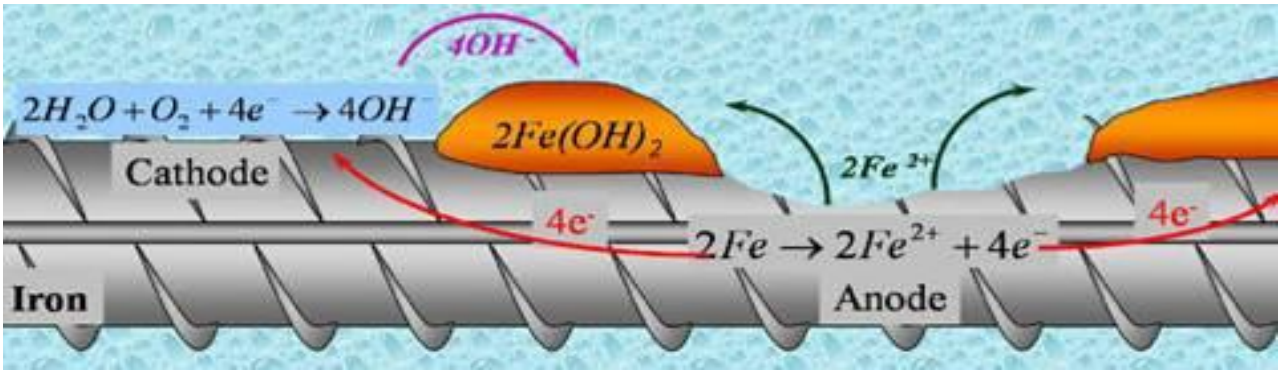

Figure 2–3The Electrochemical Process of Corrosion

[http://www.cement.org/images/default-source/contech/corrosion_water_graphic.jpg?sfvrsn=2]

2-5 Corrosion Cell Components

Corrosion of any metal is its natural breakdown into a more stable state, as a metal oxide. Corrosion does not exist unless five main components are present [Ahmad S. 2003, Ann K. Y., and Song H 2007, and Basheer, L 2001].

1- Presence of starter reactants at the local site of corrosion, such as O_2,H_2O and (Cl or Co_2).

2- An anode pole where metal is oxidized, $Fe \rightarrow Fe^{+2} + 2e^{-}$.

3-A cathode pole to accept (reduce) electrons, $2H_2O + O_2 + 2e^{-} \rightarrow 4OH -$

4-An electrical path (current conductivity) between the anode and cathode to transfer electrons.

5- A conductive electrolytic environment to transfer ions and complete the circuit.

The Figure (2-4) simulates the corrosion path in reinforced concrete.

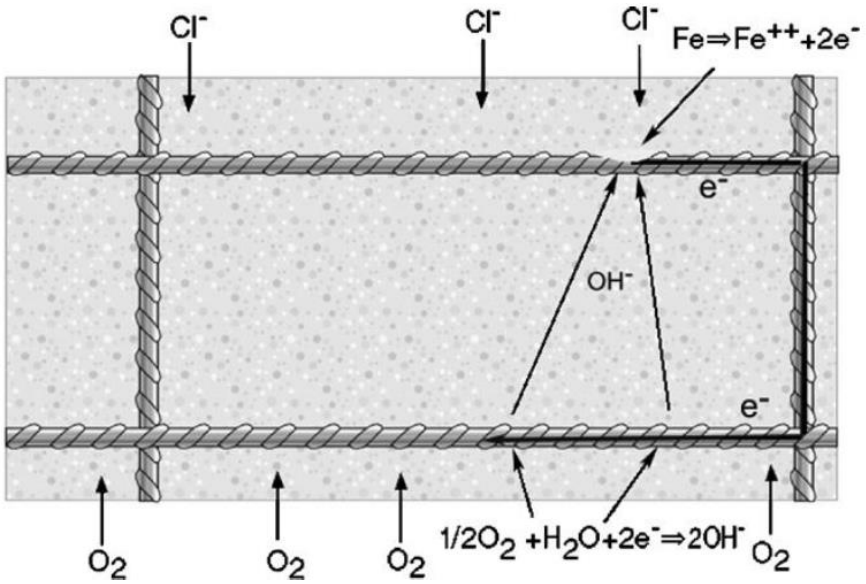

Figure 2–42–2 The Corrosion Path in Reinforced Concrete Member

[Bertolini, L 2004]

2-6 Corrosion Products Size

The final production of corrosion is hydrated ferric oxide ($Fe_2\ O_3$) which has a volume approximatly 3 to 10 the original size of the original reacting steel [ACI 222R 1996 and Ahmed S. 2003], figure (2-5). This huge expansion leads to cracking, delamination, and finally spalling of the concrete surrounding the reinforcing steel bars.

2-7 Corrosion Thermodynamic and Kinetics

The electrochemical reactivity of the surface of steel reinforced bars has a significant effect on their inclination to corrosion initiation. By using Gibb's free energy, the following result could be driven [Perez N 2004]

$$\Delta G = \Delta H - T\Delta S + \Delta W \qquad \text{Eq. (2-8)}$$

Where:

ΔG: Change in Gibb's free energy

ΔH: Change in enthalpy

T: Temperature

ΔS: Change in entropy, and

ΔW: Change in additional external work

However, Thomas [Thomas, D. 2003] concluded that in the case of a typical corrosion reaction, environmental conditions are relatively constants and changes in entropy and enthalpy tend towards zero.

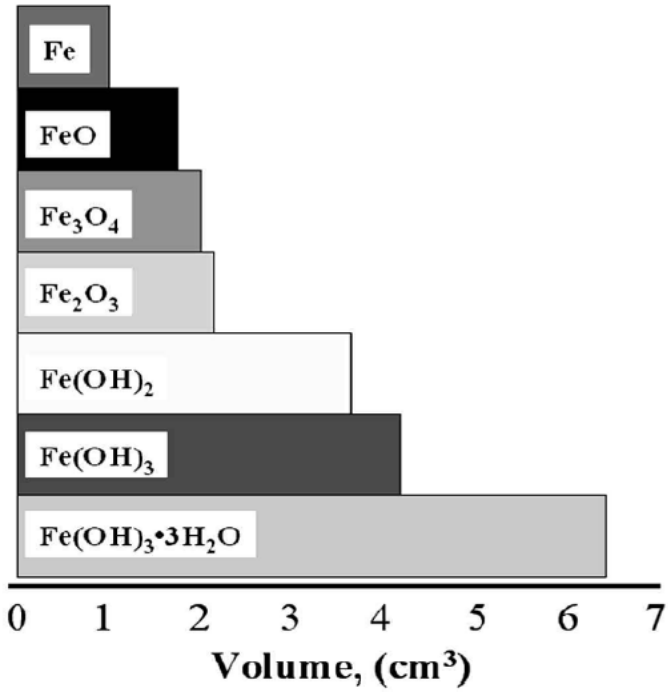

Figure 2–52–3 Relative Volumes of Fe Oxides

[Hope et al. 2001]

Therefore, we can correlate the corrosion free energy by:

$$\Delta G = \Delta W \qquad \text{Eq. (2-9)}$$

It is known in electrochemical system,

$$\Delta W = -Q * E \qquad \text{Eq. (2-10)}$$

Where:

Q: is the charge / ion transfer present at the interface between the metal and the electrolyte, and the negative sign is included by convention for electrochemical potential measurements.

E: is the electrochemical potential difference formed by the spatial distribution of ions in the double layer.

Depending on Faraday,

$$Q = n * F \qquad \text{Eq. (2-11)}$$

Where:

N: is the number of electrons transferred in the reaction.

F: is Faraday's constant (96,500 C/mol).

Now we can rewrite the change in Gibb's free energy to the electrochemical potential present at the surface as shown in equation (2-12) below.

$$\Delta G = -n * F * E \qquad \text{Eq. (2-12)}$$

Negative values of ΔG indicates a reduction in free energy and a spontaneous reaction. Positive values of ΔG indicates an increase in the free energy of the system and a thermodynamically unstable condition [13].

2-8 Corrosion Monitoring Techniques

The corrosion monitoring, however, means using advanced technologies to track and observe the corrosion parameters and phenomena as well. The following are the most popular and widely used techniques of corrosion monitoring. It is very important to emphasize that all these techniques are not necessarily able to measure all the corrosion parameters.

2-8-1: Visual Inspection

It is the simple way to monitor the corrosion process. This method includes periodic intervals to take a look at the structural members such as bridge decks in order to monitor whether or not there are corrosion cracks, rust stains, spalled concrete cover, concrete disintegration, and leach out [ACI 222R 1996]. This method could be used to make up the first conception of corrosion present, then the treatment consequences might take place

depending on the suitable available rehabilitation methods. This method could be used with any type of other monitoring process.

2-8-2: Open Circuit Potential (OCP) or Half-Cell Potential Method

As a result of the reaction between the steel rebars and the other ions, O, OH, and Cl, an electrochemical cell is formed [Hyoung seok and Stephen Geoffrey millard 2007]. Figure (2-6) below shows the open circuit method.

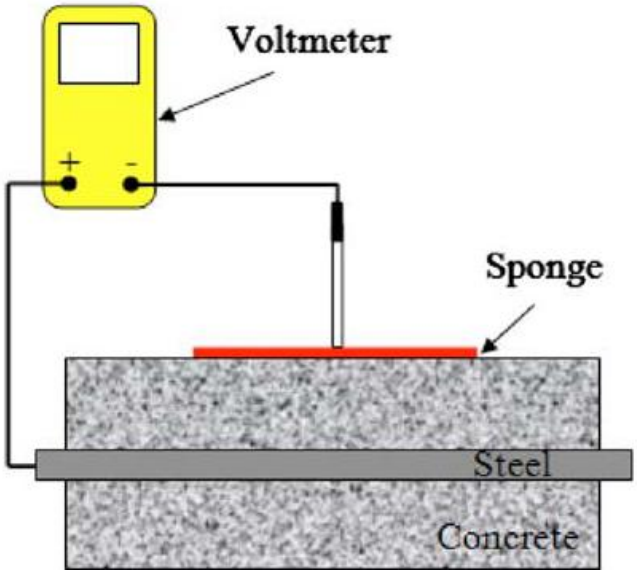

Figure 2–6 Open Circuit Set up

[Hyoung seok and Stephen Geoffrey millard 2007]

In this method, we should notice that the probability of corrosion is estimated; it is not the actual rate of corrosion. The ASTM C 876 illustrates the method of work of this test. The probability of corrosion depends on the open circuit activity; for example the more potentials stands for more corrosion suspension.

The half-cell potential consists of a strand electrode as Cu/CuSO4 and a voltmeter while the rebar works as a working electrode. Table (2-1) shows the probability of corrosion depending on corrosion cell potentials.

Table 2-1 The probability of Corrosion via Corrosion Cell Potentials

[ASTM C 876]

Half-Cell Potential Reading Versus Cu/CuSo4	Corrosion Activity
More positive than -200 mV	90% probability of no corrosion
Between -200 and -350 mV	An increase probability of corrosion
More negative than -350 mV	90% probability of corrosion

2-8-3: Macro-Cell Corrosion Method

The macro-cell means the two poles of corrosion cell separated by different areas, normally called anode and cathode. In the case of the bridge deck, the top bar always reacts as anode while the bottom bar plays as cathode. The ASTM G109 [ASTM G109 2007] gives the working method for this test. The figure (2-7) below shows the test set up.

2-8-4: Concrete Resistivity Measurements

One of the most important parameters that controls the corrosion process is the electrical resistivity of concrete. This resistance prevents the electrical current from passing between the anode and cathode through the concrete mass [Bezad Bavarian & Lisa Reiner 2003].

Figure 2–7 ASTM G109 Test Set Up

The electrical resistivity of concrete was proposed as an effective parameter to evaluate the risk of reinforcing steel corrosion, particularly when corrosion is induced by chloride attack [Ahmad S 2003]. The resistivity of concrete is strongly dependent on the concrete quality and on the exposure conditions, such as the relative humidity. Also, temperature affects the degree of concrete pore saturation and so the resistivity values [Ann K. Y. and Song 2007, ASTM A416 / A416M 2006]. Concrete resistivity is generally measured by using the Wenner four probe method as showed in figure (2-8 and 2-9) below. Also the relation between corrosion and concrete resistivity is listed in table (2-2) below.

Table 2-2 The Relation Between Corrosion and Concrete Resistivity

Resistivity (Ohm.cm.)	Corrosion risk
Greater than 20,000	Negligible
10,000 to 20,000	Low
5,000 to 10,000	High
Less than 5,000	Very high

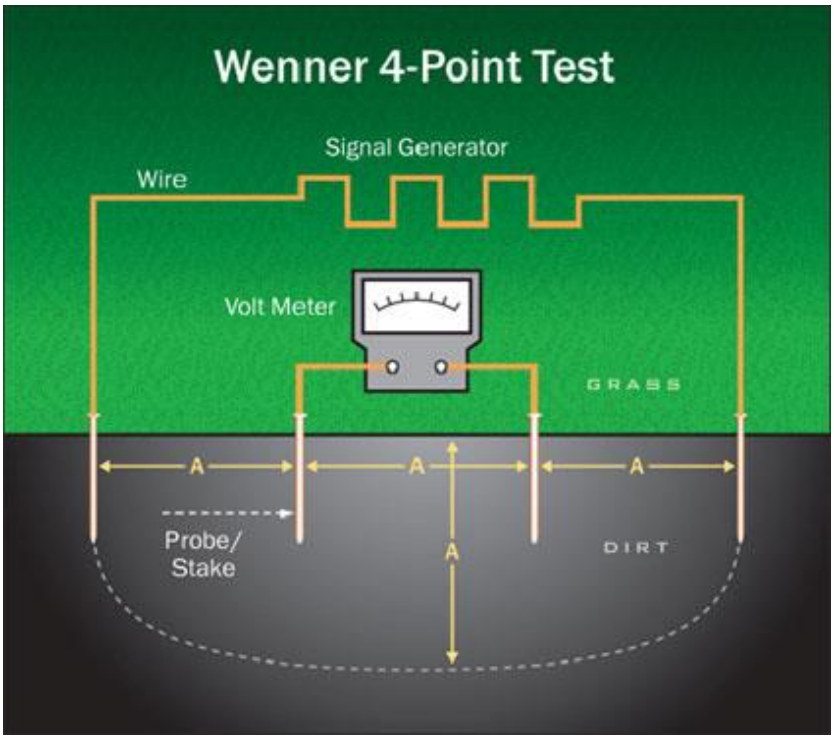

Figure 2–8 Wenner Array Principles and Probe

[http://www.esgroundingsolutions.com]

Figure 2–9 Wenner Array Set Up

.

2-8-5: Linear Polarization Resistance Method (LPR)

It is one of the most advanced and widly used methods for determining the instantaneous activity and rate of corrosion in the world [Perez N 2004]. There are three types of polarization, concentration, ohmic, and activation.

i. Concentration polarization [Thomas D 2003]: is due to the fact that the current depletes the ions available near the electrode surface, which reduces the voltage and inhibits the current.

ii. Ohmic polarization.

iii. Activation polarization [Thomas D 2003]: is a drop-in electrode potential due to changes caused by the current magnitude in the mechanism of ion transfer through the steel-concrete interface. The reinforcement is interrupted by a small amount from its equilibrium potential in this method. This can be accomplished

potentiostatically by changing the potential of the reinforcing steel by a fixed amount, ΔE, and monitoring the current decay, ΔI, after a fixed time. Alternatively, it can be done galvanostatically by applying a small fixed current, ΔI, to the reinforcing steel and monitoring the potential change, ΔE, after a fixed time period. In each case the conditions are selected such that the change in potential, ΔE, falls within the linear Stern–Geary range of 10–30 mV [Jones D. A. 1996]. The polarization resistance, Rp, of the steel is then calculated from the equation:

$$Rp=\Delta E/\Delta I \text{----------(2-13)}$$

The corrosion rate, I corr:

$$Icorr=B/Rp \text{ ----------(2-14)}$$

Where

B is the Stern–Geary constant

The corrosion density, I corr: need to know the axact surface are of corroded steel,

icorr=Icorr/A

C.Andrade, et.al. correlated the relation between Icorr and the service life of structure [ASTM C876 2006] as presented in table (2-3) below.

Table 2-3 The Relation Between Icorr and the Service Life of Structure

Corrosion current (Icorr)	Condition of the Rebar
Icorr < 0.1 μA/cm2	Passive condition
Icorr 0.1 - 0.5 μA/cm2	Low to moderate corrosion
Icorr 0.5 - 1.0 μA/cm2	Moderate to high corrosion
Icorr > 1.0 μA/cm2	High corrosion rate

2-8-6 Embbeded Sensors:

This method implies puting sensors inside the concrete mass to monitor the corrosion factors and corrosion development as well. There are varity of sensors that could be used to monitor the corrosion activity. Following are the most used sensors:

1- CMS V2000 Silver-Silver Chloride Electrode Monitoring

This sensor consists of silver-silver chloride electrode. It is embedded in the concrete mass along with the steer rebars to measure the potential differences between the anodic rebar and this electrode and by using Farady's law the corrosion activity ought to be calculated [K.C. Clear 1989].

2- Embedded Corrosion Instrument:

This type of sensors represents the most advanced generation of sensors for corrosion monitoring. This kind is able to measure the majority of corrosion parameters such as oxygen content, temperature, chloride content, humidity, and some properties as LPR. In addition to this, it is able to intergrate these parameters to find the corrosion activity and rate, and it sends this information to data loger to gather them and give the early corrosion warning.

2-9 Previous Corrosion Studies

The corrosion resistance of different types of steel reinforcement was evaluated by Brent M. Phares, et. Al [33. Brent M. 2006]. To perform this study, ASTM G109 and Rapid Macrocell accelerated Corrosion Tests were used. Basic type of sensors CMS V2000

silver-silver chloride electrode was used to measure the electrochemical activity of corrosion for both reinforcement types. The test results illustrated that there are no corrosion issues noticed within the first 40 weeks of exposure age for both MMFX and the as-delivered epoxy-coated reinforcement; while the uncoated mild steel specimens underwent corrosion within the fifth week.

Wiss et. al used ASTM G 109 to measure the corrosion activity of modified corrosion samples. [Wiss Janney Elstner Associates 2008]. The chloride solution was 15 % NaCl to simulate the occurring deicing salts on in-land bridge structure. They concluded that the corrosion threshold cannot start before 20 weeks. Also, the results indicated the stainless steel 304 had the highest corrosion resistance (5 times that of black steel), and the MMFX had 3 time that of black steel.

In order to understand the relation between the different crack widths and the corrosion rate and propagation, M.B. Otino et al [carried out a significance experimental study. A total of 48 beams (100*100*500 mm) were casted with different w/binder ratios, (0.4 and 0.7 mm) crack widths, and many binder types. All specimens were exposed to 5 % NaCl for about 32 weeks. The corrosion rate (by using Galvanostatic linear polarization resistance technique), half-cell potentials (HCP), and concrete resistivity were measured. The most important conclusions were: (i) in contrast to general agreed upon opinion, the crack width (less than 0.4 mm) may significantly affect both corrosion rate and propagation, (ii) it is impossible to find the universal threshold crack width for all concretes, and (iii) the presence of cracks increased the corrosion rate by 210% for normal concrete.

In the same direction, the effect of cover depth, w/c ratio, and crack width on half-cell potential in cracked concrete exposed to salt sprayed condition has been investigated by Yun Yong Kim et al. The test parameters were cover depth (1.18 and 2.36 inches), crack widths (0.0 and 0.06 inches) w/c ratio (0.35, 0.55, and 0.70). A salt spraying test was used to accelerate the corrosion on reinforced concrete beams. The spraying duration was nearly of 35 days. The following conclosion was derived: (i) in control condition (w/c 0.55 and cover depth 30 mm), HCP measurements increase with crack width, by 14–16% in 0.50 mm crack width, 24% in 1.0 mm crack width, and 34–42% in 1.50 mm crack width respectively. (ii) when crack width reaches 1.0 mm in w/c 0.55, HCP increasing ratio was 112–122% in cover depth 10 mm, 116–120% in cover depth 30 mm, and 166–200% in cover depth 60 mm respectively.

Continuously, Brent M. Phares etal. [Brent M. Phares etal. 2002] investigated the corrosion resistance of epoxy coated reinfoced rebars and the impact of bridge deck cracking on durability. Cores taken from many bridges have been selected across Iowa state. Preliminary results showed the conditions of epoxy coated rebars at cracked area is worser than the other locations. They concluded that the ingress of chloride ions throw cracked deck is faster than uncracked position which destroy the epoxy protection layer on the surface of rebar. Due to the fact that the exestance of defects in the epoxy coating layer of rebars, this makes the epoxy coating reinforcing steel rebars are susceptible to corrosion and deterioration.

In contrast, A. W. Beeby [ACI 222.3R 2011] studied the cracking, cover and corrosion of reinforcement. Though this study, many beams were broken after 1, 2, 4, and

10 years, and the progress of corrosion was studied by measuring the depth of corrosion at each crack. The cover was 0.9 to 1.38 inches while the bar types were plain and deformed. The experimental results revealed that (i) crack widths have little influence on corrosion, (ii) cover of concrete and quality of concrete are the major parameters controlling corrosion.

In the same direction, C. Arya and F.K. Ofori-Darko [C. Arya 2010] studied the relationship between crack frequency and reinforcement corrosion (2 years lab investigation). The techniques that used to start corrosion were (i) 3% sodume chloride (spray method). and (ii) 5% NaCl dosage (by weight of cement) to the concrete mix. The study concluded that an effective measure against corrosion may be to limit the frequency of cracking (i.e. by increasing the thickness of concrete cover). In other words, increasing the cover thickness limits the crack's frequencies.

An experimental study has been done by Aimin Xu and Ahmed Shayan [Aimin Xu 2011]. They studied the relation between rienforcement corrosion rust growth at the concrete steel interface and concrete cover cracking. Their expermintal program included preparing a reinforced concrete slabs (15*12*7 inches) to predict the first cracking of the concrete cover based on the depth of the corrosion on the reinforcing steel. The variables were two types of concretes (4351 and 7252 psi), three kinds of steel bars reinforcement, three levels of chloride contamination (by dissolving $N_a C_l$ in concrete mixing water), and three concrete cover thickness (1, 2, and 2.8 inches). A corrosion rate meter which implies LRP was used to measure the corrosion rate. The main finding were the corrosion depth of steel bars was found vary from 0.2 mil for 0.9" bar under 1" cover, to 5.9 mil for 0.2"

bar under 2.9” cover. That clearly means the critical corrosion depth to cause cover cracking is larger for smaller sized bars and thicker cover.

David W. Law et al.[David W 2009] carried out research in order to study the relation between the concrete strength and the width of surface crack. Average surface crack widths of 0.05, 0.5, 1 and 1.5 mm were adopted as the target crack widths. They computed the following aspects: (i) The correlation was better for maximum crack width than for mean crack width and bond stress. (ii) Confined bars displayed a higher bond stress at the point of initial cracking than where no corrosion had occurred. As crack width increased, the bond stress decreased significantly. (iii) Unconfined bars displayed a decrease in bond stress at initial cracking, followed by a further decrease as cracking increased. Generally, the results indicated a potential relationship between the maximum crack width and the bond.

An extensive study to model the Time-to-Corrosion cracking of the cover concrete in chloride contaminated reinforced concrete structures has been done by Youping Liu [Youping 1996]. The following parameters were considered: two diameters of reinforcing steel rebar, W/C ration 0.45, seven sodume chloride contents, two different exposure conditions, and three different concrete cover depths. In the monthly basis, the authors computed corrosion potentials, rate of corrosion, resistance of concrete, and temperature . They also matched the actual corrosion weight loss of rebars to the results of measurement devices. Based on the corrosion-cracking conceptual model and critical mass of corrosion products, the time-to-corrosion cracking model was suggested. They anticipated times to corrosion cracking are in a good agreement with the observed times to corrosion cracking of the cover concrete.

Ali S. Al-Harthy et al. [Ali S. 2006], however, reviewed and studied the crack initiation and propagation of RC slab specimens subjected to accelerated corrosion testing. For the experimental part, six RC specimens (550 * 1000 mm rectangular slabs of thickness 250 mm) were constructed. It was found that crack initiation time and crack propagation time increased with increasing of concrete cover and with decreasing the reinforcing bar diameter and concrete compressive strength. Also, the experimental crack initiation time was compared with nine predictive models. The predictive models were found to give widely scattered results and more data are needed in order to better assess the accuracy of the predictive models.

Kolluru V. Subramaniam and Mingdong Bi [Kolluru V 2012] carried out an experimental work in order to: (i) predict the macrocell response of a steel bar embedded in cracked concrete using the polarization responses of active and passive steel; and (ii) to evaluate the relative contributions of the macro and micro cell components to the total corrosion of steel located in cracked concrete. The dimensions of the concrete beam specimen were 15*15*100 cm. An artificial crack was introduced using a plastic insert placed in the middle of the specimen. Potentials, LPR and Tafel slope were measured. The following conclusions were found: (i) In the spatially inhomogeneous corrosion along the length of the steel bar embedded in cracked concrete, the relationship between the flow of macrocell current and the potential can be predicted by the polarization response of steel located at the crack and the passive steel located away from the steel; and (ii) In the macrocell corrosion system established along the length of the steel bar in cracked concrete, the macrocell corrosion mechanism is the dominant component contributing significantly to local metal loss at the crack.

To monitor the corrosion parameters for structural concrete, Carmen Andrade and Isabel Martinez [Carmen and Isabel 2009] used embedded sensors. In order to correlate these results on the field, they studied only the effect of temperature on corrosion activity. The test results showed the resistivity of concrete conversely proportional to the increase of temperature . However, in my opinion this parameter isn't enough to correlate the corrosion issue. The researcher thinks it would be adequate had it included the effect of other parameters such as the presence of Oxygen and moisture content. Also, there is a lot of missing information about the characteristics and properties of each testing group.

In the same direction, Brain, M.Pailes statistics did a based approach of half-cell potential and concrete resistivity to identify the corrosion threshold of bridge decks at different places [Brian M. Pailes 2014]. In this research, the statistical correlation method is used to identify half-cell potential and electrical resistivity threshold values. The data of HCP and CR bridge decks has been collected from New Jersey, New York, Virginia, Minnesota, and Iowa. The researcher has concluded that there is a correlation between the HCP and the CR with respect to corrosion threshold. This correlation isn't enough to predict the precise threshold, since the effective correlation should be between the threshold and its parameter such as chloride content, temperature at reinforcement depth, Oxygen content, and ohmic resistance of concrete.

The correlation regarding to accelerated corrosion tests had been done by M.P. Papadopoulos et al [M.P. Papadopoulos 2011]. They collected a large number of samples of old marine buildings (96 years old) in Greece, and they tested these samples for mechanical properties and corrosion. Their calculation has been estimated by taking into

account two different parameters: the corrosion attack rate and the mass loss rate. The results were; in the first case, the acceleration factor was about 74.5, whereas in the second case it was about 79.The researcher believes that the test results were not adequate and had a wide range of scatters. They are not applicable just in the same place in Greece because (i) they used a very simply mathematical formula for corrosion curve fittings ”straight relation,” (ii) they didn’t correlate to the actual corrosion parameters such as chloride content, the presence of oxygen, and humidity inside the pore water. Figure (2-10) presents the test results.

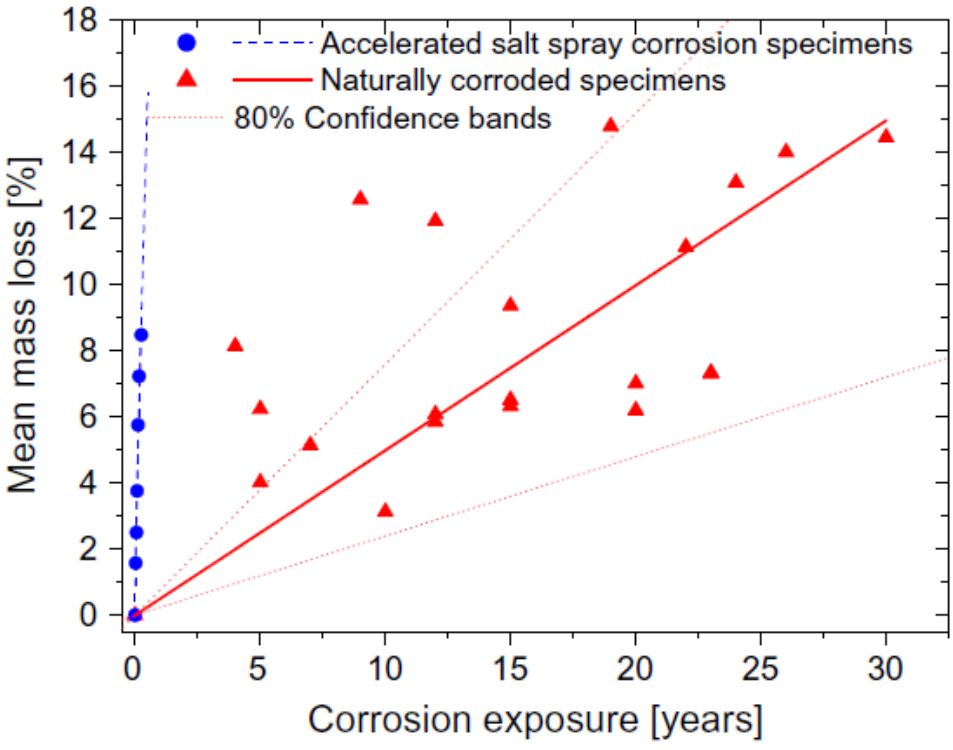

Figure 2–10 Correlation Factor

[M.P. Papadopoulos 2011]

2-10 Summary of the Previous Crack Effects Studies

The sumarry of the most recent cracks effects studies of corrosion process is listed in tables (2-4) below. It shows clearly, there is no one research that studies or correlates the relation of the crack width/ and depth with the corrosion process so far.

Table 2-4 Summary of Crack Characteristics Effects

Author	Year	Crack Characterstics			Type Of Concrete	Type Of Reinforcement	Measurements Techniques	Nacl Dosage	Sample Size (Inches)
		Width	Depth	Pattern					
C. Arya & F.K. darko	1996	0.012	1.575	T	A	B.S.	LPR, Galvanic current	3% & 5%	4*5*35 & 6.7*6*157
S.J. Jaffer & C.N. Hansson	2008	N/A	N/A	N/A	A & HPC	B.S.	Potentios-tatic LPR & Potentiod-ynamic LPR	3%	2.7*4.7*47
Kolluru V.	2010	0.014, .016	1	T	A	BS.	LPR, macrocell	3%	6*6*47
M.B. Otieno	2010	0.016, 0.0275	0.4	T	A	B.S.	Galvanostatic LPR	5%	4*4*19.7

Continue table (2-4) Summary of Crack Charactrestics Effects

Author	Year	Crack			Type of Concrete	Type of Reinforcement	Measurements Techniques	Nacl Dosage	Sample Size (Inches)
		Width	depth	pattern					
Ali S. Al-Harthy	2011	0.04*, 0.084*	N/A	N/A	A	B.S.	LPR	3%	21.6*39.3*9.8
A. Michel	2013	N/A	N/A	Tc	A	B.S. & SFR	Macrocell	3%	11.4* 12.2* 25.6
Aimin Xu and Ahmed Shayan	2016	N/A	N/A	N/A	A & HPC	B.S.	Macrocell,LPR	.25, .98, 1.97 by weight of cement	15*12*7
The researcher suggestion		.011, 0.035	0.5, 1	Lc	A & HPC	B.S., EC, S.S.,	Macrocell,LPR	3%, 15%	4.5*6*11 & 24*24*10

Where,

A: ordinary concrete; B.S.: Black Steel; LPR: linear Polarization Resistance; Tc: Transversal Crack, HPC: High Performance Concrete; SFR: steel fiber reinforcing; *: Induced cracks due to corrosion; Lc: Longitudinal; N/A: Not Applicable; EC: Epoxy Coated; S.S.: stainless steel; G.S.: Galvanized Steel.

3. Chapter Three

Experimental Study

3.1.General

Relating to the previous studies and researches, there is no single adequate research that studied neither the correlation between the chloride content and the corrosion potentials nor the correlation between the crack depth and width. For this reason, there is a necessity to correlate the lab-based accelerated tests with the field performance and crack depth/ width effects.

Fortunately, we have a corrosion data of a 20 year old bridges decks which is suitable to correlate with ongoing lab tests. To get the correlation process as close as possible, we simulated the two existing bridges (in other words, we eliminated the variables between the lab and the field performance). For example, we used the same mix proportions and properties, material characteristics, and exposure conditions. To get this task done, the following plan of study is carried out:

i. Compressive Strength-ASTM C39
ii. Tensile strength-ASTM C496
iii. Flexural strength- ASTM C78
iv. Static Modulus of Elasticity- ASTM C469
v. Free Shrinkage- ASTM C157
vi. Rapid Chloride Permeability- AASHTO T 277
vii. Surface resistivity- AASHTO T 358

viii. Corrosion potentials and currents ASTM G109.

ix. Chloride Content- ASTM C1152.

x. Visual Inspection.

xi. Corrosion Autopsy.

3.2.Concrete and Reinforcement Types

The materials used through this research are primarily locally sourced. The availability of each material is very important if it is to be implemented by agencies in the area. All coarse and fine aggregates, along with cement and silica fume, were acquired from Clayton Concrete in Edison, New Jersey. The concrete chemical admixtures such as water reducer, air entraining, high range water reducing admixture, were supplied by Great Eastern Technologies Company. Herein concrete class (A) and HPC are used in this research since they are widely used nowadays at bridge decks. The mix proportions and essential physical and mechanical properties of these mixes are listed in tables (3-1) and (3-2) respectively. Also, in order to cover the most frequently used rbars, the following types are used, figure (3-1):

i. Black steel (conventional steel rebars)

ii. Epoxy Coated steel rebars

iii. Duplex 2205 (318) Stainless steel rebars

iv. Hot Dip Galvanized Steel.

v. Chrome X 9000 MMFX rebars, Martensitic Microcomposite Formable Steel (MMFX).

Figure (3-2) below shows the chemical admixture that used in this research.

Figure 3–1 Types of the Reinforced Steel Rebars Used in This Research

3.3.Plan of the Research

This study aims to cover the most significant parameters that influence the corrosion process such as the effects of the crack patterns and rebars types. Also, it is trying to simulate the bridge deck in the field. The following aspects are considered:

Table 3-1 Concrete Class (A) Mix Proportions and Properties

Design Strength	Class A (TPKE-AR57A)
Cement (lbs.)	658
Sand (lbs.)	1282
Rock (lbs.)	1850
Water (gal.)	30
W/C Ratio	0.38
Admixture (1) (ml.) (Great Eastern Technologies- section 6A-Air Entraining Admixture ASTM C-260)	6.6
Admixture (2) (ml.) (Great Eastern Technologies- Chemstrong A- Water Reducer Admixture- Type A- ASTM C494	15.1
Slump (inches)	3+/-1
Air (%)	6+/-1

Table 3-2 High Performance Concrete (HPC) Mix Design and Properties

Design Strength	HPC
Cement (lbs.)	501
Sand (lbs.)	1184
Rock (lbs.)	1850
Fly Ash	132
Silica Fume	25
Water (gal.)	31.6
W/C Ratio	0.4
Admixture No. 1 (ml.), AE. (Great Eastern Technologies- section 6A-Air Entraining Admixture ASTM C-260)	162
Admixture (2) (ml.), WRA. (Great Eastern Technologies- Chemstrong A- Water Reducer Admixture- Type A- ASTM C494).	486
Admixture (3) (ml.), HRWRA. (Great Eastern Technologies- Chemstrong A- High Range Water Reducing Admixture- Type F- ASTM C494.	2025
Slump- maximum (inches)	8
Air (%)	6

Figure 3–2 Chemical admixtures which used through the current research

3-3-1 Laboratory Studies on the Crack Effects of Corrosion Process of Reinforced Concrete Members by Using ASTM G-109

This part aims to correlate the crack depth and/ or width with the corrosion initiation and progress. The variable parameters are concrete class (A), HPC, black steel, duplex

stainless Steel, MMFX, Galvanized Steel, and Epoxy-coated steel Rebars. Tables (3-3) through (3-7) and flow chart in figure (3-3) show the crack effect aspects.

3-3-2 Bridge Deck Service Life Corrosion Model

It stands to correlate the laboratory-based accelerated corrosion testing with the field performance of steel rebars to predict the service life of reinforced concrete structure. The variable parameters are HPC, duplex stainless steel, MMFX, galvanized steel, and Epoxy-coated steel Rebars. Table (3-8) and flow chart in figure (3-4) show the Bridge Deck Simulation.

3-3-3 The Crack-Sealer Performance

This part of research is attempting to investigate the performance of the crack sealants. As mentioned earlier, two kinds of sealant, T-70 MX and Seal Krete -SK, are used through this research. The T-70 is a High Molecular Weight Methacrylate (HMWM) while the Seal Krete is an acrylic sealant. The two different types of the crack sealant are presented in the figure (3-9) below.

Table 3-3 Testing Program of Black Steel

Samples ID	Concrete Type	Reinforcement Type	Crack Width (inch)	Crack Depth (inch)		Chloride Solution Concentration (%)	Notes
A-BS-LCL	A	Black Steel	0	0	0	3%	A = Class A concrete HPC= high performance concrete BS= Black Steel EC= Epoxy Coated MMFX= Martensitic Microcomposite Formable Steel SS =Stainless Steel GS = Galvanized Steel LCL = Low concentration 3% HCL= high concentration 15%
A-BS-HCL			0	0	0	15%	
A-BS-0.011-LCL			0.011	.5	1	3%	
A-BS-0.011-HCL			0.011	.5	1	15%	
A-BS-0.035-LCL			0.035	.5	1	3%	
A-BS-0.035-HCL			0.035	.5	1	15%	

Table 3-4 Testing Program of Epoxy Coated Steel

Samples ID	Concrete Type	Reinforcement Type	Crack Width	Crack Depth		Chloride Solution Concentration (%)
A-EC-LCL	A	Epoxy Coated	0	0	0	3%
A-EC-HCL			0	0	0	15%
A-EC-0.011-LCL			0.011	.5	1	3%
A-EC-0.011-HCL			0.011	.5	1	15%
A-EC-0.035-LCL			0.035	.5	1	3%
A-EC-0.035-HCL			0.035	.5	1	15%
HP-EC-LCL	HPC		0	0	0	3%
HP-EC-HCL			0	0	0	15%
HP-EC-0.011-LCL			0.011	.5	1	3%
HP-EC-0.001-HCL			0.011	.5	1	15%
HP-EC-0.035-LCL			0.035	.5	1	3%
HP-EC-0.035-HCL			0.035	.5	1	15%

Table 3-5 Testing Program of Stainless Steel

Samples ID	Concrete Type	Reinforcement Type	Crack Width	Crack Depth		Chloride Solution Concentration (%)
A-SS-LCL	A	Stainless Steel	0	0	0	3%
A-SS-HCL			0	0	0	15%
A-SS-0.011-LCL			0.011	.5	1	3%
A-SS-0.011-HCL			0.011	.5	1	15%
A-SS-0.035-LCL			0.35	.5	1	3%
A-SS-0.035-HCL			0.035	.5	1	15%
HP-SS-LCL	HPC		0	0	0	3%
HP-SS-HCL			0	0	0	15%
HP-SS-0.011-LCL			0.011	.5	1	3%
HP-SS-0.001-HCL			0.011	.5	1	15%
HP-SS-0.035-LCL			0.035	.5	1	3%
HP-SS-0.035-HCL			0.035	.5	1	15%

Table 3-6 Testing Program of Galvanized Steel

Samples ID	Concrete Type	Reinforcement Type	Crack Width	Crack Depth		Chloride Solution Concentration (%)
A-GS-LCL	A	Galvanized Steel	0	0	0	3%
A-GS-HCL			0	0	0	15%
A- GS -0.011-LCL			0.011	.5	1	3%
A- GS -0.011-HCL			0.011	.5	1	15%
A- GS -0.035-LCL			0.035	.5	1	3%
A- GS -0.035-HCL			0.035	.5	1	15%
HP- GS -LCL	HPC		0	0	0	3%
HP- GS -HCL			0	0	0	15%
HP- GS -0.011-LCL			0.011	0.011	.5	3%
HP- GS -0.001-HCL			0.011	0.011	.5	15%
HP- GS -0.035-LCL			0.035	0.35	.5	3%

Table 3-7 Testing Program of MMFX

Samples ID	Concrete Type	Reinforcement Type	Crack Width	Crack Depth		Chloride Solution Concentration (%)
A-MMFX-LCL	A	MMFX	0	0	0	3%
A-MMFX-HCL			0	0	0	15%
A-MMFX-0.011-LCL			0.011	.5	1	3%
A- MMFX -0.011-HCL			0.011	.5	1	15%
A- MMFX -0.035-LCL			0.035	.5	1	3%
A- MMFX -0.035-HCL			0.035	.5	1	15%
HP-MMFX-LCL	HPC		0	0	0	3%
HP-MMFX-HCL			0	0	0	15%
HP- MMFX-0.011-LCL			0.011	0.011	.5	3%
HP- MMFX-0.001-HCL			0.011	0.011	.5	15%
HP- MMFX-0.035-LCL			0.035	0.35	.5	3%

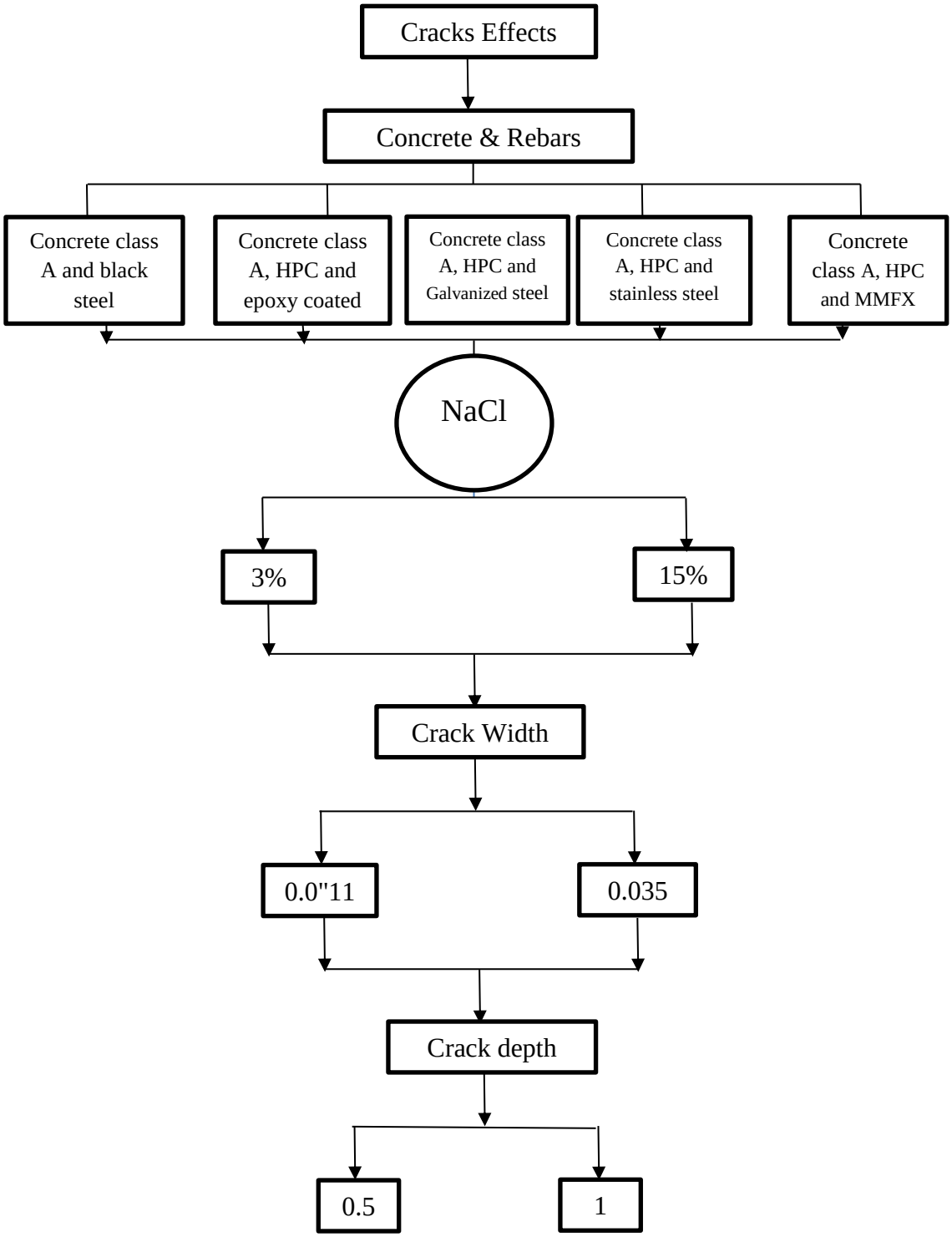

Figure 3–3 Flow Chart of Crack Effects

Table 3-8 Summary of Testing Program of Bridge Deck Simulation

Samples ID	Concrete type	Reinforcement type	Chloride Solution Concentration (%)	notes
HP-EC-HCL	HPC	Epoxy Coated Steel	15%	HPC= high performance concrete EC= Epoxy Coated MMFX= Martensitic Microcomposite Formable Steel GS: galvanized Steel SS =Stainless Steel HCL= high concentration 15%
HP-SS-HCL		Stainless steel		
HP-GS-HCL		Galvanized Steel		
HP-MMFX-HCL		MMFX		

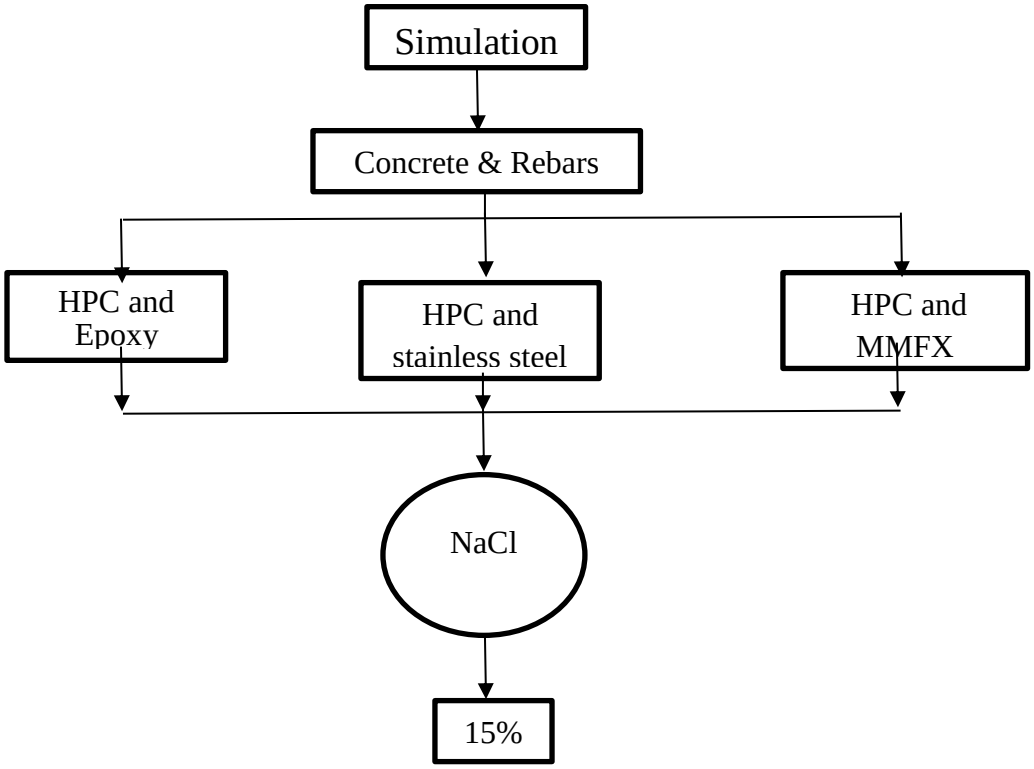

Figure 3–4 Flow Chart of Experimental Work-Bridge Deck Simulation

3-4 Types and Sizes of Corrosion Samples

Two types of concrete samples are used throughout this study, prisms and slabs, as shown in Figures (3-5) and (3-6). The prismatic samples (11×6×4.5 inches) made in accordance with ASTM G109. The specimens reinforced with 3 #5 (5/8 inches bar diameter) of different types of steel reinforcement. While the slabs (24×24×10 inches) has the same dimensions and steel reinforcement details of the two bridge decks. These slabs consist of two mats of #5 steel rebars of different types of steel reinforcement.

Figure 3–5 Prismatic Samples of Corrosion Tests

Figure 3–6 Slab Samples of Corrosion Tests

3-5 Sealed Corrosion Samples.

In order to investigate the performance of the cracked samples, two types of High Molecular Weight Methacrylate (**HMWM**) and **Acrylic** Crack Sealers were used, T-70 MX and Seal Krete from two different manufacturing companies. The crack sealer was applied to the surface of concrete before exposing to the chloride solutions figures (3-7 and 3-8). The following abbreviations are used to refer to the effects of crack sealers in the corrosion activities:

Control: Concrete has no sealant.

T70-∥: corrosion potentials and/ or currents of samples sealed with T-70 MX and have cracks parallel to the longitudinal reinforcement.

T70-⊥: corrosion potentials and/ or currents of samples sealed with T-70 MX and have cracks perpendicular to the longitudinal reinforcement (transverse direction).

SK-∥: corrosion potentials and/ or currents of samples sealed with Seal Krete and have cracks parallel to the longitudinal reinforcement.

SK-⊥: corrosion potentials and/ or currents of samples sealed with Seal Krete and have cracks perpendicular to the longitudinal reinforcement (transverse direction).

Figure 3–7 Applying the Concrete Sealant on the Prismatic Concrete Samples

Figure 3–8 Applying the Concrete Sealant on the Reinforced Concrete Slabs

3-6 Chloride Concentrations:

As we stated in chapter two, literature review, there is no specific concentration of N_aC_l, but the range varies from 2.5 to 15 % of NaCl. Accordingly, we have used a normal concentration of 3% of N_aC_l as it is recommended by ASTM G-109, and 15% of N_aC_l as it exists in most of bridge decks in the USA due to deicing salt action.

Figure 3–9 Crack sealant that used in this research

3-7 Crack Formation

Artificial cracks are formed in the prismatic samples to simulate the field conditions. In order to make these cracks, stainless steel sheets are inserted to the top surfaces of concrete samples during casting as illustrated in figures (3-10), (3-11), (3-12) and (3-13).

Figure 3–10 Stainless Steel Sheets of the Artificial Crack Formation

Figure 3–11 Stainless Steel Sheets Inserted within Concrete Mass

Figure 3–12 The Cracked Concrete Samples after Removing the Stainless Steel Sheets

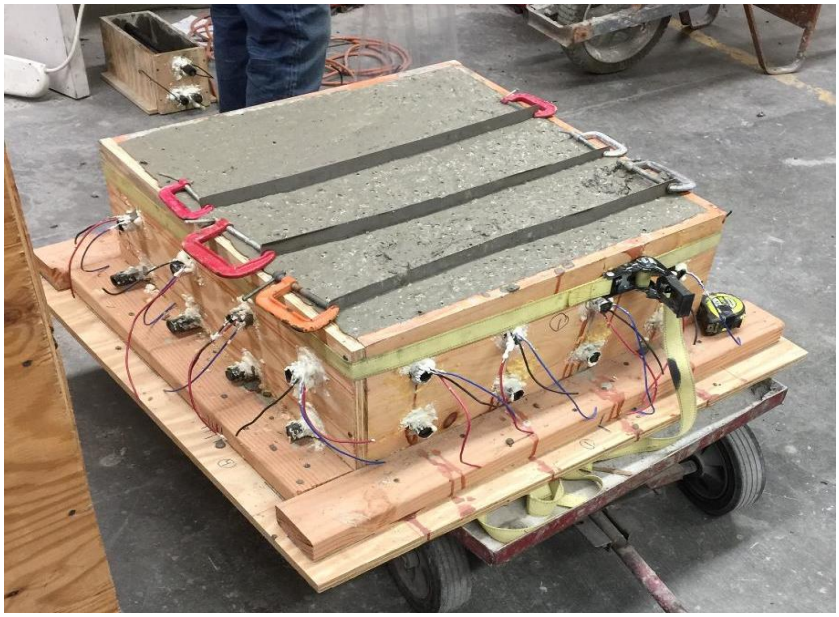

Figure 3–13 Artificial crack of slabs

3-8 Corrosion Sensors

Two types of sensors are used to monitor the corrosion process in the laboratory and field work in this research. These sensors were installed inside the bridge decks and corrosion samples before construction. The properties of each sample are as follows:

CMS V2000 Silver-Silver Chloride Electrode Monitoring

This sensor consists of silver-silver chloride electrode. It is embedded in the concrete mass along with the steel rebars to measure the potential differences between the anodic rebar and this electrode. By using Farady's law the corrosion activity could be calculated. The figure (3-14) below shows the silver-silver electrode.

Embedded Corrosion Instrument:

This type of sensors represents the most advanced generation of sensors for corrosion monitoring. This kind is able to measure the majority of corrosion parameters such as oxygen content, temperature, chloride content, humidity, and some properties as LPR. In addition to this, it is able to intergrate these parameters to find the corrosion activity and rate, and it sends this information to dataloger to gather them and give the early corrosion warning. Figure (3-15) below shows the MEP used through this reseaech. The final set up of the corrosion samples are presented in figures (3-16) and (3-17) below.

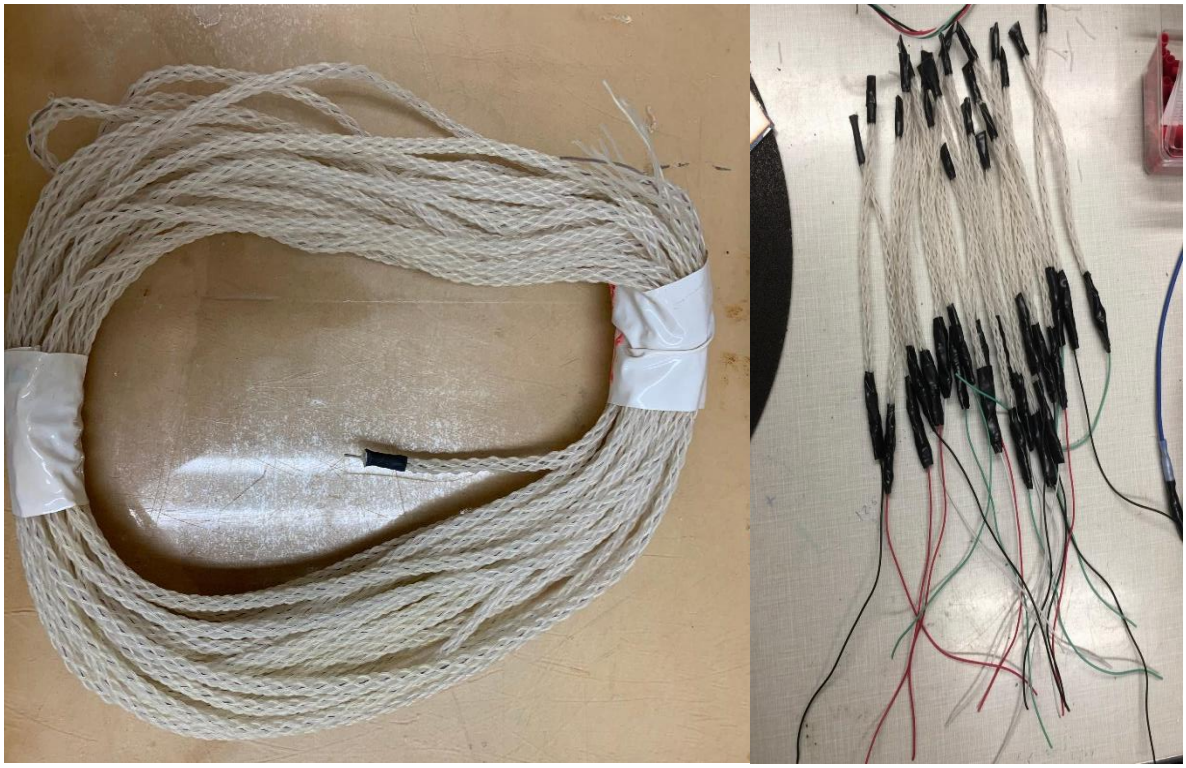

Figure 3–14 CMS V2000 Silver-Silver electrode

Figure 3–15 Advanced Corrosion Sensor, MEP

[http://www.corrosion service.com]

Figure 3–16 Set up of the prismatic corrosion samples

Figure 3–17 Set up of the corrosion slabs

4. Chapter Four

Results

4.1 General

This chapter presents the preliminary test results of the experimental work of both concrete class (A) and high performance concrete (HPC) containing black steel, Epoxy coated, stainless steel, and MMFX. The results include the mechanical properties (compressive strength, tensile strength, flexural strength, static modulus of elasticity, etc.), durability indices, and corrosion activities (potentials, currents, chloride content, correlations, etc.).

4.2 Mechanical Properties

In this chapter, the most important mechanical properties have been investigated in order to conclude the mechanical behavior of concretes. All tests were performed in accordance to their individual standards which are previously mentioned in Chapter three. Following are the results of these tests.

4.2.1 Compressive Strength

The compressive strength of concrete class (A) and high performance concrete (HPC) have been carried out in this test. The testing was done in accordance with ASTM C39 at ages of 1, 7, 14, and 28 days. Table (4-1) and Figure (4-1) below show the test results of compressive strength of all concretes.

Figure (4-1) shows clearly that the compressive strength developed with time, but the HPC has improved greatly. This improvement is due to the use of the concretes admixtures such as silica fume, fly ash, and high range water reducing admixtures. That obviously leads to increase the density of the hydration products, especially at an early age.

Table 4-1 Compressive Strength of Concretes

Age (days)	Compressive Strength (Ksi)	
	Concrete Type	
	A	HPC
1	2.77	3.7
3	3.1	4.1
7	4	5
14	4.3	7
28	4.5	8.1

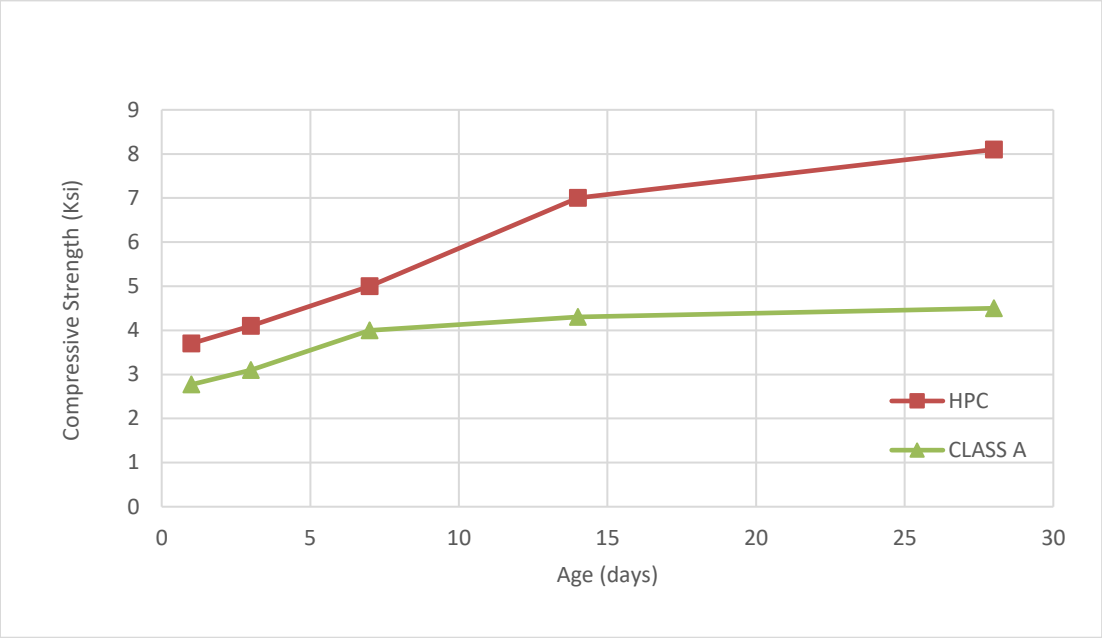

Figure 4–1 Compressive Strength of Concretes

4-2-2 Tensile Strength

The tensile test of both types of concretes, A, and HPC, was performed in accordance with ASTM C496. The testing was also done at ages of 1, 7, 14, and 28 days. Table (4-2) and figure (4-2) illustrate the results of tensile strength test. The tensile strength of HPC is higher than that of concrete class (A) at all ages. The reason for the superior behavior of HPC is related to the strong microstructure of HPC due to use of cementitious materials such as fly ash and silica fumes compared with concrete class (A).

Table 4-2 Tensile Strength of Concretes

Age (days)	Tensile Strength (psi)	
	Concrete Type	
	A	HPC
1	250	320
3	330	480
7	430	650
14	470	720
28	480	860

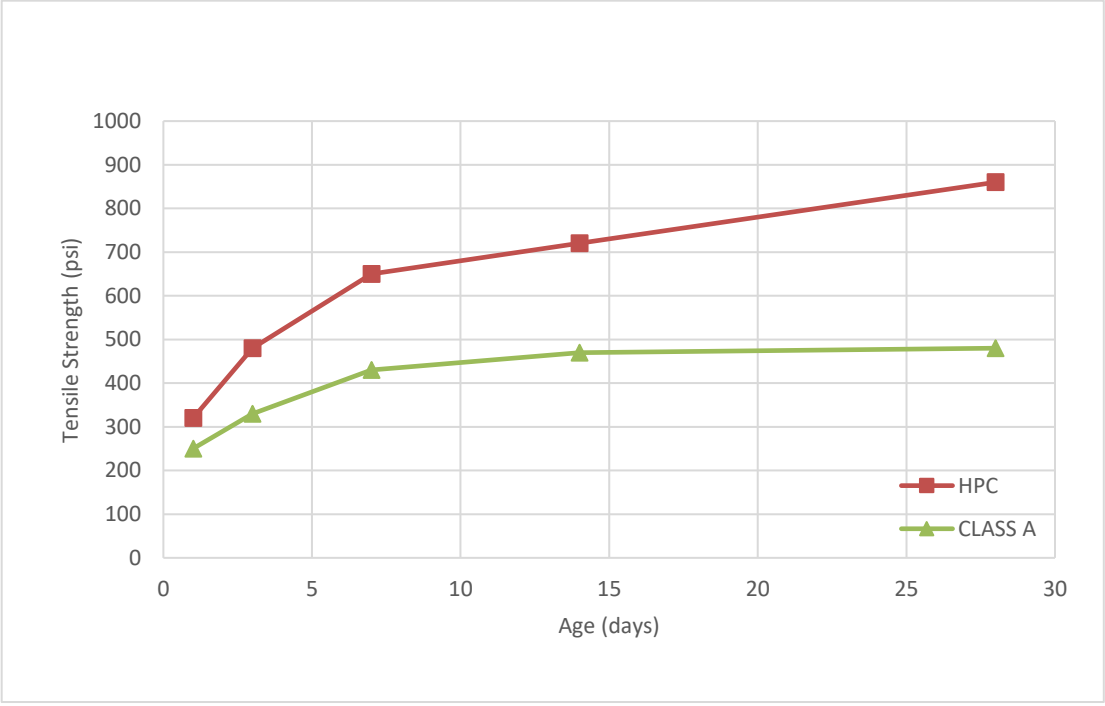

Figure 4–2 Tensile Strength of Concretes

4-2-3 Flexural Strength

The testing was done with accordance to ASTM C78 by using simple beam third-point loading. All concretes developed a noticeable flexural strength. The flexural strength increased with the age progress. The high increment ratio was of HPC as revealed in table (4-3) and figure (4-3) below.

4-2-4 Static Modulus of Elasticity

The table (4-4) and figure (4-4) below include the test results of static modulus of elasticity of all concretes. The test was made according to ASTM C617. As usual, HPC developed the higher static modulus of elasticity. It is most noticeable that the increment ration of the modulus of elasticity of HPC was 65% which is less than that of other mechanical tests.

Table 4-3 Flexural Strength of Concretes

Age (days)	Flexural strength (psi)	
	Concrete type	
	A	HPC
1	320	480
3	375	540
7	520	658
14	538	918
28	589	1060

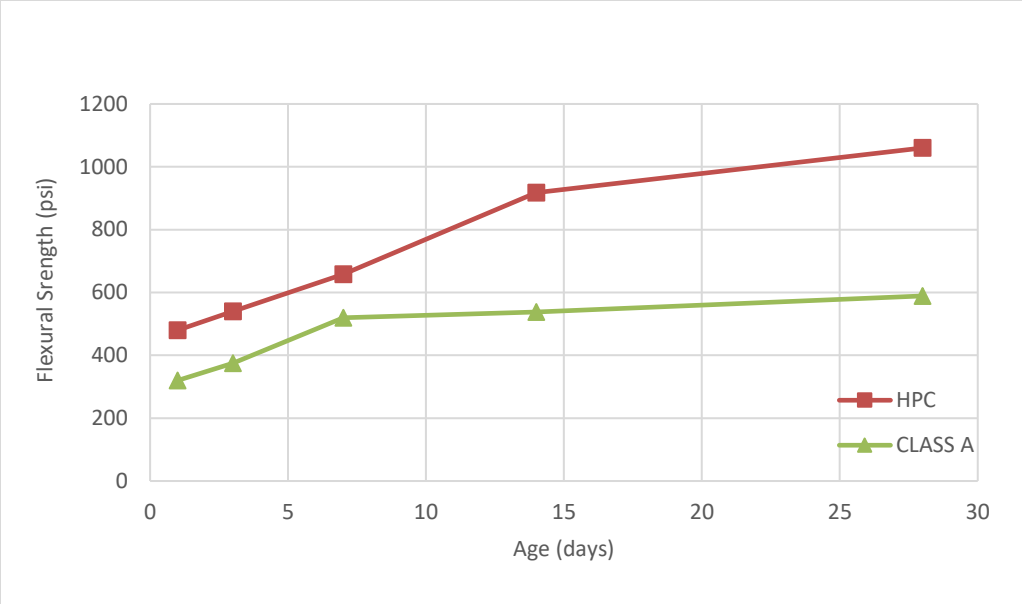

Figure 4–3 Flexural Strength of Concretes

Table 4-4 Modulus of Elasticity of Concretes

Age (days)	Modulus of Elasticity (ksi)	
	Concrete type	
	A	HPC
1	1560	2900
3	1990	3300
7	3110	4255
14	3525	6041
28	4125	6815

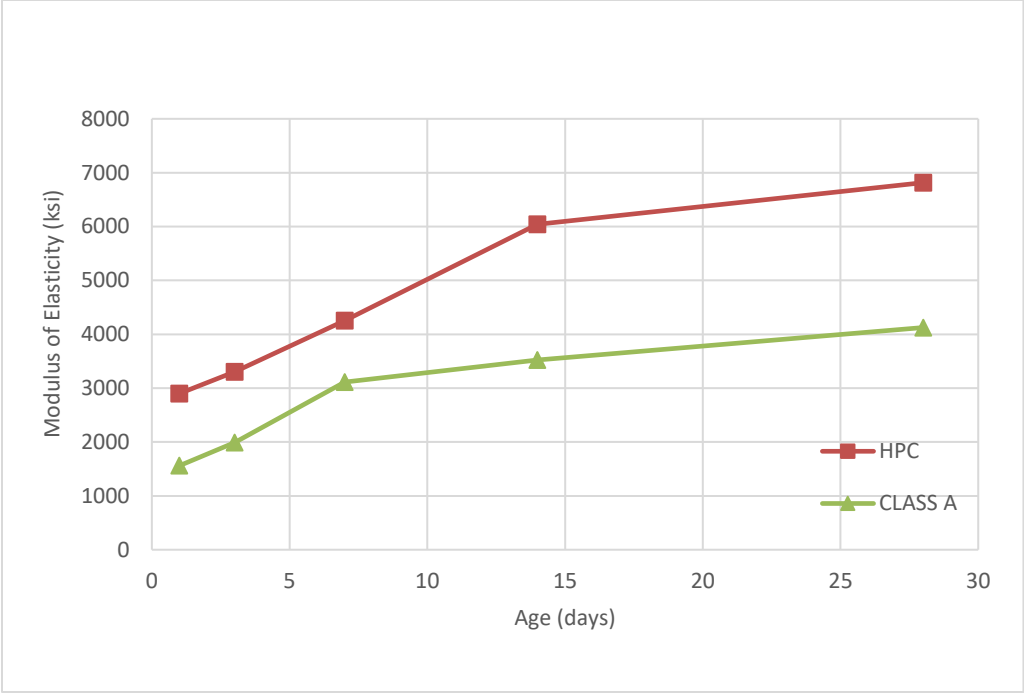

Figure 4–4 Modulus of Elasticity of Concretes

4-3 Free Shrinkage

The value of free shrinkage is presented and plotted in table (4-5) and figure (4-5). The result indicates a low free shrinkage of HPC comparing with concrete class (A), also the rate of free shrinkage decreases with the age progress. The lower ratio of free shrinkage considers a good indicator of low associated unrestrained cracks of e according to [ASTM C157].

4-4 Surface Resistivity

HPC has a superior surface resistivity compared to concrete class (A) especially at later ages. Table (4-6) and figure (4-6) illustrate that the rate of improvement is more than 1000% at age of 90 days. As mentioned earlier in chapter two, table 2-2, HPC has a very low Chloride Ion Permeability [ASTM C1202 and AASHTO T 277], according to ASTM C1202 and AASHTO T277.

Table 4-5 Free Shrinkage of Concretes

Age (days)	Free Shrinkage (µ€)	
	Concrete Type	
	A	HPC
1	0	0
3	-241	-168
7	-356	-249
28	-555	-333
60	-642	-417
90	-725	-478

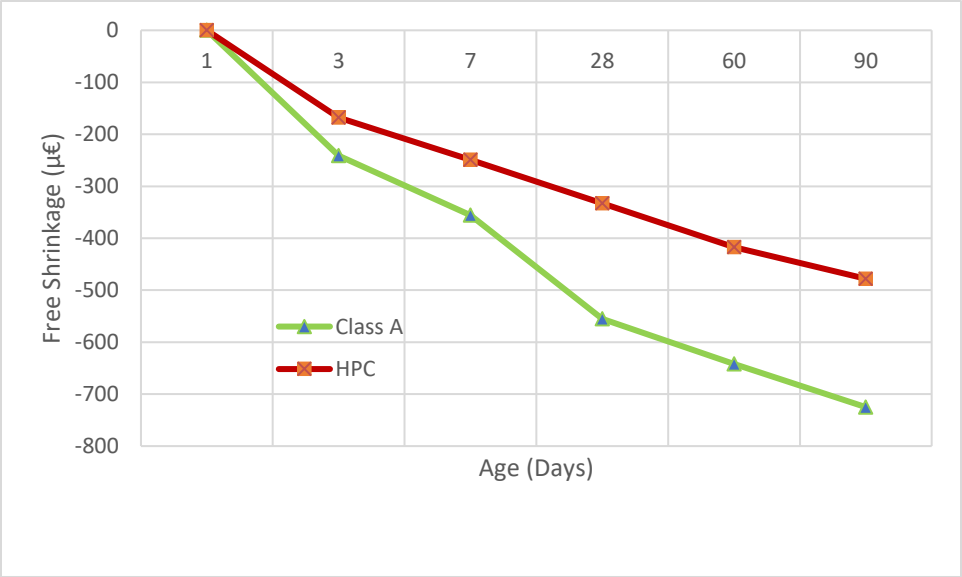

Figure 4–5 Free Shrinkage of Concretes

Table 4-6 Surface Resistivity of Concretes

Age (days)	Surface Resistivity KΩ/cm	
	Concrete Type	
	A	HPC
1	8.2	15
3	10	45
7	10.6	63
14	11.3	112
28	12.5	151
According to ASTM C1202 and AASHTO T277: If the concrete has a surface resistivity value as (37-254), this concrete considers a low chloride ion permeability concrete.		

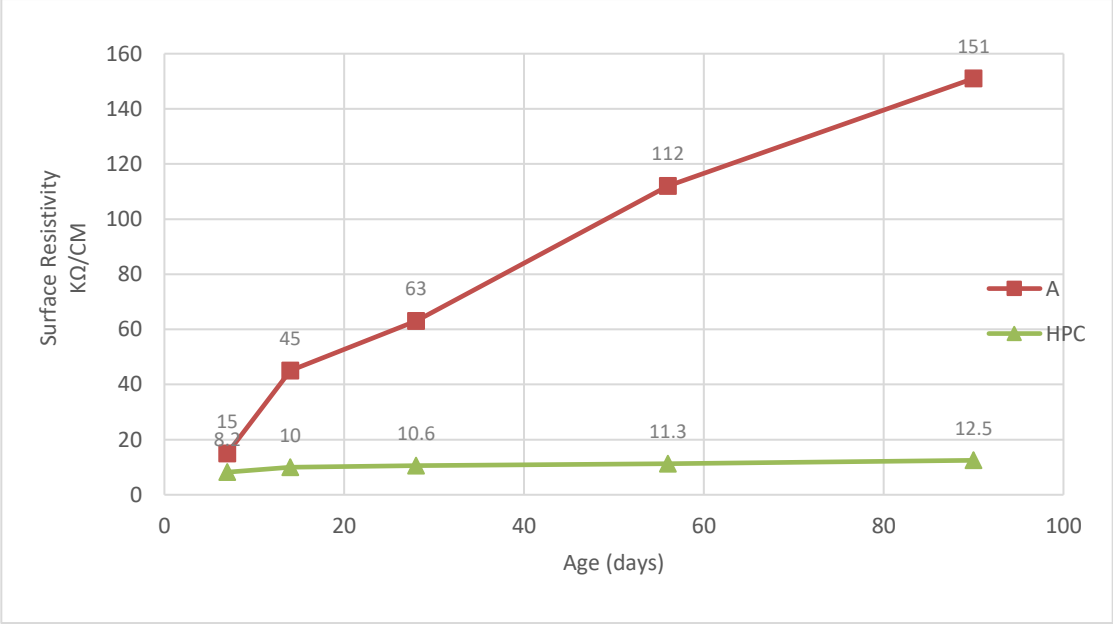

Figure 4–6 Surface Resistivity of Concretes

4-5 Rapid Chloride Permeability Test (RCPT)

Test results of RCPT listed in table (4-7) and plotted in figure (4-7) below. Obviously, HPC shows a superior durability index relating to concrete class (A). This enhancement refers to a dense concrete structure and discontinuity of micro pores within the concrete mass.

Table 4-7 Rapid Chloride Permeability Results of Concretes

Age (days)	Total Charges Columbus	
	Concrete Type	
	A	HPC
56	3615	356
90	3300	335
180	3000	330

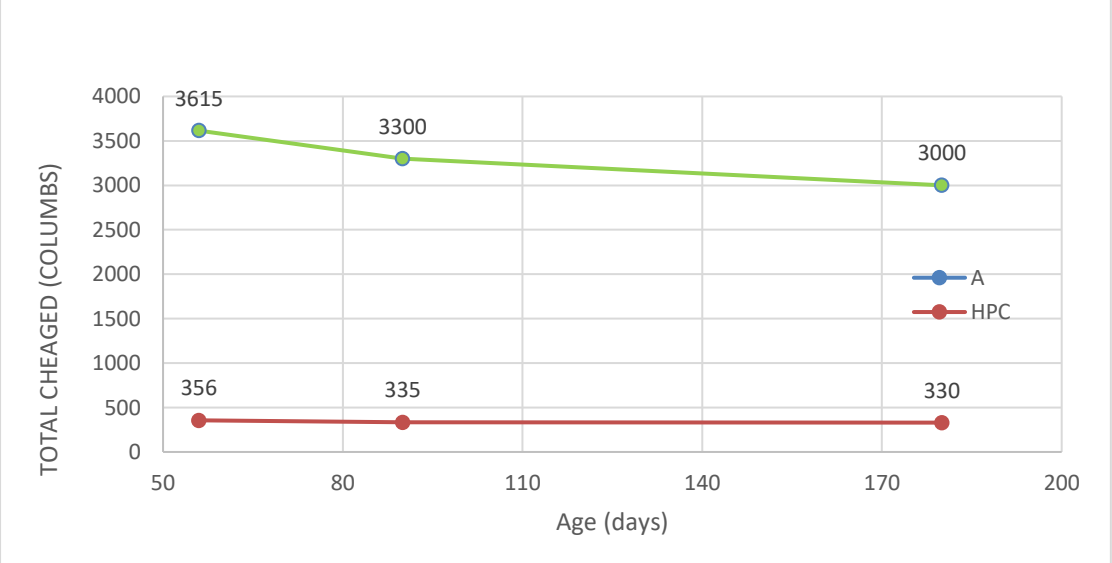

Figure 4–7 Rapid Chloride Permeability Results of Concretes

4.6 Corrosion Data

For all corrosion samples, prisms and slabs, the ASTM G109 was used to measure the corrosion activities. This test method has been used elsewhere with good agreement between corrosion and corrosion damage on the embedded steel. After casting the corrosion samples, all specimens were demolded after one day, then kept inside the curing room for 28 days. Then they were left for 14 days inside in the ambient room temperature until they sealed with epoxy sealant. Continually, the chloride solutions were placed on the plastic dams on the top surface of samples. The Sodium chloride solution was ponded for two weeks, and the corrosion measurements were taken during the second week of ponding. Finally, the chloride solution was vacuumed from the dam, and the samples were left inside the laboratory to dry for two weeks.

For all the laboratory corrosion samples, the corrosion potentials and currents, chloride content, and visual inspection were maintained to monitor the corrosion process.

4-6-1 Prismatic samples (4.5×6×11")

There are many parameters or indices used to determine the corrosion activities of different concretes and rebars, such as potentials (voltage), current, chloride content, visual examination, and so forth. The following are some corrosion tests used in this research.

4-6-1-1 Corrosion Potentials (ASTM G109 Method)

The potentials of different steel reinforcement rebars were obtained according to ASTM G-109. An average of three replicates were made for each test series. The corrosion activities were measured on a monthly basis to figure out the behavior of steel rebars under

the effect of two chloride concentrations. The results of voltages are plotted in figures (4-8) through (4-22).

4-6-1-1-1 Corrosion Potentials of Concrete Class (A)

Following are the corrosion potentials of concrete class A which containes Black Steel, Epoxy Coated, MMFX, and Stainless Steel reinforcement, cracks patterns, and chloride concentrations. All potentials are measured according to ASTM G109 in mV.

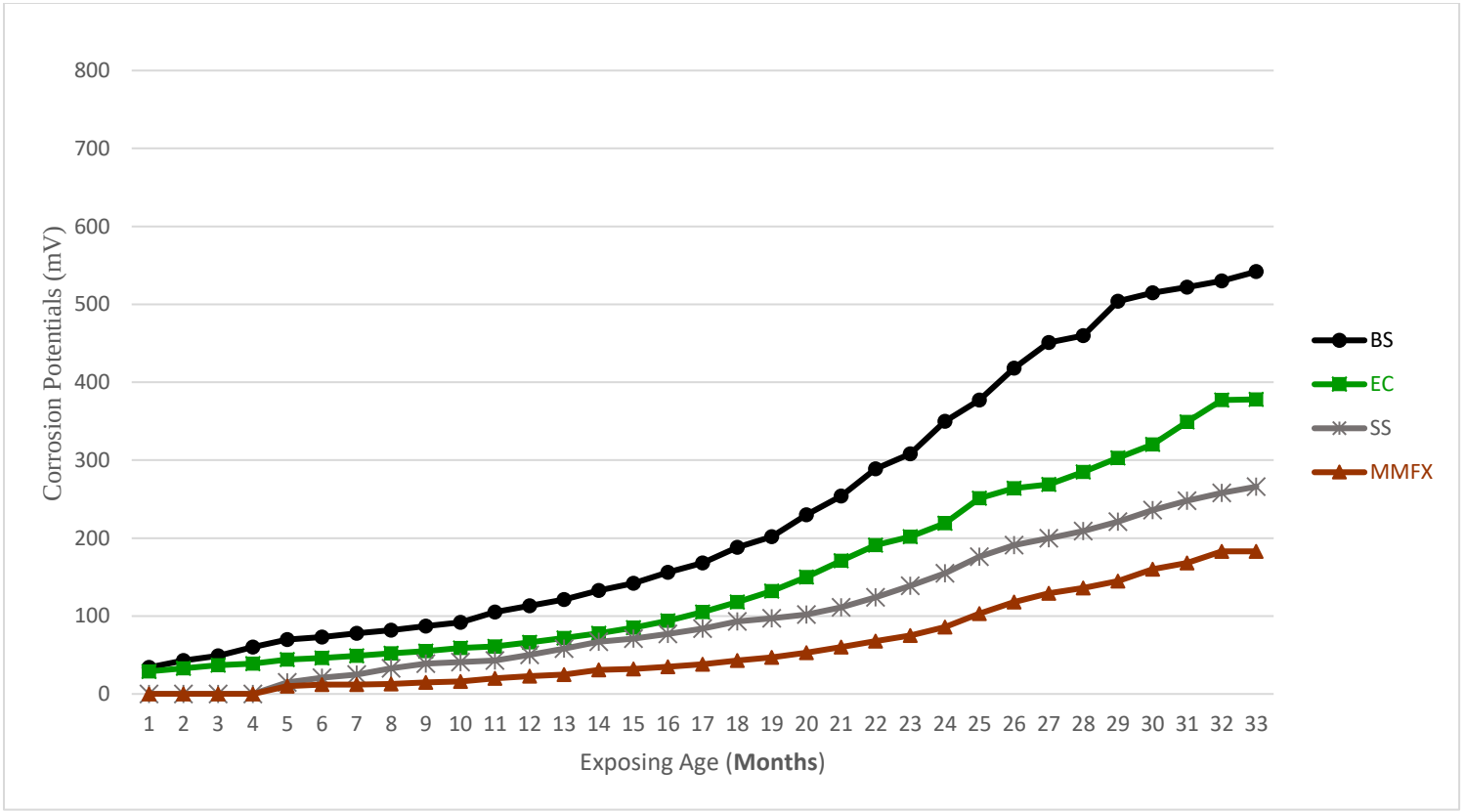

Figure 4–8 Corrosion Potentials of Un Cracked Concrete Class A Exposing to 3% Concentration of Sodium Chloride

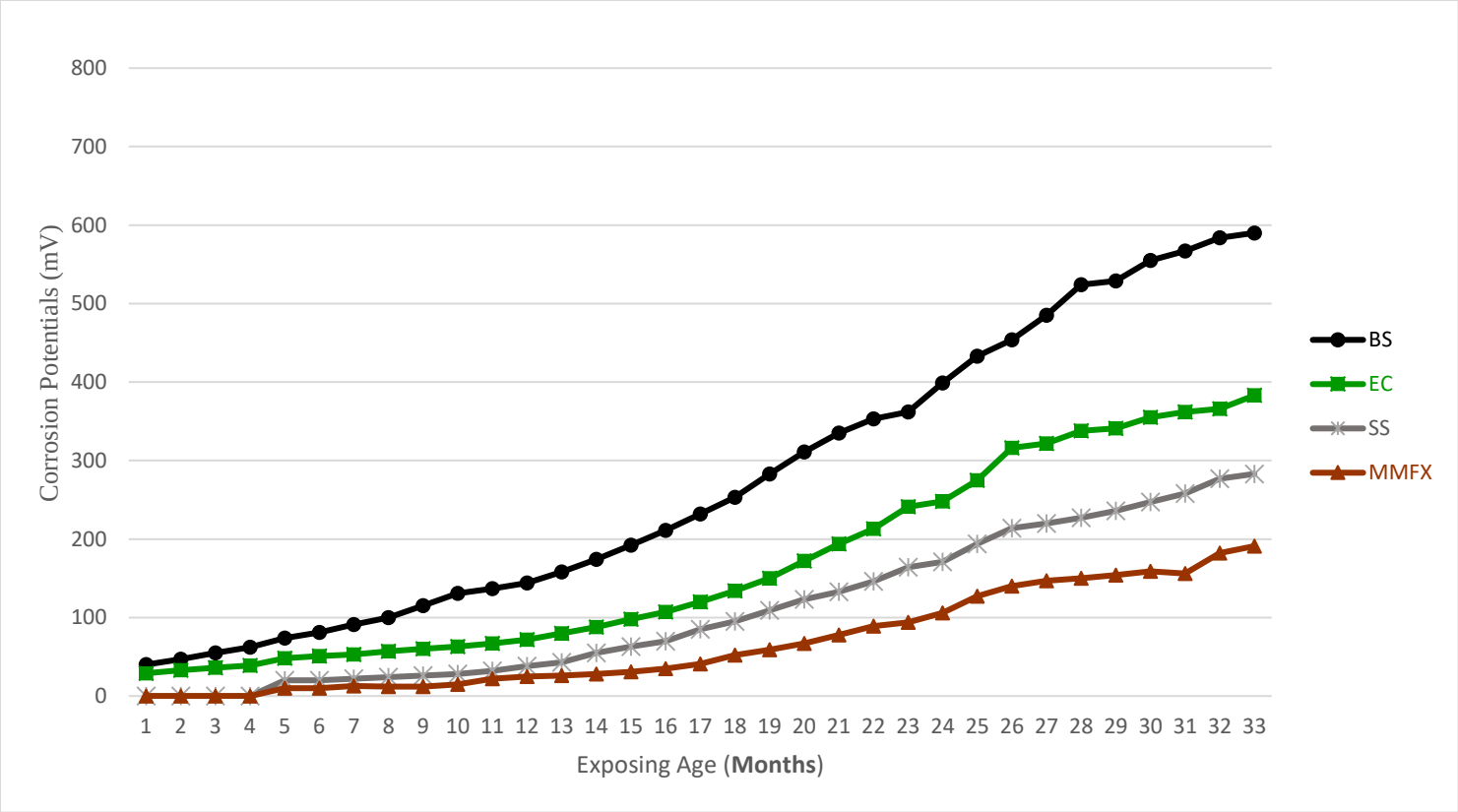

Figure 4–9 Corrosion Potentials of Cracked Concrete Class A (Crack Width=.011", Crack Depth=.5") Exposing to 3% Concentration of Sodium Chloride

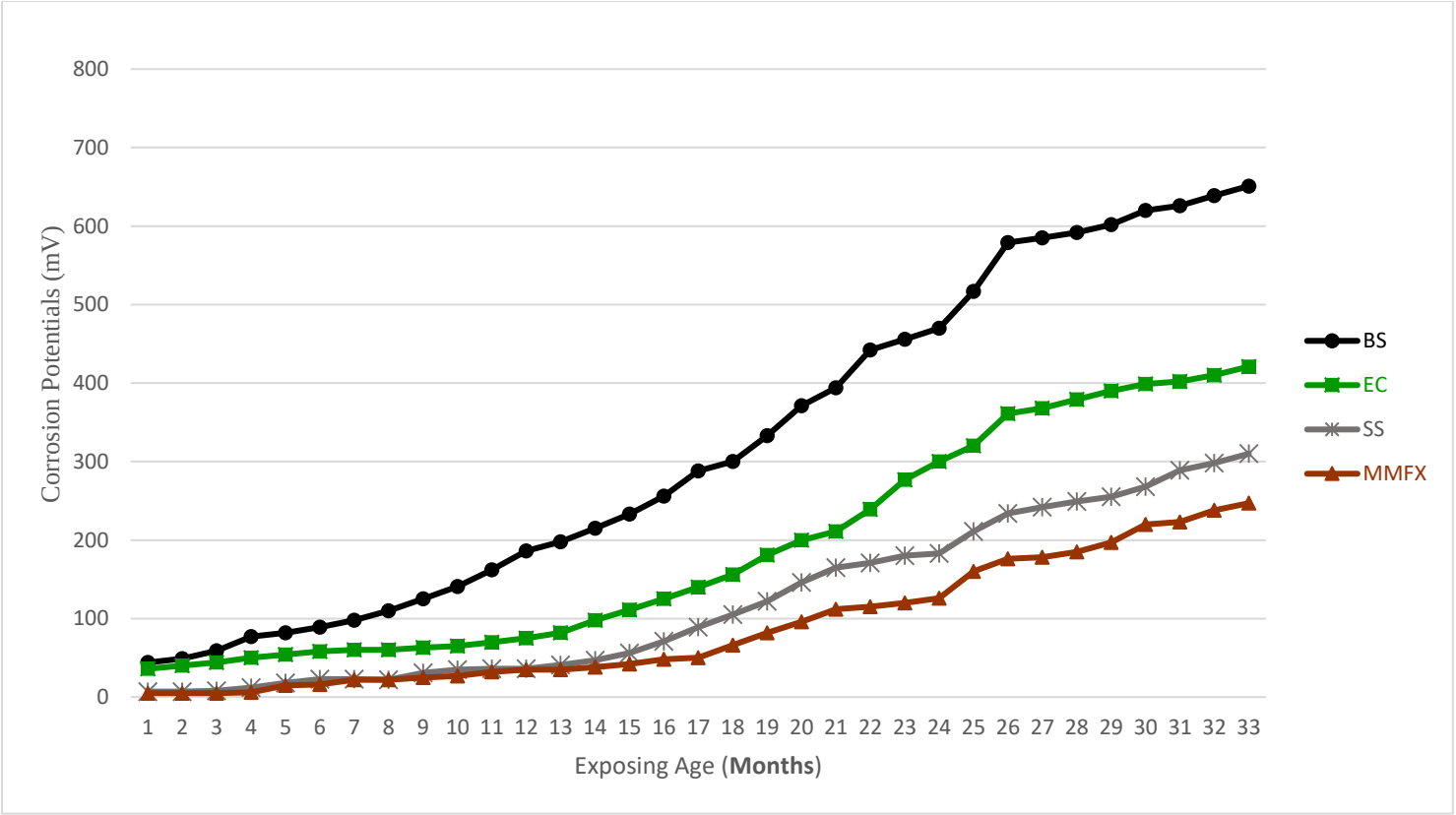

Figure 4–10 Corrosion Potentials of Cracked Concrete Class A (crack width=.011", crack depth=1") Exposing to 3% Concentration of Sodium Chloride

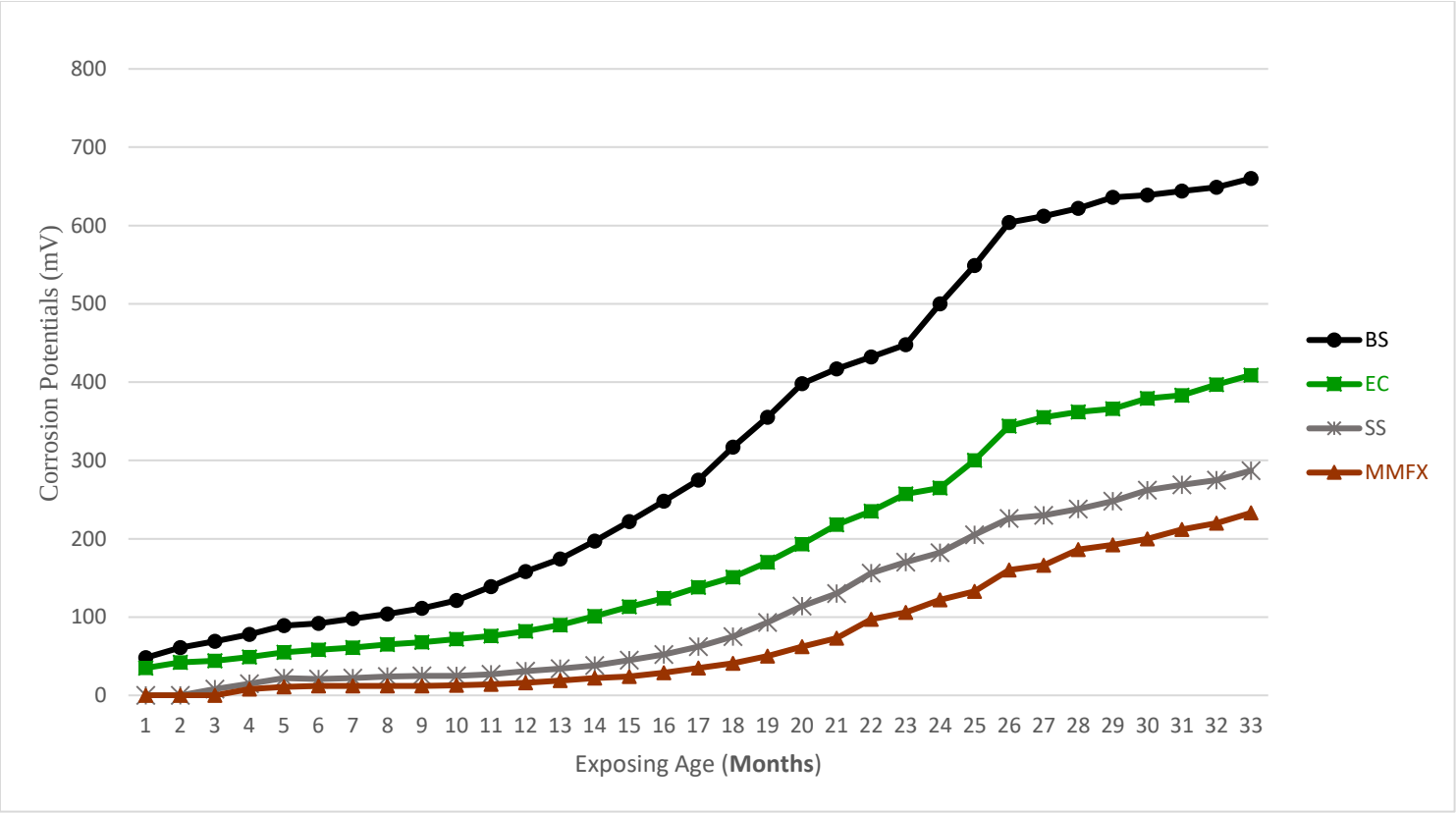

Figure 4–11 Corrosion Potentials of Cracked Concrete Class A (crack width=..035", crack depth=.5") Exposing to 3% Concentration of Sodium Chloride

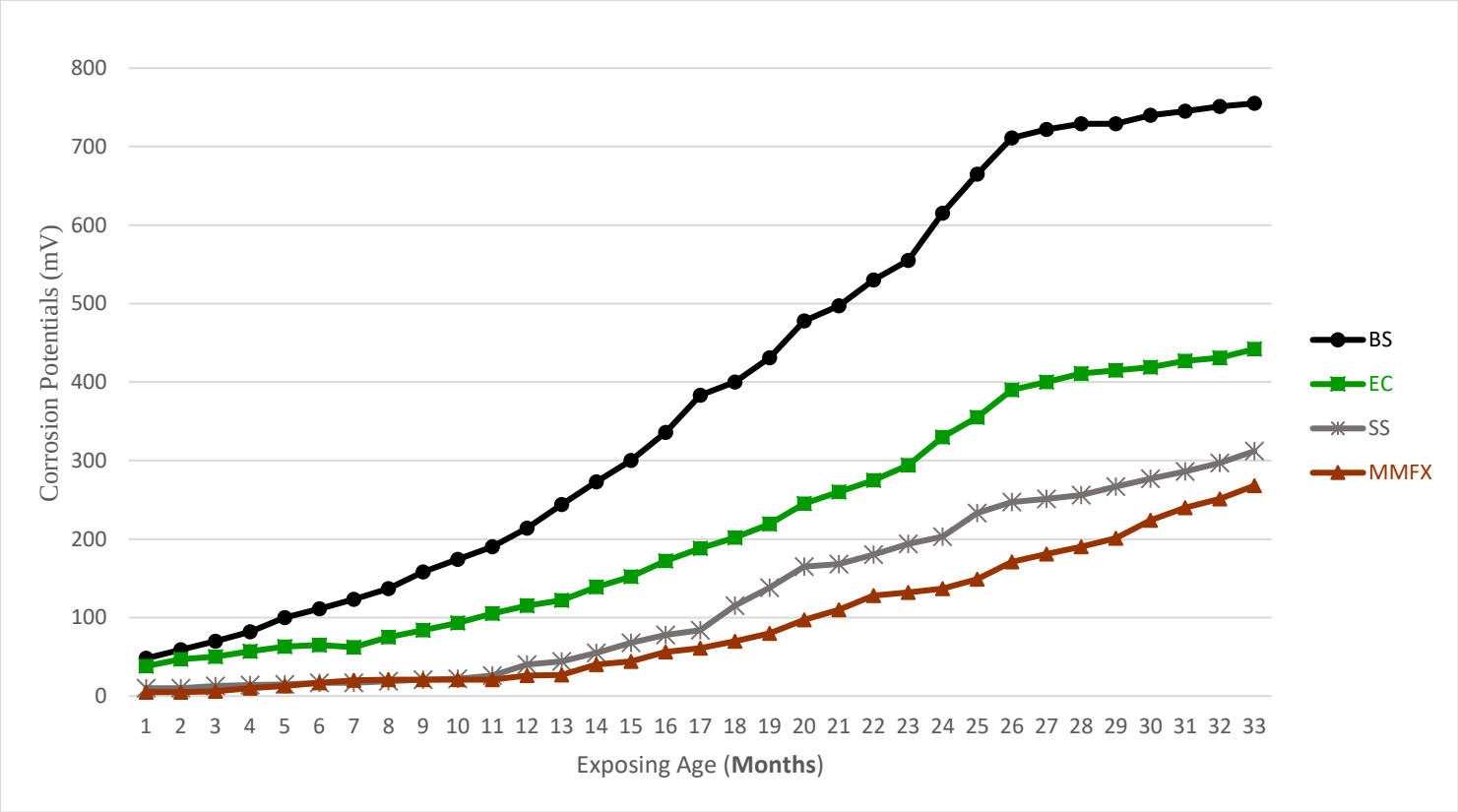

Figure 4–12 Corrosion Potentials of Cracked Concrete Class A (crack width=..035", crack depth=1") Exposing to 3% Concentration of Sodium Chloride

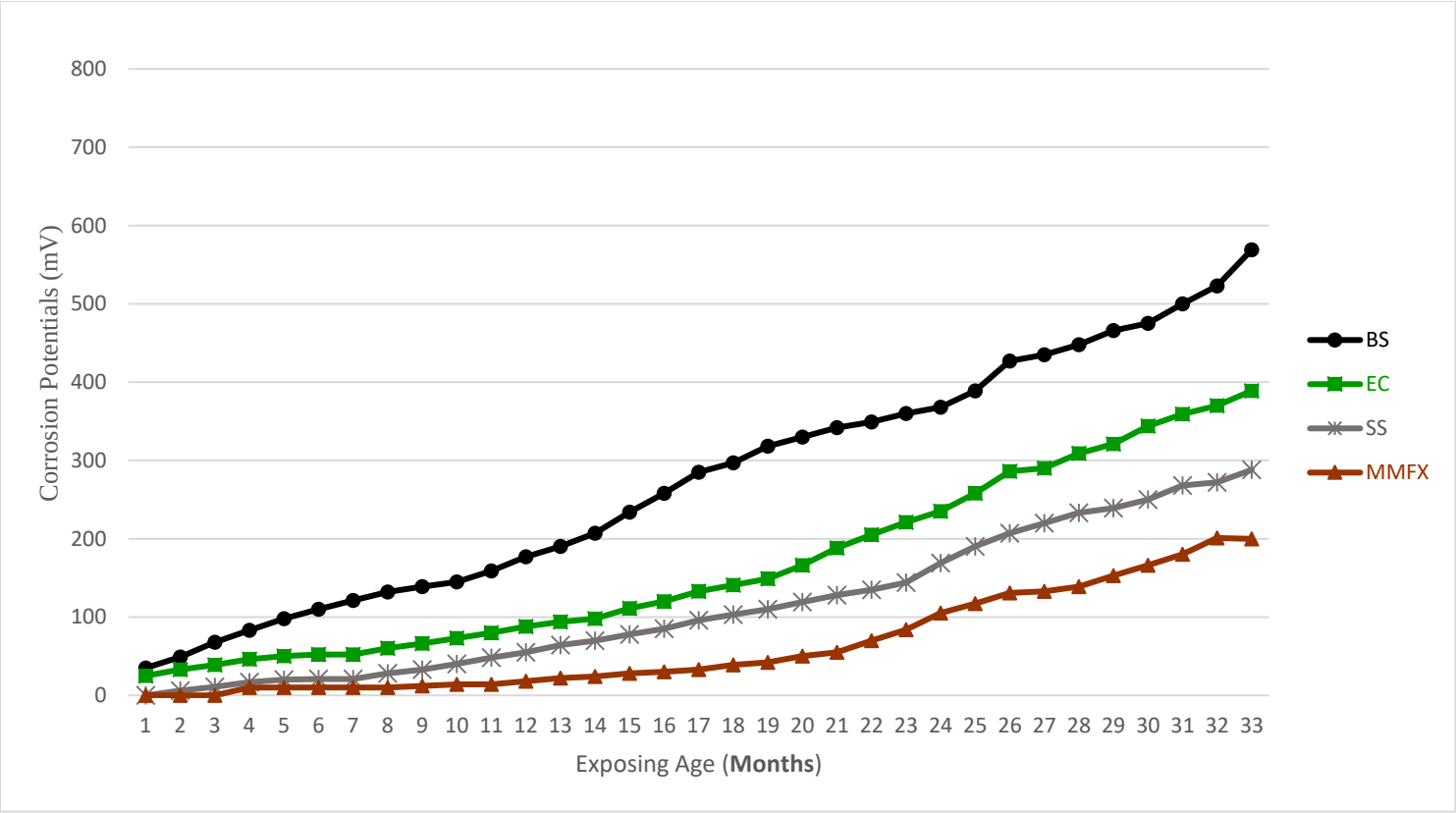

Figure 4–13 Corrosion Potentials of Un Cracked Concrete Class A Exposing to 15% Concentration of Sodium Chloride

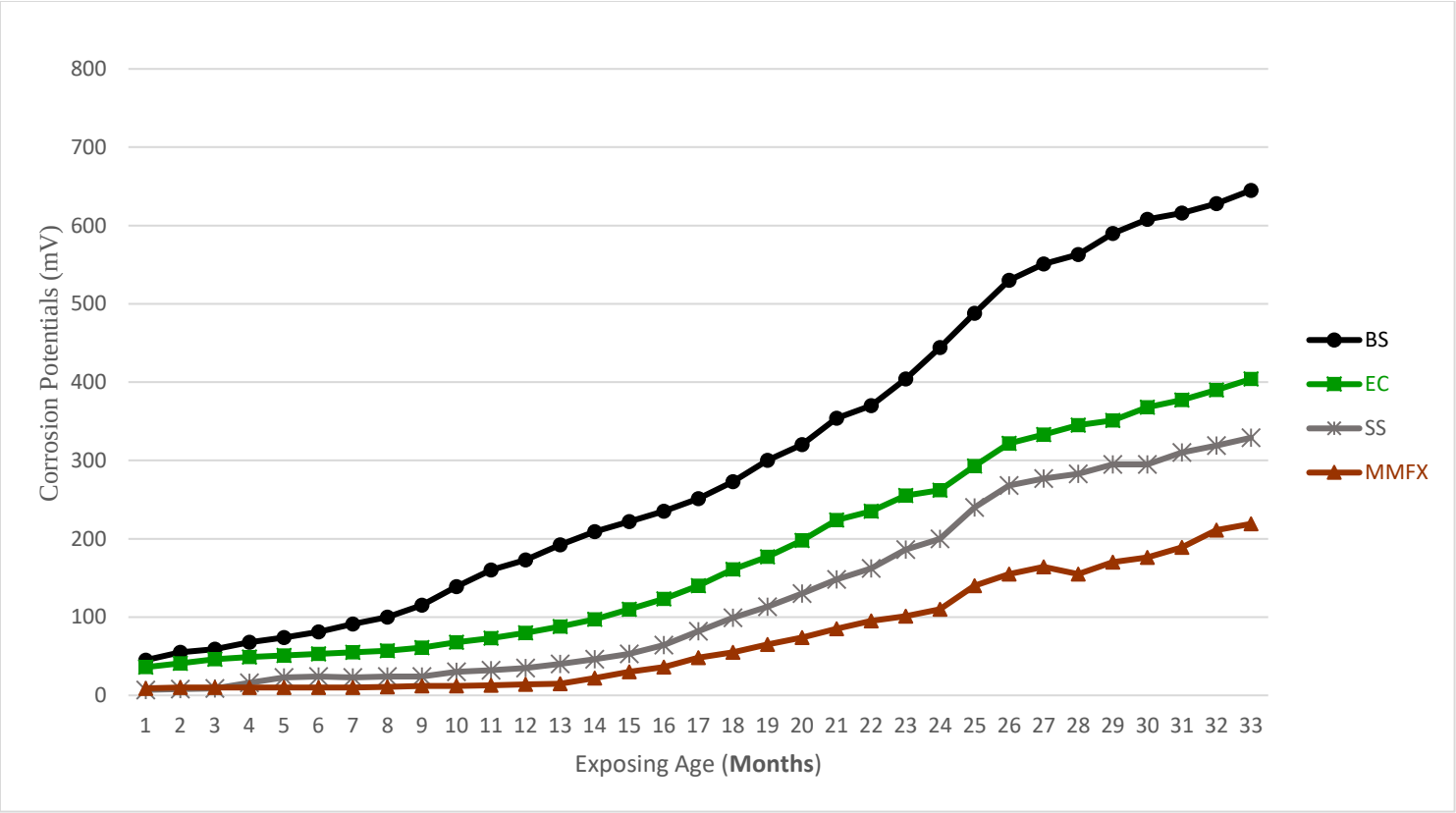

Figure 4–14 Corrosion Potentials of Cracked Concrete Class A (crack width=.011", crack depth=.5") Exposing to 15% Concentration of Sodium Chloride

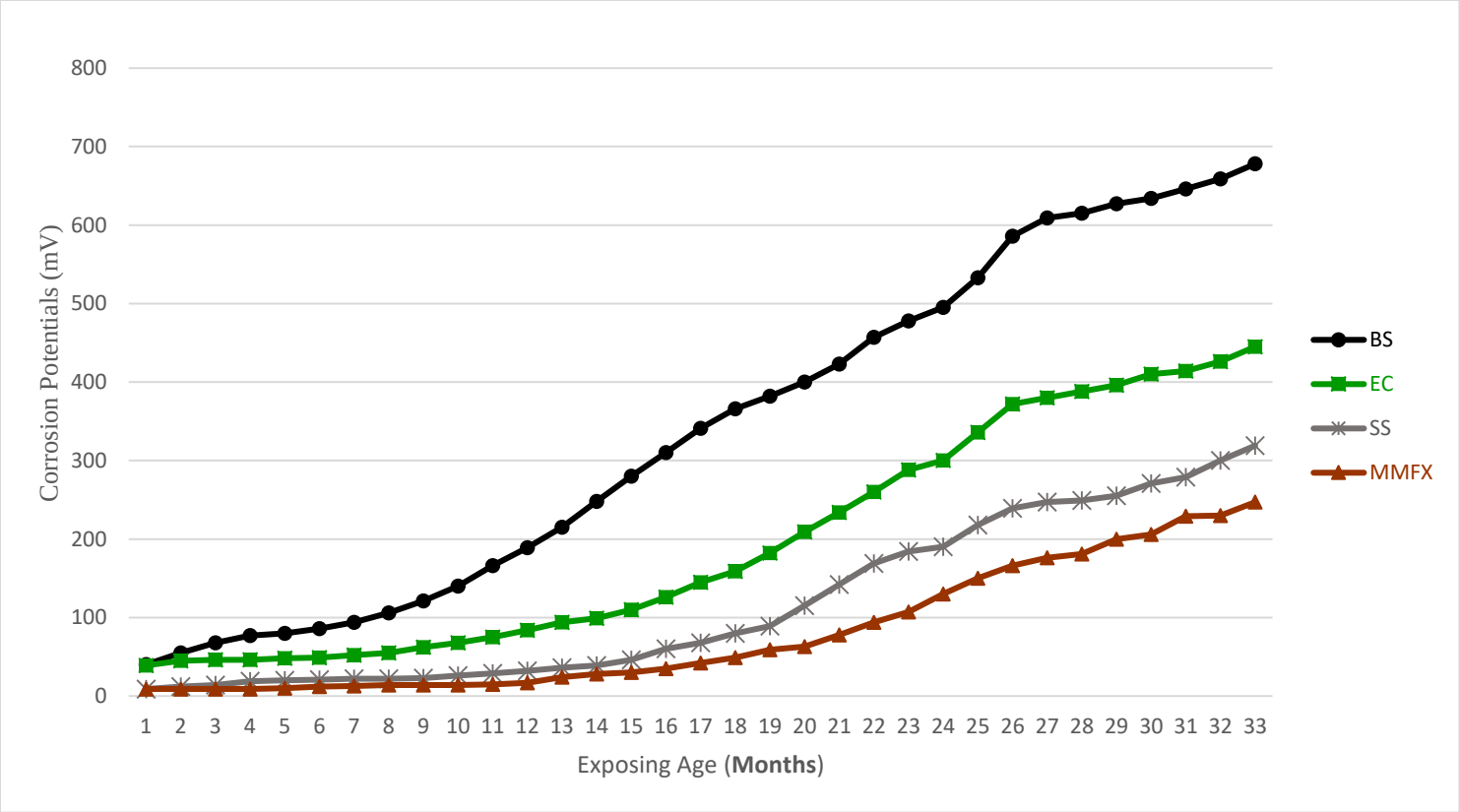

Figure 4–15 Corrosion Potentials of Cracked Concrete Class A (crack width=.011", crack depth=1") Exposing to 15% Concentration of Sodium Chloride

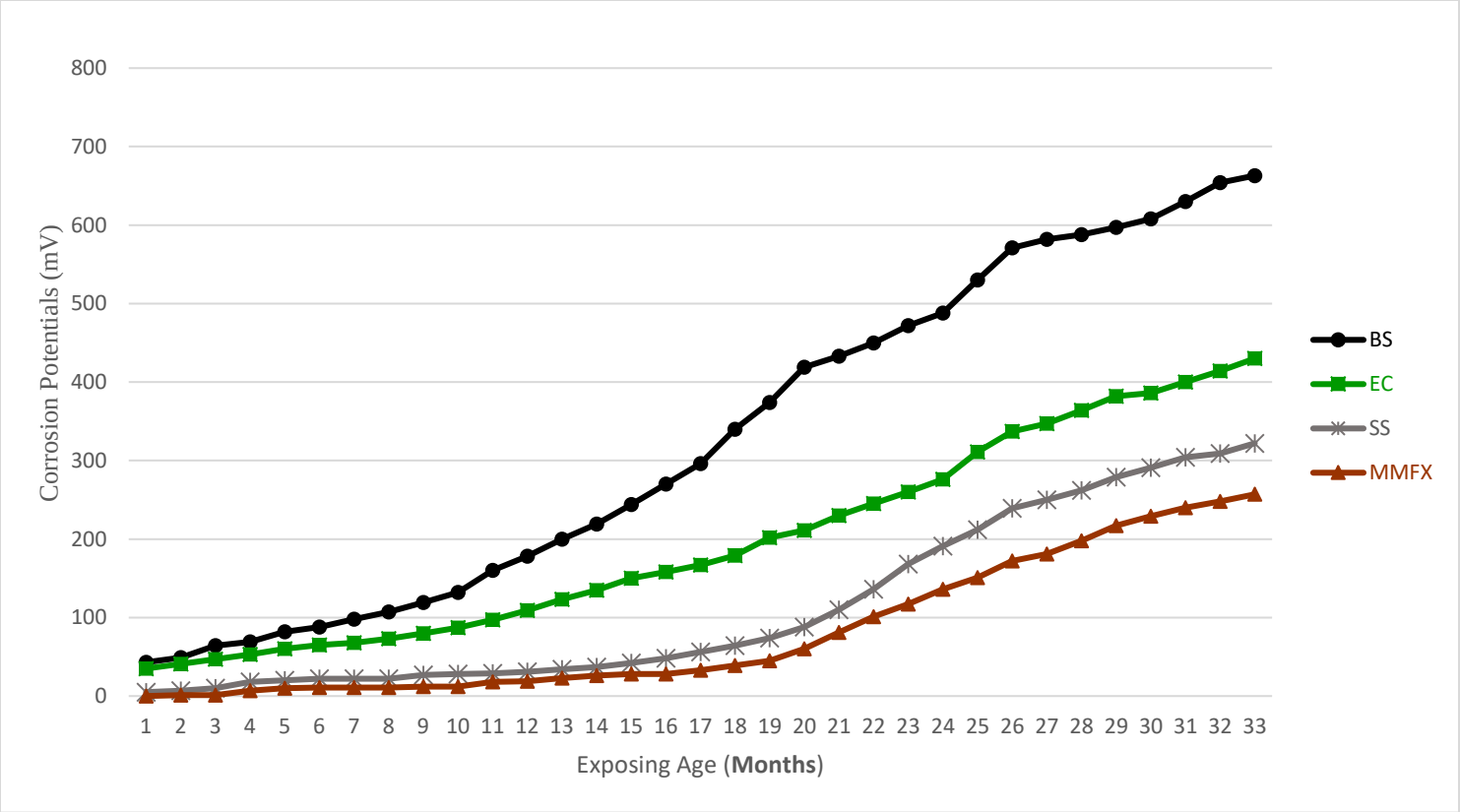

Figure 4–16 Corrosion Potentials of Cracked Concrete Class A (crack width=..035", crack depth=.5") Exposing to 15% Concentration of Sodium Chloride

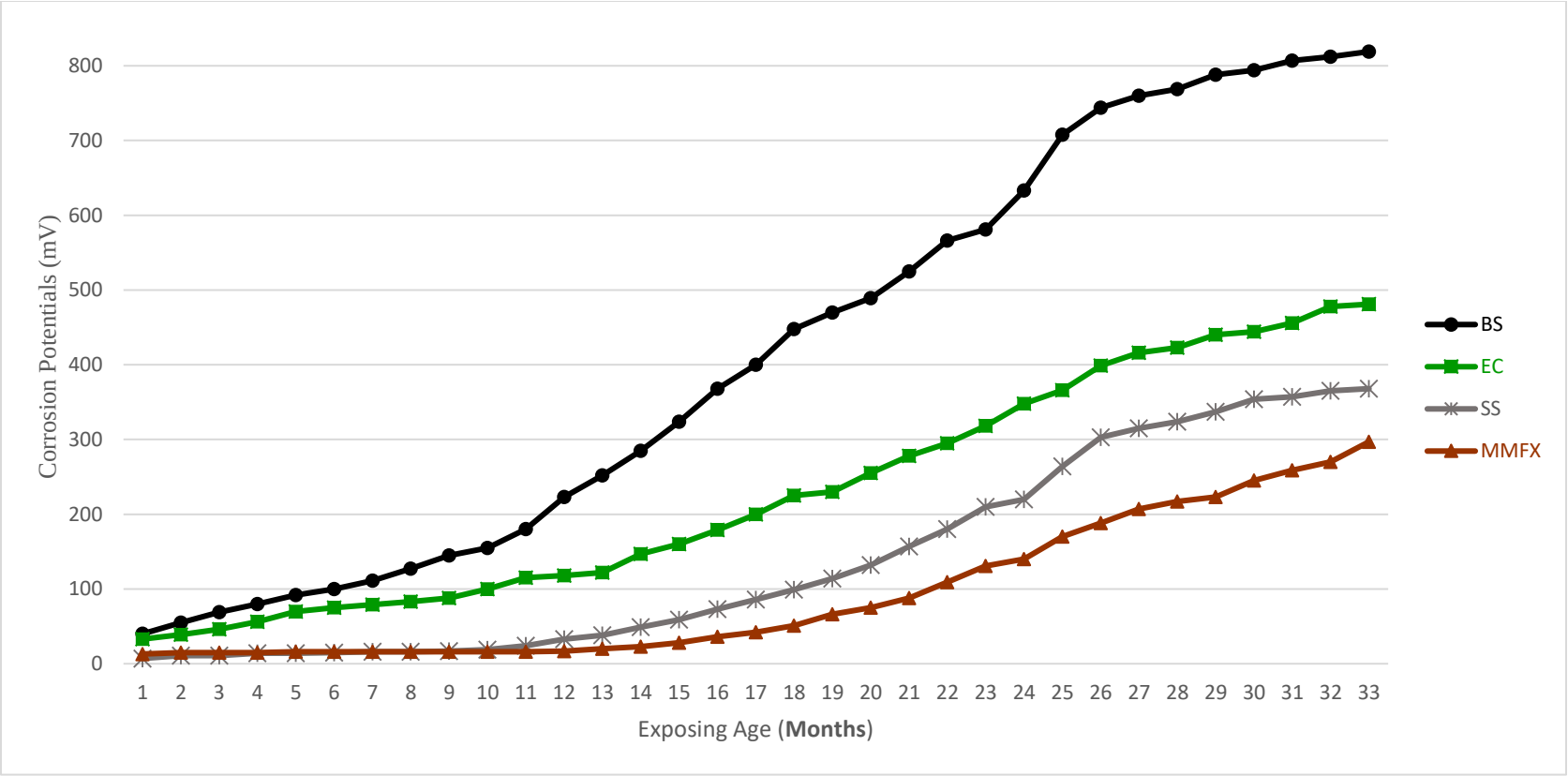

Figure 4–17 Corrosion Potentials of Cracked Concrete Class A (crack width=..035", crack depth=1") Exposing to 15% Concentration of Sodium Chloride

4-6-1-1-2 Corrosion Potentials of High Performance Concrete (HPC)

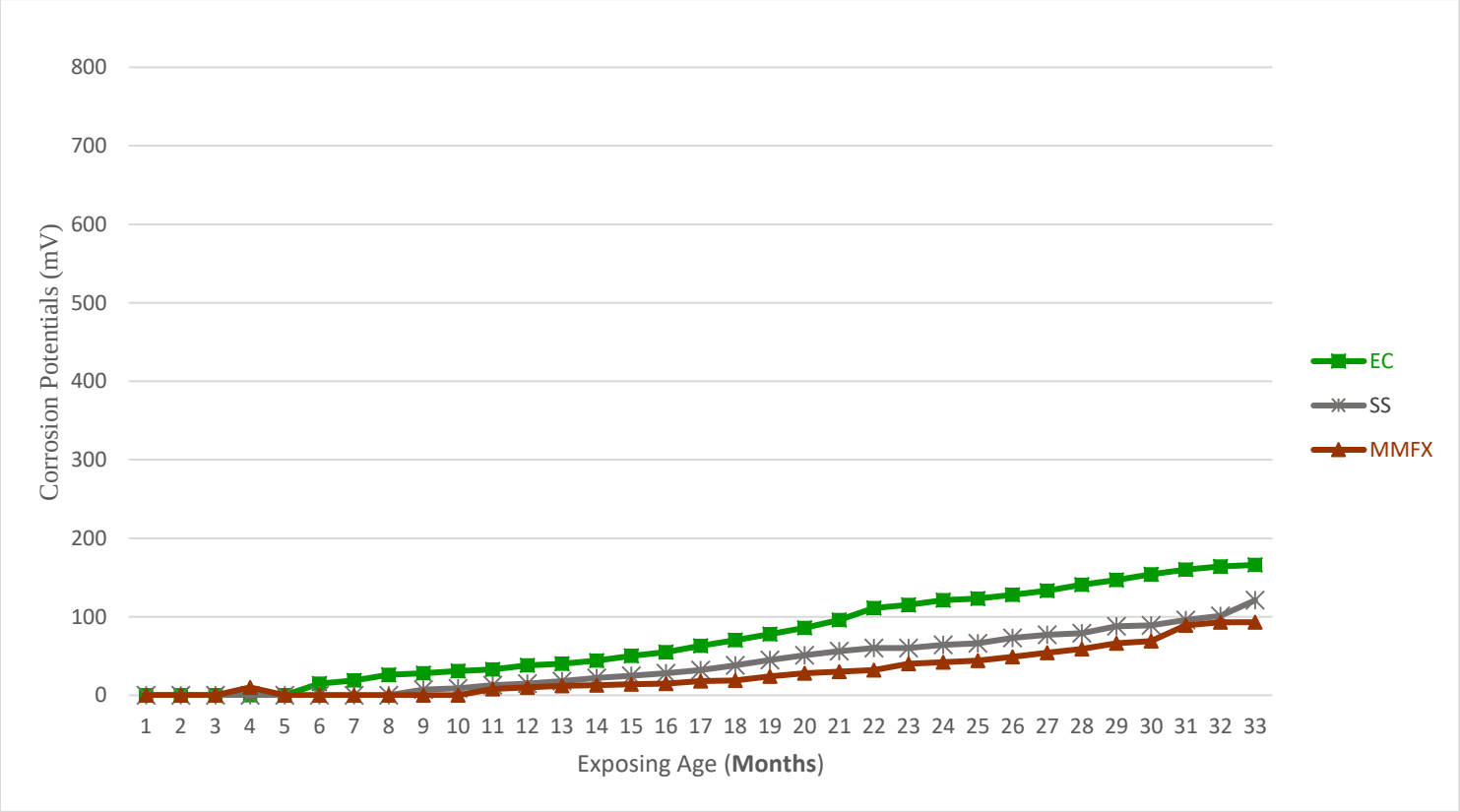

Figure 4–18 Corrosion Potentials of Un Cracked HPC Exposing to 15% Concentration of Sodium Chloride

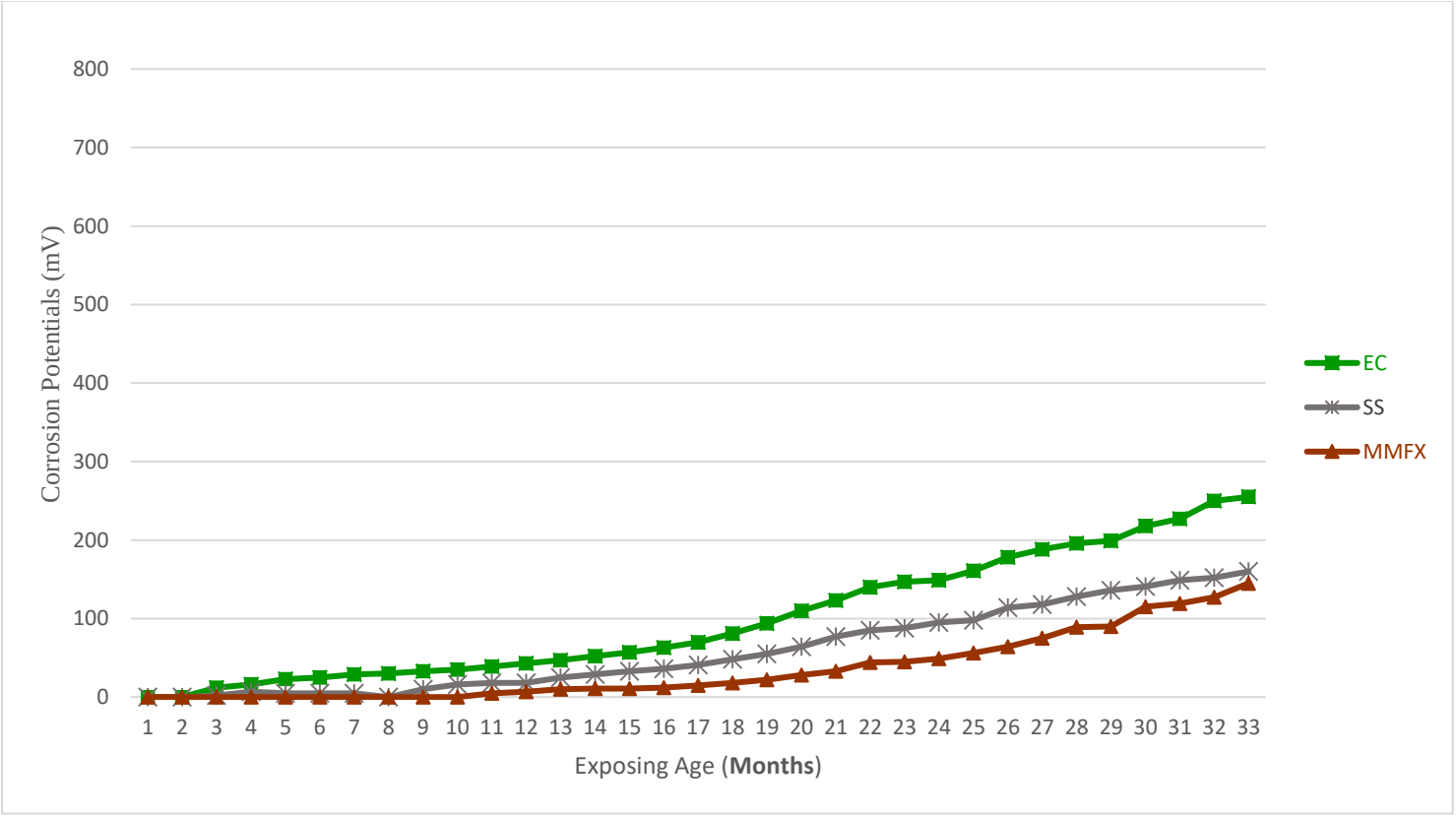

Figure 4–19 Corrosion Potentials of Cracked HPC (crack width=.011", crack depth=.5”) Exposing to 15% Concentration of NaCl

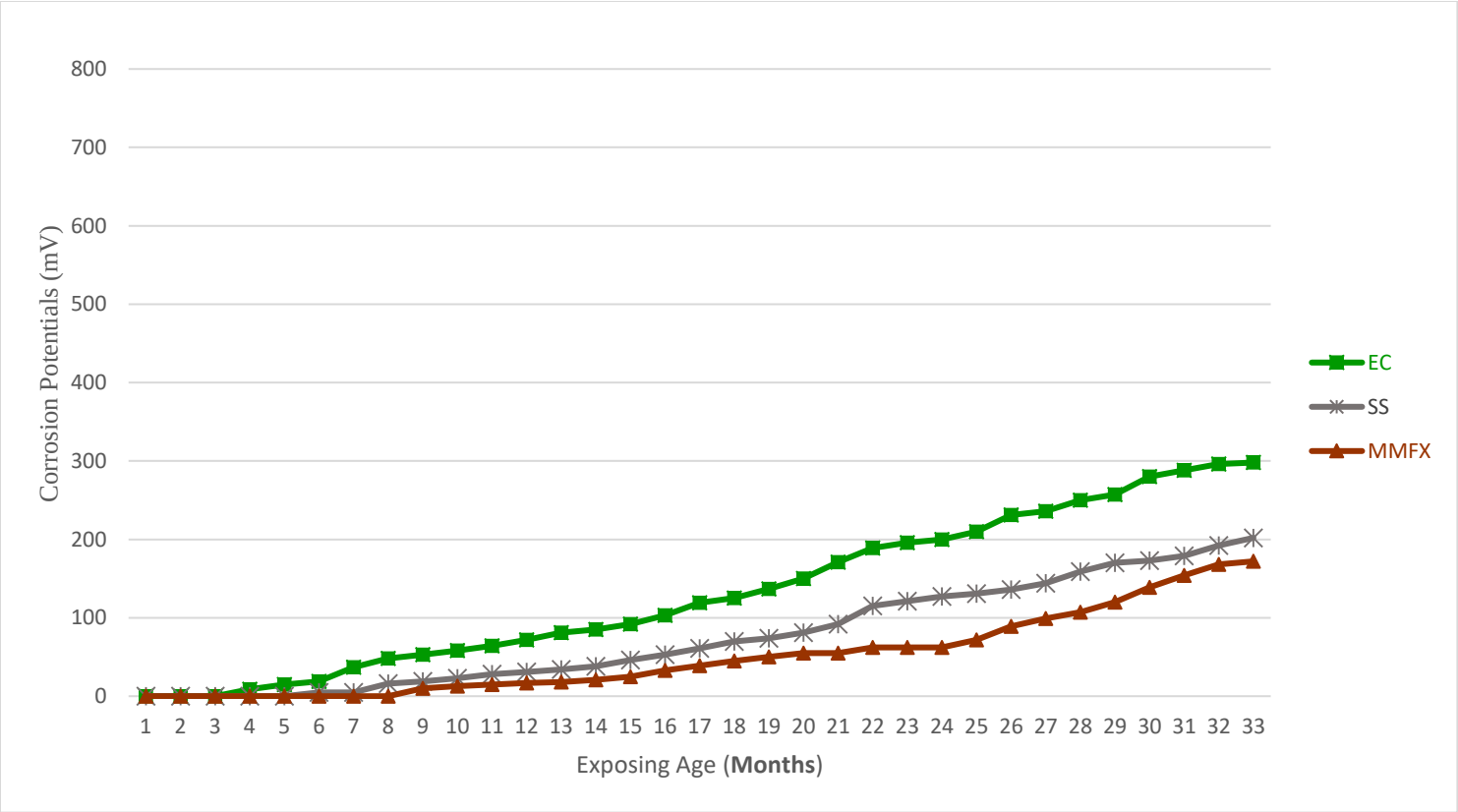

Figure 4–20 Corrosion Potentials of Cracked HPC (crack width=.011", crack depth=1") Exposing to 15% Concentration of NaCl

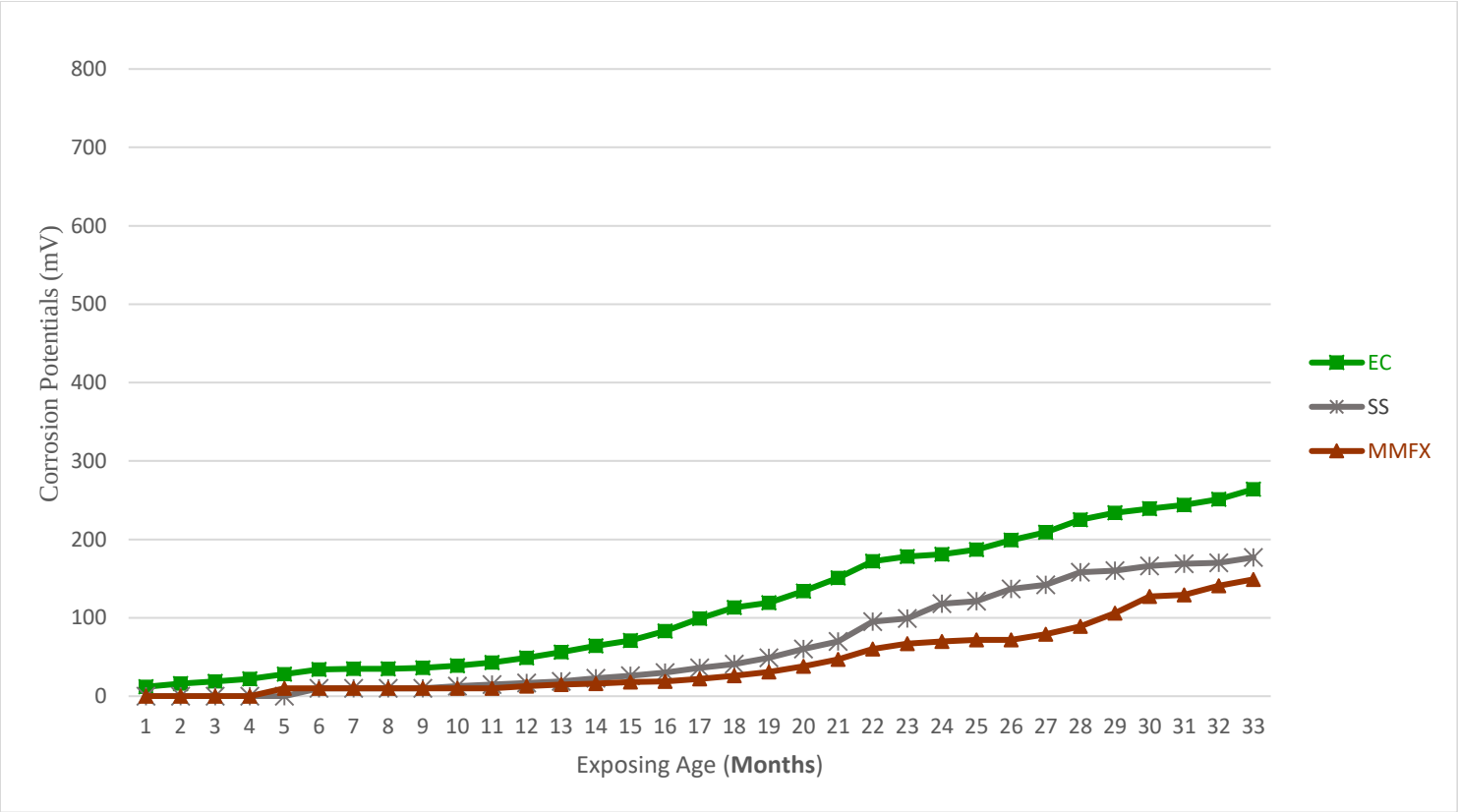

Figure 4–21 Corrosion Potentials of Cracked HPC (crack width=.035", crack depth=.5") Exposing to 15% Concentration of NaCl

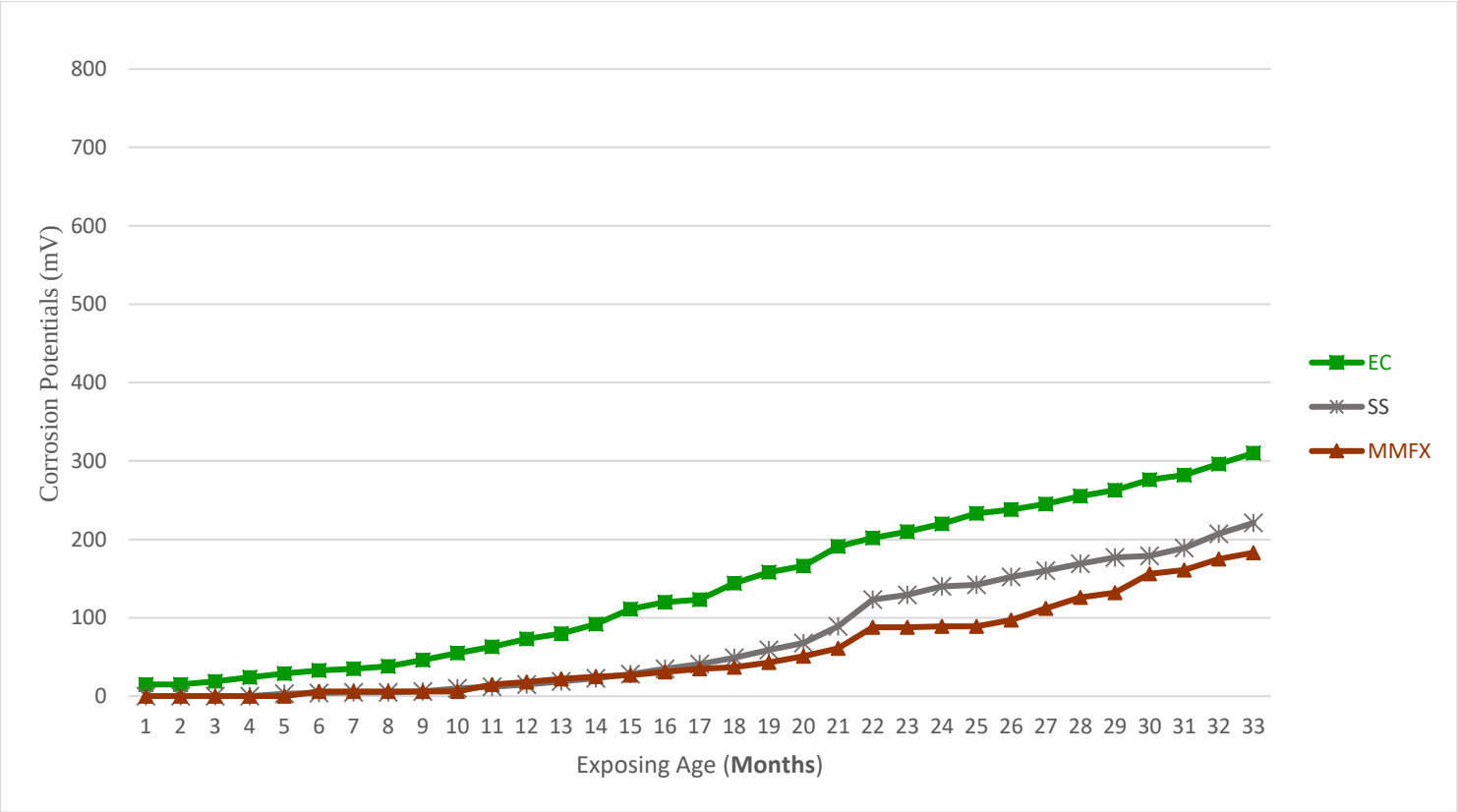

Figure 4–22 Corrosion Potentials of Cracked HPC (crack width=.035", crack depth=1") Exposing to 15% Concentration NaCl

Figure (4-22)

4-6-1-2 Corrosion Currents

4-6-1-2-1 Corrosion Currents of Concrete Class (A)

The corrosion currents of concrete class A and high performance concrete (HPC) presented figures (4-23) through (4-37). The value of the current in mA and measured according to ASTM G109.

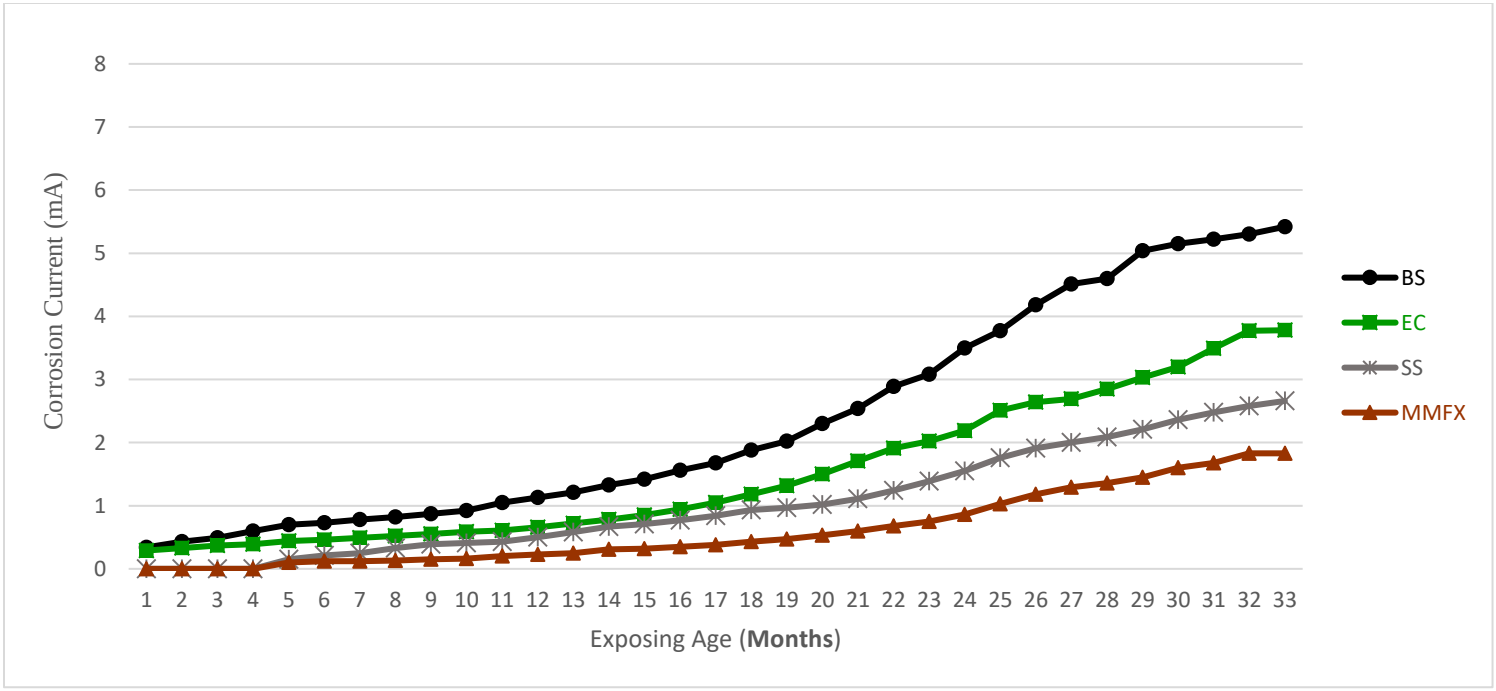

Figure 4–23 Corrosion Currents of Un Cracked Concrete Class A Exposing to 3% Concentration of Sodium Chloride

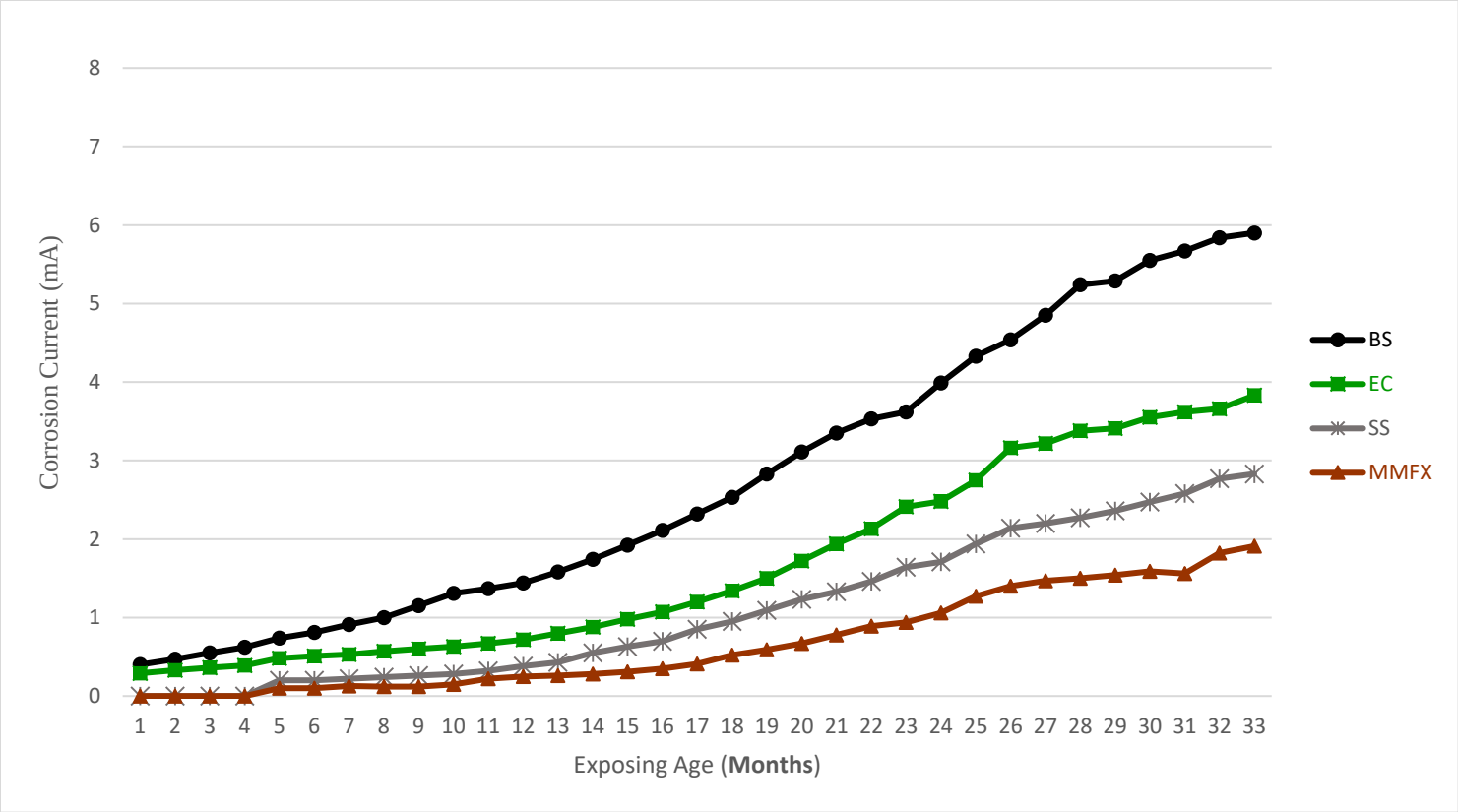

Figure 4–24) Corrosion Currents of Cracked Concrete Class A (crack width=.011", crack depth=.5") Exposing to 3% Concentration of Sodium Chloride

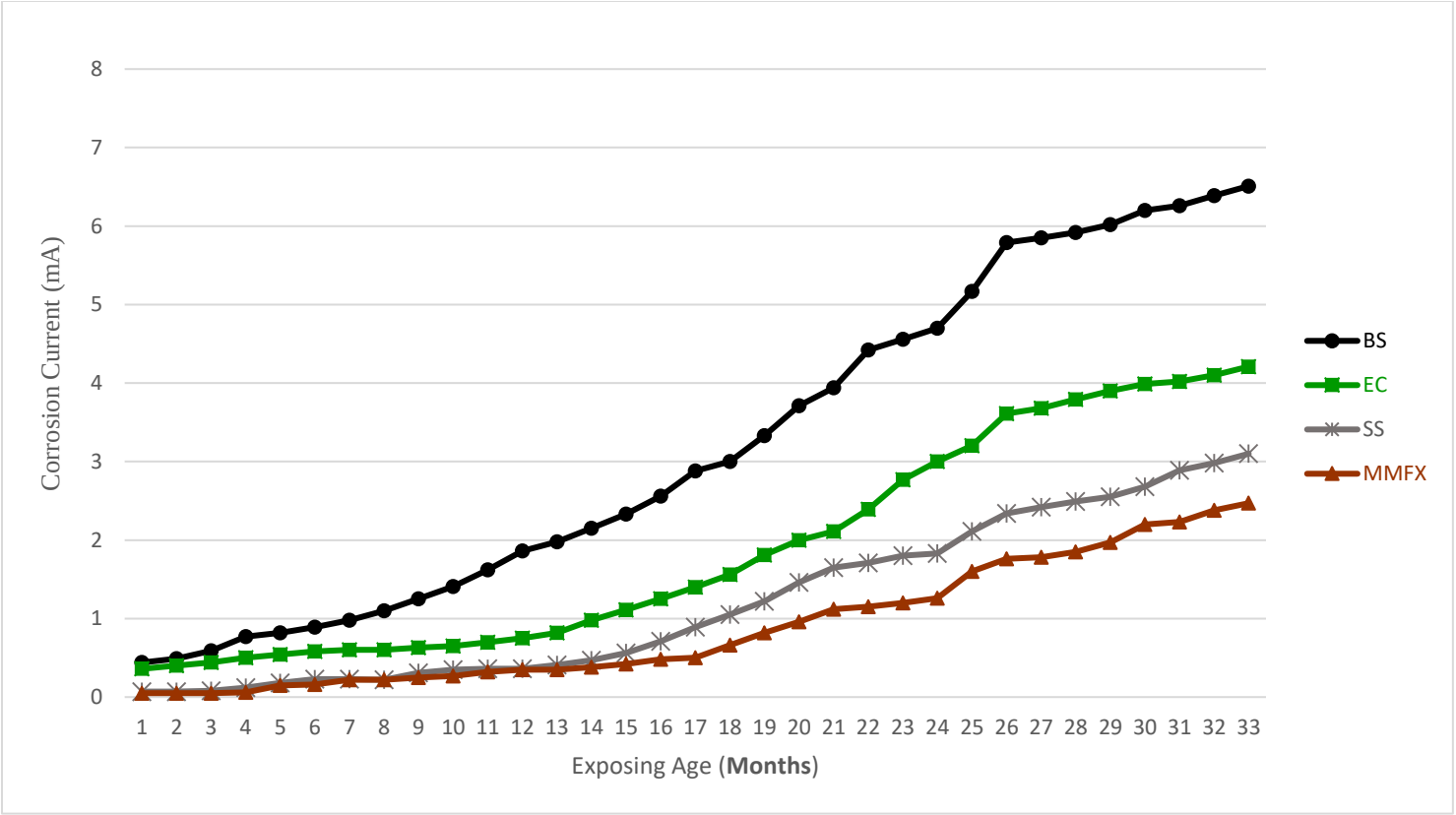

Figure 4–25 Corrosion Currents of Cracked Concrete Class A (crack width=.011", crack depth=1") Exposing to 3% Concentration of Sodium Chloride

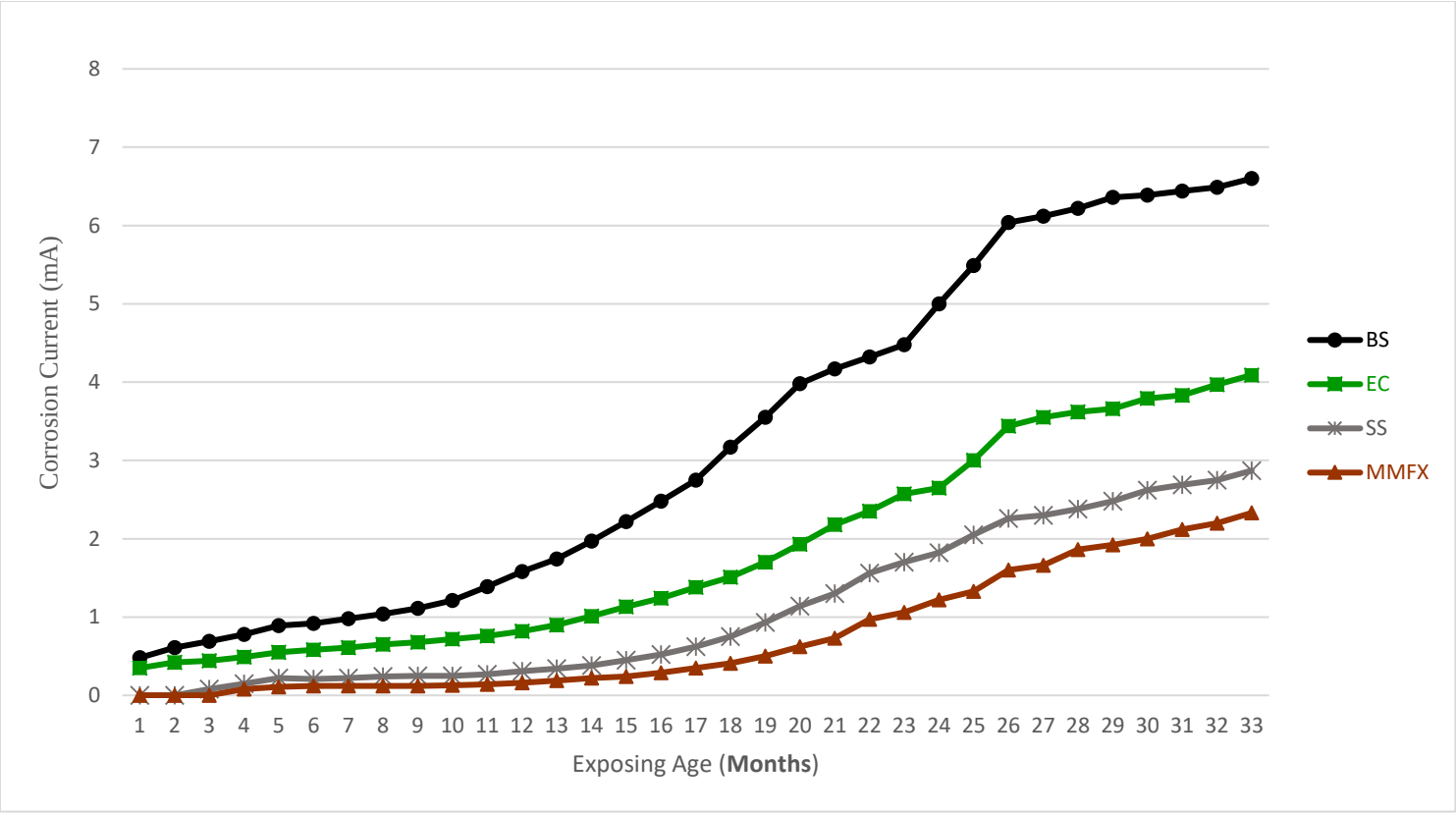

Figure 4–26 Corrosion Currents of Cracked Concrete Class A (crack width=..035", crack depth=.5") Exposing to 3% Concentration of Sodium Chloride

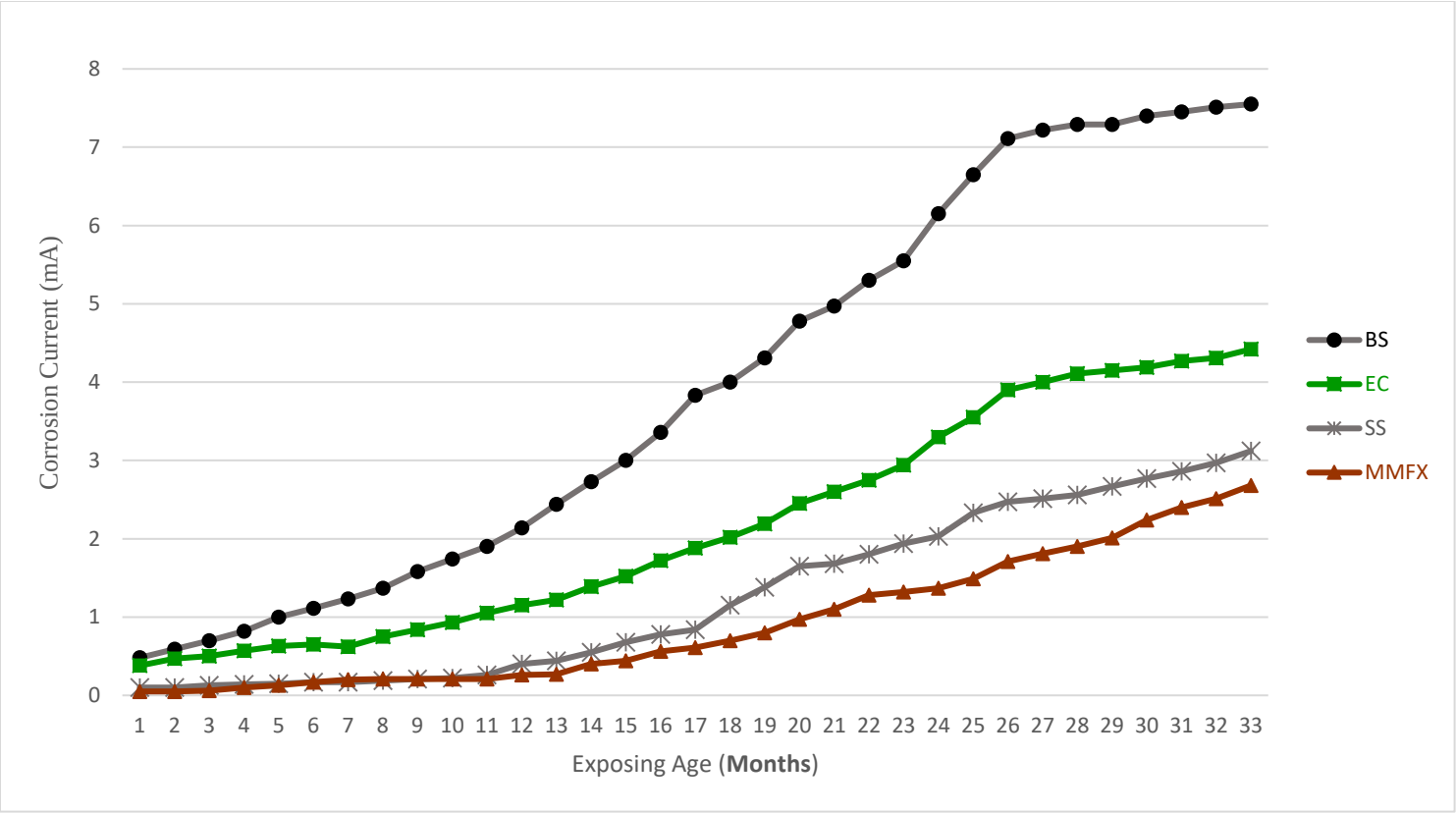

Figure 4–27 Corrosion Currents of Cracked Concrete Class A (crack width=..035", crack depth=1") Exposing to 3% Concentration of Sodium Chloride

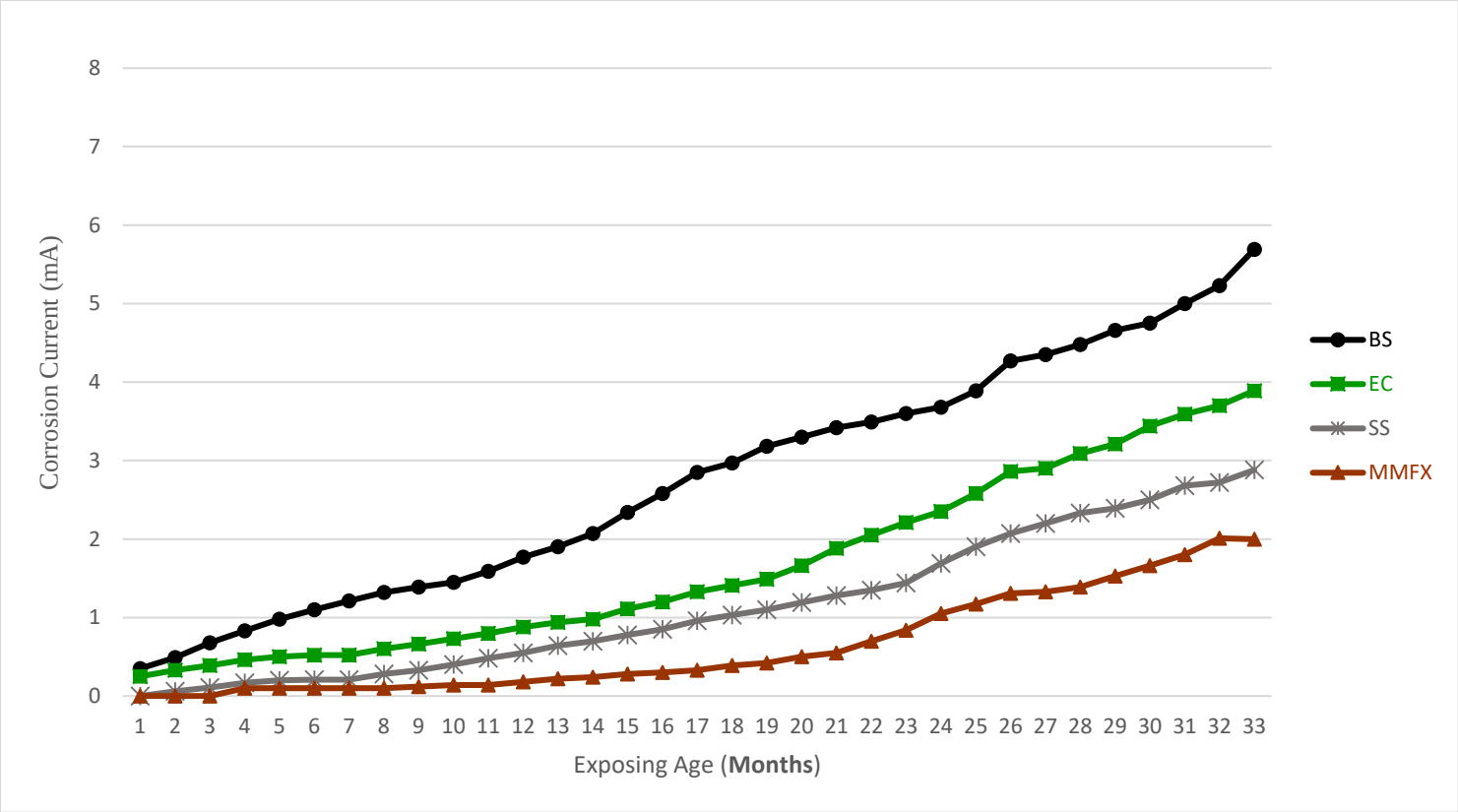

Figure 4–28 Corrosion Currents of Un Cracked Concrete Class A Exposing to 15% Concentration of Sodium Chloride

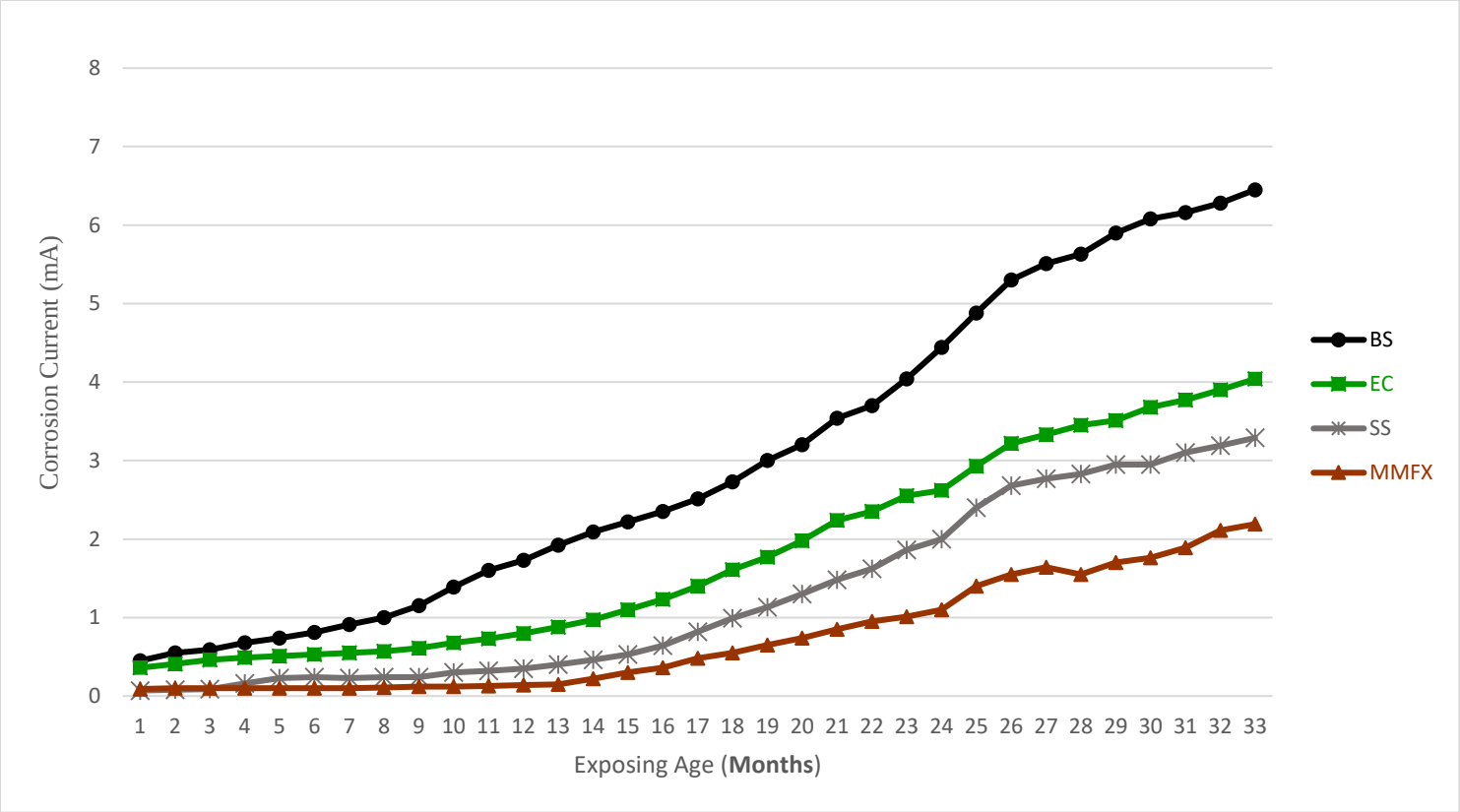

Figure 4–29 Corrosion Currents of Cracked Concrete Class A (crack width=.011", crack depth=.5") Exposing to 15% Concentration of Sodium Chloride

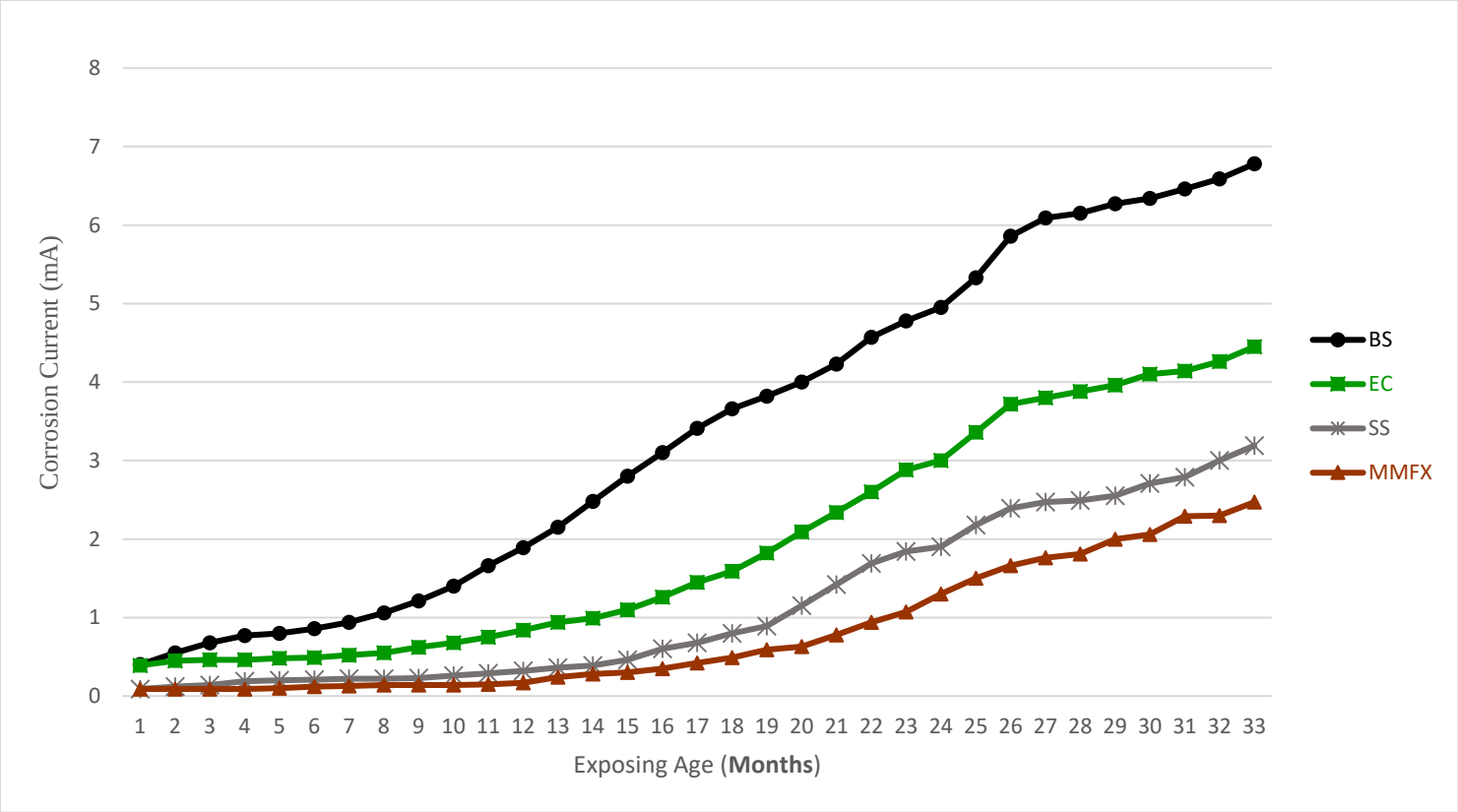

Figure 4–30 Corrosion Currents of Cracked Concrete Class A (crack width=.011", crack depth=1") Exposing to 15% Concentration of Sodium Chloride

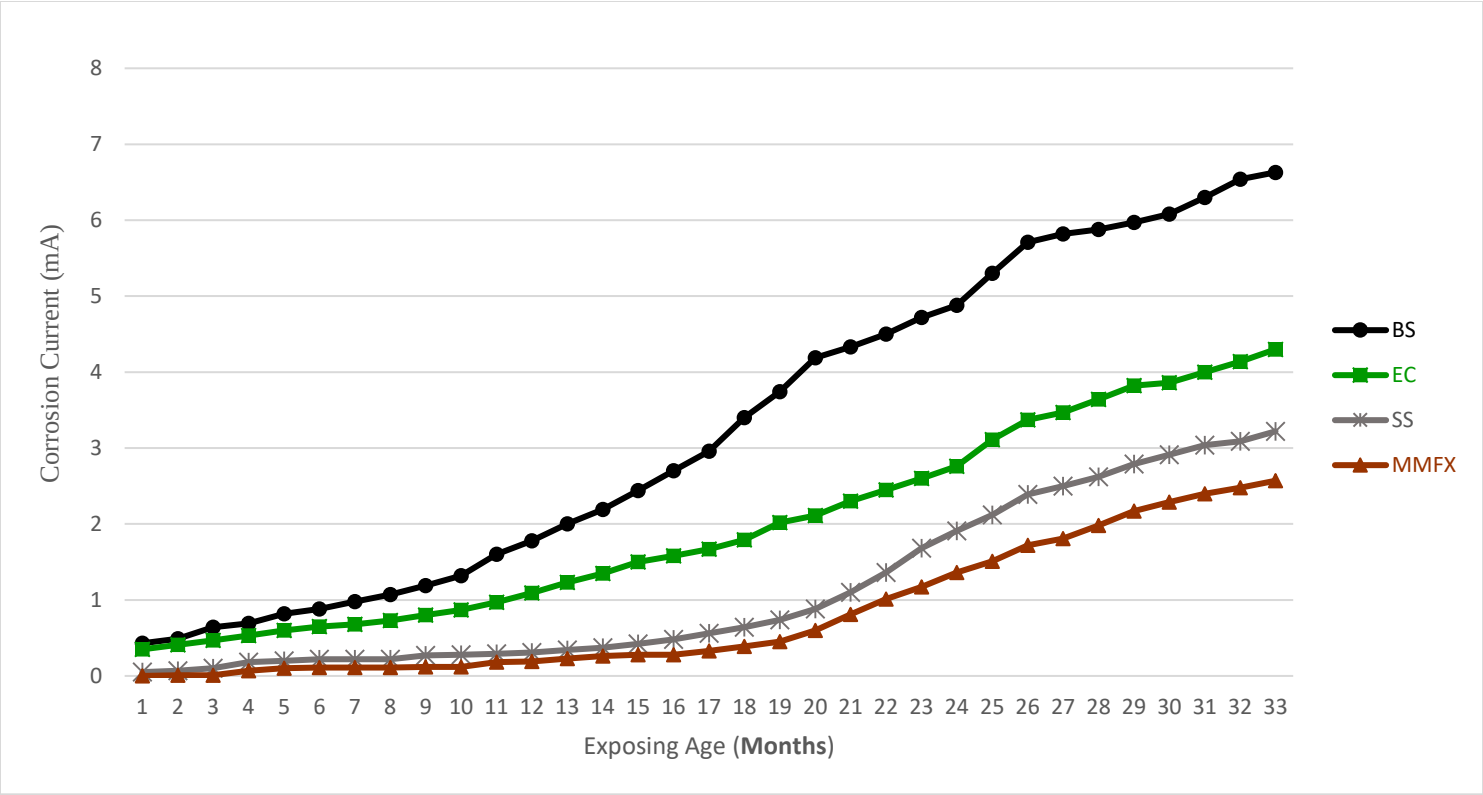

Figure 4–31 Corrosion Currents of Cracked Concrete Class A (crack width=..035", crack depth=.5") Exposing to 15% Concentration of Sodium Chloride

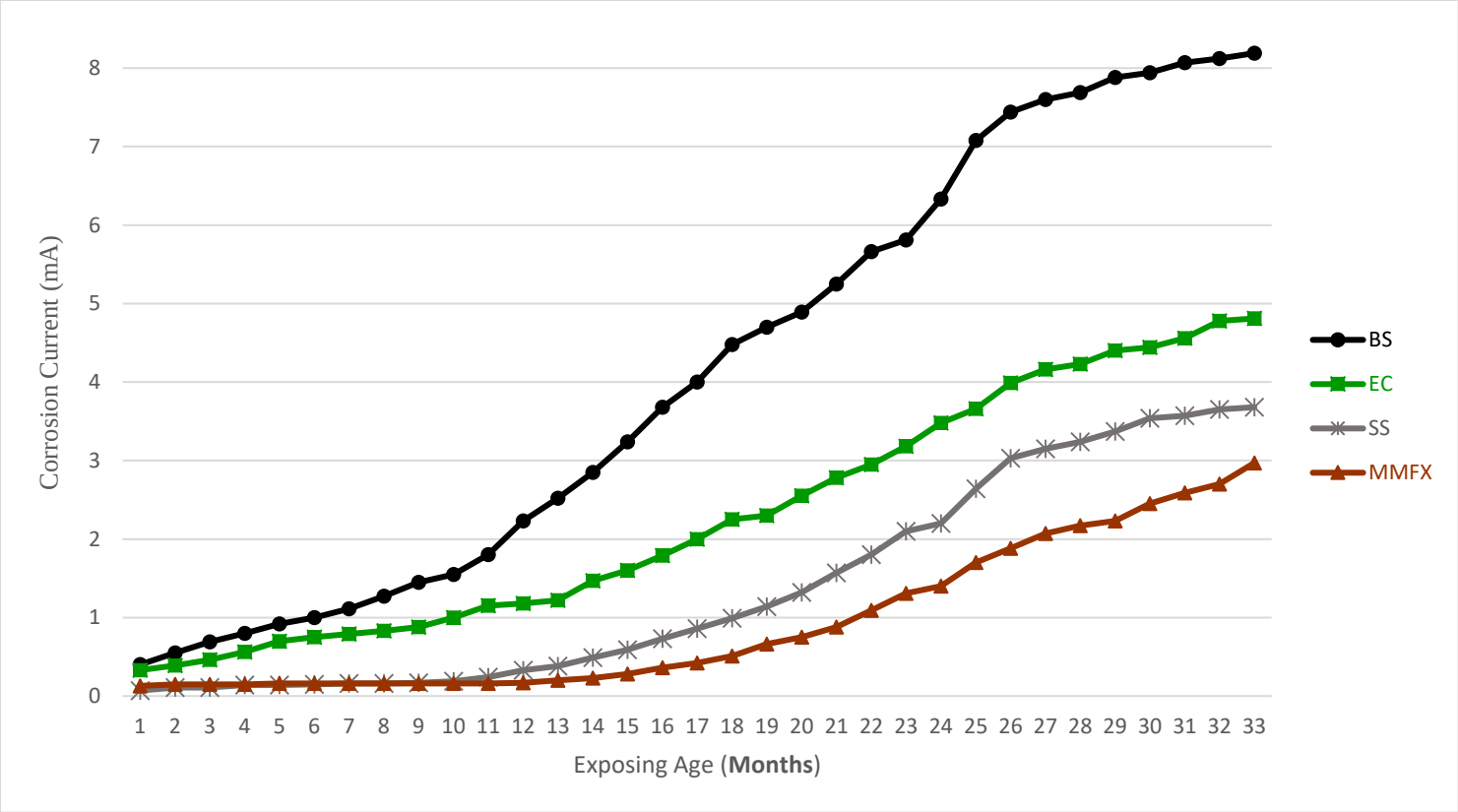

Figure 4–32 Corrosion Currents of Cracked Concrete Class A (crack width=..035", crack depth=1") Exposing to 15% Concentration of Sodium Chloride

4-6-1-2-2 Corrosion Currents of High Performance Concrete (HPC)

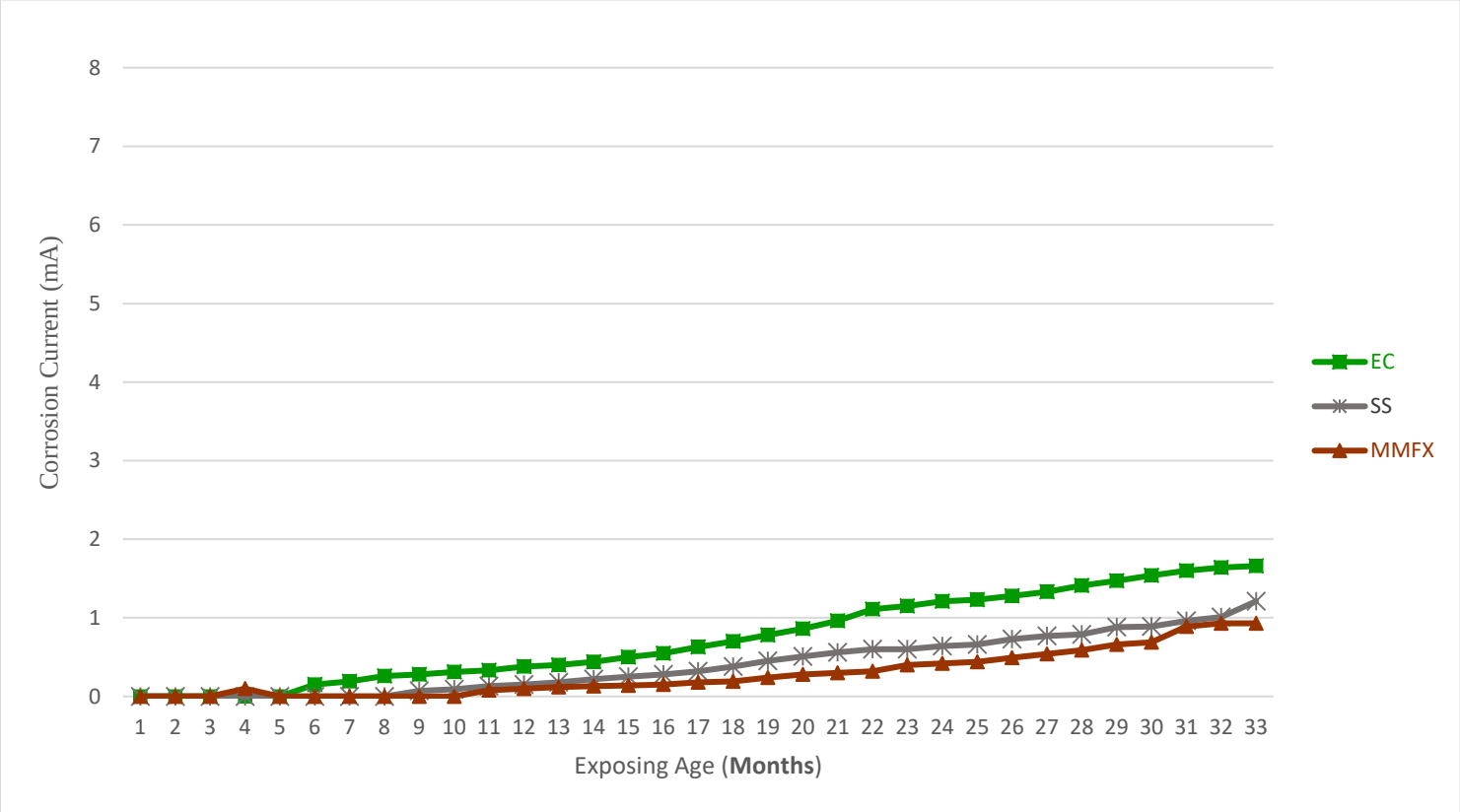

Figure 4–33 Corrosion Currents of Un Cracked HPC Exposing to 15% Concentration of Sodium Chloride

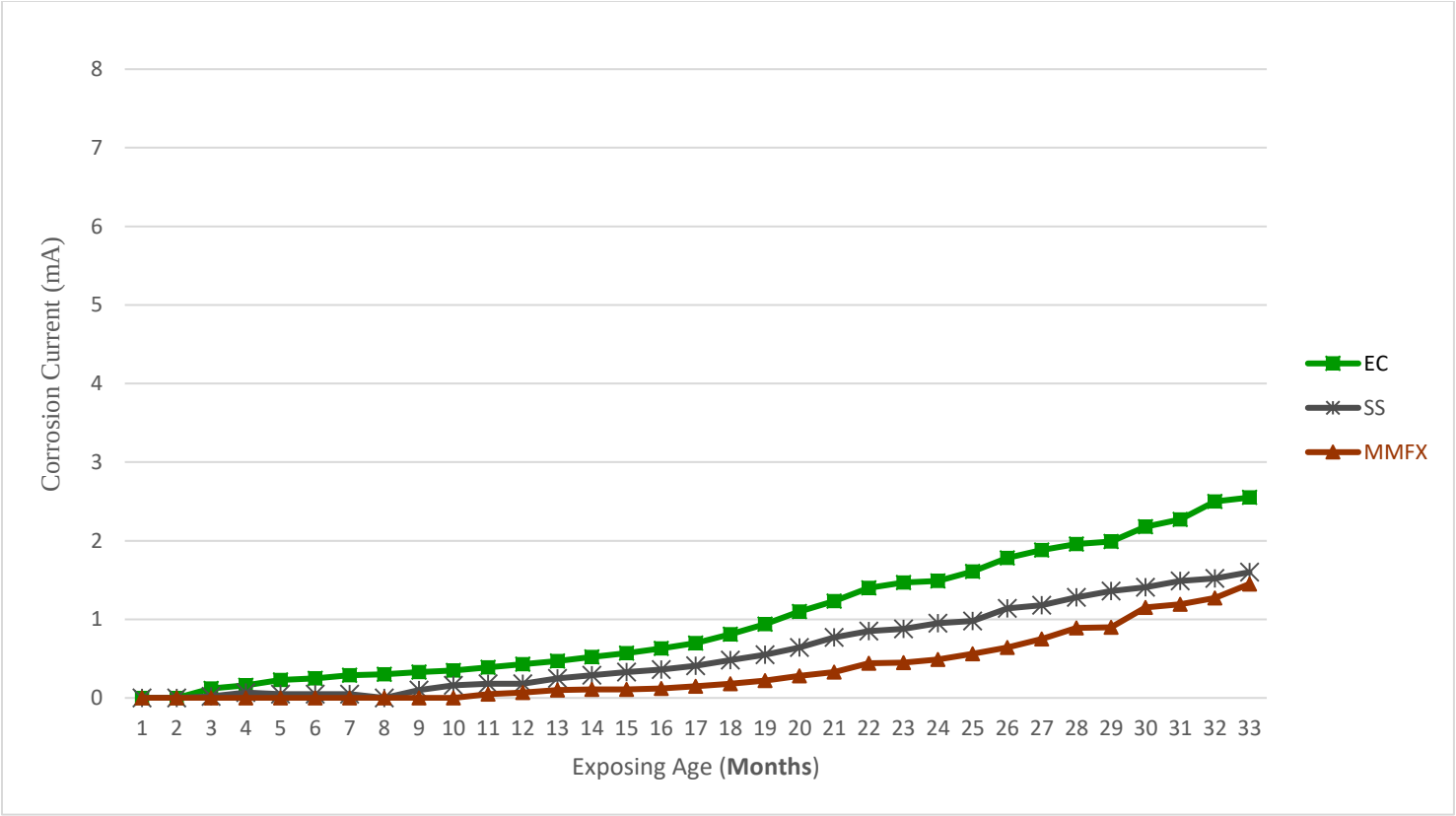

Figure 4–34 Corrosion Currents of Cracked HPC (crack width=.011", crack depth=.5") Exposing to 15% Concentration of NaCl

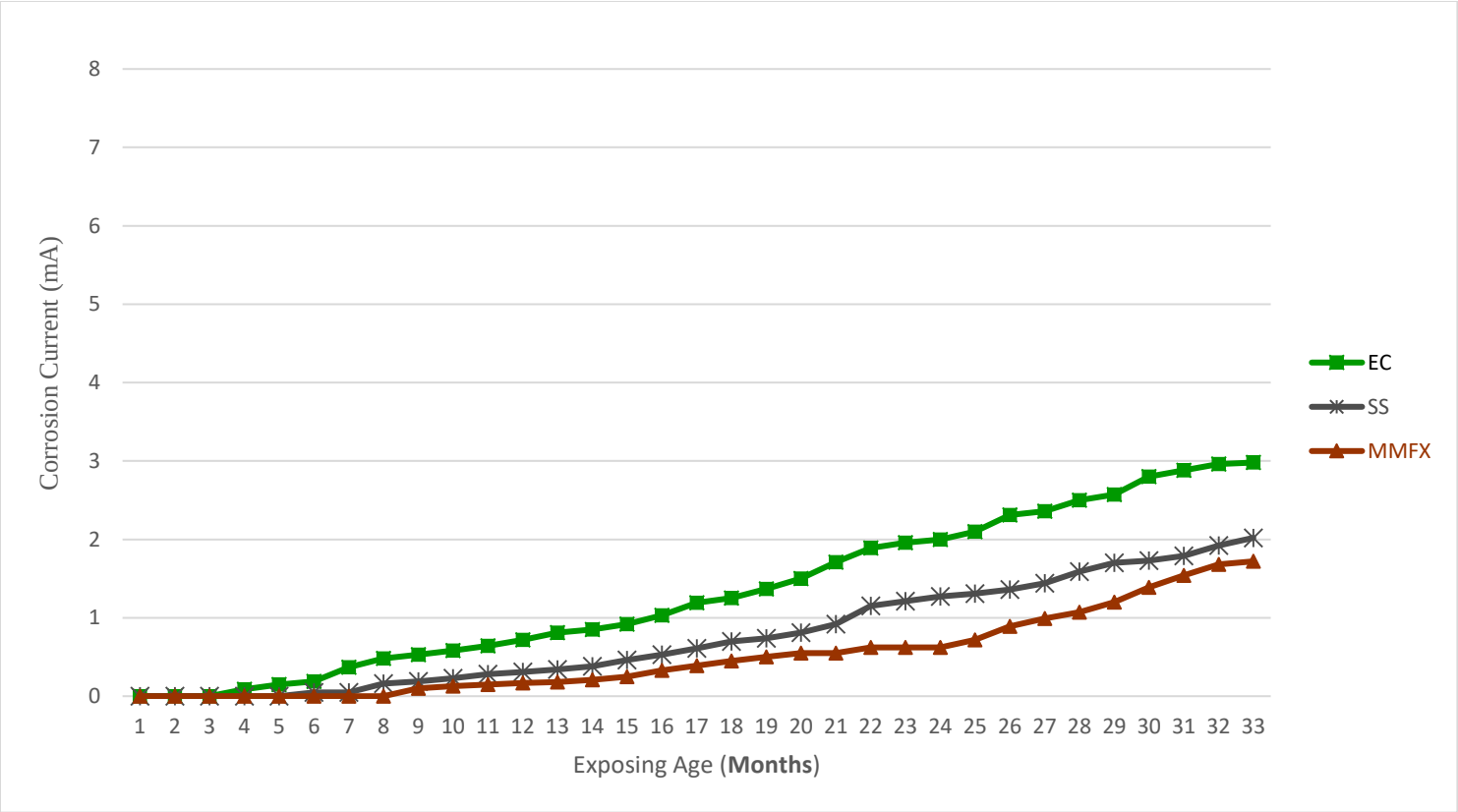

Figure 4–35 Corrosion Currents of Cracked HPC (crack width=.011", crack depth=1") Exposing to 15% Concentration of NaCl

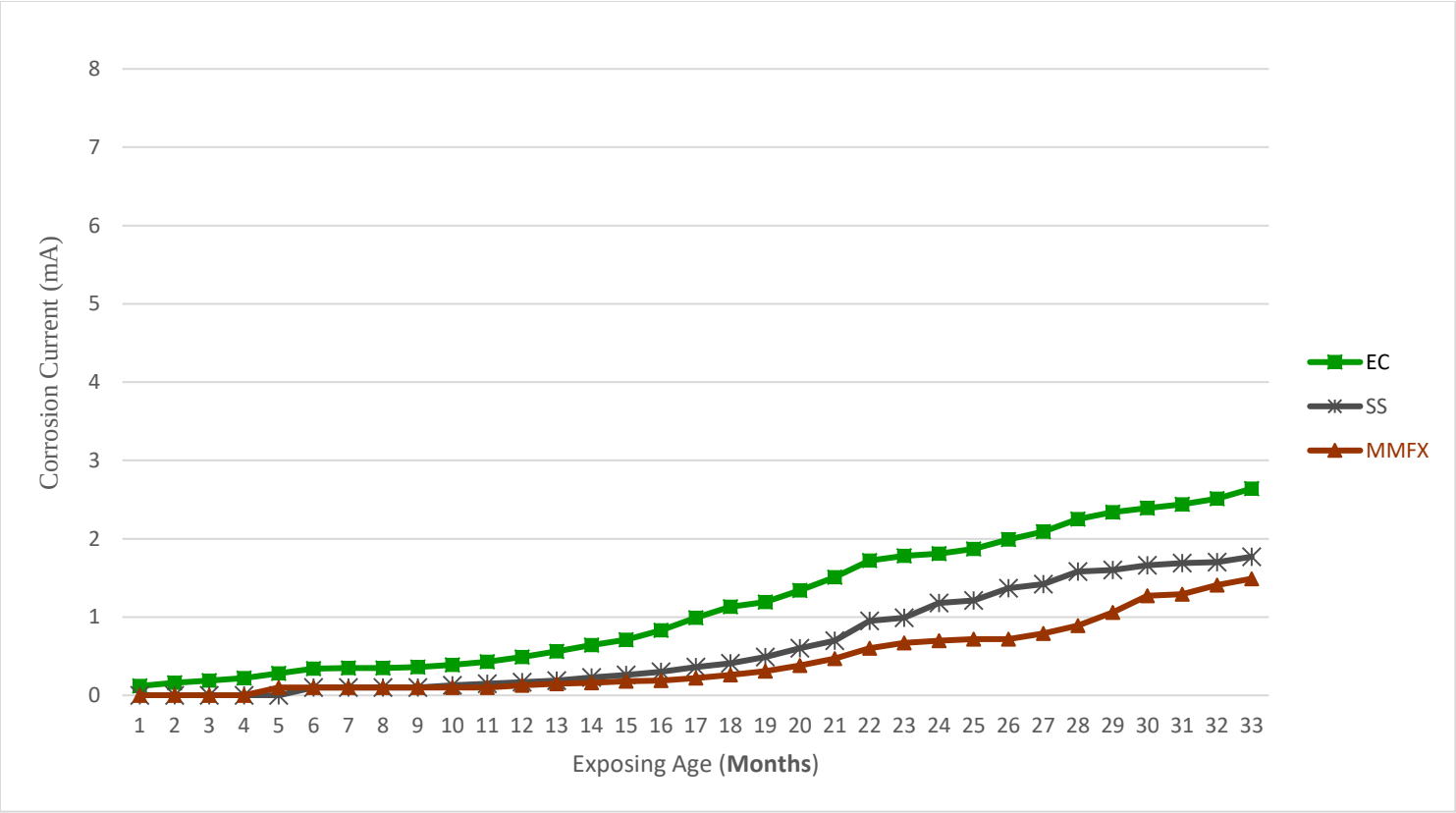

Figure 4–36 Corrosion Currents of Cracked HPC (crack width=.035", crack depth=.5") Exposing to 15% Concentration of NaCl

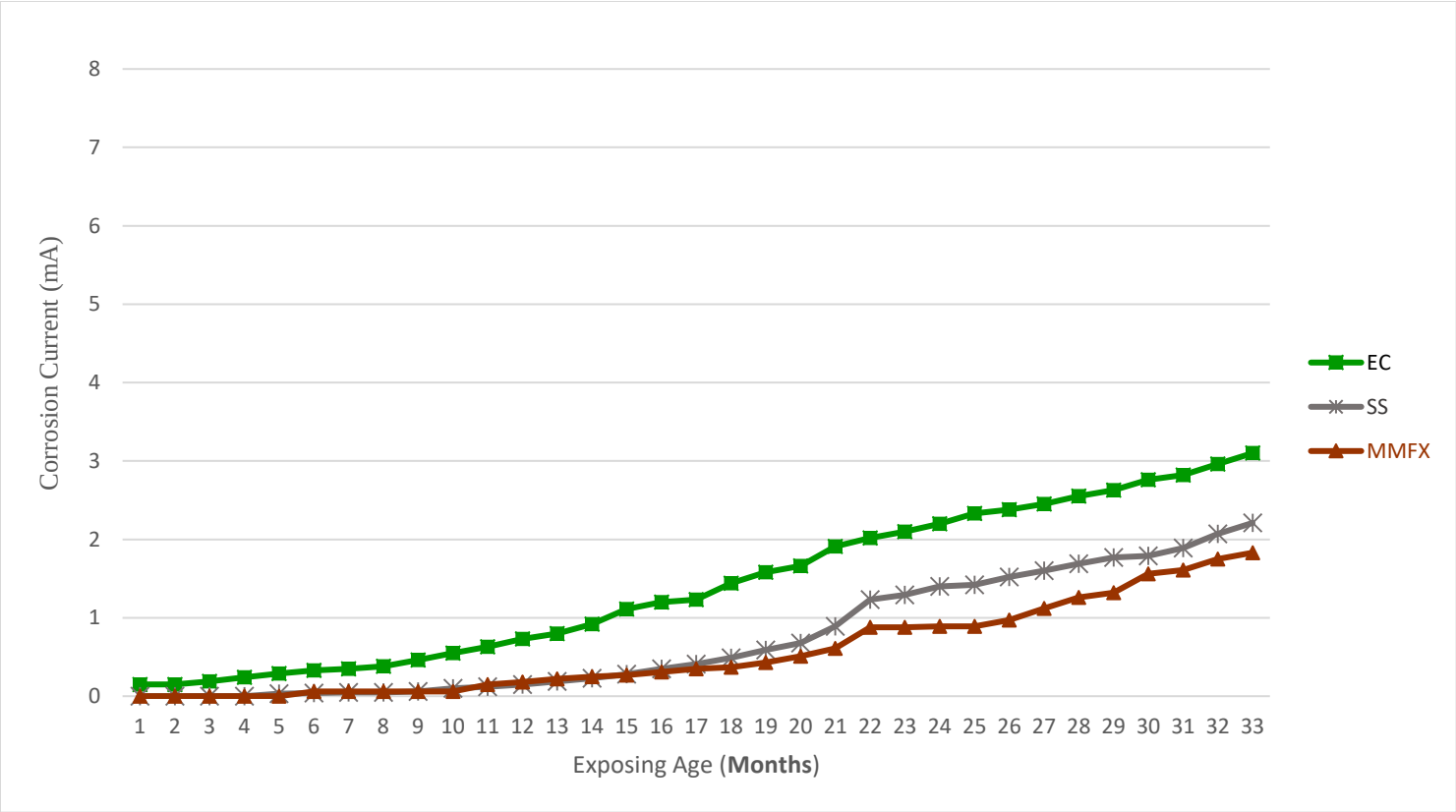

Figure 4–37 Corrosion Currents of Cracked HPC (crack width=.035", crack depth=1") Exposing to 15% Concentration of NaCl

4-6-1-3-1 Corrosion Potentials Of Sealed Samples

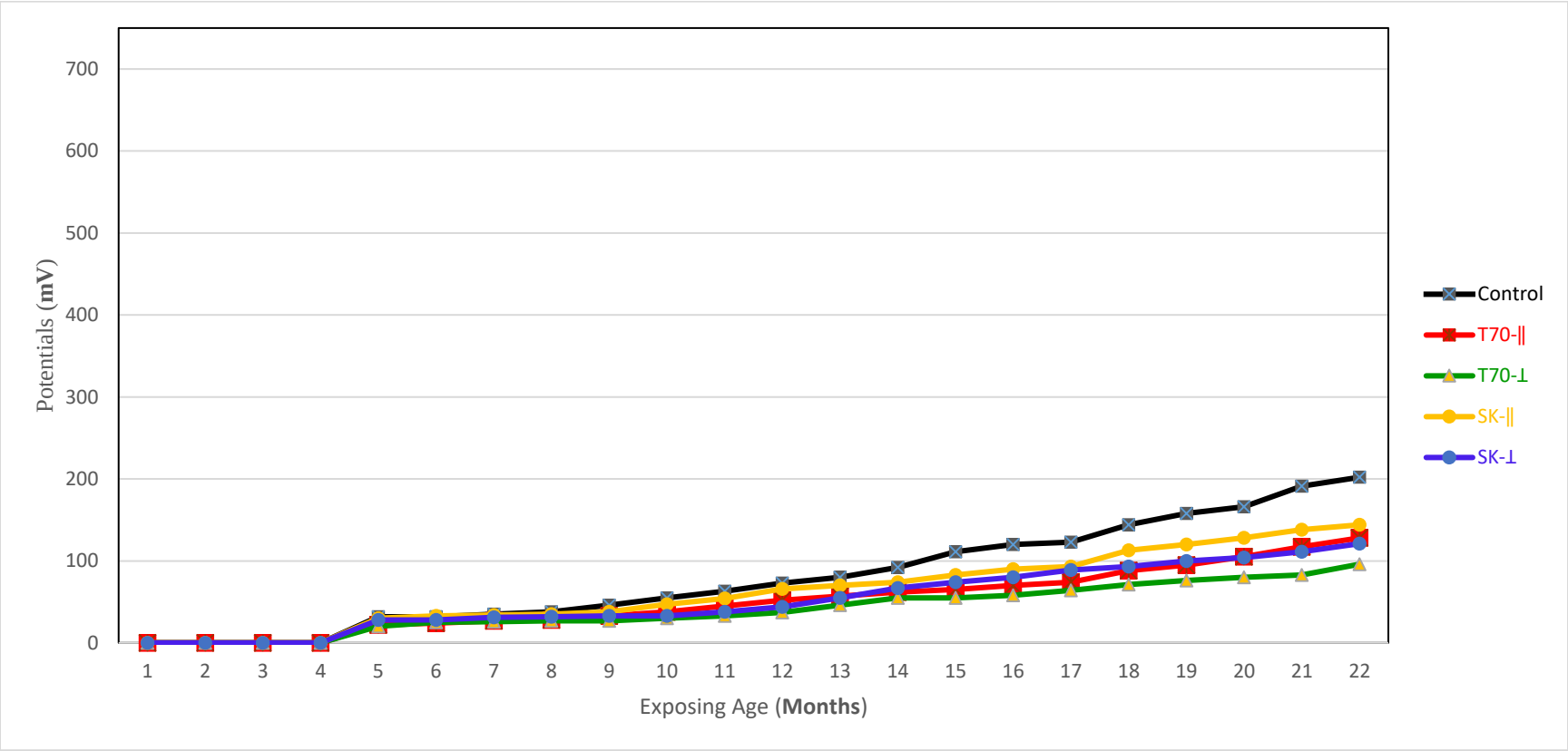

Figure 4–38 Corrosion Potentials of Cracked Epoxy Coated HPC(crack width=.035", crack depth=1"); Sealed with Two Concrete Crack Sealants (T70-MX Methacrylate and Seal Krete- Acrylic) Exposing to 15% Concentration of Sodium Chloride

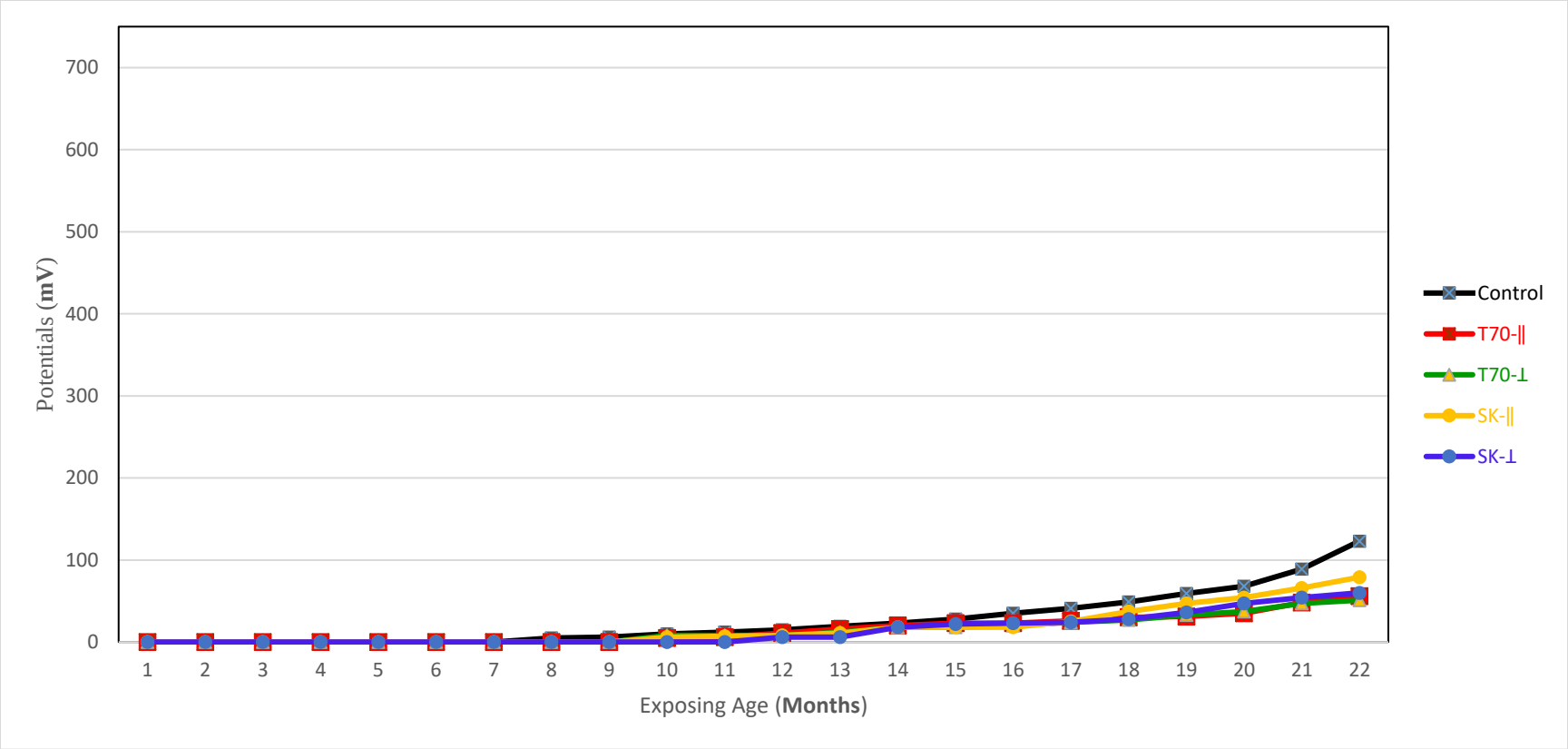

Figure 4–39 Corrosion Potentials of Cracked Stainless Steel HPC(crack width=.035", crack depth=1"); Sealed with Two Concrete Crack Sealants (T70-MX Methacrylate and Seal Krete- Acrylic) Exposing to 15% Concentration of Sodium Chloride

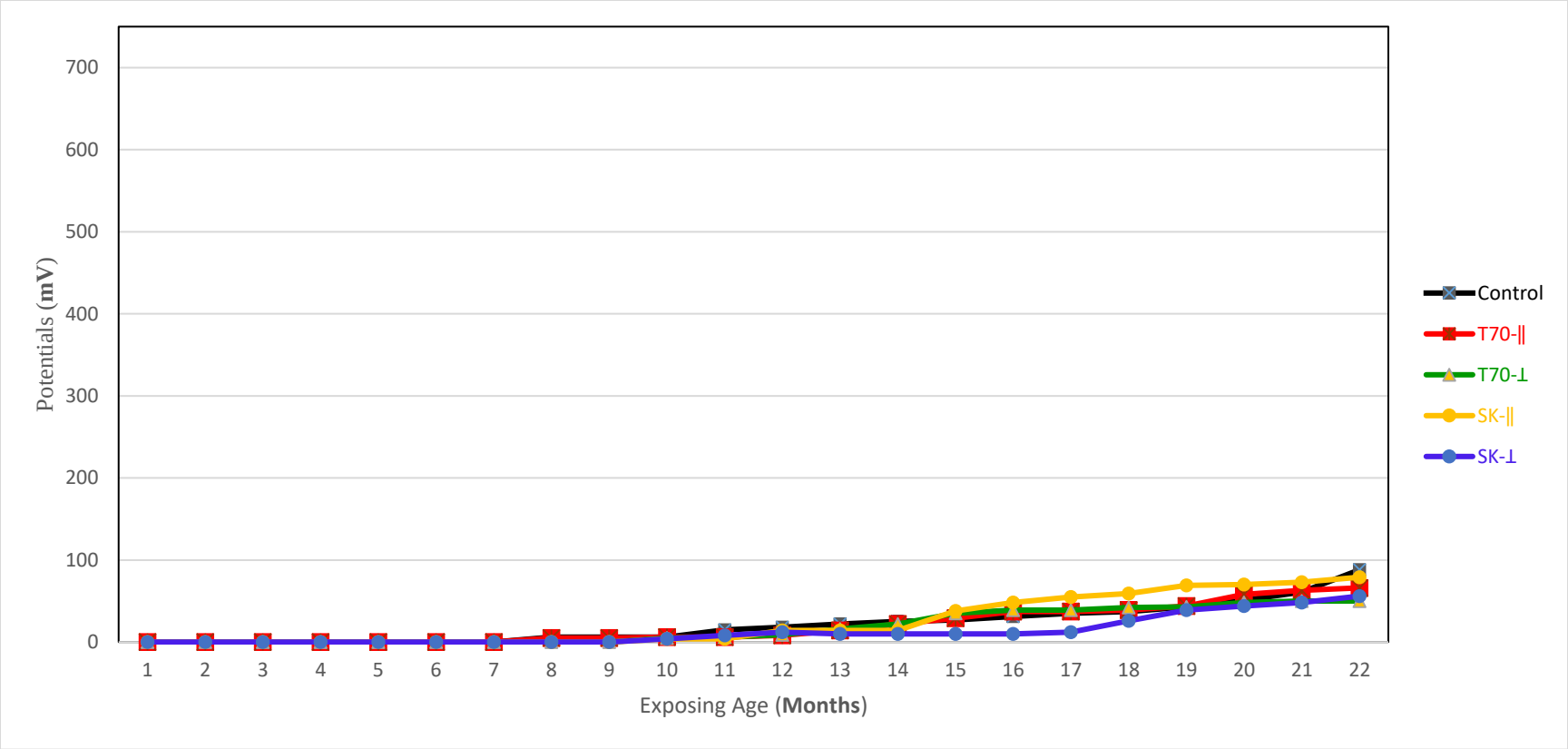

Figure 4–40 Corrosion Potentials of Cracked MMFX-HPC (crack width=.035", crack depth=1"); Sealed with Two Concrete Crack Sealants (T70-MX Methacrylate and Seal Krete- Acrylic) Exposing to 15% Concentration of Sodium Chloride

4-6-1-3-2 Corrosion Currents of Sealed Samples

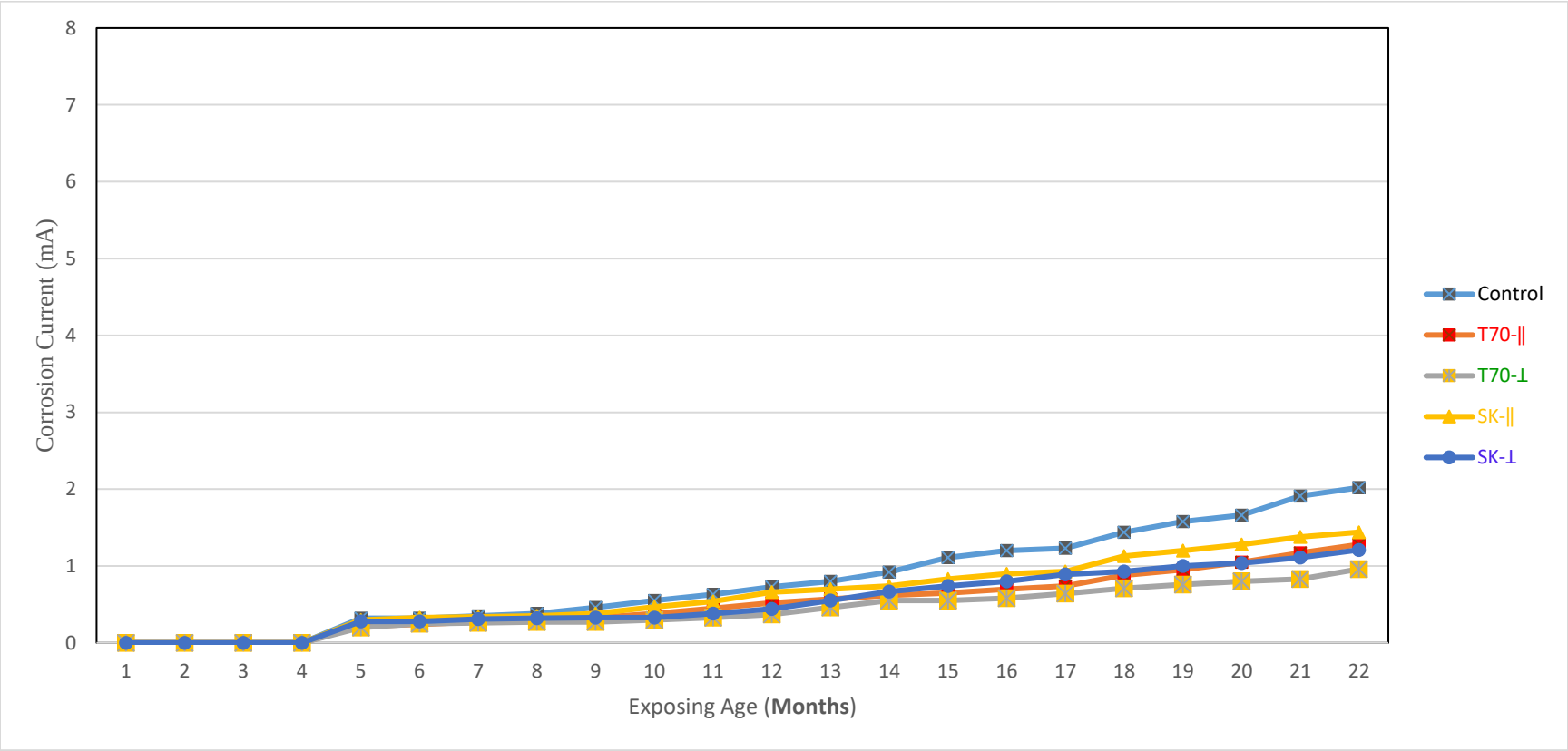

Figure 4–41 Corrosion Currents of Cracked Epoxy Coated-HPC(crack width=.035", crack depth=1"); Sealed with Two Concrete Crack Sealants (T70-MX Methacrylate and Seal Krete- Acrylic) Exposing to 15% Concentration of Sodium Chloride

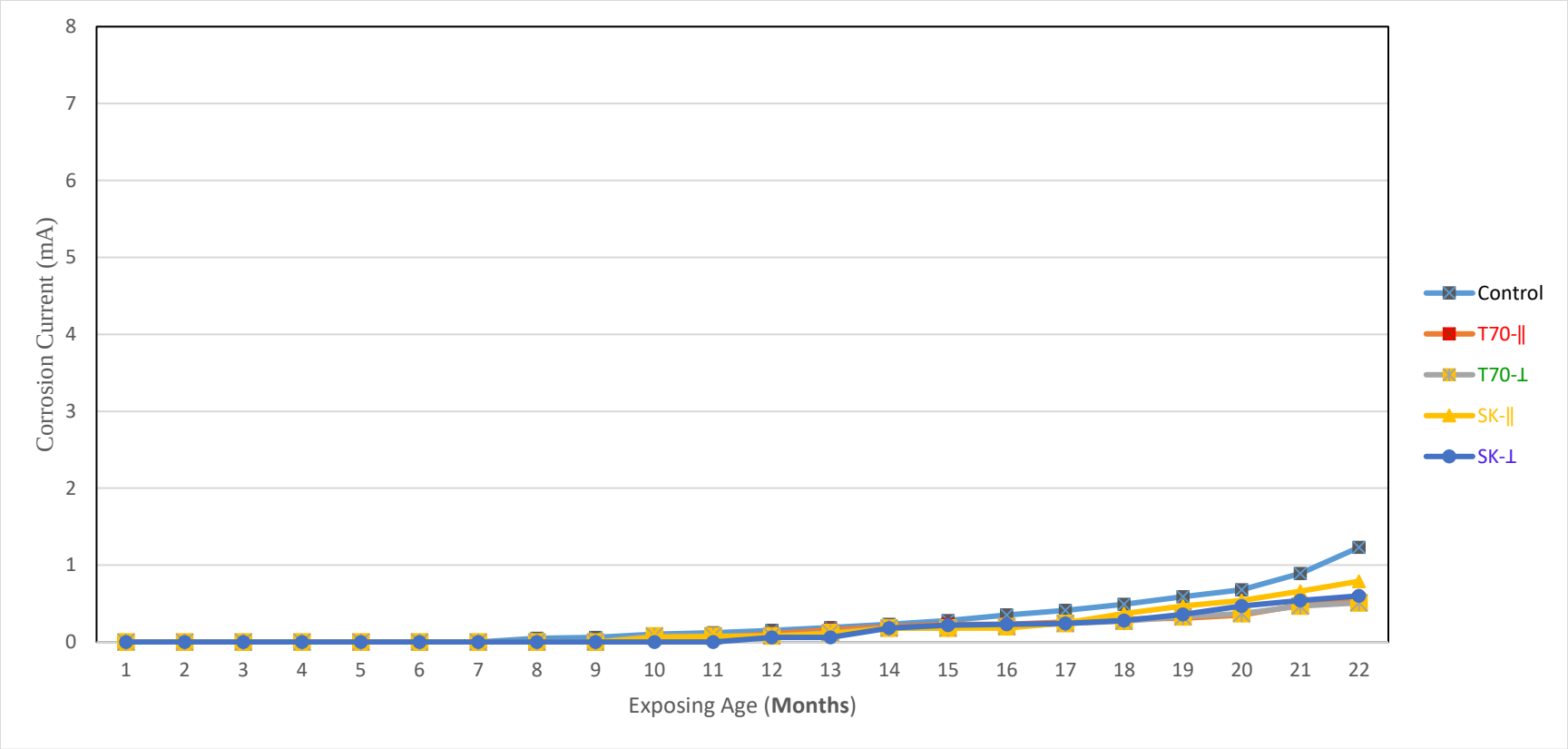

Figure 4–42 Corrosion Currents of Cracked Stainless Steel-HPC (crack width=.035", crack depth=1"); Sealed with Two Concrete Crack Sealants (T70-MX Methacrylate and Seal Krete- Acrylic) Exposing to 15% Concentration of Sodium Chloride

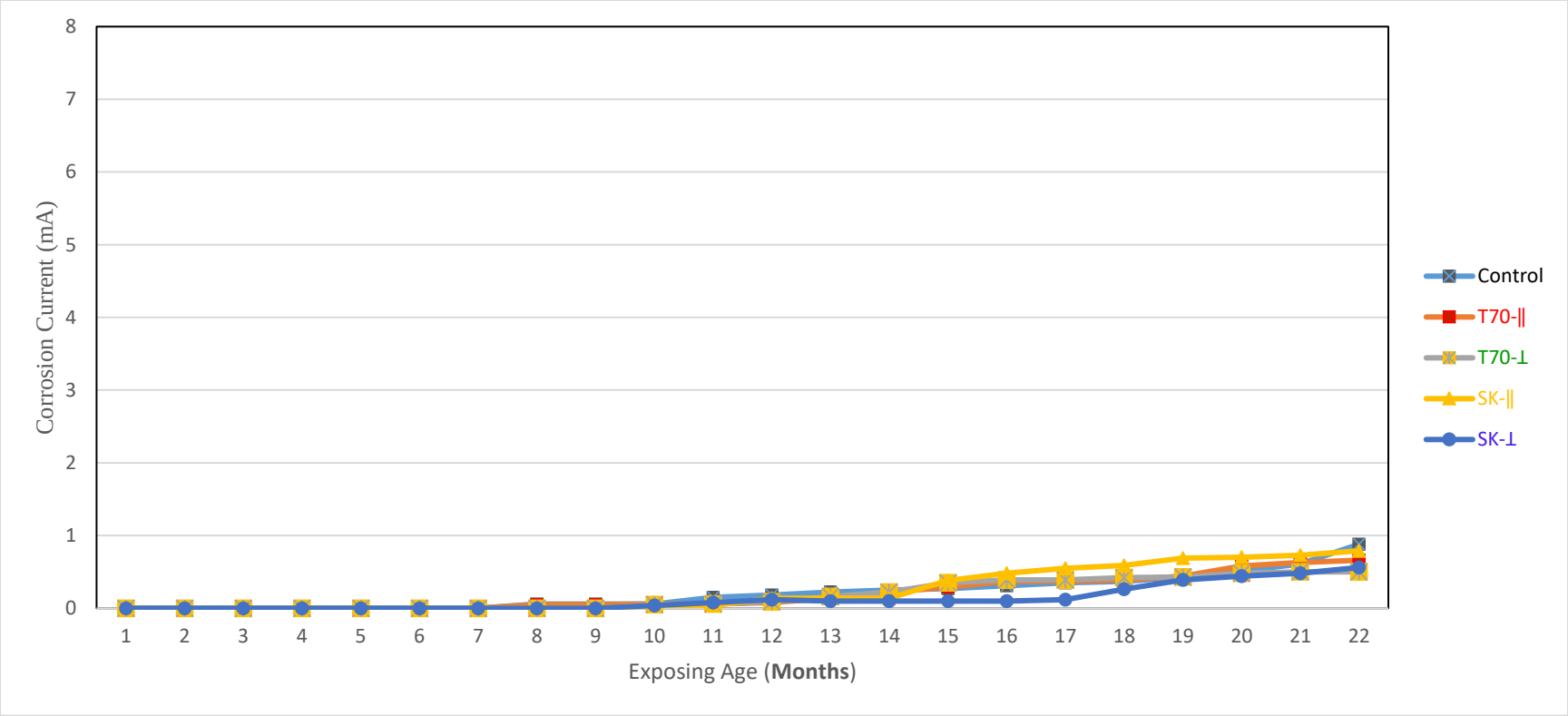

Figure 4–43 Corrosion Currents of Cracked MMFX-HPC (crack width=.035", crack depth=1"); Sealed with Two Concrete Crack Sealants (T70-MX Methacrylate and Seal Krete- Acrylic) Exposing to 15% Concentration of Sodium Chloride

4-6-2 Slab Samples of Corrosion (24×24×10")

In this part of the research there are many parameters or indices that were used to determine the corrosion activities of different concretes and rebars, such as potentials (voltage), current, corrosion map, chloride content, visual examination, and so on. Following are the tests used to investigate the corrosion process.

4-6-2-1 Corrosion Potentials of un Cracked Slabs

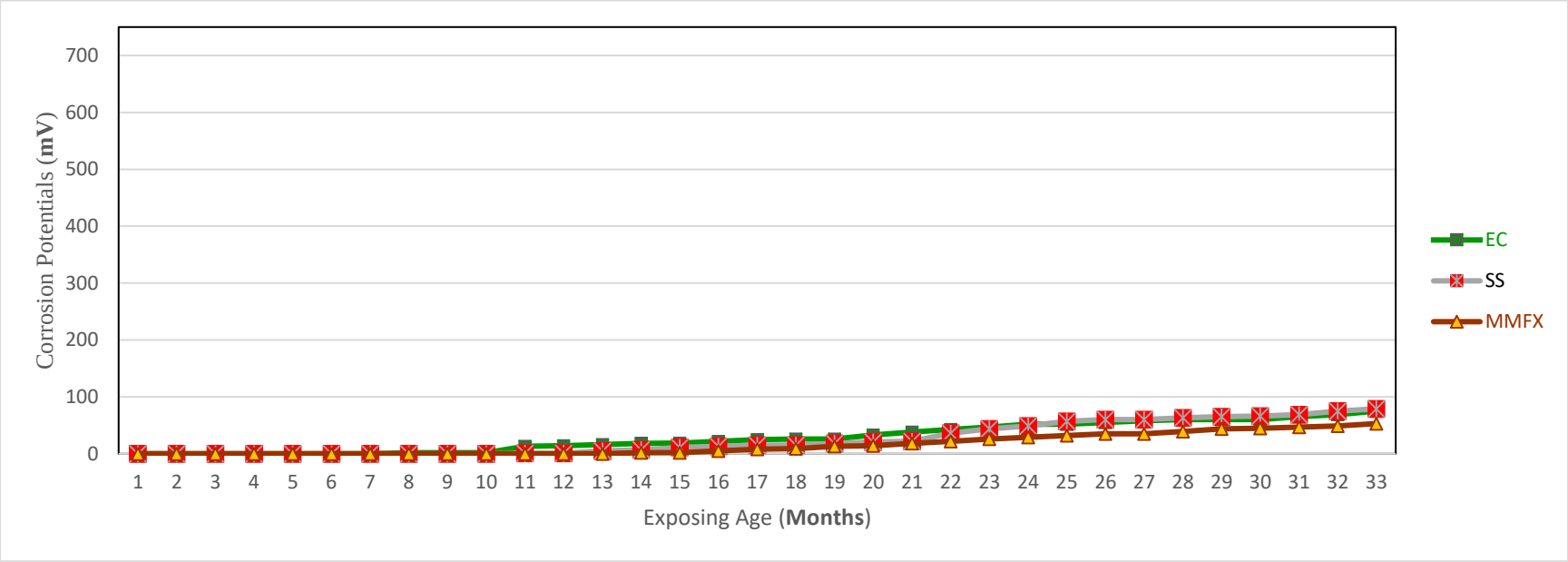

Figure 4–44 Corrosion Potentials of Un Cracked High Performance Concrete Slabs Exposing to 15% Concentration of Sodium Chloride

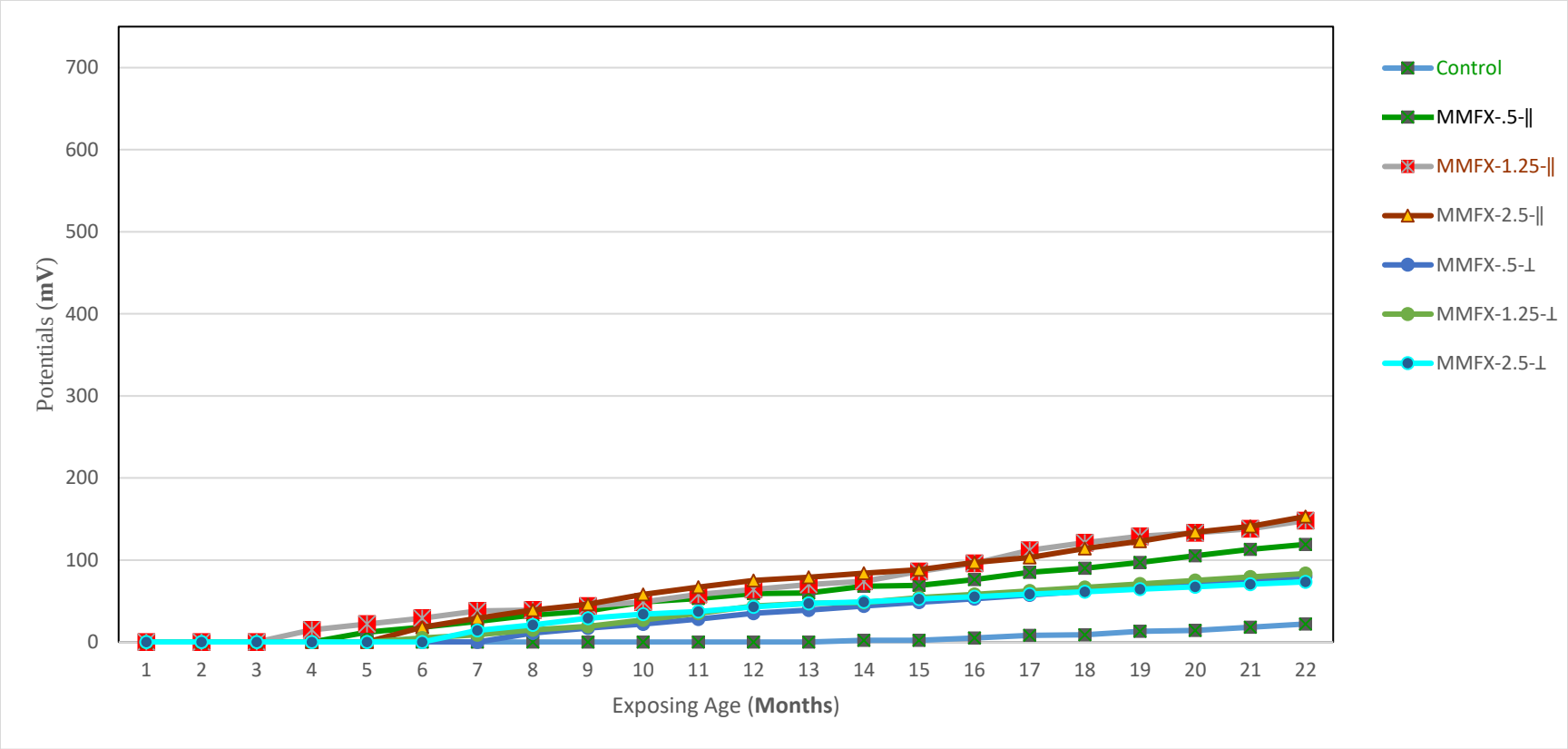

Figure 4–45 Corrosion Potentials of Cracked Un sealed MMFX HPC (crack width=.035", crack depth=.5, 1.25, and 2.5") Exposing to 15% Concentration of Sodium Chloride

4-6-2-2 Corrosion Potentials of Sealed Slabs

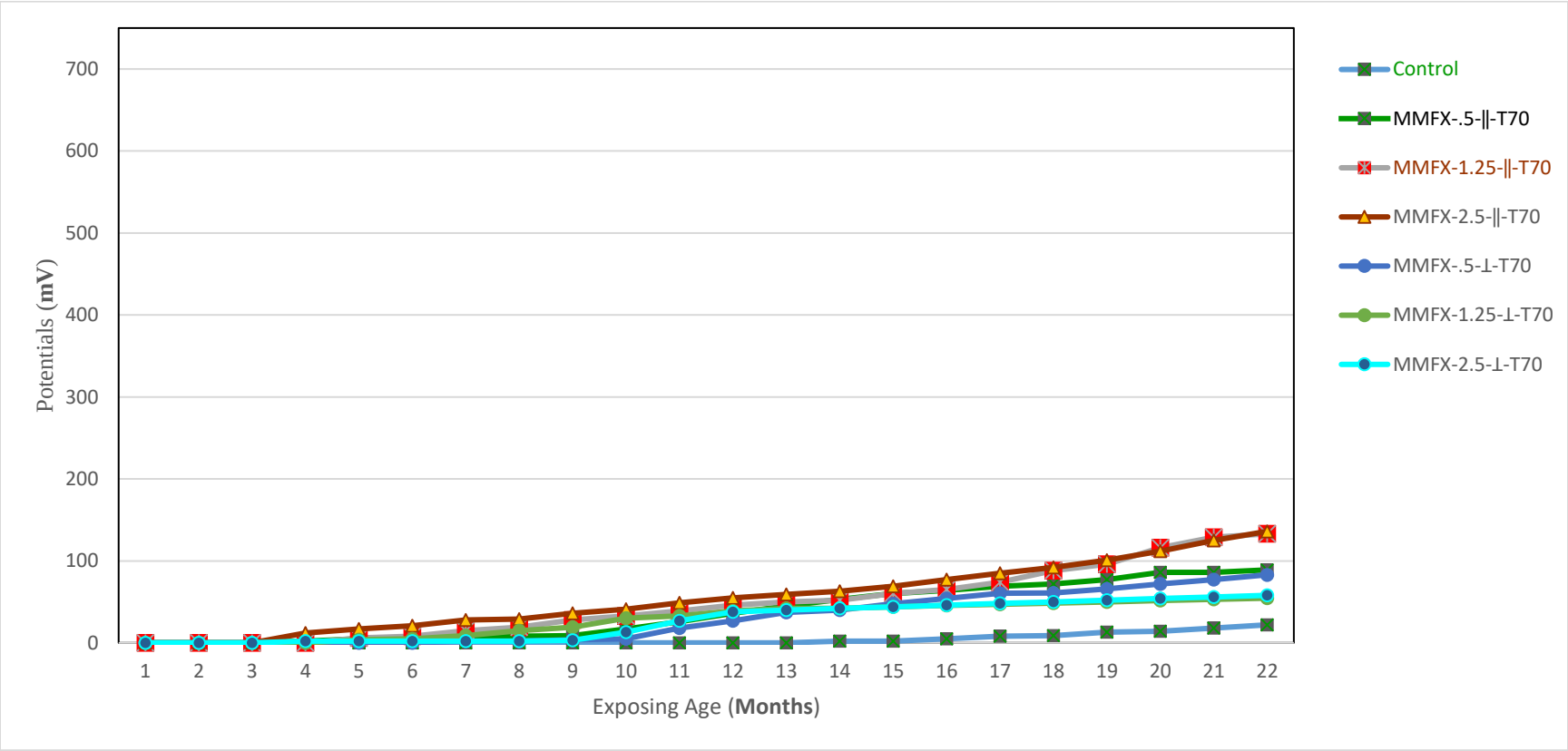

Figure 4–46 Corrosion Potentials of Cracked MMFX HPC (crack width=.035", crack depth=.5, 1.25, and 2.5"); Sealed with T70-MX High Wight Methacrylate Concrete Crack Sealant Exposing to 15% Concentration of Sodium Chloride

4-6-2-3 Corrosion Currents of Slabs Samples

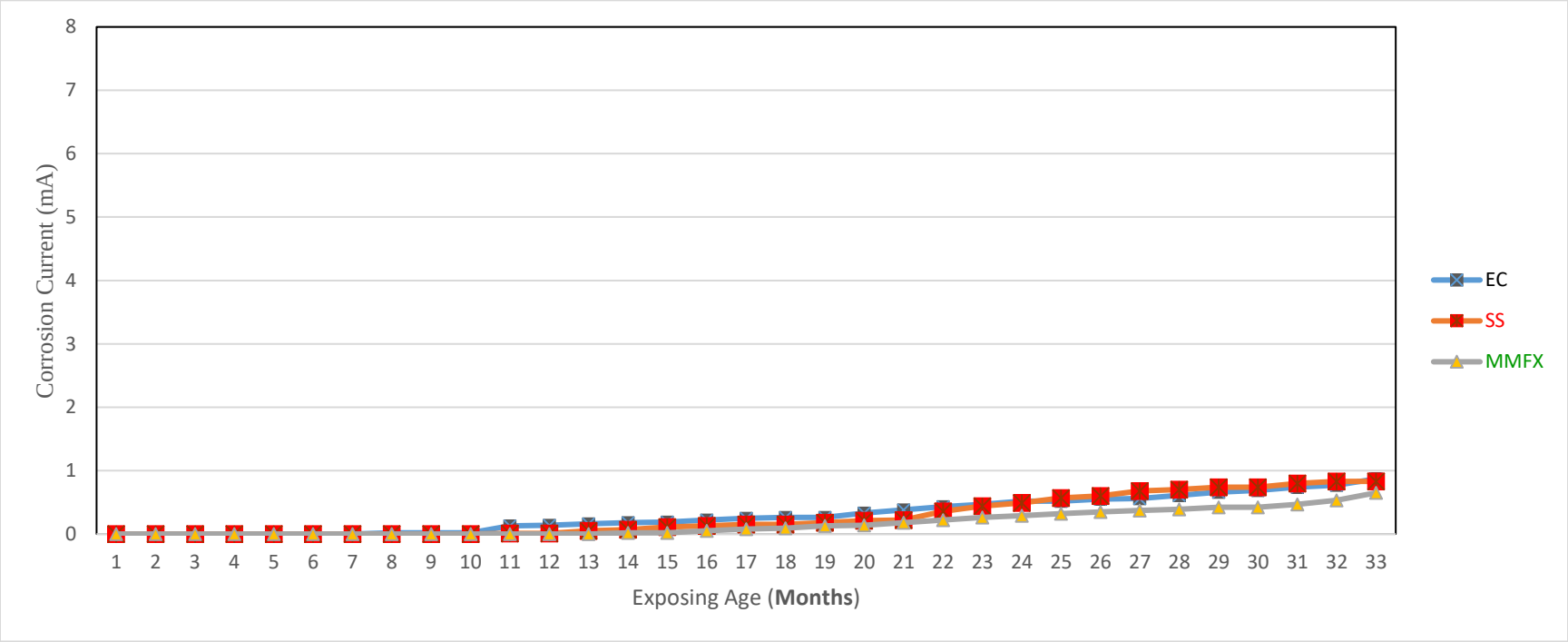

Figure 4–47 Corrosion Currents of Un Cracked High Performance Concrete Slabs Exposing to 15% Concentration of Sodium Chloride

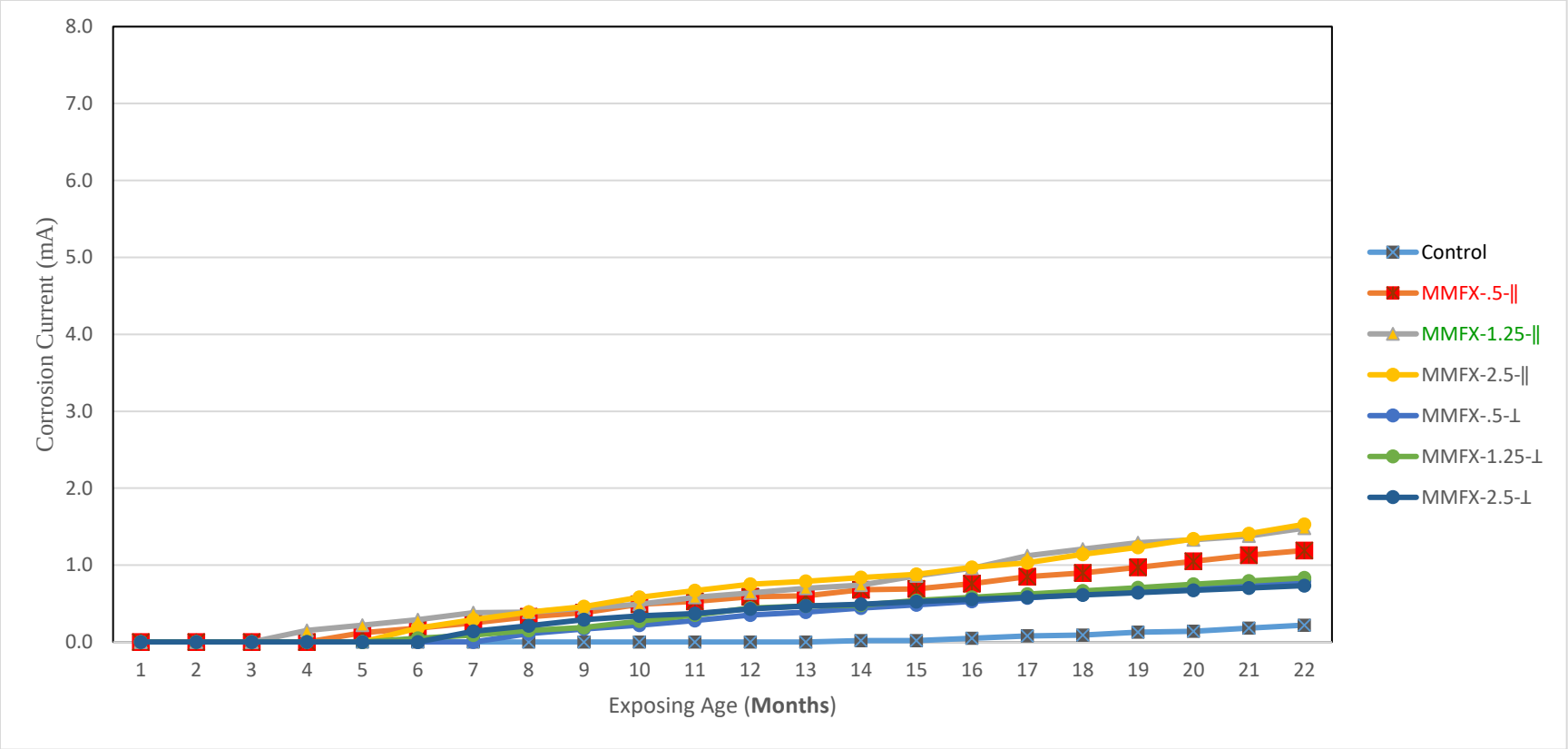

Figure 4–48 Corrosion Currents of Cracked Un sealed MMFX HPC (crack width=.035", crack depth=.5, 1.25, and 2.5") Exposing to 15% Concentration of Sodium Chloride

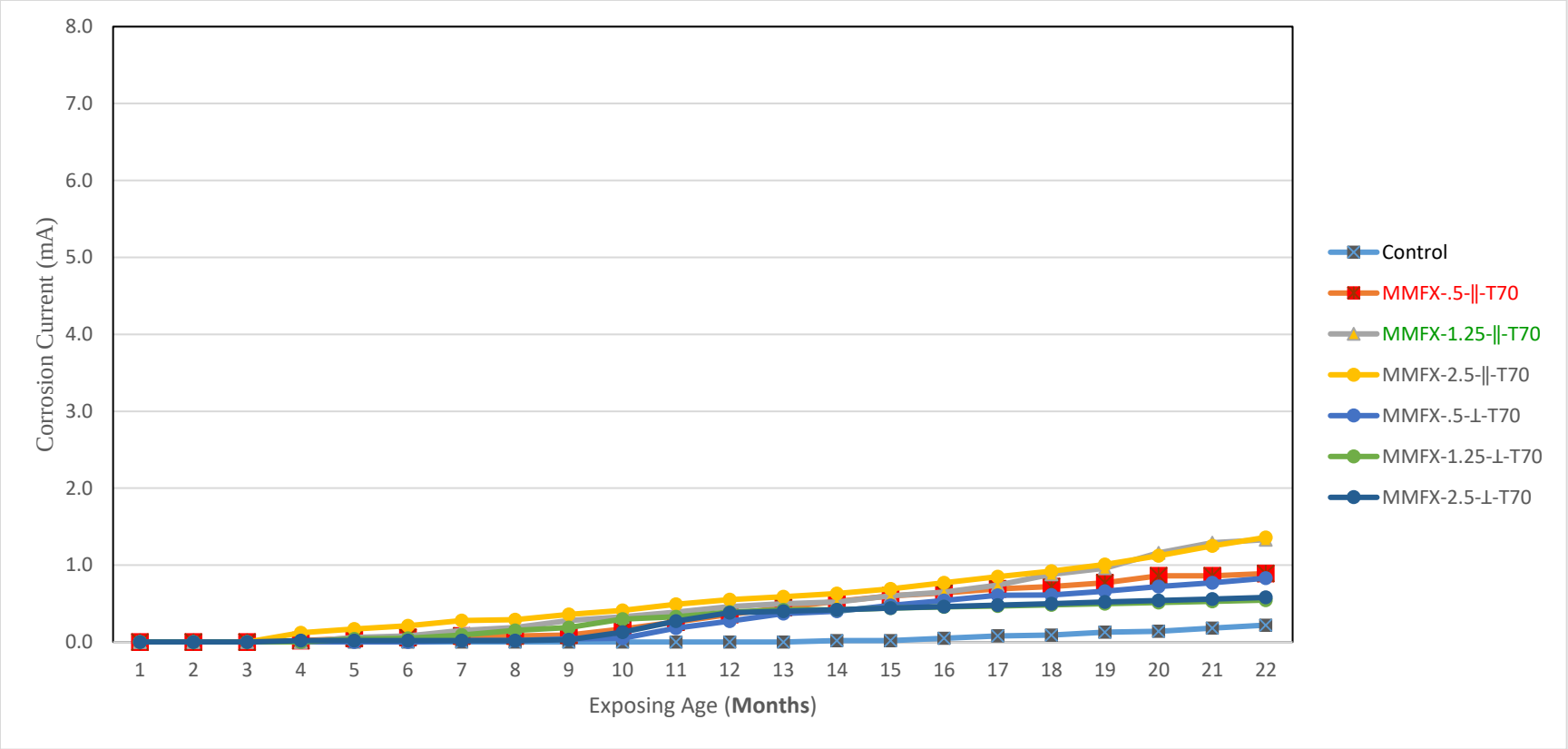

Figure 4–49 Corrosion Currents of Cracked MMFX HPC (crack width=.035", crack depth=.5, 1.25, and 2.5"); Sealed with T70-MX High Wight Methacrylate Concrete Crack Sealer Exposing to 15% Concentration of Sodium Chloride

4-6-3 Corrosion Map of Slabs

The corrosion maps were determined by measuring the corrosion potentials between the top rebars of the concrete and the V2000 Silver-Silver as working electrode.

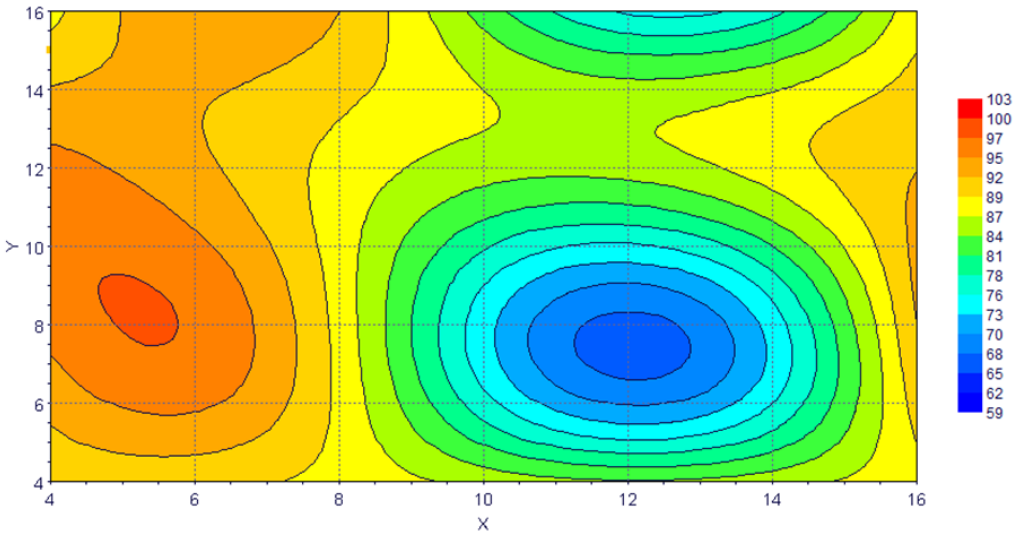

Figure 4–50 Epoxy Coated Un Cracked High Performance Concrete Slab.

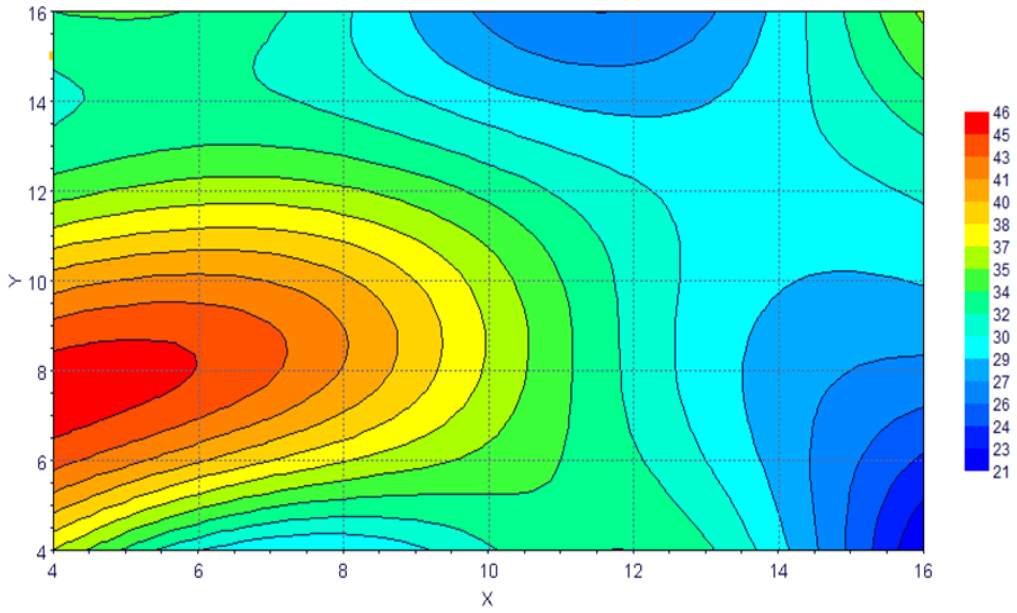

Figure 4–51 Stainless Steel Un Cracked High Performance Concrete Slab

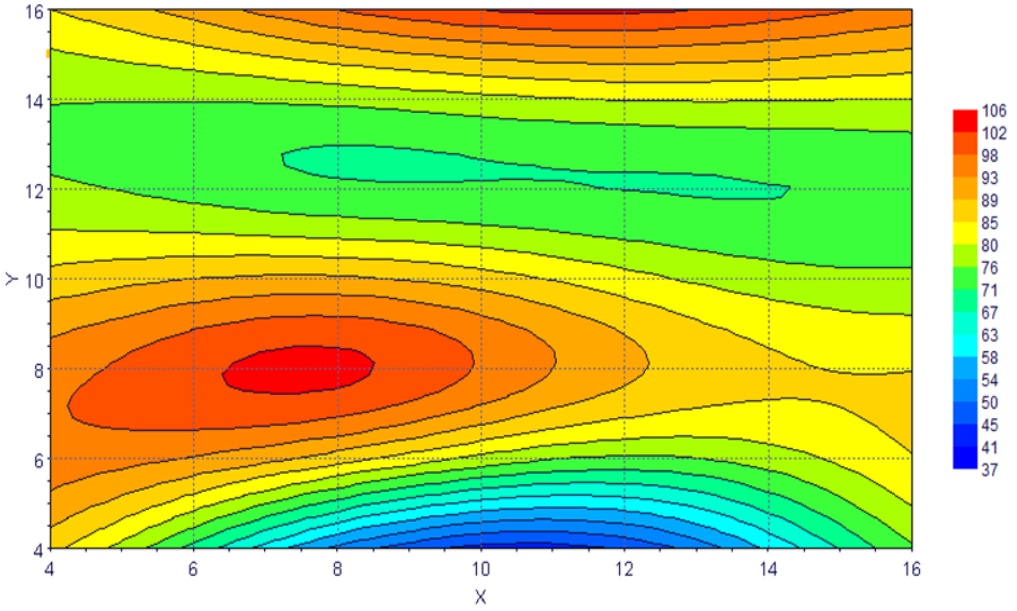

Figure 4–52 MMFX Un Cracked High Performance Concrete Slab

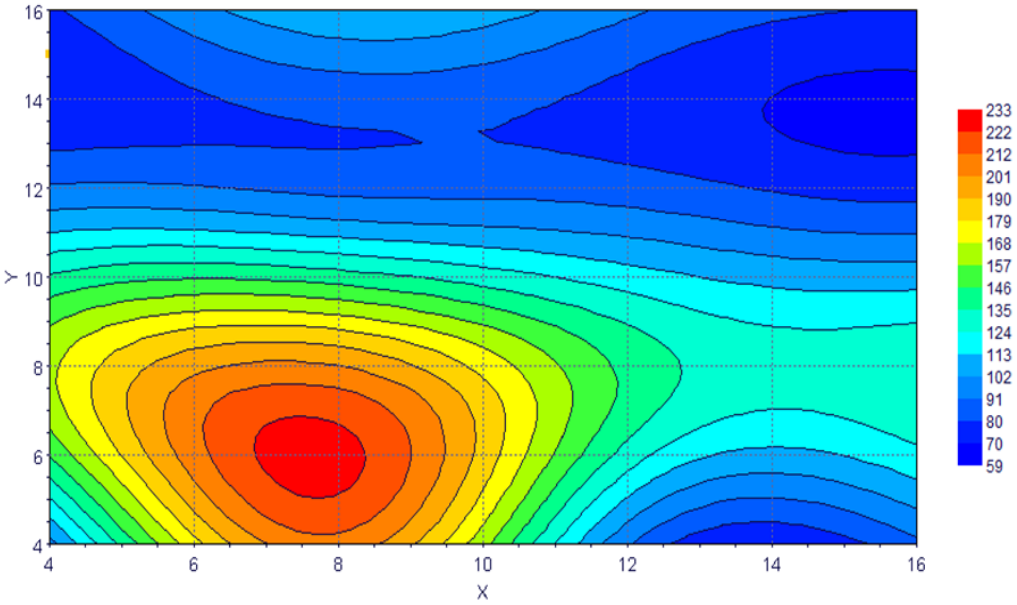

Figure 4–53 MMFX Cracked High Performance Concrete Slab Non-Sealed

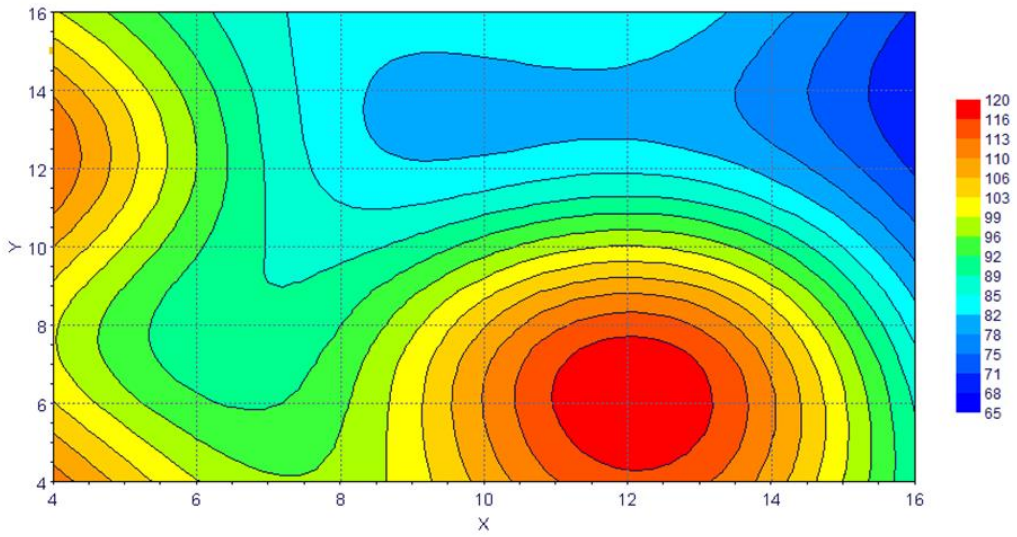

Figure 4–54 MMFX Cracked High Performance Concrete Slab Sealed with T-70 MX

4-7 Discussion and Conclusion of the Laboratory Results

The current research is using the laboratory tests and the field performances to investigate the effects of crack on the corrosion process of reinforced concrete members, predicting the service life of bridge decks, and to compute the efficiency of two different types of crack sealants. The results of experimental and theoretical work are summarized in this part.

4-7-1 Mechanical Properties

Both types of concretes, Concrete class A and HPC, developed noticeable strength properties with the progress of age, but HPC had the superior achievement compared with concrete class A. the improvement ratios were about 80, 80, 79, and 65% for compressive

strength, tensile strength, flexural strength, and modulus of elasticity at age of 28 days as summarized in the table (4-8) below.

Table 4-8 Mechanical Properties of Concretes at Age 28 Days

Strength properties	Concrete Class A	HPC	Increment Ratio (%)
Compressive Strength (psi)	4500	8100	80%
Tensile Strength (psi)	480	860	79%
Flexural Strength (psi)	589	1060	80%
Modulus of Elasticity	4125	6815	65%

The improvement in the strength properties of HPC is attributed to the use of the cementitious materials such as silica fume and fly ash along with the chemical admixtures, high range water reducing admixtures.

4-7-2 Durability Indices

High performance concrete (HPC) has proven its effectiveness throughout this research by developing some superior durability characteristics such as surface resistivity, rapid chloride permeability, and free shrinkage. The test results indicate that HPC had less free shrinkage and permeability compared to concrete class A, while developing a significant surface resistivity. Table (4-9) below illustrates the improvement ratios of durability indices at age of 90 days.

Table 4-9 Durability Properties of Concretes

Durability properties	Concrete Class A	HPC	Increment Ratio (%)
Surface Resistivity	12.5	151	1000%
Rapid Chloride permeability	330	3000	800%
Free Shrinkage	-725	-478	34%

The superior durability properties of HPC comes from fact that the cementitious material interact with the hydration products of cement to produce a dense microstructure of concrete. This reaction between the Silica fume, fly ash, and chemical admixtures leads to the cut of the continuity of the porosity and micro voids within the concrete mass.

4-7-3 Conclusion and Discussion of the Laboratory Corrosion Data

4-7-3-1 Corrosion Data of non-Sealed Prismatic Samples

Depending on the test results of the corrosion data obtained from the prismatic samples of corrosion, the following aspects have been concluded:

1- All samples didn't show any noticeable corrosion signals at age 5 months or earlier for concrete class A, and age 8 months for High performance concrete.

2- The corrosion rate increased with the progress of exposing age for all samples. The increment ratios are not constant and vary from month to month.

3- All samples developed different corrosion potentials, but the black steel has the highest corrosion potentials which indicates to high corrosion activity.

4- Compared with MMFX, Epoxy Coated Rebars have low corrosion invitation. This reduction is attributed to the debond of the Coating layer from the steel surface [R.E. Weyers 1995] which make the rebars more vulnerable to corrosion. This result is with good agreement with others [128.B.S. Covino Jr. 2000].

5- The MMFX has a high corrosion resistance compared to Black Steel, Epoxy Coated, and Stainless Steel at all ages and exposing conditions. The improvement ratio at exposing age of 33 months is 63 % compared to black steel of un cracked concrete samples class A.

6- The Epoxy Coated and Stainless Steel rebars developed a very good corrosion resistance compared to Black Steel; the improvement ratios are 37% and 54% respectively.

7- The crack width has a slight effect on corrosion potentials while the crack depth has a significant effect. For example, if we increase the crack width from .011" to .035" for the same depth (0.5"), the increment ratios of corrosion potentials are 12, 7, 2, and 22% respectively. While if we increase the crack depth from .5" to 1" or the same width (.011), the corrosion potentials increment ratios are 10, 10, 10, and 29 % respectively.

8- At age of 33 months, the high sodium chloride concentration (15%) shows a high risk of corrosion compared to low sodium chloride concentration (3%). For instance, the corrosion potentials are 755, 442, 312, and 268 for the cracked samples of Black Steel, Epoxy Coated, and MMFX respectively exposed to 3% of NaCl. These values become 819, 481, 368, and 297 when we use 15% of NaCl for the same concretes. This conclusion is applicable also for all cracked corrosion samples.

9- The HPC concrete develops a high corrosion resistance compared to concrete class A at all ages and crack patterns.

10- The HPC has superior corrosion resistance up to age of 33 months, where there is no noticeable corrosion activity for all samples of EC, SS, and MMFX; they showed a very low corrosion probability compared to concrete class A.

11- The corrosion threshold (initiation) differs from conditions to other depending on the concrete and steel reinforcement types, crack patterns, and chloride solution concentrations. The corrosion threshold (initiation) for different scenarios of exposing conditions are tabulated in table (4-10) below. From this table the following aspects can be concluded:

i. The Stainless Steel and MMFX have superior corrosion resistance. Whereas exposing age of 33 months, there is no corrosion initiation.

ii. The corrosion threshold of uncracked concrete class A with Black Steel starts after 24 and 22 months of exposure when subjected to 3 and 15 % of NaCl respectively. The corrosion threshold of Epoxy Coated concrete starts after 31 and 30 months for the same conditions.

iii. For concrete class A, when increasing the crack width to .035” and depth to 1”, the corrosion threshold value decreases approximately one third; the corrosion threshold is 16 months only. While the corrosion threshold of Epoxy Coated concrete diminishes to 25 months compared to Black Steel for the same conditions.

iv. All HPC samples don’t show any corrosion threshold even after 33 months of exposure.

4-7-3-2 Corrosion Data of the Sealed Prismatic Samples

The compression of the efficiency of the two types of crack sealants regarding the steel reinforcement types is plotted in the figure (4-58) below. A conclusion could be drawn as following:

1- The sealed corrosion prisms still have low corrosion activities even after subjected to 22 months of exposure of 15% of NaCl.
2- The samples which have the longitudinal cracks developed noticeable corrosion signals compared with those have the transverse cracks.
3- Both sealant T-70 MX and Seal Krete are considered a very good crack sealer, but the T-70 MX has a superior corrosion resistance compared with the Seal Krete.
4- When we use the crack sealant, T-70 MX, for The Epoxy Coated concrete samples, the potentials improvement ratios are 36 and 52% in the longitudinal and transverse cracks directions at exposing age of 22 months. While the improvement ratios are 29 and 40% if we use the other crack sealant, Seal Crete, for the same conditions.

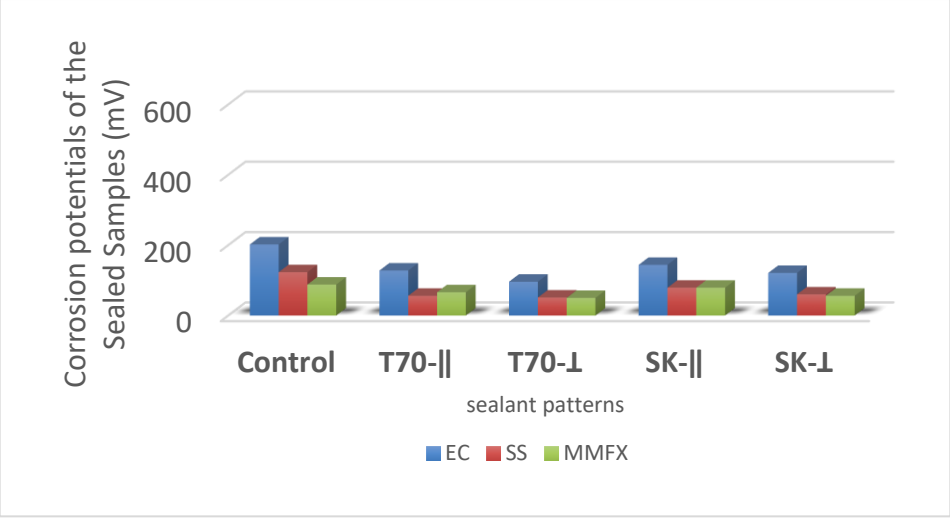

Figure 4–55 Performances of the Crack Sealants

Table 4-10 Crack Influences on the Corrosion Process

Scenario	Corrosion Threshold Exposing Age (Months)		Scenario	Corrosion Threshold Exposing Age (Months)	
	3% NaCl	15 % NaCl		3% NaCl	15 % NaCl
A- BS-No cracks	24	22	---	---	
A- EC-No cracks	31	30	---	---	
A- SS-No cracks	---	---	---	---	
A- MMFX-No cracks	---	---	---	---	
A- BS- 0.011”- 0.5”	22	21	HPC- BS- 0.011”- 0.5”	---	
A- EC- 0.011”- 0.5”	29	29	HPC - EC- 0.011”- 0.5”	---	
A- SS- 0.011”- 0.5”	---	---	HPC - SS- 0.011”- 0.5”	---	
A- MMFX- 0.011”- 0.5”	---	---	HPC - MMFX- 0.011”- 0.5”	---	
A- BS- 0.011”- 1”	19	17	HPC - BS- 0.011”- 1”	---	
A- EC- 0.011”- 1”	26	25	HPC - EC- 0.011”- 1”	---	
A- SS- 0.011”- 1”	---	---	HPC - SS- 0.011”- 1”	---	
A- MMFX- 0.011”- 1”	---	---	HPC - MMFX- 0.011”- 1”	---	
A- BS- 0.035”- 0.5”	19	18	A- BS- 0.035”- 0.5”	---	
A- EC- 0.035”- 0.5”	26	27	A- EC- 0.035”- 0.5”	---	
A- SS- 0.035”- 0.5”	---	---	A- SS- 0.035”- 0.5”	---	
A- MMFX- 0.035”- 0.5”	---	---	A- MMFX- 0.035”- 0.5”	---	
A- BS- 0.035”- 1”	16	16	A- BS- 0.035”- 1”	---	
A- EC- 0.035”- 1”	25	24	A- EC- 0.035”- 1”	---	
A- SS- 0.035”- 1”	---	30	A- SS- 0.035”- 1”	---	
A- MMFX- 0.035”- 1”	---	---	A- MMFX- 0.035”- 1”	---	

4-7-3-3 Corrosion Data of the Slab Samples

1- The corrosion potentials of slabs (ASTM G-109) are still very low or vanish until age of 22 months.
2- Approximately all reinforcements have the same corrosion potentials and currents. This is because the reinforcements attributed to 2.5 inches concrete.
3- The deeper the crack, the more corrosion probability for all slabs.
4- The concrete crack sealer, T70 MX performs a very good corrosion resistance so far.
5- Depending on the corrosion map, the most sever corrosion occurs close to the edges or the rims rather than the slab center. I think this is attributed to the fact that the edges adsorb and evaporate the sodium chloride faster than the slab center.

4-8 Corrosion Autopsy

After the end of the test duration, the highest corrosion potentials samples were broken in order visually examine the corrosion effects on the steel reinforcement. The corrosion autopsy proves that following:

i. The samples that reinforced with Black Steel underwent a serious corrosion damage on the rebars surface. It is clearly showed that the corrosion products (rust) built up on the surface of the rebars. Also, the surrounding concrete in the intermediate zoon between the steel reinforcing bars and the cement matrix was partially disintegrated.
ii. The samples that reinforced with Epoxy Coated rebars had a noticeable corrosion rust without any damage in the intermediate zoon.

iii. The samples that reinforced with Stainless Steel and MMFX rebars didn't show any corrosion products on the reinforcing steel surface neither a damage in the cement matrix.

This result proves the point of view of the corrosion parameters that were measured during the exposing age such as potentials and currents. The following figure (4-56) illustrates the corrosion autopsy and visual examination of corrosion samples.

Figure 4–56 Autopsy and Visual Examination of Corrosion

5. Chapter Five

Field Work

5-1 General

In 1998 and 1999 the State of New Jersey constructed two bridges on the Garden State Parkway, GSP. The first bridge, 84.1 A, is located in the southern part of New Jersey while the other one, 159.7, is in northern New Jersey. Thus, in order to structurally monitor the serviceability and stability of these bridges, the NJHA installed sets of advanced generation of sensors, MEP's, within the reinforced concrete bridge decks. The MEP's are able to monitor the corrosion activities such as potentials, currents, concrete resistivity, corrosion rate, LRP, and inside bridge deck temperature. Since then, the corrosion process was monitored, and the corrosion data measured on the annual basis.

Fortunately, these two bridges are included in the current research. The corrosion data for 20 years is suitable to correlate with the lab performance. To get the correlation process as close as possible and eliminate the variables, we simulated the bridge decks in the lab. So, we use the same concrete mixes, reinforcement types, material characteristics, and exposure conditions.

5-2 Field Study

The other part of the research deals with monitoring the structural health of two real bridges. These bridges were constructed on the Garden State Parkway in 1998 and 1999. Following are the details of these bridges:

5-2-1 Bridge 84.1 A

This is a 2-Span continuous bridge highly skewed deck. It has 263 ft. long and 38 ft. wide. This bridge constructed with Galvanized steel reinforcement and high performance concrete (HPC), and located in South New Jersey, Figure (5-1) and (5-2).

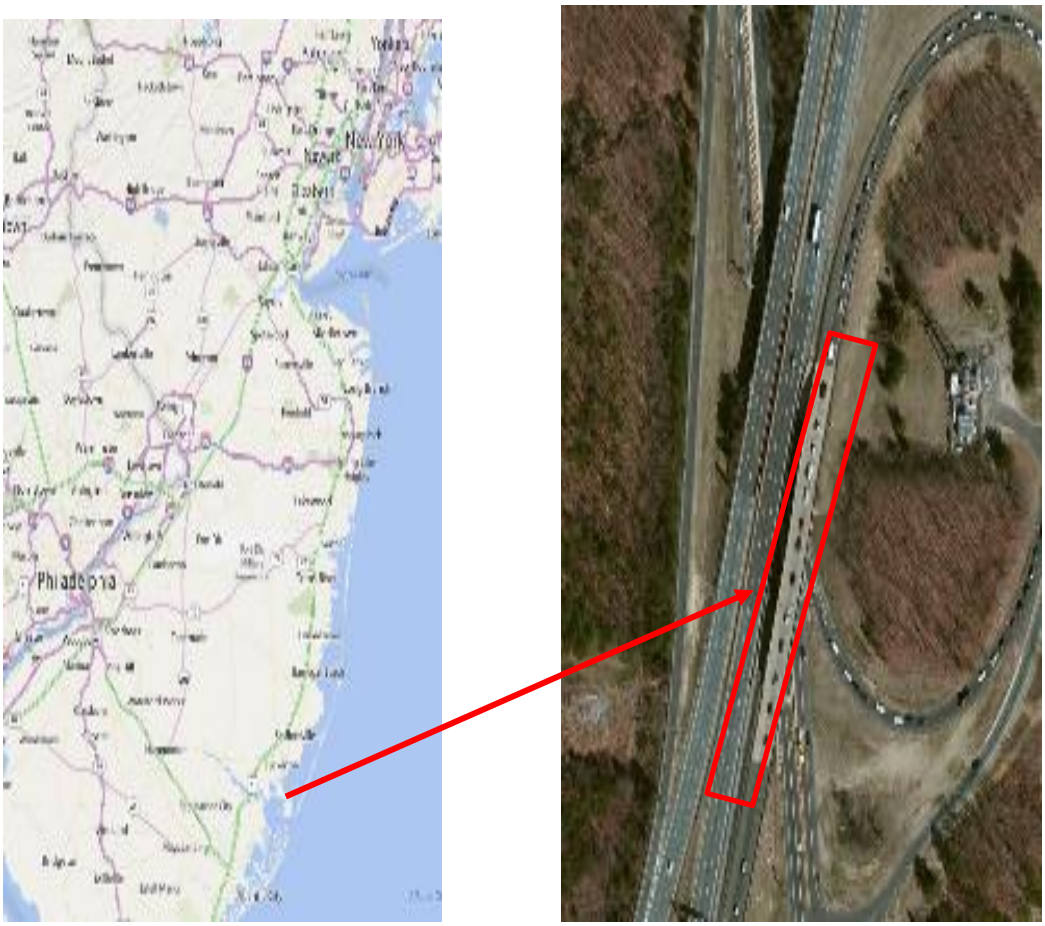

A (B)

Figure 5–1 Bridge 84.1 A, (A) the Location, and (B) the Top View

Figure 5–2 Field Corrosion Measurement of Bridge 84.1A

5-2-1-1 Corrosion Sensors Layout of Bridge 84.1 A

A total of 25 multi-function probes were attached to the top mat of steel prior to pouring the deck. Readings from these probes can be taken at 5 junction boxes cast into the west fascia barrier (figure 5-3). A series of five tests, potential, corrosion current, concrete resistivity, corrosion rate, and deck temperature are to be taken on a yearly basis. Once deterioration begins, a sixth test, linear polarization resistance (LPR), is to be performed. Figure (5-4) below shows the layout of sensors of bridge 84.1 A; 6 MEPs at 4

locations (B1 through B4) and 1 MEP at 1 location (B5), while figure (5-5) illustrates the MEPs inside of the corrosion monitoring boxes.

Figure 5–3 Junction Boxes on the West Fascia Barrier of Bridge 84.1A

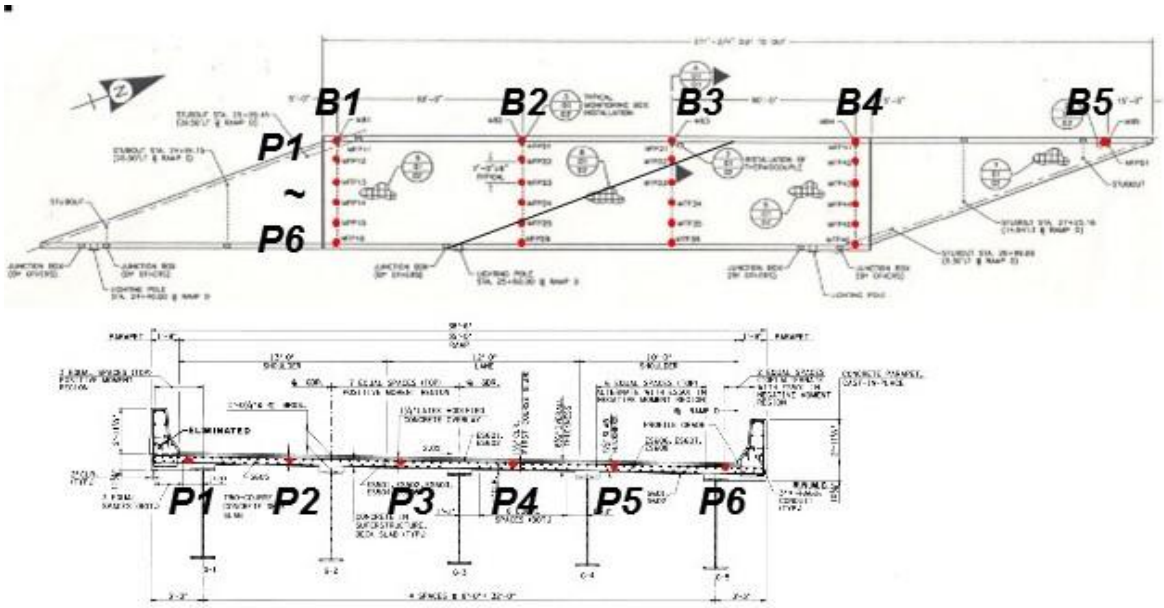

Figure 5–4 Corrosion Sensors Layout of Bridge 84.1 A

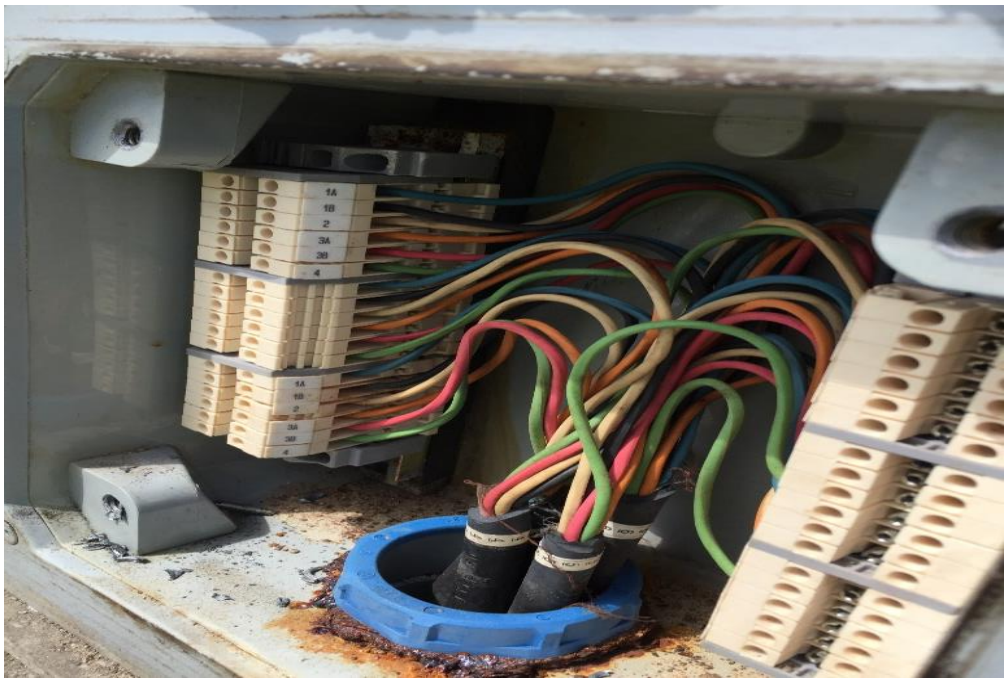

Figure 5–5 Monitoring Box of Six MEP Sensors Placed in the Parapet of the Bridge

5-2-2 Bridge 159.7

This bridge is located on the Garden State Parkway (GSP) north. This bridge was constructed in 1998 as a new ramp to I-80 EB. This bridge is 8-Span continuous highly curved bridge. It was constructed with Duplex 2205 (318) SS and high performance concrete. Figures (5-5) and (5-6) show bridge location, while figures (5-7) and (5-8) illustrate sensors layout and monitoring box.

(A) (B)

Figure 5–6 Annual Corrosion Measurements of Bridge 159.7

Figure 5–7 Bridge 159.7 (A) the Location, and (B) the Top View

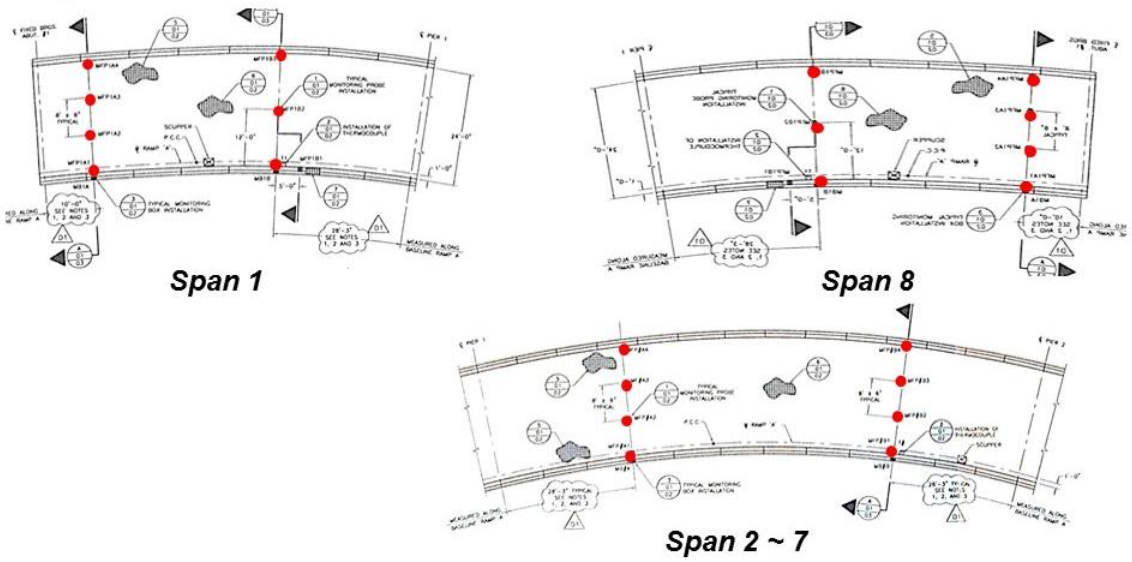

Figure 5–8 Sensors Layout of Bridge 159.7

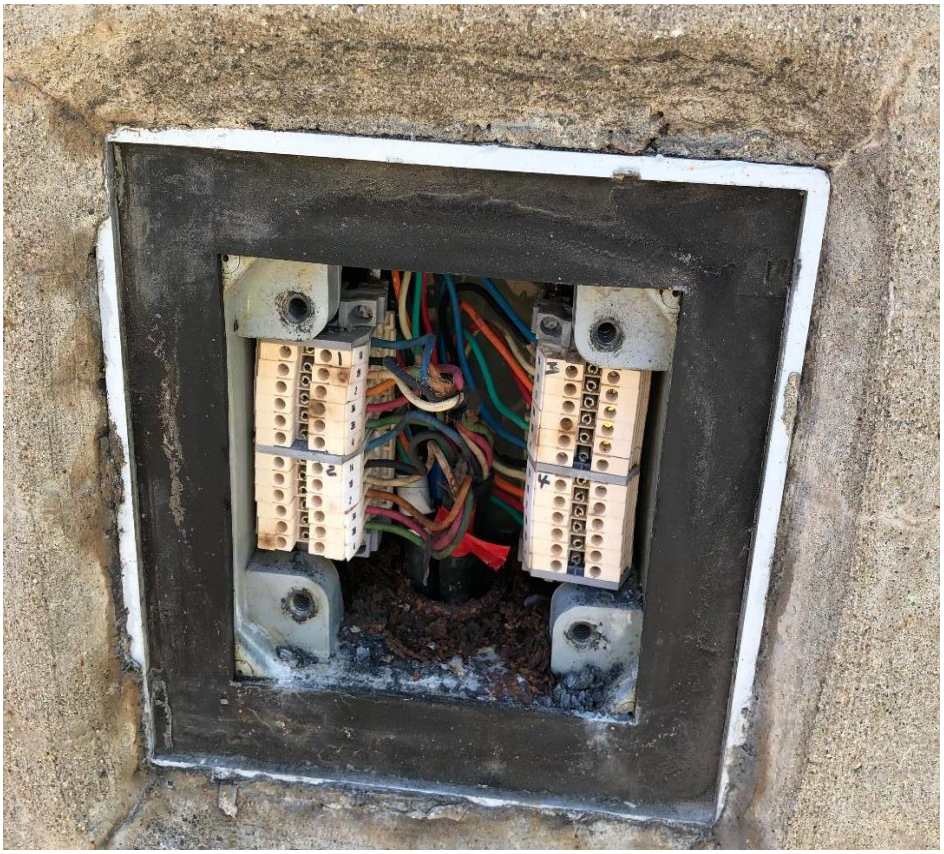

Figure 5–9 Corrosion Monitoring Box, 4 MEPs of Bridge 159.7

5-3 Results

The field work includes the corrosion data that was collected from the two existing bridges on the Garden State Parkway, 84.1 and 159.7. All corrosion tests which include corrosion potentials, corrosion current, corrosion rate, concrete resistivity, and bridge deck inside temperature are measured through the corrosion monitoring multi element sensor which was installed inside the bridge decks. For the two bridges the following tolls are used to maintain the aforementioned test parameters: Zero Resistance Ammeter, Nilsoon Resistance Meter model 400, Pronto Digital Thermometer, and Multimeter.

5-3-1 Corrosion Data of the Field Work

5-3-1-1 Bridge 84.1 A:

5-3-1-1-1 Corrosion Potentials of Bridge 84.1

The potentials (voltage) were measured by connecting a high resistance voltmeter between the carbon steel working electrode and the MnO2 as reference electrode in the monitoring boxes of the MEP'S. The potentials of corrosion potentials of bridge 84.1 that were monitored from 1998 to 2018 are illustrated in table (5-1) and plotted in figure (5-9) below. All values are volts.

Table 5-1 Corrosion Potentials of Bridge 84.1 (May 1998 through June 2018)

May, 1998	B1	B2	B3	B4	B5	Average per Probe-line
P1	-0.27	-0.24	-0.45	-0.26	-0.29	-0.30
P2	-0.55	-0.51	-0.33	-0.44		-0.46
P3	-0.33	-0.38	-0.29	-0.48		-0.37
P4	-0.27	-0.36	-0.45	-0.27		-0.34
P5	-0.24	-0.45	-0.31	-0.27		-0.32
P6	-0.26	-0.30	-0.29	-0.32		-0.29
Average per Span-line	-0.32	-0.37	-0.35	-0.34	-0.29	-0.34
Nov, 1999						Average per Probe-line
P1	-0.18	-0.31	-0.95	-0.21	-0.24	-0.38
P2	-0.51	-0.63	-0.22	-0.62		-0.49
P3	-0.61	-0.50	-0.24	-0.52		-0.47
P4	-0.19	-0.57	-0.47	-0.20		-0.36
P5	-0.12	-0.55	-0.24	-0.20		-0.28
P6	-0.16	-0.21	-0.22	-0.17		-0.19
Average per Span-line	-0.29	-0.46	-0.39	-0.32	-0.24	-0.36

Continue table (5-1) Corrosion Potentials of Bridge 84.1 (May 1998 through June 2018)

Jul, 2013	B1	B2	B3	B4	B5	Average per Probe-line
P1	-0.26	-0.39	-0.03	-0.15	-0.64	-0.29
P2	-0.67	-0.77	-0.17	-0.55		-0.54
P3	-0.61	-0.18	-0.23	-0.53		-0.39
P4	-0.30	-0.53	-0.57	-0.36		-0.44
P5	-0.13	-0.70	-0.50	-0.28		-0.40
P6	-0.17	-0.13	-0.14	-0.22		-0.16
Average per Span-line	-0.35	-0.45	-0.27	-0.35	-0.64	-0.37
May, 2016						Average per Probe-line
P1	-0.40	-0.17	-0.27	-0.14	-0.42	-0.28
P2	-0.65	-0.72	-0.15	-0.59		-0.53
P3	-0.59	-0.35	-0.18	-0.30		-0.35
P4	-0.19	-0.45	-0.64	-0.39		-0.42
P5	-0.11	-0.65	-0.48	-0.38		-0.40
P6	-0.16	-0.11	-0.12	-0.21		-0.15
Average per Span-line	-0.35	-0.41	-0.31	-0.33	-0.42	-0.35

Continue table (5-1) Corrosion Potentials of Bridge 84.1 (May 1998 through June 2018)

June, 2017	B1	B2	B3	B4	B5	Average per Probe-line
P1	-0.47	-0.21	-0.06	-0.14	-0.42	-0.26
P2	-0.63	-0.68	-0.16	-0.65		-0.53
P3	-0.60	-0.33	-0.20	-0.17		-0.32
P4	-0.22	-0.50	-0.62	-0.39		-0.43
P5	-0.11	-0.68	-0.43	-0.31		-0.38
P6	-0.14	-0.10	-0.13	-0.53		-0.23
Average per Span-line	-0.36	-0.42	-0.27	-0.37	-0.42	-0.36
June, 2018						Average per Probe-line
P1	-0.244	-0.400	0.000	-0.305	0.42	-0.106
P2	-0.36	-0.300	-0.360	-0.420		-0.360
P3	-0.26	-0.215	-0.405	0.000		-0.220
P4	-0.23	-0.220	-0.410	-0.444		-0.326
P5	-0.323	-0.240	-0.266	-0.310		-0.285
P6	-0.315	-0.260	-0.331	-0.355		-0.315
Average per Span-line	-0.289	-0.273	-0.295	-0.306	0.42	

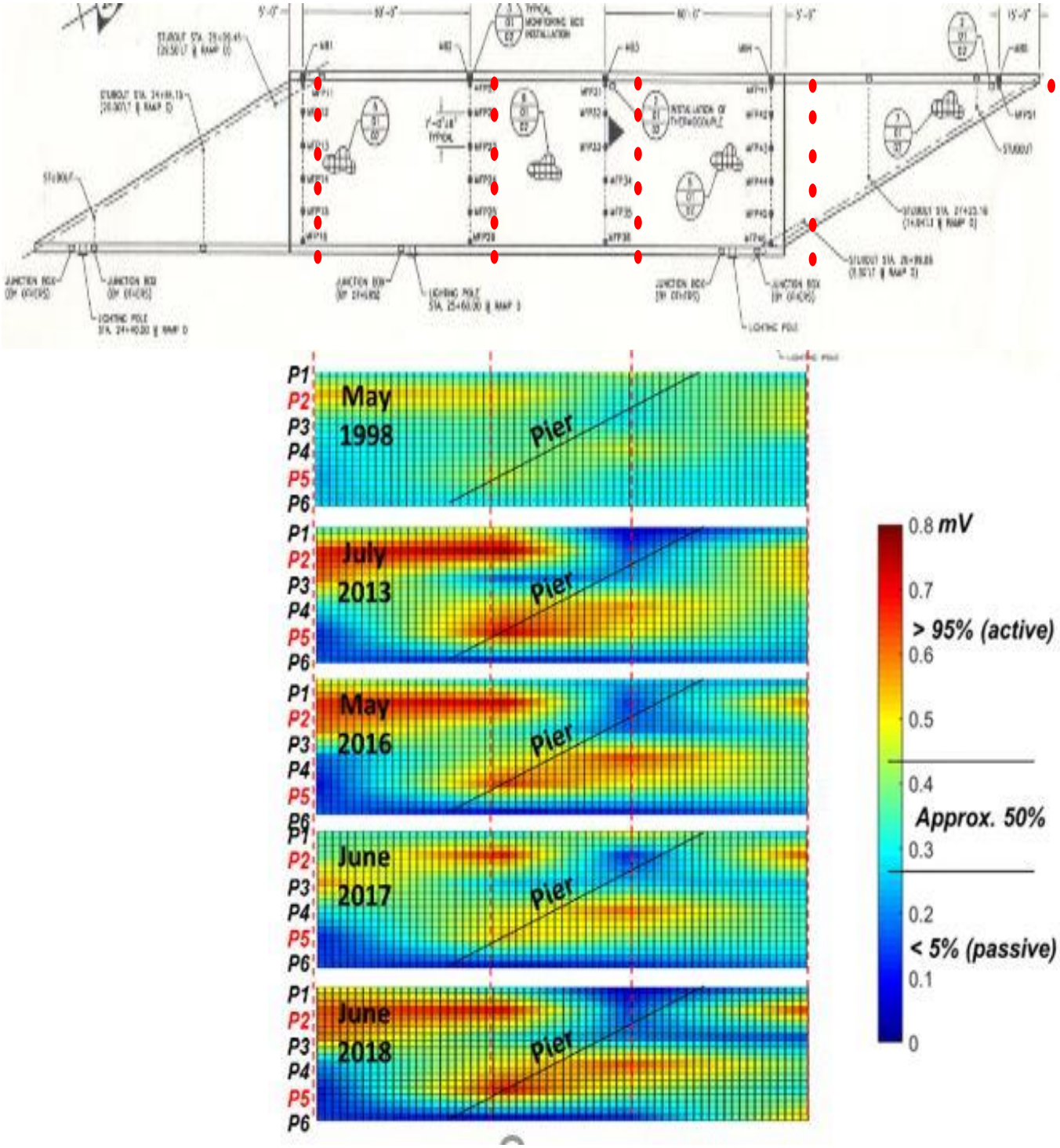

Figure 5–10 Corrosion Potentials of Bridge 84.1 (May 1998 through June 2018)

5-3-1-1-2 Corrosion Currents of Bridge 84.1

The current was measured by connecting the Zero resistance ammeter between the carbon steel working electrode and the stainless steel as counter electrode. Then connect the High resistance voltmeter to the output measurement jack. The corrosion current values are presented in table (5-2).

Table 5-2 Corrosion Currents of Bridge 84.1(May 1998 through June 2018)

May 1998	B1	B2	B3	B4	B5
P1	0.10	-0.40	0.70	0.00	0.00
P2	1.40	0.25	0.20	-0.10	
P3	0.10	0.50	0.15	1.20	
P4	0.10	0.20	1.00	0.10	
P5	0.00	-0.80	0.15	0.00	
P6	0.00	0.35	0.00	0.30	
Average per Span-line	0.28	0.42	0.37	0.28	0.00
Nov 1999					
P1	0.20	0.10	11.8?	0.50	0.00
P2	0.70	1.60	0.00	1.50	
P3	2.00	0.80	0.00	0.30	
P4	0.50	1.50	0.30	0.10	
P5	1.60	0.50	0.70	0.40	
P6	0.00	0.10	0.10	0.10	
Average per Span-line	0.83	0.77	0.22	0.48	0.00

Continue Table (5-2) Corrosion Currents of Bridge 84.1(May 1998 through June 2018)

July 2013	B1	B2	B3	B4	B5
P1	0.30	0.20	1.70	0.40	0.60
P2	1.80	1.20	0.60	1.00	
P3	1.00	1.00	0.30	1.20	
P4	1.20	0.20	0.40	0.30	
P5	0.10	0.70	0.00	0.60	
P6	0.00	0.00	0.20	0.10	
Average per Span-line	0.73	0.55	0.53	0.60	0.60
May 2016					
P1	4.00	0.20	0.70	0.00	1.70
P2	5.80	6.60	0.10	3.30	
P3	7.40	0.40	0.10	3.70	
P4	0.10	0.80	5.00	0.80	
P5	0.10	3.70	1.50	0.40	
P6	0.00	0.00	0.00	1.00	
Average per Span-line	2.90	1.95	1.23	1.53	1.70

Continue Table (5-2) Corrosion Currents of Bridge 84.1(May 1998 through June 2018)

June 2017	B1	B2	B3	B4	B5
P1	3.60	0.00	0.60	0.20	1.70
P2	4.20	2.00	0.00	4.50	
P3	6.00	0.10	0.50	3.80	
P4	0.00	1.50	3.00	0.60	
P5	0.60	1.90	1.50	1.00	
P6	0.30	0.20	0.10	0.80	
Average per Span-line	2.45	0.95	0.95	1.82	1.70
June 2018					
P1	4.50	0.20	0.60	0.00	2.00
P2	1.00	5.50	0.10	4.00	
P3	4.60	0.50	0.10	1.90	
P4	0.70	2.90	4.50	2.00	
P5	0.10	6.50	1.50	0.50	
P6	0.00	0.40	0.00	1.80	
Average per Span-line	1.82	2.67	1.13	1.70	2.00

5-3-1-1-3 Corrosion Rate of Bridge 84.1, (mpy)

The corrosion rate of bridge (84.1 A) was computed by using the following equation:

Corrosion rate (mpy) = 0.045 × corrosion current (μA). The test results are included in table (5-3) and plotted in figure (5-10) below.

Table 5-3 Corrosion Rate of Bridge 84.1(May 1998 through June 2018)

Corrosion rate (mpy)	B1	B2	B3	B4	B5
May 1998					
P1	0.00	0.00	0.03	0.00	0.00
P2	0.06	0.01	0.01	0.00	
P3	0.00	0.02	0.01	0.05	
P4	0.00	0.01	0.05	0.00	
P5	0.00	0.00	0.01	0.00	
P6	0.00	0.02	0.00	0.01	
Average per Span-line	0.01	0.01	0.02	0.01	0.00
Nov 1999					
P1	0.01	0.00	0.00	0.02	0.00
P2	0.03	0.07	0.00	0.07	
P3	0.09	0.04	0.00	0.01	
P4	0.02	0.07	0.01	0.00	
P5	0.07	0.02	0.03	0.02	
P6	0.00	0.00	0.00	0.00	
Average per Span-line	0.04	0.03	0.01	0.02	0.00

Continue able (5-3) Corrosion Rate of Bridge 84.1(May 1998 through June 2018)

Corrosion rate (mpy)	B1	B2	B3	B4	B5
July 2013					
P1	0.01	0.01	0.08	0.02	0.03
P2	0.08	0.05	0.03	0.05	
P3	0.05	0.05	0.01	0.05	
P4	0.05	0.01	0.02	0.01	
P5	0.00	0.03	0.00	0.03	
P6	0.00	0.00	0.01	0.00	
Average per Span-line	0.03	0.02	0.02	0.03	0.03
May 2016					
P1	0.18	0.01	0.03	0.00	0.08
P2	0.26	0.30	0.00	0.15	
P3	0.33	0.02	0.00	0.17	
P4	0.00	0.04	0.23	0.04	
P5	0.00	0.17	0.07	0.02	
P6	0.00	0.00	0.00	0.05	
Average per Span-line	0.13	0.09	0.06	0.07	0.08

Continue able (5-3) Corrosion Rate of Bridge 84.1(May 1998 through June 2018)

Corrosion rate (mpy)	B1	B2	B3	B4	B5
June 2017					
P1	0.16	0.00	0.03	0.01	0.08
P2	0.19	0.09	0.00	0.20	
P3	0.27	0.00	0.02	0.17	
P4	0.00	0.07	0.14	0.03	
P5	0.03	0.09	0.07	0.05	
P6	0.01	0.01	0.00	0.04	
Average per Span-line	0.11	0.04	0.04	0.08	0.08
June 2018					
P1	0.20	0.01	0.03	0.00	0.09
P2	0.05	0.25	0.00	0.18	
P3	0.21	0.02	0.00	0.09	
P4	0.03	0.13	0.20	0.09	
P5	0.00	0.29	0.07	0.02	
P6	0.00	0.02	0.00	0.08	
Average per Span-line	0.08	0.12	0.05	0.08	0.09

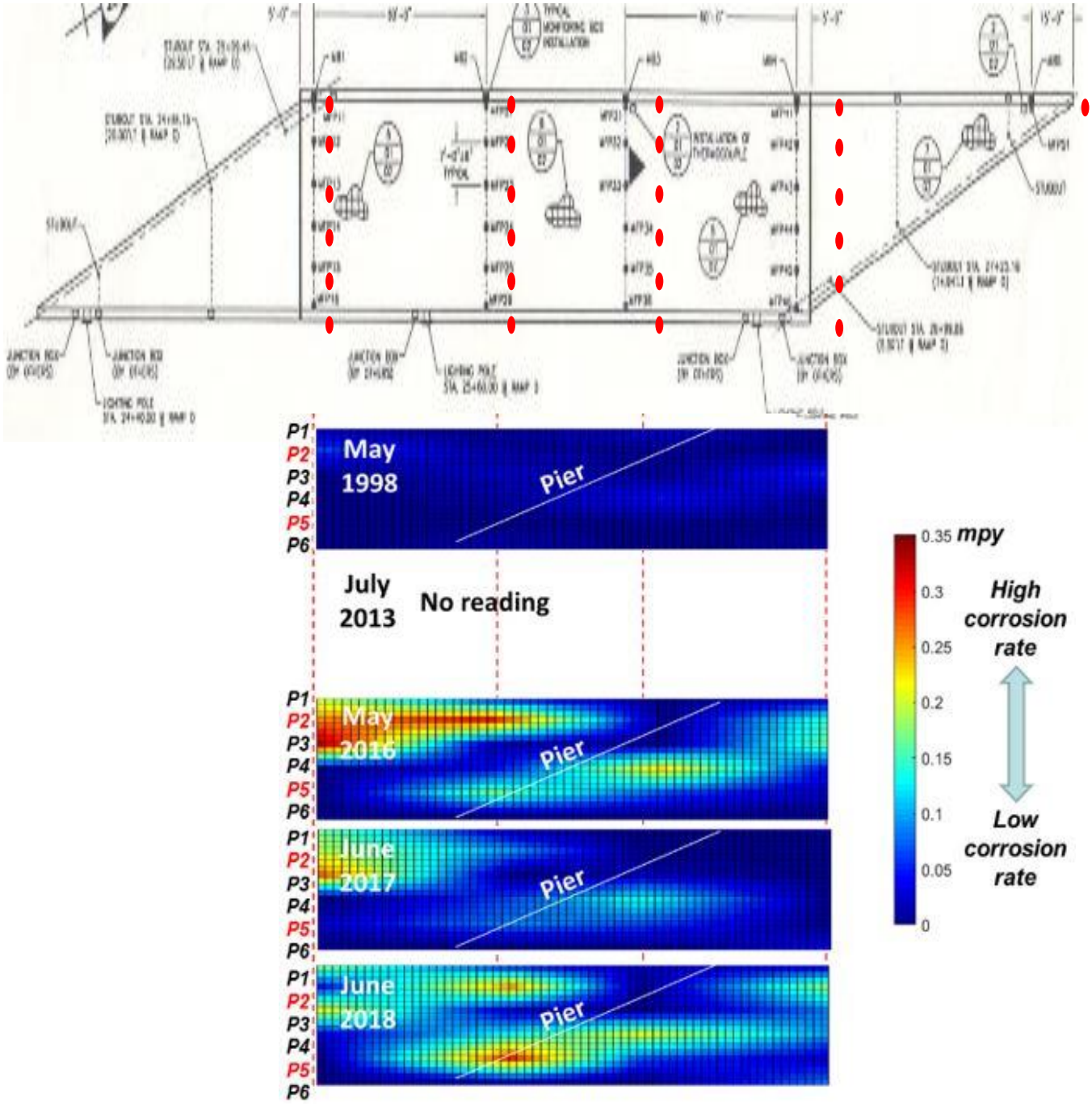

Figure 5–11 Corrosion Rate of Bridge 84.1(May 1998 through June 2018)

5-3-1-1-4 Concrete Resistivity of Bridge 84.1, (kohm-cm)

This test was carried out to monitor the resistivity of the concrete bridge deck in order to assess the depth of chloride contamination and moisture penetration. The test measured by connecting the Earth resistance meter props to the carbon steel sensor electrode, carbon steel working electrode, and the stainless steel. The test results are summarized in table (5-4) below and plotted in figure (5-11).

Table 5-4 Concrete Resistivity (kohm-cm) of Bridge 84.1(May 1998 - June 2018)

May 1998	B1	B2	B3	B4	B5
P1	70	64	39	109	56
P2	40	54	59	41	
P3	46	50	53	43	
P4	89	43	52	59	
P5	70	39	59	60	
P6	84	58	60	61	
Average per Span-line	67	51	54	62	56
Nov 1999					
P1	230	89	70	283	133
P2	84	80	172	75	
P3	89	89	167	70	
P4	317	70	80	177	
P5	235	75	123	177	
P6	351	99	240	162	
Average per Span-line	218	84	142	157	133

Continue table (5-4) Concrete Resistivity (kohm-cm) of Bridge 84.1(May 1998 through June 2018)

July 2013	B1	B2	B3	B4	B5
P1	55	65	61	366	33
P2	41	47	109	41	
P3	47	48	80	39	
P4	64	49	56	14	
P5	206	49	64	133	
P6	278	64	215	41	
Average per Span-line	115	54	98	106	33
May 2016					
P1	84	118	104	160	46
P2	48	160	160	36	
P3	58	56	118	29	
P4	104	67	59	84	
P5	63	60	67	123	
P6	65	109	160	46	
Average per Span-line	70	95	111	80	46

Continue able (5-4) Concrete Resistivity (kohm-cm) of Bridge 84.1(May 1998 through June 2018)

June 2017	B1	B2	B3	B4	B5
P1	65	54	46	160	54
P2	60	65	58	55	
P3	70	60	55	65	
P4	63	63	60	65	
P5	46	70	65	70	
P6	42	46	70	63	
Average per Span-line	58	60	59	80	54
June 2018					
P1	65	54	46	160	54
P2	60	65	58	55	
P3	70	60	55	65	
P4	63	63	60	65	
P5	46	70	65	70	
P6	42	46	70	63	
Average per Span-line	58	60	59	80	54

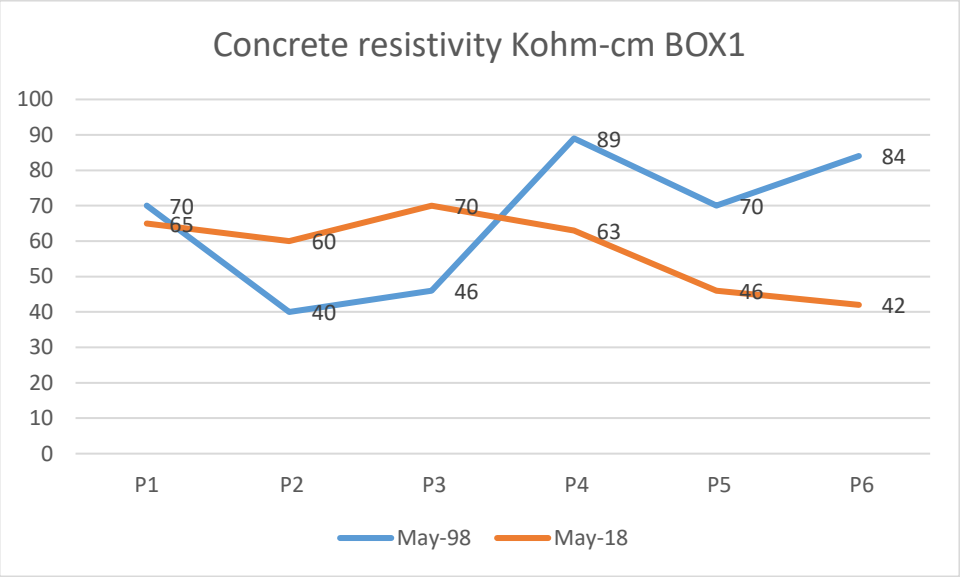
Concrete resistivity Kohm-cm BOX1
100
90
80
70
60
50
40
30
20
10
0
P1
P2
P3
P4
P5
P6
May-98
May-18
70
40
46
89
70
84
65
60
70
63
46
42

(A)

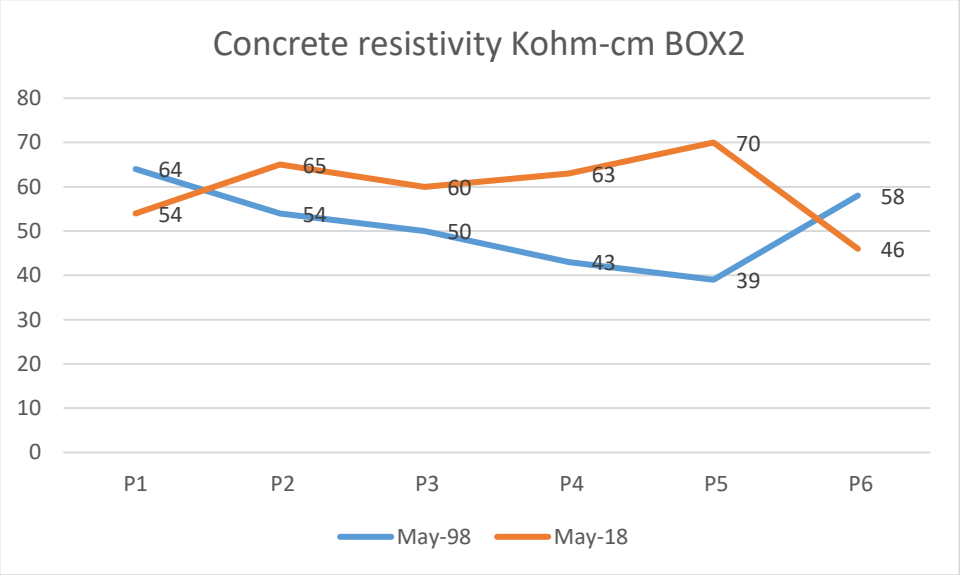
Concrete resistivity Kohm-cm BOX2
80
70
60
50
40
30
20
10
0
P1
P2
P3
P4
P5
P6
May-98
May-18
64
54
50
43
39
58
54
65
60
63
70
46

(B)

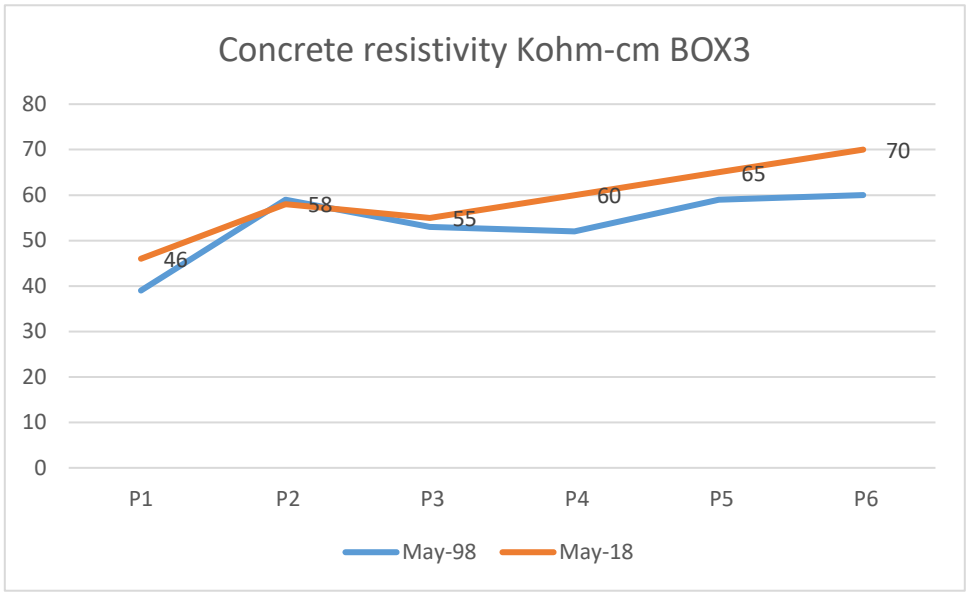

(C)

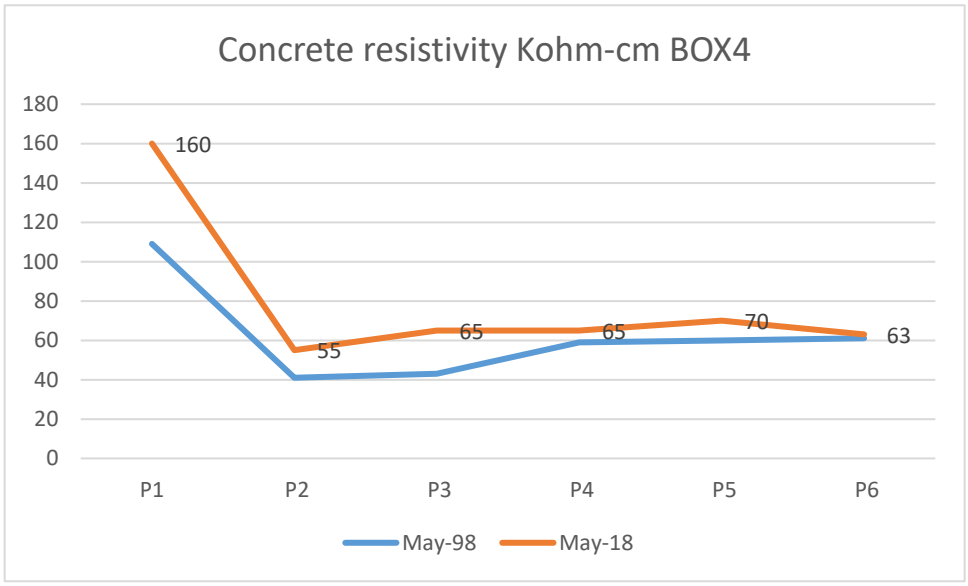

(D)

Figure 5–12 Concrete Resistivity of Bridge 84.1(May 1998 through June 2018)

5-3-1-2 Bridge 159.7

5-3-1-2-1 Corrosion Potentials

Table 5-5 Corrosion Potentials, Volts, of Bridge 159.7 (Dec. 1998 through June 2018)

Bridge 159.7	S1		S2		S3		S4		S5		S6		S7		S8		
	A	B	A	B	A	B	A	B	A	B	A	B	A	B	A	B	
Dec, 1998																	
1	-0.37	-0.31	-0.31	-0.35	-0.38	-0.35	-0.33	-0.36	-0.33	-0.39	-0.38	-0.34	-0.36	-0.41	-0.27	-0.33	-0.35
2	-0.33	-0.34	-0.38	-0.33	-0.41	-0.35	-0.37	-0.35	-0.37	-0.35	-0.44	-0.36	-0.44	-0.40	-0.33	-0.31	-0.36
3	-0.28	-0.34	-0.33	-0.41	-0.34	-0.35	-0.40	-0.39	-0.35	-0.32	-0.39	-0.36	-0.44	-0.34	-0.33	-0.31	-0.35
4	-0.34	-0.36	0.00	-0.41	-0.38	-0.35	-0.41	-0.37	-0.37	-0.36	-0.35	-0.39	-0.34	-0.32	-0.34	-0.35	-0.34
Average per Span line	-0.33	-0.34	-0.25	-0.37	-0.38	-0.35	-0.38	-0.37	-0.35	-0.35	-0.39	-0.36	-0.39	-0.37	-0.32	-0.32	-0.35

Continue table (5-5) Corrosion Potentials of Bridge 159.7 (Dec. 1998 through June 2018)

Bridge 159.7	S1		S2		S3		S4		S5		S6		S7		S8		
	A	B	A	B	A	B	A	B	A	B	A	B	A	B	A	B	
Nov. 1999																	
1	-0.19	-0.21	-0.19	-0.24	-0.20	-0.24	-0.19	-0.20	-0.23	-0.19	-0.21	-0.24	-0.32	-0.22	-0.20	-0.24	-0.22
2	-0.18	-0.19	-0.18	-0.16	-0.19	-0.18	-0.19	-0.19	-0.19	-0.19	-0.34	-0.20	-0.34	-0.30	-0.22	-0.15	-0.21
3	-0.27	-0.19	-0.18	-0.26	-0.18	-0.16	-0.21	-0.26	-0.21	-0.22	-0.29	-0.17	-0.34	-0.25	-0.22	-0.21	-0.23
4	-0.22	-0.18	0.00	-0.21	-0.23	-0.22	-0.21	-0.24	-0.24	-0.21	-0.32	-0.21	-0.31	-0.25	-0.21	-0.22	-0.22
Average per Span-line	-0.21	-0.19	-0.14	-0.22	-0.20	-0.20	-0.20	-0.22	-0.22	-0.20	-0.29	-0.20	-0.33	-0.25	-0.21	-0.21	-0.22

Continue table (5-5) Corrosion Potentials of Bridge 159.7 (Dec. 1998 through June 2018)

Bridge 159.7	S1		S2		S3		S4		S5		S6		S7		S8		
	A	B	A	B	A	B	A	B	A	B	A	B	A	B	A	B	
July 2013																	
1	-0.14	-0.25	-0.32	-0.26	-0.81	-0.03	-0.25	-0.13	-0.25	-0.22	-0.45	-0.30	-0.29	-0.22	-0.18	-0.14	-0.26
2	-0.18	-0.26	-0.19	-0.25	-0.27	-0.04	-0.28	-0.12	-0.21	-0.13	-0.30	-0.18	-0.29	-0.12	-0.22	-0.27	-0.21
3	-0.13	-0.26	-0.21	-0.22	-0.29	-0.16	-0.08	-0.29	-0.16	-0.21	-0.21	-0.20	-0.30	-0.19	-0.22	-0.06	-0.20
4	-0.04	-0.20	-0.08	-0.20	-0.20	-0.08	-0.09	-0.19	-0.12	-0.13	-0.28	-0.12	-0.27	-0.17	-0.33	-0.13	-0.16
Average per Span-line	-0.12	-0.24	-0.20	-0.23	-0.39	-0.08	-0.18	-0.18	-0.18	-0.17	-0.31	-0.20	-0.29	-0.17	-0.24	-0.15	-0.21

Continue table (5-5) Corrosion Potentials of Bridge 159.7 (Dec. 1998 through June 2018)

Bridge 159.7	S1		S2		S3		S4		S5		S6		S7		S8		
	A	B	A	B	A	B	A	B	A	B	A	B	A	B	A	B	
May 2016																	
1	-0.25	-0.25	-0.25	-0.18	-0.18	-0.01	-0.28	-0.06	-0.23	-0.33	-0.35	-0.24	-0.27	-0.26	-0.21	-0.10	-0.21
2	-0.14	-0.16	-0.15	-0.25	-0.25	-0.04	-0.18	-0.07	-0.31	-0.10	-0.26	-0.14	-0.26	-0.09	-0.23	-0.27	-0.18
3	-0.14	-0.16	-0.02	-0.12	-0.21	-0.13	-0.06	-0.29	-0.17	-0.18	-0.16	-0.14	-0.27	-0.49	-0.23	-0.08	-0.18
4	-0.01	-0.22	-0.08	-0.21	-0.15	-0.04	-0.08	-0.12	-0.05	-0.15	-0.28	-0.09	-0.26	-0.16	-0.25	-0.12	-0.14
Average per Span-line	-0.13	-0.20	-0.12	-0.19	-0.20	-0.06	-0.15	-0.13	-0.19	-0.19	-0.26	-0.15	-0.26	-0.25	-0.23	-0.14	-0.18

Continue table (5-5) Corrosion Potentials of Bridge 159.7 (Dec. 1998 through June 2018)

Bridge 159.7	S1		S2		S3		S4		S5		S6		S7		S8		
	A	B	A	B	A	B	A	B	A	B	A	B	A	B	A	B	
June 2017																	
1	-0.22	-0.26	-0.27	-0.17	-0.29	-0.02	-0.27	-0.08	-0.21	-0.23	-0.32	-0.27	-0.28	-0.27	-0.23	-0.33	-0.23
2	-0.30	-0.15	-0.15	-0.24	-0.26	-0.04	-0.27	-0.08	0.00	-0.10	-0.28	-0.14	-0.27	-0.06	-0.19	-0.27	-0.18
3	-0.15	-0.15	-0.01	-0.09	-0.21	-0.11	-0.03	-0.27	-0.15	-0.19	-0.16	-0.17	-0.30	-0.25	-0.06	-0.08	-0.15
4	-0.04	-0.23	-0.07	-0.21	-0.10	-0.07	-0.08	-0.12	-0.09	-0.16	-0.28	-0.09	-0.26	-0.16	-0.28	-0.14	-0.15
Average per Span-line	-0.18	-0.20	-0.12	-0.18	-0.21	-0.06	-0.16	-0.14	-0.11	-0.17	-0.26	-0.17	-0.28	-0.19	-0.19	-0.21	-0.18

Continue table (5-5) Corrosion Potentials of Bridge 159.7 (Dec. 1998 through June 2018)

Bridge 159.7	S1		S2		S3		S4		S5		S6		S7		S8		
	A	B	A	B	A	B	A	B	A	B	A	B	A	B	A	B	
June 2018																	
1	-0.29	-0.26	-0.36	-0.18	-0.28	-0.02	-0.43	-0.08	-0.26	-0.18	-0.31	-0.48	-0.27	-0.26	-0.22	-0.24	-0.26
2	-0.39	-0.15	-0.14	-0.23	-0.16	-0.03	-0.29	-0.09	0.00	-0.08	-0.25	-0.12	-0.25	-0.07	-0.22	-0.28	-0.17
3	-0.15	-0.15	0.04	0.03	-0.19	-0.10	-0.01	-0.28	-0.17	-0.18	-0.16	-0.13	-0.27	-0.21	-0.22	-0.09	-0.14
4	-0.38	-0.17	-0.08	-0.23	-0.08	-0.04	-0.08	-0.12	-0.05	-0.15	-0.27	-0.08	-0.25	-0.19	-0.25	-0.11	-0.16
Average per Span-line	-0.30	-0.18	-0.13	-0.15	-0.18	-0.05	-0.20	-0.14	-0.12	-0.15	-0.25	-0.20	-0.26	-0.18	-0.23	-0.18	-0.18

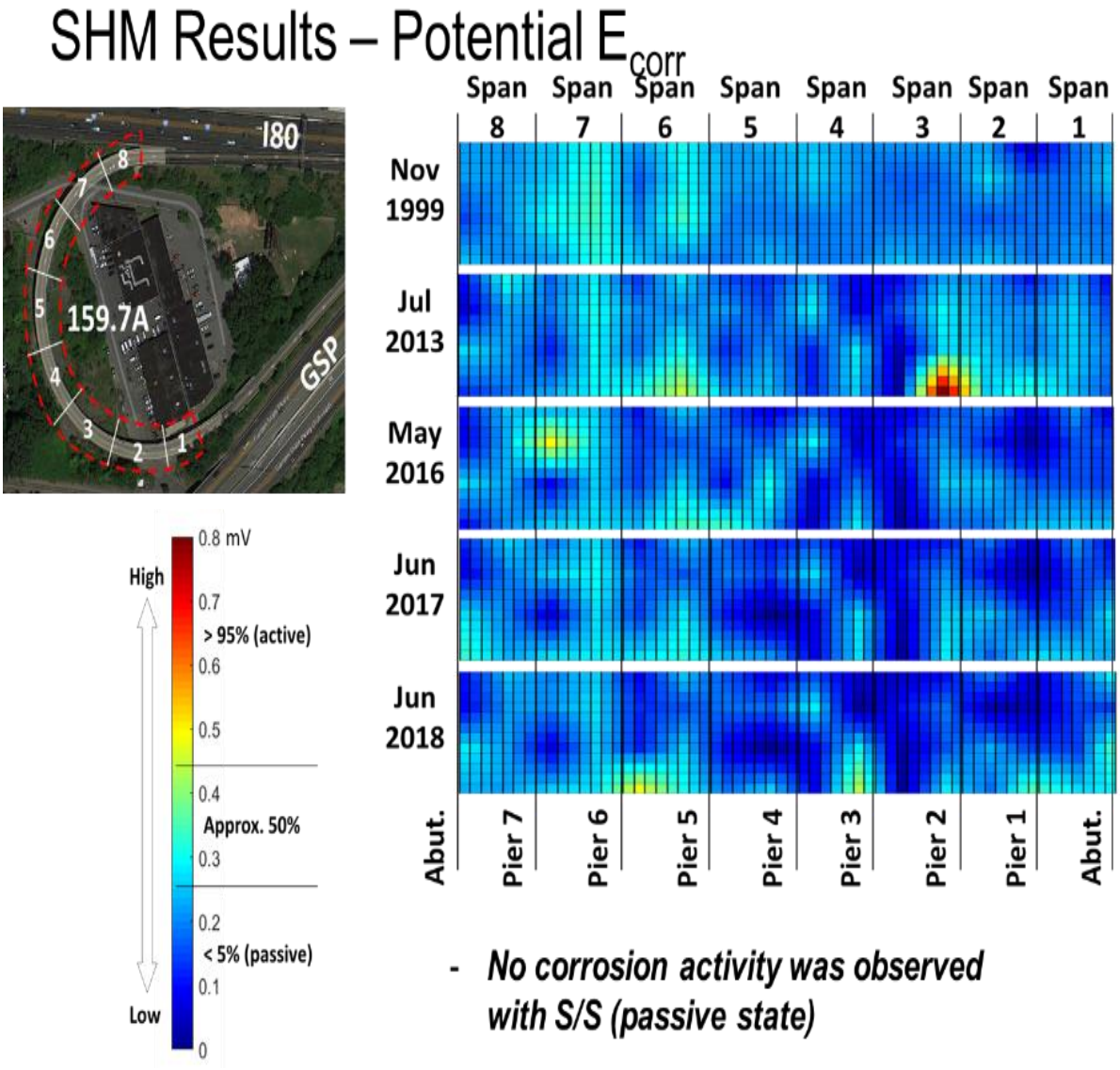

Figure 5–13 Corrosion Potentials of Bridge 159.7 (Dec. 1998 through June 2018)

5-3-1-2-2 corrosion Currents

The test results of corrosion currents are presented in table (5-6) below.

Table 5-6 Corrosion Currents of Bridge 159.7 (Dec. 1998 through June 2018)

Bridge 159.7	S1		S2		S3		S4		S5		S6		S7		S8		
	A	B	A	B	A	B	A	B	A	B	A	B	A	B	A	B	
Dec, 1998																	
1	0.00	0.10	0.20	0.20	0.20	0.50	0.00	0.40	0.20	0.60	0.30	0.20	0.30	0.40	0.10	0.10	0.24
2	0.10	0.10	0.20	0.20	0.60	0.30	0.50	0.40	0.00	0.20	0.50	0.20	0.80	0.40	0.10	0.00	0.29
3	0.00	0.10	0.10	0.40	0.10	0.30	0.60	0.40	0.20	0.10	0.10	0.10	0.60	0.00	0.10	0.10	0.21
4	0.20	0.40	0.10	0.30	0.30	0.20	0.30	0.40	0.20	0.20	0.40	0.30	0.10	0.10	0.20	0.50	0.26
Average per Span line	0.08	0.18	0.15	0.28	0.30	0.33	0.35	0.40	0.15	0.28	0.33	0.20	0.45	0.23	0.13	0.18	0.25

Continue table (5-6) Corrosion Currents of Bridge 159.7 (Dec. 1998 through June 2018)

Bridge 159.7	S1		S2		S3		S4		S5		S6		S7		S8		
	A	B	A	B	A	B	A	B	A	B	A	B	A	B	A	B	
Nov. 1999																	
1	0.00	0.00	0.10	0.10	0.10	0.20	0.10	0.00	0.10	0.10	0.00	0.10	0.50	0.10	0.00	0.20	0.11
2	0.20	0.20	0.10	0.00	0.00	0.10	0.00	0.20	0.00	0.10	0.40	0.00	0.70	0.00	0.00	0.00	0.13
3	0.10	0.20	0.10	0.30	0.10	0.20	0.00	0.20	0.10	0.20	0.10	0.10	0.40	0.10	0.00	0.00	0.14
4	0.10	0.10	0.10	0.10	0.10	0.10	0.10	0.20	0.00	0.00	0.40	0.20	0.40	0.20	0.10	0.10	0.14
Average per Span-line	0.10	0.13	0.10	0.13	0.08	0.15	0.05	0.15	0.05	0.10	0.23	0.10	0.50	0.10	0.03	0.08	0.13

Continue table (5-6) Corrosion Currents of Bridge 159.7 (Dec. 1998 through June 2018)

Bridge 159.7	S1		S2		S3		S4		S5		S6		S7		S8		
	A	B	A	B	A	B	A	B	A	B	A	B	A	B	A	B	
May 2016																	
1	1.60	1.50	1.30	0.30	0.10	0.10	0.30	0.00	0.30	0.70	2.30	0.10	1.10	0.50	0.70	0.10	0.69
2	0.60	0.20	0.10	0.20	0.90	0.00	0.00	0.10	0.00	0.10	0.30	0.10	2.20	0.60	0.20	1.90	0.47
3	0.50	0.20	0.10	0.10	0.10	0.10	0.50	1.10	0.40	1.20	0.00	0.30	0.70	1.50	0.20	0.00	0.44
4	0.00	0.20	0.00	0.30	0.10	0.00	0.00	0.20	0.20	0.20	0.70	0.20	0.50	0.00	0.20	0.20	0.19
Average per Span-line	0.68	0.53	0.38	0.23	0.30	0.05	0.20	0.35	0.23	0.55	0.83	0.18	1.13	0.65	0.33	0.55	0.45

Continue table (5-6) Corrosion Currents of Bridge 159.7 (Dec. 1998 through June 2018)

Bridge 159.7	S1		S2		S3		S4		S5		S6		S7		S8		
	A	B	A	B	A	B	A	B	A	B	A	B	A	B	A	B	
June 2017																	
1	3.80	0.80	0.90	0.40	0.50	0.10	0.50	0.00	0.40	0.20	2.50	0.40	1.00	0.20	0.60	1.20	0.84
2	0.85	0.20	0.10	0.40	1.20	0.20	0.70	0.10	0.00	0.20	0.20	0.00	1.50	0.50	0.30	1.70	0.51
3	1.20	1.90	0.30	0.00	0.10	0.10	0.20	1.70	0.50	1.20	######	0.50	0.70	0.60	0.20	0.20	#VALUE!
4	0.00	0.00	0.00	3.00	0.00	0.00	0.00	0.20	0.10	0.00	0.70	0.30	0.30	0.10	1.20	0.00	0.37
Average per Span-line	1.46	0.73	0.33	0.95	0.45	0.10	0.35	0.50	0.25	0.40	######	0.30	0.88	0.35	0.58	0.78	#VALUE!

Continue table (5-6) Corrosion Currents of Bridge 159.7 (Dec. 1998 through June 2018)

Bridge 159.7	S1		S2		S3		S4		S5		S6		S7		S8		
	A	B	A	B	A	B	A	B	A	B	A	B	A	B	A	B	
June 2018																	
1	6.00	2.00	3.00	0.30	0.50	0.10	0.20	0.00	0.80	0.00	1.60	0.20	2.00	0.50	0.90	1.30	1.21
2	2.00	0.40	0.10	0.50	0.50	0.10	0.50	0.20	0.00	0.30	0.20	0.00	2.80	0.40	0.30	2.70	0.69
3	0.40	0.80	3.00	0.20	0.60	0.10	0.10	0.10	0.60	1.50	0.00	0.20	2.60	0.00	0.20	0.60	0.69
4	1.70	0.00	0.00	0.40	0.20	0.00	0.00	0.10	0.70	0.20	0.60	0.70	0.50	0.20	1.30	0.20	0.43
Average per Span-line	2.53	0.80	1.53	0.35	0.45	0.08	0.20	0.10	0.53	0.50	0.60	0.28	1.98	0.28	0.68	1.20	0.75

5-3-1-2-3 Corrosion Rate

Table 5-7 Corrosion Rate of Bridge 159.7 (Dec. 1998 through June 2018)

Bridge 159.7	S1		S2		S3		S4		S5		S6		S7		S8		
	A	B	A	B	A	B	A	B	A	B	A	B	A	B	A	B	
Dec, 1998																	
1	0.00	0.00	0.01	0.01	0.01	0.02	0.00	0.02	0.01	0.03	0.01	0.01	0.01	0.02	0.00	0.00	0.01
2	0.00	0.00	0.01	0.01	0.03	0.01	0.02	0.02	0.00	0.01	0.02	0.01	0.04	0.02	0.00	0.00	0.01
3	0.00	0.00	0.00	0.02	0.00	0.01	0.03	0.02	0.01	0.00	0.00	0.00	0.03	0.00	0.00	0.00	0.01
4	0.01	0.02	0.00	0.01	0.01	0.01	0.01	0.02	0.01	0.01	0.02	0.01	0.00	0.00	0.01	0.02	0.01
Average per Span line	0.00	0.01	0.01	0.01	0.01	0.01	0.02	0.02	0.01	0.01	0.01	0.01	0.02	0.01	0.01	0.01	0.01

Continue table (5-7) Corrosion Rate of Bridge 159.7 (Dec. 1998 through June 2018)

Bridge 159.7	S1		S2		S3		S4		S5		S6		S7		S8		
	A	B	A	B	A	B	A	B	A	B	A	B	A	B	A	B	
Nov. 1999																	
1	0.00	0.00	0.00	0.00	0.00	0.01	0.00	0.00	0.00	0.00	0.00	0.00	0.02	0.00	0.00	0.01	0.00
2	0.01	0.01	0.00	0.00	0.00	0.00	0.00	0.01	0.00	0.00	0.02	0.00	0.03	0.00	0.00	0.00	0.01
3	0.00	0.01	0.00	0.01	0.00	0.01	0.00	0.01	0.00	0.01	0.00	0.00	0.02	0.00	0.00	0.00	0.01
4	0.00	0.00	0.00	0.00	0.00	0.00	0.00	0.01	0.00	0.00	0.02	0.01	0.02	0.01	0.00	0.00	0.01
Average per Span-line	0.00	0.01	0.00	0.01	0.00	0.01	0.00	0.01	0.00	0.00	0.01	0.00	0.02	0.00	0.00	0.00	0.01

Continue table (5-7) Corrosion Rate of Bridge 159.7 (Dec. 1998 through June 2018)

Bridge 159.7	S1		S2		S3		S4		S5		S6		S7		S8		
	A	B	A	B	A	B	A	B	A	B	A	B	A	B	A	B	
May 2016																	
1	0.07	0.07	0.06	0.01	0.00	0.00	0.01	0.00	0.01	0.03	0.10	0.00	0.05	0.02	0.03	0.00	0.03
2	0.03	0.01	0.00	0.01	0.04	0.00	0.00	0.00	0.00	0.00	0.01	0.00	0.10	0.03	0.01	0.09	0.02
3	0.02	0.01	0.00	0.00	0.00	0.00	0.02	0.05	0.02	0.05	0.00	0.01	0.03	0.07	0.01	0.00	0.02
4	0.00	0.01	0.00	0.01	0.00	0.00	0.00	0.01	0.01	0.01	0.03	0.01	0.02	0.00	0.01	0.01	0.01
Average per Span-line	0.03	0.02	0.02	0.01	0.01	0.00	0.01	0.02	0.01	0.02	0.04	0.01	0.05	0.03	0.01	0.02	0.02

Continue table (5-7) Corrosion Rate of Bridge 159.7 (Dec. 1998 through June 2018)

Bridge 159.7	S1		S2		S3		S4		S5		S6		S7		S8		
	A	B	A	B	A	B	A	B	A	B	A	B	A	B	A	B	
June 2017																	
1	0.17	0.04	0.04	0.02	0.02	0.00	0.02	0.00	0.02	0.01	0.11	0.02	0.05	0.01	0.03	0.05	0.04
2	0.04	0.01	0.00	0.02	0.05	0.01	0.03	0.00	0.00	0.01	0.01	0.00	0.07	0.02	0.01	0.08	0.02
3	0.05	0.09	0.01	0.00	0.00	0.00	0.01	0.08	0.02	0.05	######	0.02	0.03	0.03	0.01	0.01	#VALUE!
4	0.00	0.00	0.00	0.14	0.00	0.00	0.00	0.01	0.00	0.00	0.03	0.01	0.01	0.00	0.05	0.00	0.02
Average per Span-line	0.07	0.03	0.01	0.04	0.02	0.00	0.02	0.02	0.01	0.02	######	0.01	0.04	0.02	0.03	0.03	#VALUE!

Continue table (5-7) Corrosion Rate of Bridge 159.7 (Dec. 1998 through June 2018)

Bridge 159.7	S1		S2		S3		S4		S5		S6		S7		S8		
	A	B	A	B	A	B	A	B	A	B	A	B	A	B	A	B	
June 2018																	
1	0.27	0.09	0.14	0.01	0.02	0.00	0.01	0.00	0.04	0.00	0.07	0.01	0.09	0.02	0.04	0.06	0.05
2	0.09	0.02	0.00	0.02	0.02	0.00	0.02	0.01	0.00	0.01	0.01	0.00	0.13	0.02	0.01	0.12	0.03
3	0.02	0.04	0.14	0.01	0.03	0.00	0.00	0.00	0.03	0.07	0.00	0.01	0.12	0.00	0.01	0.03	0.03
4	0.08	0.00	0.00	0.02	0.01	0.00	0.00	0.00	0.03	0.01	0.03	0.03	0.02	0.01	0.06	0.01	0.02
Average per Span-line	0.11	0.04	0.07	0.02	0.02	0.00	0.01	0.00	0.02	0.02	0.03	0.01	0.09	0.01	0.03	0.05	0.03

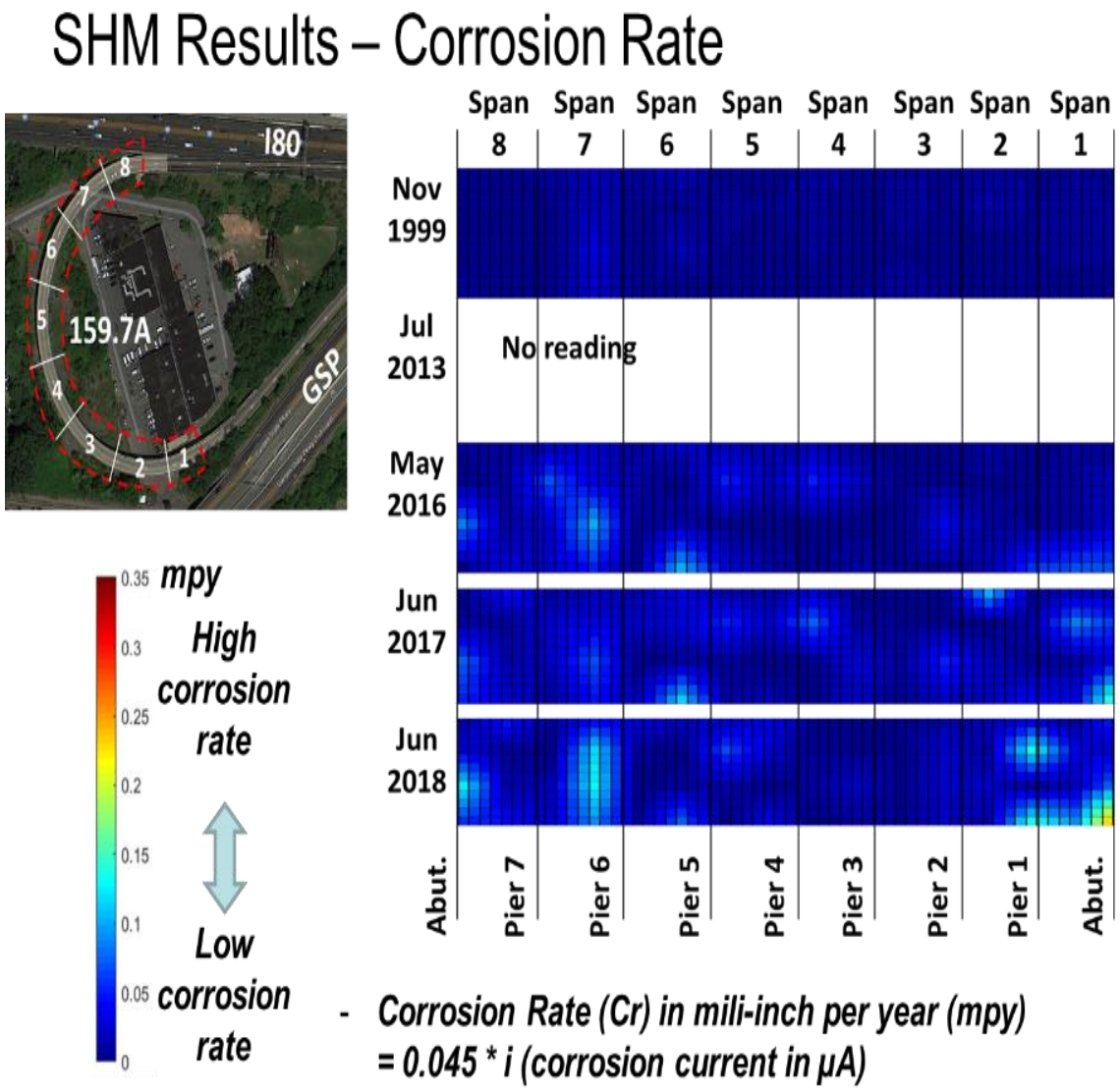

Figure 5–14 Corrosion potentials of bridge159.7 (May 1999 through June 2018)

5-3-1-2-4 Concrete Resistivity of Bridge159.7

Table 5-8 Concrete Resistivity of Bridge159.7 (Dec. 1998 through June 2018)

	May, 1999	Nov, 1999	May, 2016	June, 2017	June, 2018
Corrosion Probe- MEP	Resistivity (kohm-cm)				
Bridge Span Number 1					
1A1	20	9	9	160	160
1A2	11	10	19	48	160
1A3	6	6	11	24	160
1A4	9	18	33	54	160
1B1	10	14	33	160	160
1B2	13	15	27	40	160
1B3	12	10	22	14	160
Bridge Span Number 2					
2A1	17	5	9	50	160
2A2	11	15	27	160	160
2A3	9	14	37	34	160
2A4	160	160	#VALUE!	46	160
2B1	11	15	160	160	160
2B2	9	12	29	21	160
2B3	6	8	21	51	160
2B4	9	6	13	56	160
Bridge Span Number 3					
3A1	13	21	24	40	160
3A2	9	16	33	160	160
3A3	8	6	11	160	160
3A4	9	9	15	63	160
3B1	16	10	29	160	160

Continue table (5-8) Concrete Resistivity of Bridge159.7 (Dec. 1998 through June 2018)

	May, 1999	Nov, 1999	May, 2016	June, 2017	June, 2018
Corrosion Probe- MEP	Resistivity (kohm-cm)				
Bridge Span Number 3					
3B2	11	12	22	160	160
3B3	8	8	16	160	160
3B4	11	13	160	160	160
Bridge Span Number 4					
4A1	15	11	15	70	160
4A2	10	9	21	68	160
4A3	9	9	21	30	160
4A4	14	160	#VALUE!	6	160
4B1	12	128	160	160	160
4B2	9	89	160	160	160
4B3	9	7	14	160	160
4B4	11	6	18	60	160
Bridge Span Number 5					
5A1	10	10	16	160	160
5A2	9	20	#VALUE!	160	160
5A3	7	11	31	60	160
5A4	8	7	13	160	160
5B1	12	14	11	160	160
5B2	5	6	13	160	160
5B3	4	0	9	160	160
5B4	6	6	10	65	160
Bridge Span Number 6					
6A1	23	17	39	65	160
6A2	3	8	7	23	160

Continue table (5-8) Concrete Resistivity of Bridge159.7 (Dec. 1998 through June 2018)

	May, 1999	Nov, 1999	May, 2016	June, 2017	June, 2018
Corrosion Probe- MEP	Resistivity (kohm-cm)				
Bridge Span Number 6					
6A3		6	#VALUE!	49	160
6A4	9	9	16	42	160
6B1	19	160	160	160	160
6B2	8	7	12	33	33
6B3	9	46	99	66	66
6B4	9	8	6	67	67
Bridge Span Number 7					
7A1	5	3	6	65	160
7A2	4	2	6	36	160
7A3	2	2	1	55	160
7A4	4	7	15	70	160
7B1	14	12	18	66	58
7B2	6	7	11	46	60
7B3	12	138	16	46	30
7B4	9	10	18	54	65
Bridge Span Number 8					
8A1	22	9	15	59	160
8A2	6	6	10	138	160
8A3	10	15	13	70	160
8B1	10	9	15	160	160
8B2	4	6	9	49	160
8B3	5	27	22	152	160
8B4	8	7	10	50	160

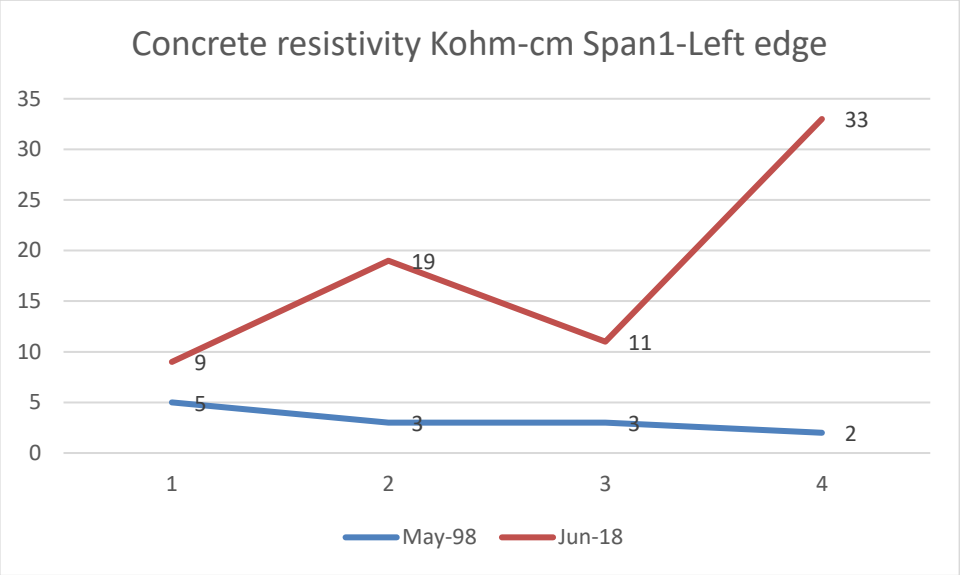
Concrete resistivity Kohm-cm Span1-Left edge
35
30
25
20
15
10
5
0
1
2
3
4
9
19
11
33
5
3
3
2
May-98
Jun-18

(A)

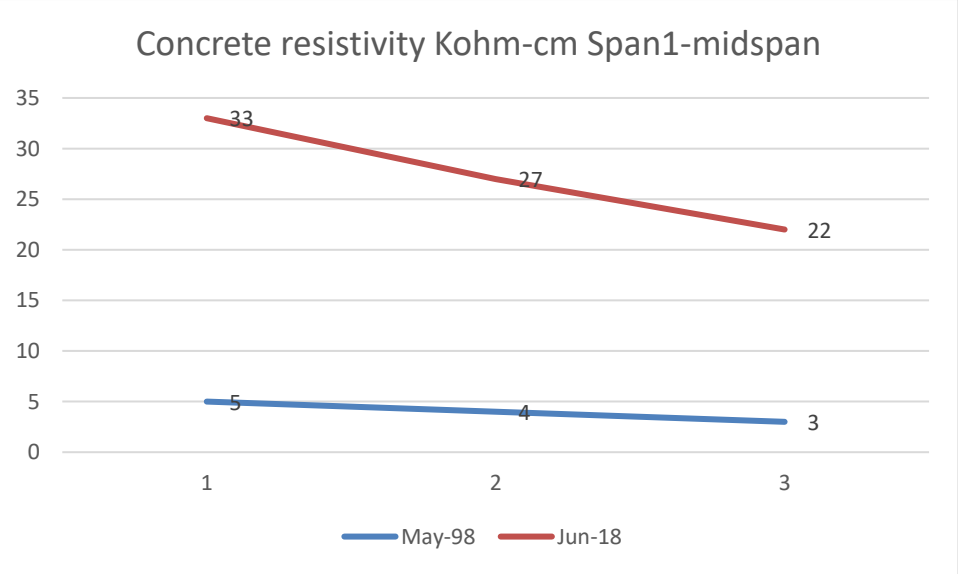
Concrete resistivity Kohm-cm Span1-midspan
35
30
25
20
15
10
5
0
1
2
3
33
27
22
5
4
3
May-98
Jun-18

(B)

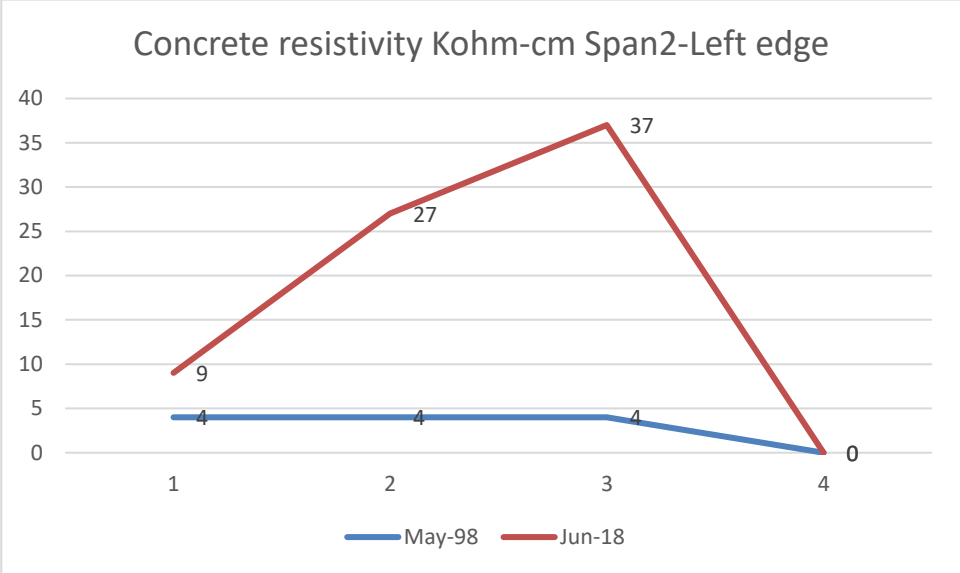
Concrete resistivity Kohm-cm Span2-Left edge
40
35
30
25
20
15
10
5
0
1
2
3
4
9
27
37
0
4
4
4
May-98
Jun-18

(C)

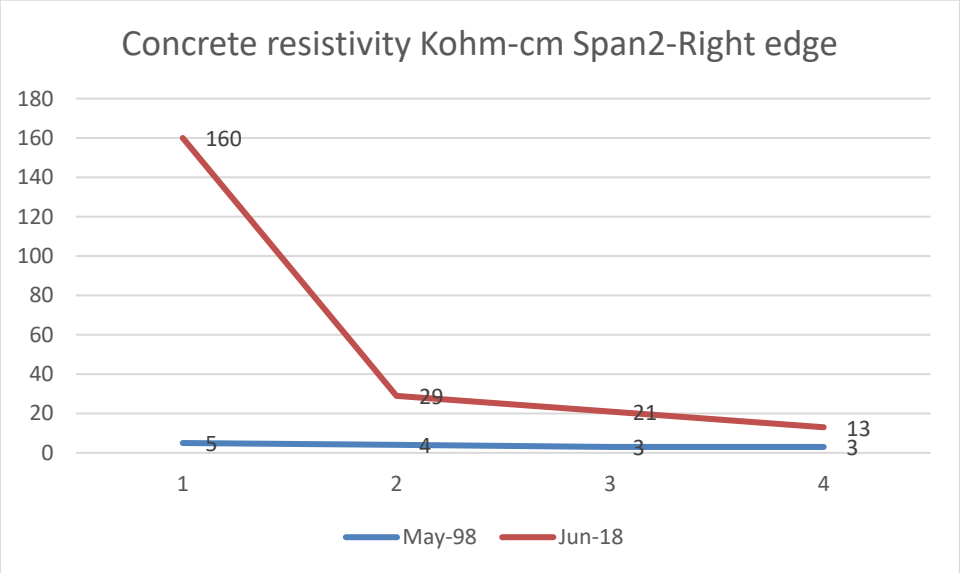
Concrete resistivity Kohm-cm Span2-Right edge
180
160
140
120
100
80
60
40
20
0
1
2
3
4
160
29
21
13
5
4
3
3
May-98
Jun-18

(D)

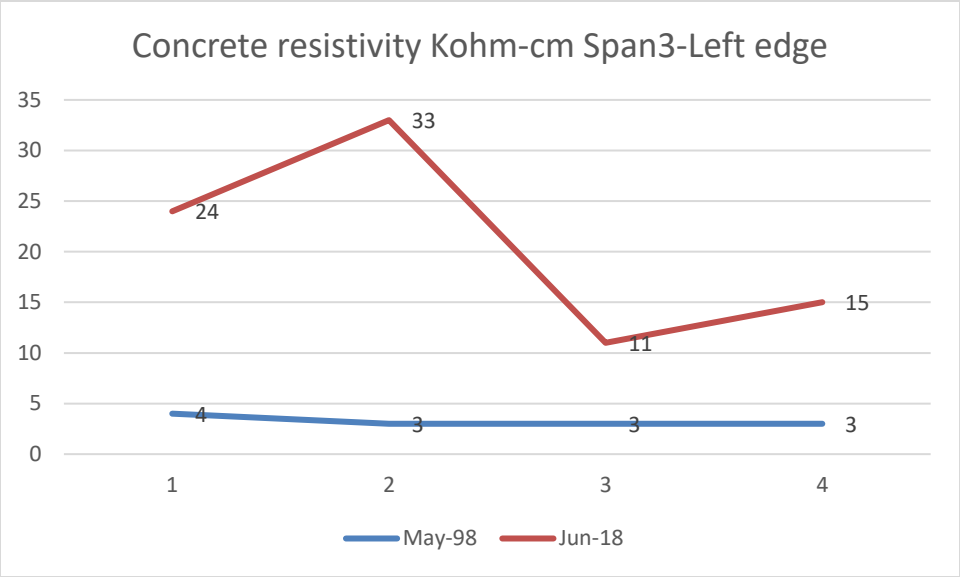
Concrete resistivity Kohm-cm Span3-Left edge
35
30
25
20
15
10
5
0
1
2
3
4
24
33
11
15
4
3
3
3
May-98
Jun-18

(E)

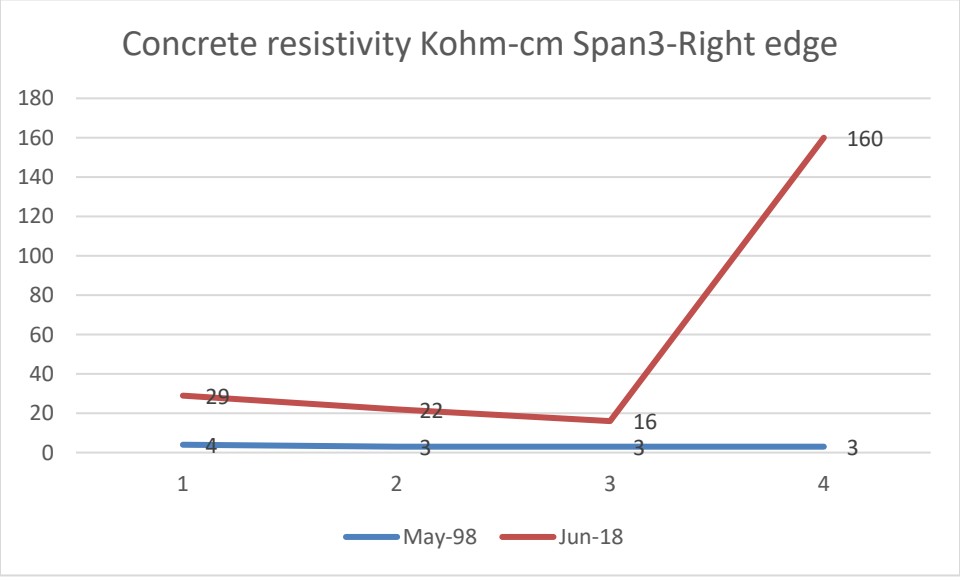
Concrete resistivity Kohm-cm Span3-Right edge
180
160
140
120
100
80
60
40
20
0
1
2
3
4
29
22
16
160
4
3
3
3
May-98
Jun-18

(F)

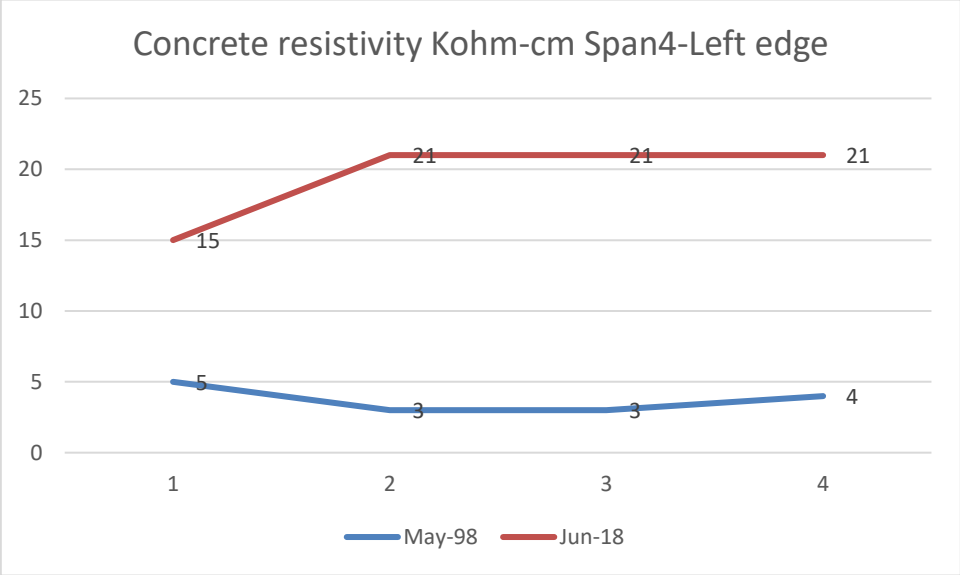
Concrete resistivity Kohm-cm Span4-Left edge
25
20
15
10
5
0
21
21
21
15
5
3
3
4
1
2
3
4
May-98
Jun-18

(G)

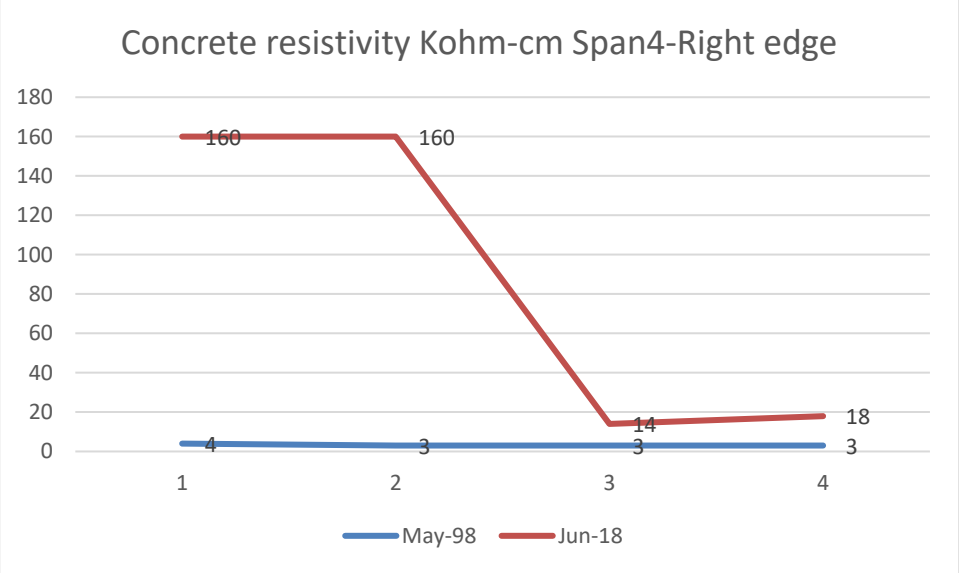
Concrete resistivity Kohm-cm Span4-Right edge
180
160
140
120
100
80
60
40
20
0
160
160
14
18
4
3
3
3
1
2
3
4
May-98
Jun-18

(H)

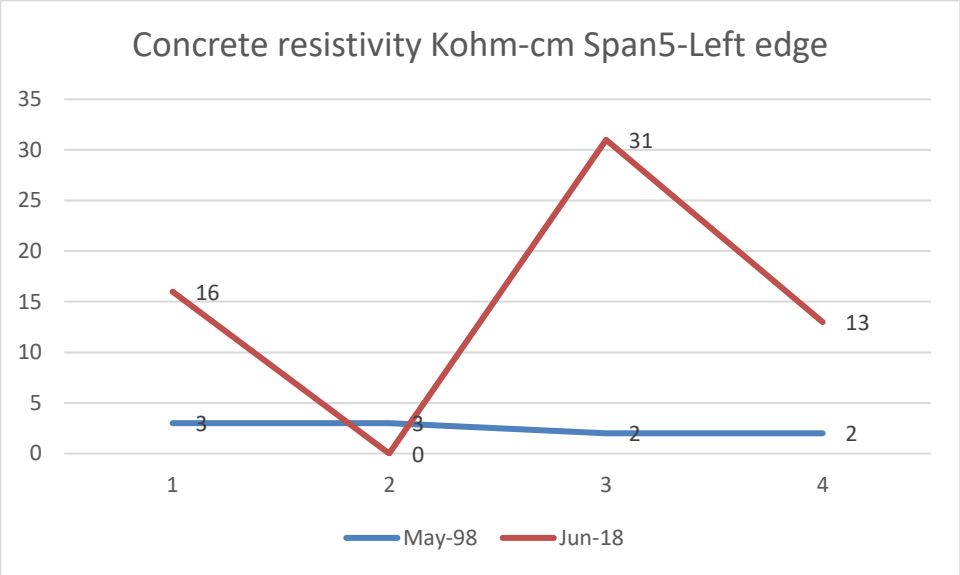
Concrete resistivity Kohm-cm Span5-Left edge
35
30
25
20
15
10
5
0
1
2
3
4
16
0
31
13
3
3
2
2
May-98
Jun-18

(I)

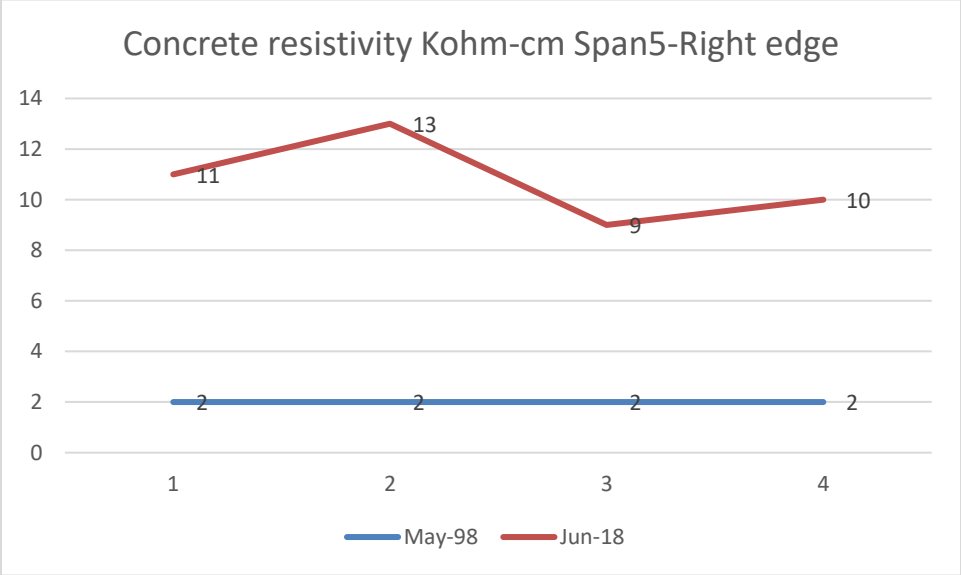
Concrete resistivity Kohm-cm Span5-Right edge
14
12
10
8
6
4
2
0
1
2
3
4
11
13
9
10
2
2
2
2
May-98
Jun-18

(J)

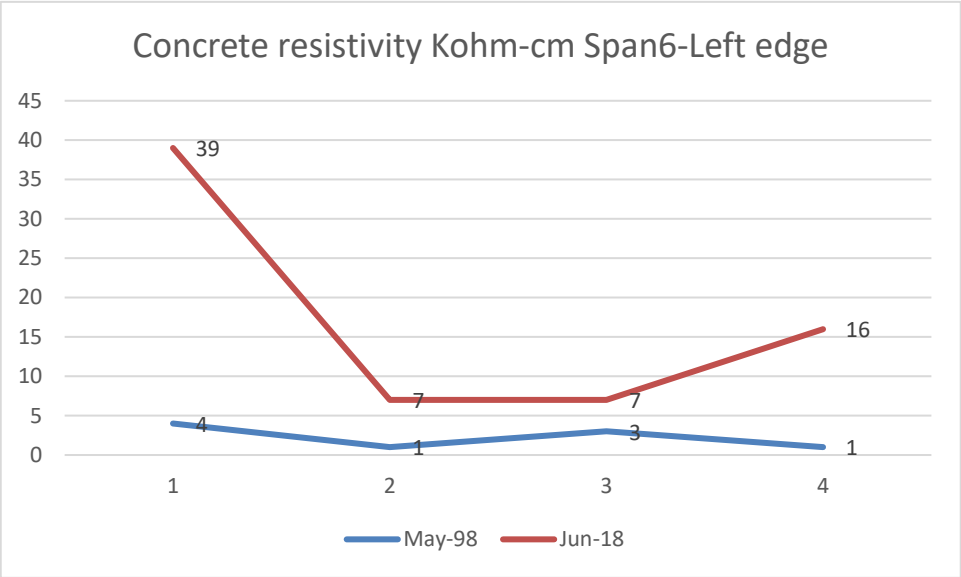
Concrete resistivity Kohm-cm Span6-Left edge
45
40
35
30
25
20
15
10
5
0
39
7
7
16
4
1
3
1
1
2
3
4
May-98
Jun-18

(K)

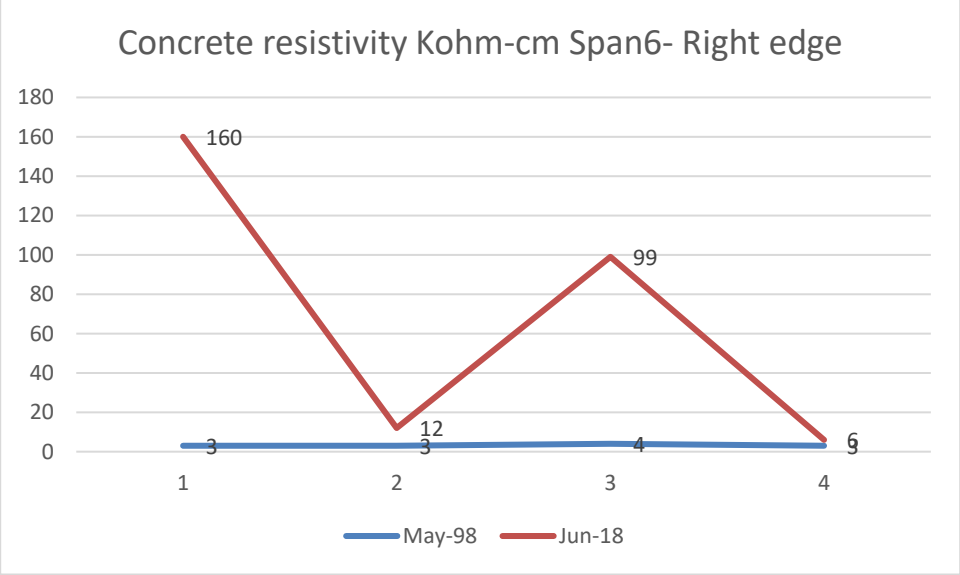
Concrete resistivity Kohm-cm Span6- Right edge
180
160
140
120
100
80
60
40
20
0
160
12
99
3
3
4
1
2
3
4
May-98
Jun-18

(L)

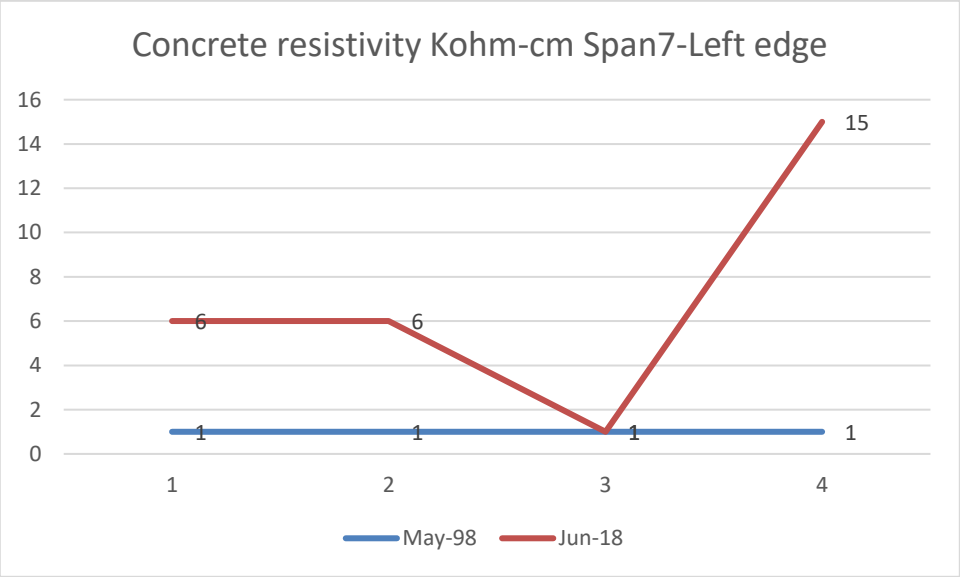
Concrete resistivity Kohm-cm Span7-Left edge
16
14
12
10
8
6
4
2
0
1
2
3
4
6
6
1
1
1
15
1
May-98
Jun-18

(M)

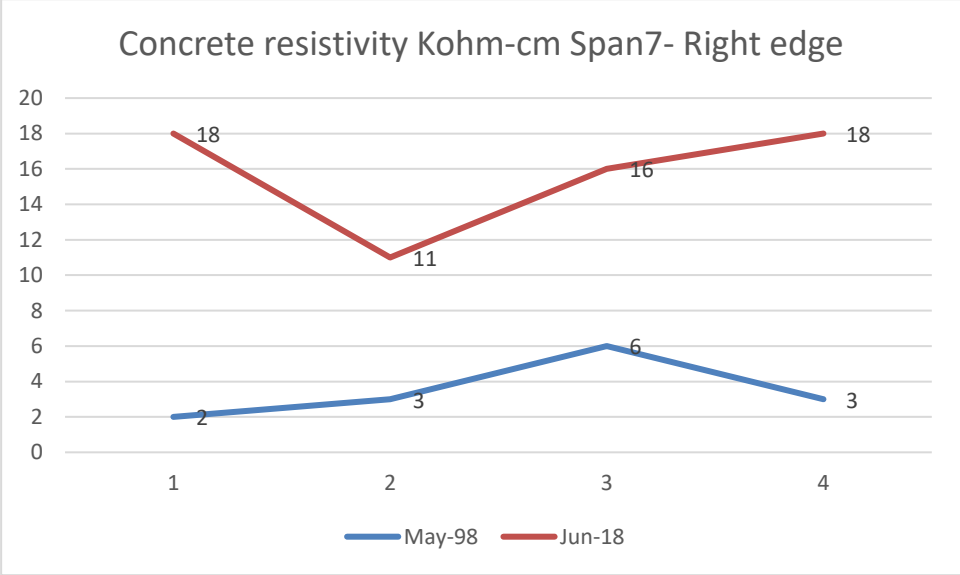
Concrete resistivity Kohm-cm Span7- Right edge
20
18
16
14
12
10
8
6
4
2
0
1
2
3
4
18
11
16
18
2
3
6
3
May-98
Jun-18

(N)

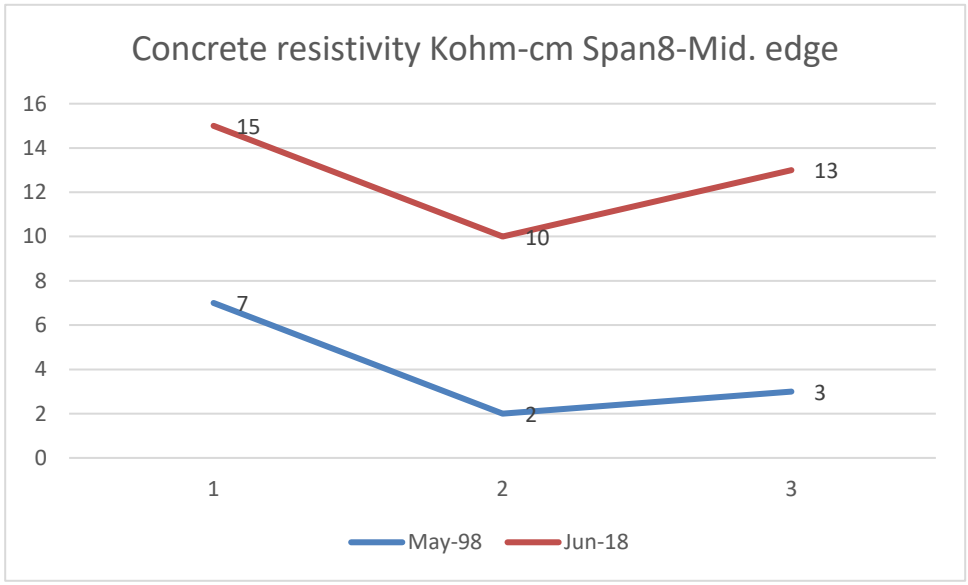

(O)

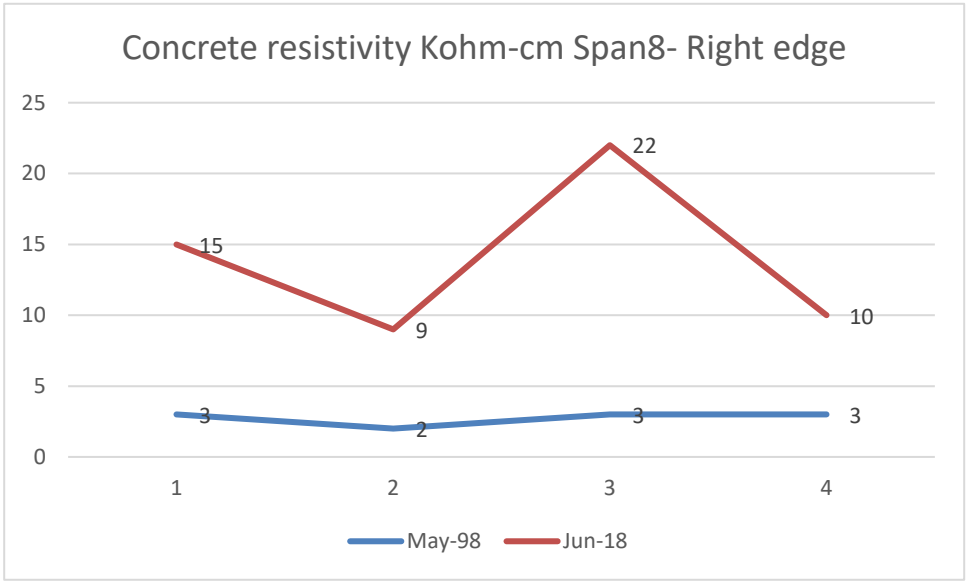

(P)

Figure 5–15 Concrete Resistivity of Bridge159.7 (Dec. 1998 through June 2018)

5-3-2-3 Discussion of the Field Data

5-3-2-3-1 Bridge 84.1(Galvanized Steel)

Depending on the test results of this bridge, the following observation are concluded.

1- In June 2018 compared to May 1998, the potentials test results observed a high corrosion activity; that obviously means a higher probability of corrosion is observed in the bridge deck. This clearly refers to a significant corrosion occuring in the main traffic sections (between P2 and P5) and in the negative moment region (B2). In other words, that means there is a high risk of corrosion is observed in this bridge deck.

2- Depending on the corrosion density, there is a high probability that there is a noticeable reduction in the Galvanized steel reinforcement diameter.

3- The corrosion rate increased significantly from 0.0191 to 0.114 mpy (mili-inch per year).

4- The test results observed a decrease in concrete resistivity especially in the negative moment area of bridge 84.1. This refers to the fact that the reduction in the resistivity of the surrounding concrete leads to acceleration of the corrosion on the vicinity territory.

5-3-2-3-2 Bridge 159.7 (Duplex Stainless Steel)

Depending on the corrosion potentials, currents, corrosion rates, and concrete resistivity, all test results indicate that no significant corrosion activity was observed in this bridge. This indicates the stainless steel rebars are in passive state.

6. Chapter Six

Service Life Model

6-1 General

In this chapter, we review the most used and cutting-edge corrosion models. The corrosion modeling parameters, types of induced corrosion, corrosion methodology, and service life of reinforced concrete structures are discussed and studied in this chapter too. The author herein, proposed a method to predict the service life of a reinforced concrete structure by linking the corrosion potentials and the associated Sodium chloride content. Consequently, the results of the service life model are presented in this chapter also.

6-2 Corrosion Terminology

The corrosion process is very complex, and the modeling is often based on observations rather than a clear understanding of the physical and chemical point of view. It is very important to understand some terminology of corrosion modeling process:

i. Corrosion threshold: the certain minimum concentration of chloride at the surface of reinforcing steel that is necessary to destroy the steel passivation layer to initiate the corrosion.

ii. Corrosion deterioration: the time when the reinforced concrete members will not be able to meet the functional design criteria due to the corrosion process.

iii. Corrosion propagation: the interval after the corrosion initiation during which the corrosion products grow to launch cracks and disintegrate the concrete mass, and

iv. Corrosion Service life: the period of time after placement of concrete during which all properties exceed the minimum acceptable maintained values.

6-3 Types of Induced Corrosion

The corrosion might be initiated by ingress of Sodium chloride or carbon dioxide within the concrete mass. The corrosion induced by carbon dioxide is beyond the scope of this research.

The corrosion of steel reinforcement in concrete structures induced by chloride ion contamination is a major problem. Deterioration starts with the loss of protection provided by the concrete cover as the result of chloride ingress. This is followed by corrosion initiation and then propagation.

The modeling of corrosion implies using different approaches to predict the corrosion phenomena and its effects on the stability and/ or reliability of the reinforced concrete structures. There are many corrosion models that have been used during the past few decades. These models attempted to predict the influences of the corrosion process on the reinforced concrete structure. Depending on corrosion modeling, many researchers aimed to find out the service life of the structures, the time to corrosion initiation, corrosion propagation, and the effects of the concrete cover, bar diameter and cracks presences.

6-4 The Methodology of the Reinforced Concrete Service Life

The methodology of the models of corrosion are either depending on experimental data from the fields or the laboratories results (empirical), or depending on the mechanics

of corrosion process (theoretical). In all cases many parameters and values need to be assumed. Therefore, the outcome or the predicting results of the corrosion models differs from researcher to another. Following is a review of the most used models of corrosion of the reinforced concrete structures.

6-5 Service Life of Reinforced Concrete Structures

The service life of structure is the stage when the structure is able to maintain the design safety conditions and resist the loads and environmental effects without an extensive maintenance requirement. It is very important to define and determine the service life of the reinforced concrete structures. By finding out the service life of any structures, the owners will know when and how to start the maintenance and the rehabilitation.

In general, from the perspective of corrosion phenomena, the service life of any structure consists of two important stages which are corrosion initiation and corrosion propagation. The corrosion initiation is the time required of chloride ion to diffuse throughout the concrete cover and break down the protection layer of the steel reinforcement in the steel- concrete interface. On the other hand, the corrosion propagation is the time required to build up the corrosion products to reduce the cross section of reinforcement and cause concrete cracking, spalling, and delamination. Accordingly, the service life of the structure could be presented by the following equation:

$$T_{life} = t_i + t_p \qquad (6\text{-}1)$$

Many authors have defined the service life by the initiation time of corrosion, T_{corr}.

$$T_{service} = T_{corr} \qquad (6\text{-}2)$$

Several researchers modify this definition to include the time to cracks of reinforced concrete, T_{crack}

$$T_{service} = T_{crack} = T_{corr} + \Delta t_{crack} \qquad (6\text{-}3)$$

Here, P. Thoft-Christincen (Figure 8-1) suggested that the service life must be modified to include the situation after the crack initiation stage. So, it will be more significant to include the after-cracking stage up to a certain crack width of .3 mm. Thus, the model should be modified to:

$$T_{service} = T_{width} = T_{crack} + T_{width} = T_{corr} + \Delta t_{crack} + \Delta t_{width} \qquad (6\text{-}4)$$

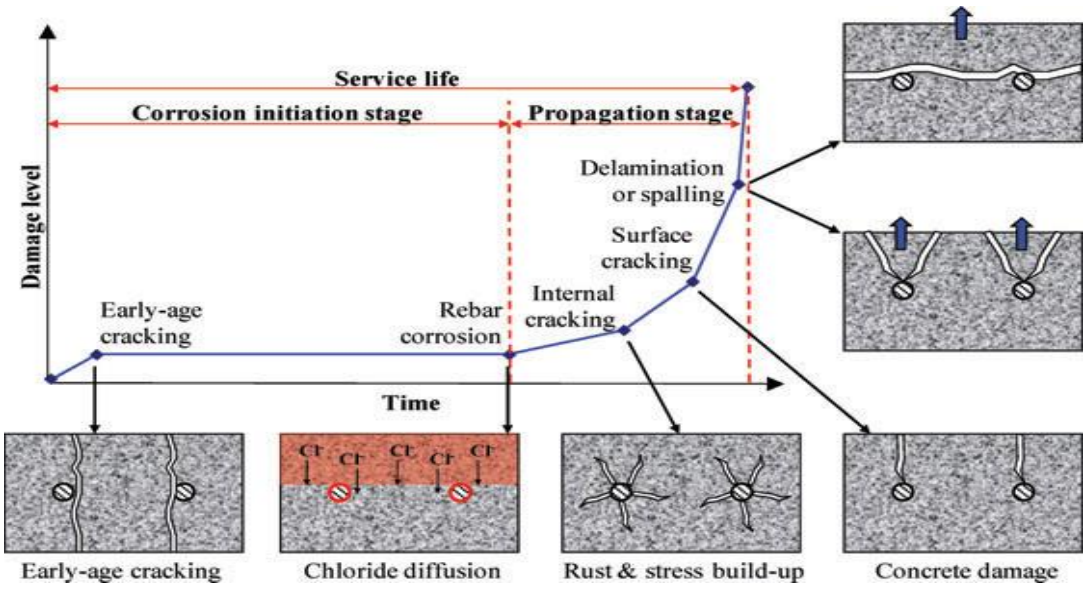

Figure 6–1 Schematic Service Life Model

[P. Thoft Christensen]

There are many factors affecting the corrosion initiation and propagation such as W/C ratio, permeability of concrete, temperature, moisture content, availability of oxygen, thickness of the concrete cover, use of additives like fly ash and silica fume, crack width and depth, and the type of reinforcing steel.

6-6 Corrosion Modeling of the Reinforced Concrete Structures-Literature Review

There are a variety of models that have been proposed to predict the corrosion modeling of the reinforced concrete structure. But in general, we could categorize them into three types:

1- Models depending on electrochemistry of corrosion
2- Models based on diffusion process, and
3- Models related to empirical approaches.

Yue Li et al. Studied the chloride transmission in cracked concrete. The influence of cracks on chloride penetration in concrete with numerical simulation were adopted for this study. They prepared a small cylindrical corrosion samples (100*50 mm) with artificial cracks (crack width of .05, .08, 0.1, and 0.2 mm). In order to initiate the corrosion, they used the rapid chloride migration method (RCM). The samples subjected to electrical current of 30-40 mA (35 v) for 2, 4,6,8,10, 12, and 24 hours. Both Fick's second law and Finite Element Method with thermal analysis module were used through this research. The test results showed that the cracks effect could be neglected if the crack width is less than .05 mm. and if the crack width is larger than 0.1 mm, the chloride transmission is similar

to that of liquids. In my opinion this method is not adequate because it depends on empirical method of simulation. Also, it couldn't predict the service life of reinforced concrete members.

P. Throft-Christensin Model suggested the corrosion initiation and the rate of chloride penetration into the concrete mass could be modeled by using Fick's law of diffusion which predicts how diffusion causes the concentration to change with time. It is a partial differential equation. P. Christensin simplifies this equation to calculate the time to corrosion initiation:

$$Ti = d2/4D\left(erf - 1\left(\frac{Ccr-C0}{Ci-C0}\right)\right) \qquad (6\text{-}5)$$

Ti: is the time to corrosion initiation

d: the cover thickness

D: chloride diffusion coefficient

Ccr: critical chloride concentration at the rebar- concrete interface.

C0: the surface chloride concentration, and

Ci: the initial chloride concentration.

Bazant used a Mathematical Models to predict the time to corrosion Cracking based on theoretical physical models for corrosion of steel in concrete exposed to seawater. He suggested a simplified mathematical model to calculate the time to corrosion cracking of concrete cover. The basic assumptions of Bazant's models are as following:

i. Oxygen and chloride ion transport through concrete cover are quasi-stationary and one dimensional.

ii. A steady-state of corrosion producing expansive rust layer begins at depassivation time, and

iii. The model is based on red rust which is more dangerous for cracking concrete.

K. C. Clear made attempts, as early as 1976, to determine the time to cover cracking based on pure empirical data. But according to Broomfield, this model is not verified or validated yet. The suggested model was:

$$0.83\sqrt{\frac{.052\ d^{1.22}\times t^{0.21}}{Cs^{0.24}/(\frac{w}{c})}} \qquad (6\text{-}6)$$

where:

t_{crack} = time to first cracking (years)

d = cover thickness (mm)

t = the age at which Cs was measured (years)

Cs = the surface (or near surface) chloride concentration (percent by weight of concrete), and

w/c = water/cement ratio

A deterioration model developed by Cady and Weyers has been used to estimate the remaining life of concrete bridge components in corrosive environments. There are three distinct phases in their model: diffusion, corrosion and deterioration. The first phase, diffusion, is defined as the time for chloride ions to penetrate the concrete cover and to

initiate corrosion. The diffusion time usually can be determined empirically using Fick's Second Law. The second phase, corrosion, is defined as a period of time from initiation of corrosion to first cracking of concrete cover, the time to cracking ranges between 2 to 5 years. The third phase, deterioration, describes the time for damage to reach a level of percent damage which is deemed as the right time for repair or rehabilitation. Accordingly, to predict the corrosion cracking time, they used the 3LP and Gecor device for this quantitively prediction.

Morinaga suggested an empirical equation to predict cracking time depending on the field and laboratory results. It assumed that the corrosion cracking will occur when the corrosion products reach a certain quantity which given by the equation below.

$Q= .602*d\ (1+2C/d)^{0.85}$

Q: the critical mass to initiate corrosion cracking

D: reinforcement diameter

C: the concrete cover

Continuously the corrosion cracking time could be calculated by:

$T_{corr}= Q/i_{crr}$, and

i_{crr}: the corrosion rate

Songkram Pyamahant Et al. proposed a simulating model for corrosion cracking of concrete cover in reinforced concrete structures located on land and subjected to airborne chloride. Chloride penetration model was proposed and verified with cores taken from the land structures. Also, a numerical formula for limited corroded mass that causing the

cracking was developed. In their study in order to find the distribution of chloride, they used the flux of chloride ions instead of the chloride concentration. They found the calculations in a good agreement with the results of cores. The numerical formula accuracy was 25% compared with previous studies.

Jin-xia XU et al. developed a nonlinear finite element model (FEM) to study the electrochemical process of the corrosion of steel reinforcement in concrete. The influences of the area ratio and the Tafel constants of the corrosion cell on the potential and corrosion current density have been examined with the model. They used the Laplace equation to simulate the potentials distribution of corrosion potentials on the surface of rebars. Results showed that the distributions of potential and corrosion current density on the steel surface, which are different from the average values measured with various electrochemical techniques, can be obtained with the finite element calculation. Therefore, the finite element calculation is more suitable for assessing the corrosion of steel reinforcement. Moreover, the calculation results show that with the decrease of both the area ratio and the Tafel constants, the local corrosion of steel reinforcement in concrete is strengthened.

Tomasz Krykowskia and Adam Zybura developed a computer program, FEM and FVM techniques, to model the degradation process of concrete cover due to induced chloride corrosion. Results were validated in two stages. In the first stage, the results from computer calculations were analyzed. For the examined cover thicknesses of 27, 47 and 70 mm, the error percentage of the calculated time *td* of the cover degradation obtained for the averaged composition of the corrosion products in comparison to the results of the experimental tests varied between 4.1 and 28.6%. Considering the comparison of the cracking time *tc* results to the experimental test results, shows the calculation error ranged

from 1.2 to 11.4%. Taking into account the level of the problem complication, considerable difficulties in determining the activation time tact and the adopted concrete model, the obtained results can be regarded as very satisfactory. In the second stage, the application of the transient layer growth model was presented for the non-uniform reinforcement corrosion around the rebar circumference.

In 2001, Trevor J. etal. Developed a model to predict the service life of Virginia bridges. The main purpose of this study was finding out the impact of specification on chloride-induced corrosion service life of bridge decks at Virginia state. The test procedure was extensive and included more than one hundred bridges. Some of these bridges were constructed between 1968 and 1972; while the rest were built between 1981 and 1994. The developed model was able to predict the time for the first repair and rehabilitation and the service life of Virginia bridges. The study depended on field data, data from literature, and Monti Carlo Simulation. Test results found that corrosion initiation time was 34 years for bridges built between 1968 and 1972, and 47 years for bridges built between 1981 and 1994.

An experimental and numerical research was carried out by **Di QIAO** to simulate the corrosion-caused damages in concrete. The study included three-dimensional level, where crack propagation and cover spalling as well as tensile performance of corroded rebars influenced by local corrosion along the rebar length direction are focused. On the other hand, a time-dependent electro-mechanical model based on Rigid Body Spring Method (RBSM) is developed for the evaluation of both concrete cracking and tensile degradation of rebars due to corrosion. Results showed that the corrosion-expansion model can simulate reasonable crack patterns compared to the test results, if the corrosion

distribution is properly assumed. The analysis indicates that for 2D cracking behavior internal crack propagation is dependent on the corrosion pattern around the rebar rather than the cover thickness. If corrosion distributes broadly, parallel cracks also appear for 10mm cover. The analysis also clarifies that the occurrence of inclined lateral crack as shown by 3D cracking behavior may be due to the confinement of concrete surface deformation by the other part with less rebar corrosion.

A study to mode the chloride-induced corrosion initiation of steel rebar in concrete has been done by **P. Ghods** Et. Al. The differential equations for the transport of

hydroxide, chloride and seven other ionic species in the concrete pore solution, coupled with the electrochemical reactions on the steel surface, were numerically modeled in simulated crevices that exist between the mill scale and the steel

surface using the COMSOL finite element software. The numerical results verify that the mill-scale on the surface of rebar enhances the initiation of corrosion which is also in agreement with experimental findings.

Modeling the time-to-corrosion cracking of the cover concrete in chloride contaminated reinforced concrete structures studied by **Youping Liu**. The researcher used both the 3LP and Gecor devices to measure the corrosion activities. An interaction model for characterizing the dynamic corrosion process was developed based on the five-year corrosion database. The model demonstrates that the corrosion rate is a function of chloride content, temperature at reinforcement depth, ohmic resistance of concrete, and corrosion time after initiation. A time-to-corrosion cracking model was suggested based on a corrosion-cracking conceptual model and critical mass of corrosion products. The model

predicted times to corrosion cracking are in good agreement with the observed times to corrosion cracking of the cover concrete.

E.L. Portela & T.N. Bitterncourt carried out a research to study the time-dependent probabilistic point-in-time approach to perform service life prediction in RC Structures. They modified Faraday's equation in their research as illustrated below:

$$\frac{D_0{}^2 - D_t{}^2}{4D_0} = \frac{A_{Fe} \times i_{corr} \times t}{\rho z F} \qquad (6\text{-}7)$$

Time-dependent reliability analysis applying FORM and Importance Sampling Monte Carlo simulation was performed. The model presented in this paper takes into account probabilistic information such as daily fluctuations of temperature and relative humidity. Live load on bridge and its actual strength are measured by means of strain gages installed in rebars and concrete. A real Brazilian bridge, which is monitored since 2011, is used as a case study in the investigation. The results showed that, in terms of the probability of failure, the difference in the predictions based on the two different ionic charges can be as large as 500%. This illustrates the importance of considering different types of chemical reactions when modeling the corrosion process.

An experimental study to estimate the residual life of structures affected by reinforcement corrosion has been done by Ne´**stor F. Ortega** and **Sandra I. Robles**. In order to accelerate the corrosion, they applied a constant current density of I_{corr}=100 (Ma/cm2). The main idea was to find the loss of natural frequency of the beams due to the

corrosion of steel reinforcement. For the numerical model they used the Finite Elements Method (FEM) and the Autodesk Algor simulation 2012 software.

A data collected in the field of 26 bridges at Virginia was used to predict the corrosion service life in the field by **Gregory S. Williamson** et al. The data includes the surface chloride concentration, diffusion coefficient, and steel cover depth. Four types of reinforcement were considered in their study: Black Steel, Galvanized steel, Stainless steel, and microcomposite-chromium steel. The probabilistic model based on the Monte Carlo simple bootstrapping technique was used for estimates

The bridge deck service life. Three distinct time periods were considered in the study as follows:

i. Time to corrosion initiation of 2% of the reinforcing steel;
ii. Time from corrosion initiation to concrete cracking and spalling of the concrete over 2% of the reinforcing steel; and.
iii. Time for corrosion propagation from 2 to 12%.

The researchers proposed the following equation to predict the time required of corrosion damage to propagate from 2 to 12% for the bridge deck reinforced with black steel:

$$Td = 8.61\left\{\sqrt[2]{(\%Det + 1.83)} - 1.45\right\} - 3.34 \qquad (6\text{-}8)$$

Where, Det: is the level of deterioration. The following aspects were drawn from their results:

1. The quality of concrete is a very important factor to diminish the corrosion process; where the service life of bridge decks expected to pass 100 years if the low

permeability concrete is used regardless of the steel reinforcement types and/or chloride exposure conditions.

2. The stainless steel is the best reinforcement type that could develop a service life of 100 years or more regardless of the concrete quality and/or chloride exposure conditions, and
3. The Micro-composite and Galvanized steel expected to need the same chloride content to initiate the corrosion.

D. Cusson Et Al. used mechanistic modeling to predict the service life of reinforced concrete bridge decks subject to chloride attack. A case study of the monitoring of a concrete highway bridge barrier wall constructed in 1996 is presented and used to illustrate the approach and its benefits. The model was validated against Monti Carlo Simulation Method. In the research a two-level decision process based on two types of deterioration models was suggested, in which critically damaged bridges are first identified by using simplified Markovian cumulative damage models, and then individually analyzed using the proposed durability monitoring and probabilistic mechanistic modeling approach. The results demonstrated that service life predictions could be improved significantly by updating the models with selected field monitoring data from embedded sensors or on-site corrosion surveys, as opposed to using selected data from the literature. The proposed approach can be used on any RC elements of bridge decks as long as the governing corrosion parameters could be monitored on site and fed to the probabilistic mechanistic prediction models.

Prediction of time to crack initiation in reinforced concrete exposed to chloride was investigated by **Nabi Y**. et al. in this study, researchers compute the effects of the chloride

concentration and silica fume on the corrosion cracks. They used an accelerated corrosion test (7 days of testing) to initiate corrosion cracks. They developed a formula for measuring the change of the current density and bars weight during the test period until the cracks initiation. The test results showed that the time to crack initiation of the reinforcing concrete structures could be estimated by using the following formula; also, they found that 40000 mg/L of Cl concentration is the minimum threshold of cracks initiation in reinforced concrete structures.

$$t = \frac{bar\ Dia.reduction}{corrosion\ rate} \qquad (6\text{-}9)$$

The service life of reinforced concrete bridge decks exposed to deicing salts was estimated by Trevor J. Kirkpatrick et al. by developing a statistical probabilistic model, Monti Carlo techniques-S-Plus 2000. They incorporated the statistical nature of chloride induced corrosion of reinforcing steel into existing models to predict the time to first repair and rehabilitation of concrete bridge decks. depending on the test results they concluded; 1) the corrosion diffusion coefficient is the control factor of corrosion process rather than cover depth. 2) the ratio of the corrosion initiation concentration/ surface chloride concentration approximately close to 1 cause a huge predicted time for diffusion corrosion initiation. 3) the bridges that subjected to the moderate chloride concentrations (such as rural areas) are less vulnerable to corrosion initiation than moderate or high exposure zones (such as interstate and US routes). 4) increasing the chloride content from 1-2 ib/cy to 8.3 ib/cy increase the time to the rehabilitation by two or more factors.

For the model parameters such as cover depth, surface chloride concentration, and apparent coefficient diffusion were obtained from field data tests (10 existing bridges in Virginia state).

6-7 Software Service Life Modeling

There are variety of computer programs that predicting the service life of reinforced concrete members. Some of the routine depend on a probabilistic, deterministic, and sochastic analysis. Following are the widely used programs:

6-7-1 Kyosti Tuutti Models

One of the oldest service life modeling depending on the corrosion performance which induced by chloride and carbonation. This model is able to predict the corrosion initiation and propagation time. This model uses the Monti Carlo Techniques and empirical data to infer the corrosion performance.

6-7-2 Duracrete Model

This is one of the most used models in Europe because it used the European experience data. The model uses the Fick's Second Law of diffusion and Monti Carlo Probability analysis. This model used with the non water saturated reinforced concrete members only. Duracrete Model is not accurate regarding to the other computer programs of corrosion service life modeling because it assumed several corrosion parameters such as surface chloride and chloride coefficient.

6-7-3 Life 365 Surface Life Prediction Model

This model predicts the service life of the induced corrosion only. The model has a wide data for the chloride peofiles of North America. It partially uses the Monti Carlo technique based on Fick's Second Law. The cover depth, exposure condition, mix proporation, concrete admixtures, steel reinforcement types, and structure location are the main parameters of this model. Also, this model is able to analyze and calculate the life cycle cost of corrosion.

6-7-4 STADIUM Model

This program requires a well knowledge about the concrete's transport properties such as concrete porosity, chloride/ hydroxide ratio, and so to predict a propabilistic model of service life. This model compute the ion transport into concrete in both saturated and non water saturated profiles.

6-8 Summary and Conclusion of Corrosion Modeling.

Different research and studies indicated significant variations in the extent of corrosion required to initiate corrosion and cracking. A thorough understanding of governing mechanisms is needed to enable effective models to be developed. many formulas and models have been proposed for the calculation of the time to onset of corrosion initiation and cracking of the concrete cover. Some analytical/mathematical models are deduced on the basis of mechanical principles and some empirical expressions are obtained according to the experimental data fitting. So far, the models for crack

initiation and propagation have been restricted to the stresses generated by the expansion of corrosion products. Models comprising the total complexity of the problem, especially generated by load induced stresses, have not been found. Most models include several empirical coefficients to adjust to experimental results from accelerated corrosion tests. The most time-to-corrosion initiation-cracking models (mathematical or based on Finite Element Methods) need input parameters for the modeling of chloride concentration, rust expansion, rate of corrosion, number of concrete pores that can be filled by corrosion products without generating bursting forced in the concrete, etc. However, reliable values of such parameters are lacking. No reliable models for predicting the time to spalling or delamination of concrete are found. This phenomenon is governed by complex interactions between corrosion, loading conditions and reinforcement detailing, which are still not well understood.

6-9 Results of Surface Life Model

As we mentioned earlier, there are variety of software models to predict the corrosion threshold and estimating the service life of reinforced concrete bridge decks. In this chapter, depending on the laboratory potentials of corrosion, sodium chloride profiles, previous literature, and the field work, the time of corrosion initiation, propagation, and the service life of structure are predicted. The data collected from laboratory tests and field performance is used to validate results of simulation model to correlate service life predictions from accelerated laboratory-based tests.

6-9-2 Chloride Profile (CTL)

The total chloride contents of the laboratory samples were determined according to ASTM C 1152/C 1152M, Standard Test Method for Acid-Soluble Chloride in Mortar and Concrete [ASTM C 1152 2003]. The test results were as follows:

1- The Initial Chloride Content

The chloride contents were measured by drilling the prismatic concrete samples before exposing to the chloride content solutions. The test results presented in table (6-1) below. Compared with concrete class A, the high performance concrete (HPC) containing the lower chloride content. This results in a good agreement with result obtained another researcher [J. C. M. Maage and S. Helland 1995].

Table 6-1 Chloride Profiles of concrete Before Exposing to Sodium Chloride

Crack Patterns/ Exposing Conditions		
	Chloride Content %	Potentials mV
A	.068	32
HPC	0.042	28

2- The Critical Chloride Threshold Level (CTL)

This test was performed for samples that already reached the critical chloride threshold level. Test results are exhibited in table (6-2) below. Depending on the results, concrete class A which reinforced with Black Steel and Epoxy Coated reached the critical chloride threshold level. In the same direction, the Stainless Steel reinforced concrete samples which had crack width of 0.035, depth of 1", and subjected to 15% NaCl were reached the critical chloride threshold level too. All other exposing conditions still below the (CTL). At the threshold level, approximately all samples had the same potentials, 350 mV.

3- The Chloride Content and Potentials at the age of 33 Months.

The corrosion potentials and associated chloride contents of all samples at current age, 33 months, are included in table (6-3) below.

6-9-3 Corrosion Threshold (Initiation) Model

Most of the research and studies emphasize the concentration of the induced chloride in the reinforced concrete mass, which is the key factor of the corrosion process. To incorporate the probabilistic nature of the process was by applying the statistical computing techniques were applied to the diffusion-cracking model [R.E. Weyers et al. 1993]. The time to corrosion initiation was predicted through using second Fick's law of diffusion [P. Thoft Christensen 2000 and Kirkpatric 2002].

Table 6-2 Chloride Profiles of concrete at Threshold level

Crack Patterns/ Exposing Conditions	BS		EC		SS	
Prismatic Corrosion Samples	Chloride Content %	Exposing Age (Months)	Chloride Content %	Exposing Age (Months)	Chloride Content %	Exposing Age (Months)
A-Uncracked-3%	0.429	24	0.696	31	---	---
A-Uncracked-15%	0.425	22	0.678	30	---	---
A-0.011-0.5-3%	0.423	22	0.613	29	---	---
A-0.011-0.5-15%	0.415	21	0.663	29	---	---
A-0.011-1-3%	0.415	19	0.602	26	---	---
A-0.011-1-15%	0.415	19	0.553	25	---	---
A-0.035-0.5-3%	0.399	18	0.580	26	---	---
A-0.035-0.5-15%	0.440	17	0.773	27	---	---
A-0.035-1-3%	0.363	16	0.638	25	---	---
A-0.035-1-15%	0.389	16	0.570	24	0.924	30

Table 6-3 the Chloride Content Profiles and Potentials for all Conditions at Exposing Age of 33 Months of Concrete Class A

Crack Patterns/ Exposing Conditions	BS		EC		SS		MMFX	
Prismatic Corrosion Samples	Chloride Content %	Potentials mV	Chloride Content %	Potentials mV	Chloride Content %	Potentials mV	Chloride Content %	Potentials mV
A-Uncracked-3%	1.018	530	0.998	377	0.978	258	1.039	183
A-Uncracked-15%	1.110	569	1.088	389	1.065	288	1.132	200
A-0.011-0.5-3%	1.105	590	1.083	383	1.061	283	1.127	191
A-0.011-0.5-15%	1.193	645	1.169	404	1.145	329	1.217	219
A-0.011-1-3%	1.193	651	1.169	421	1.145	310	1.217	247
A-0.011-1-15%	1.313	678	1.286	445	1.260	319	1.339	247
A-0.035-0.5-3%	1.149	660	1.126	409	1.103	287	1.172	233
A-0.035-0.5-15%	1.391	663	1.363	430	1.336	332	1.419	257
A-0.035-1-3%	1.264	755	1.239	442	1.213	312	1.289	268
A-0.035-1-15%	1.352	819	1.325	481	1.298	368	1.379	297

$$Ti = d2/4D\left(erf - 1\left(\frac{Ccr-C0}{Ci-C0}\right)\right) \qquad (6\text{-}10)$$

Where:

Ti: Time to corrosion initiation.

d: the concrete cover.

D: diffusion coefficient.

Cr: critical chloride concentration at the rebar surface.

C_0: the equilibrium chloride concentration at the concrete surface.

C_i: initial chloride concentration in the concrete.

6-9-4 Data Regression

The regression parameters for the laboratory data are presented in the table (8-4) and plotted in figure (6-2) below. Fortunately, there is a very good correlation between the potentials, chloride contents, and the rebar types. Depending on the test results, for a given potentials, the critical chloride threshold level to initiation corrosion for MMFX is higher than the chloride threshold levels of Stainless, Epoxy Coated, and Black Steel rebars.

6-9-5 Probabilistic Model

Numerous empirical formulas and mathematical models have been proposed to predict corrosion initiation implemented into a computer program such as FEM, SP-2000, MATLAB, and Monte Carlo techniques [Kirkpatric et al. 2002, Williamson et al 2009, and Sang-Soon Park et al 2009].

Table 6-4 Regression Parameters

Rebar Types	Regression Parameters		
	Intercept	Slope of the Regression Line	R-squared
	a0	a1	R2
BS	-5.477	547.325	0.982
EC	10.927	342.778	0.993
SS	15.143	252.75	0.992
MM	18.103	176.042	0.975

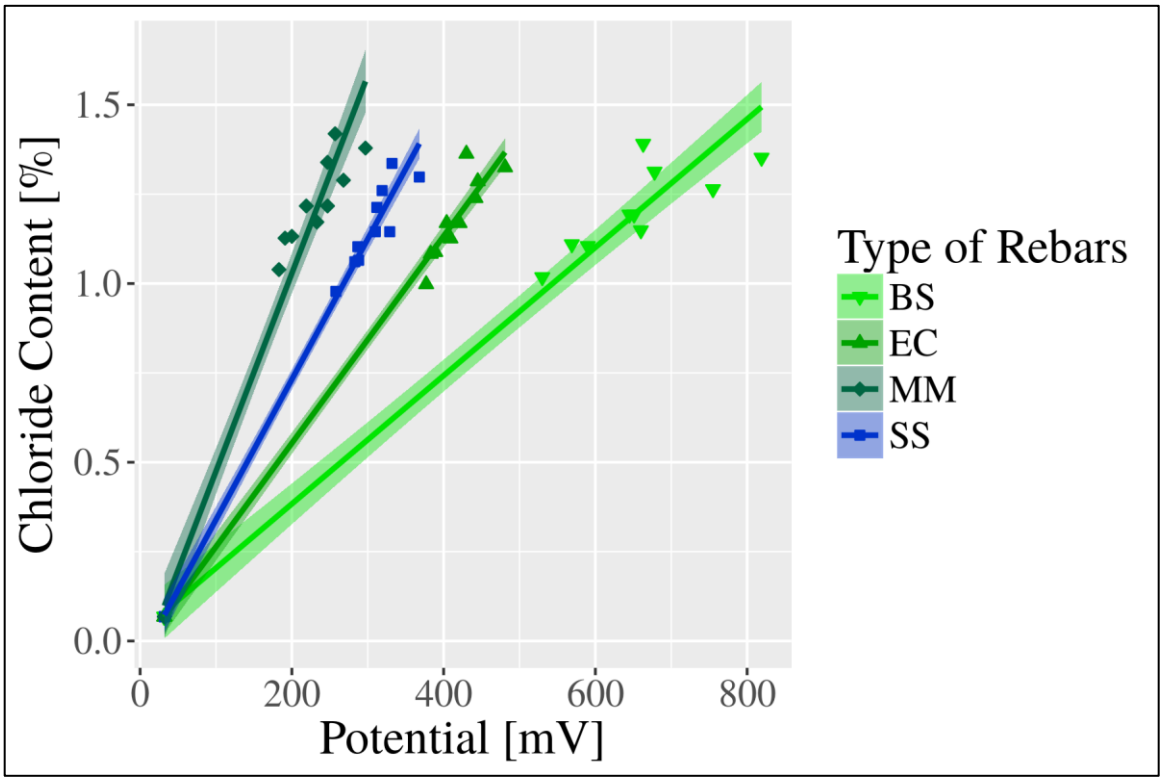

Figure 6–2 Chloride Content Vs Potentials

The schematic of simulation routine is shown in figure (6-3). In the current study, however, the Monti Carlo Simulation was used to predict the corrosion threshold. The data was analyzed, and the numerical simulations were performed to estimate the corrosion threshold level (initiation) of the deck at certain depths based on current research data and some values from previous literature [Kirkpatrick et al 2000]. The number of samples in each simulation is equal to 100,000 and each simulation is repeated 20 times to get one distribution for each condition. The parameters of the probabilistic model are presented in the table (8-5) below depending on current study laboratory data of 2 years and previous literature [Kirkpatrick et al 2000]. The random variables we used in the simulations have uniform distribution because there is no information about the shape of this variables but only the ranges.

Table 6-5 Boundaries of the Probabilistic Model

Random Variable	Type of Distribution	min	max	Reference
Initial Chloride Content, C_0	Uniform	0.3	0.8	Current Study
Diffusion, D_c [in^2/year]	Uniform	0.016	0.047	Range from Kirkpatrick et al. 2002
$C_{(x, t)}$	Uniform	0.06	0.55	Range from Kirkpatrick et al. 2002 [%]

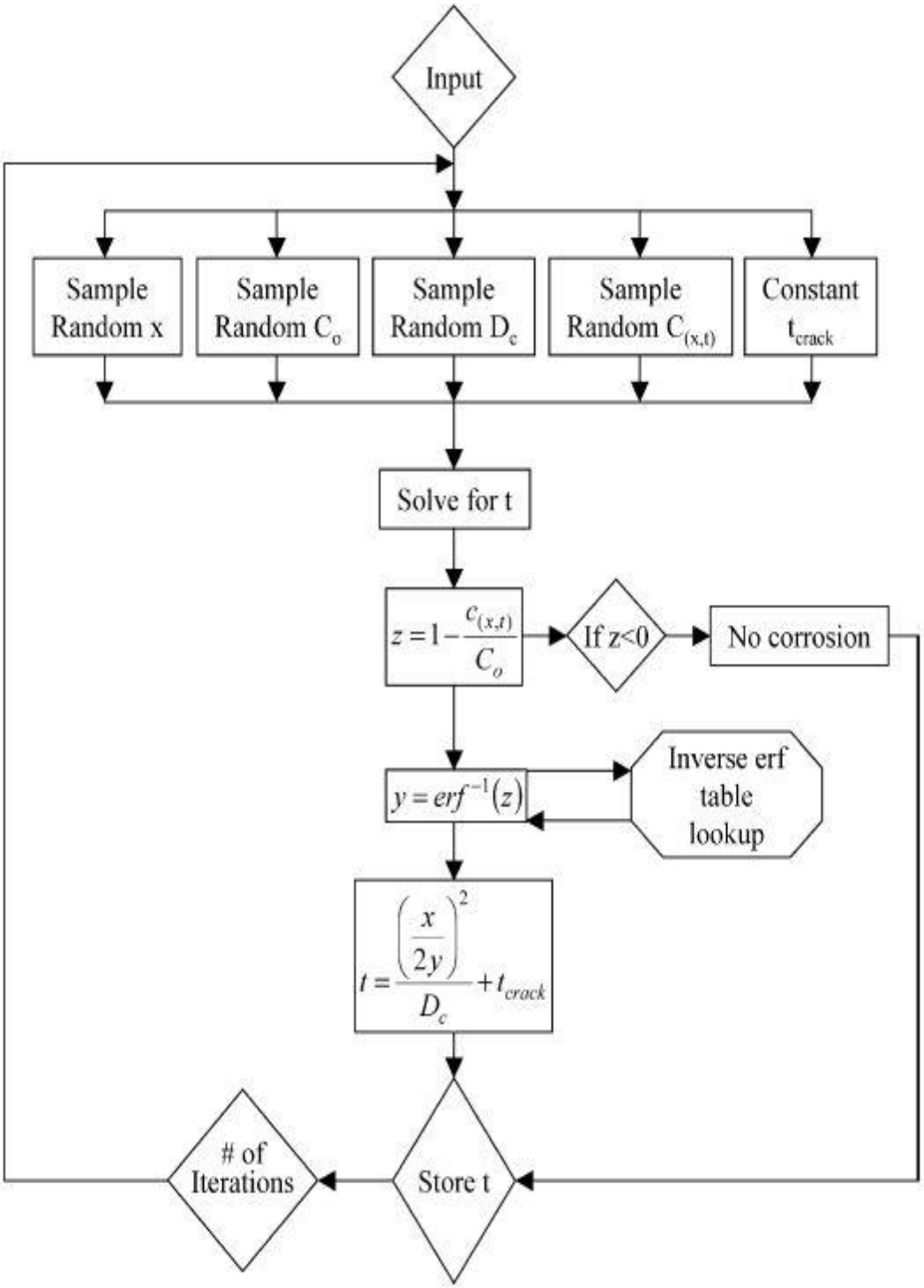

Figure 6–3 The Schematic of Simulation Routine of Service Life Model

[Kirkpatrick et al 2002]

Furthermore, the simulations process was repeated for different depths, 1 in, 2 in, and 3 in respectively. The probabilities of the corrosion initiation for each deck is equal or smaller than 20, 30, 40, 50, and 60 years are presented in table (6-6) and plotted in figures 6-4, 6-5, and 6-6 below.

Table 6-6 Probability of Corrosion Initiation

Chloride Content Depth (inches)	Probability of Corrosion Initiation (%)				
	20yrs	30yrs	40yrs	50yrs	60yrs
1	34	50	60	67	73
2	2	10	21	30	39.9
3	0	0	2	7	13

Figure 6–4 PDF of Corrosion Initiation at Depth 1”

Figure 6–5 PDF of Corrosion Initiation at Depth 3”

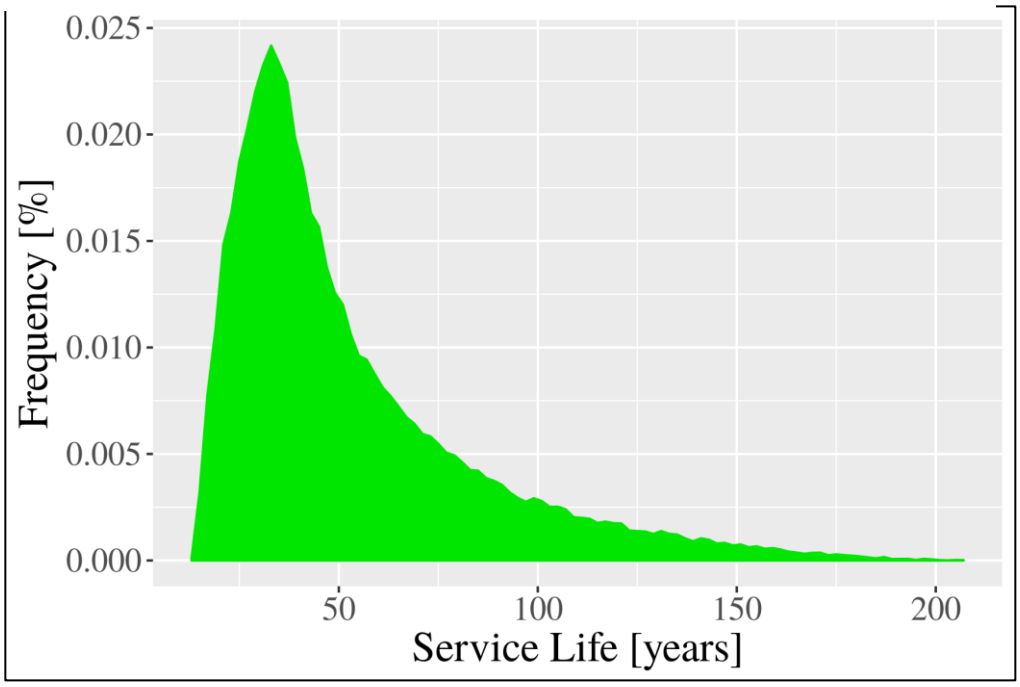

Figure 6–6 PDF of Corrosion Initiation at Depth 2”

Future Recommendations

Depending on the test results and to investigate some important issues which were not covered in this research, the following recommendations could be suggested:

i. Investigate the corrosion behavior of High performance concrete (HPC) reinforced with Black Steel.
ii. Study the correlation between laboratory and field performances of corrosion of Galvanized Steel bridge decks.
iii. Find out the corrosion behavior of reduced cover high performance concrete bridge decks reinforced with MMFX and Stainless Steel rebars.
iv. Test the effects of load-induced-cracking on the corrosion of reinforced concrete slabs.
v. Compute the induced corrosion of sodium chloride and carbon dioxide of bridge decks at un urban highway.

References:

1. Bezad Bavarian and Lisa Reiner," Migrating Corrosion Inhibitors for Steel Rebar in Concrete", Feb 2003.
2. ACI 222R-96, Corrosion of metals in concrete, state of the art, committee report.
3. Zdenek P. Bazant," physical model for steel corrosion in concrete sea structures theory", journal of the Structural division, 14651, June 1979.
4. Sang-Soon Park, Seung-Jun Kwon , and Sang Hwa Jung," Analysis technique for chloride penetration in cracked concrete using equivalent diffusion and permeation", Construction and Building Materials 29 (2012) 183–192.
5. Ahmad, S. "Reinforcement Corrosion in Concrete Structures, its Monitoring and Service Life Prediction - A Review." Cement & Concrete Composites, V. 25, pp. 459-471. 2003.
6. Ann, K. Y., and Song, H.-W. (2007). "Chloride Threshold Level for Corrosion of Steel in Concrete." Corrosion Science, V. 49 (11), pp. 4113-4133.
7. ASTM A416 / A416M - Standard Specification for Steel Strand, Uncoated Seven-Wire for Prestressed Concrete. American Society of Testing and Materials, West Conshohocken, PA. 2007.
8. Basheer, L., Kroppb, J. and Clelandc, D. J. (2001). "Assessment of the durability of concrete from its permeation properties: a review." Construction and Building Materials, V. (15), pp. 93-103.
9. Bertolini, L., Elsener, B., Pedeferri, P., and Polder, R.," Corrosion of Steel in Concrete", Wiley-VCH, 2004.
10. Mehta, P. K. (1991). Corrosion in the Marine Environment, Elsevier Applied Science.
11. Perez N," Electrochemistry and Corrosion Science, Kluwer Academic Publishers, Norwell, MA, 2004.
12. Thomas D, "Fundamentals of Electrochemistry", University of Guelph, 2003.
13. Jones D. A," Principles and Prevention of Corrosion", Prentice Hall, 1996.

ASTM C876-07, "Standard test method for half-cell potentials of uncoated reinforcing steel in concrete", West Conshohocken, PA. 2007.

14. ASTM G109-07," Standard test method for determining effects of chemical admixtures on corrosion of embedded steel reinforcement in concrete exposed to chloride environments". West Conshohocken, PA. 2007.
15. Hai-Long Wang, Jian-Guo Dai , Xiao-Yan Sun, and Xiao-Long Zhang," Characteristics of concrete cracks and their influence on chloride penetration", Construction and Building Materials 107 (2016) 216–225.
16. ACI 222R, "Corrosion of metals in concrete, state of the art", committee report, 1996.
17. W. Morris, A. Vico, M. Vazquez and S.R. De Sánchez. Corros. Sci. 44 (2002) 81.
18. S.E. Hussain M. Rasheeduzzafar, A. Al-Musallan and A.S. Al-Gahtani. Cem. Conc. Res. 25 (1995) 15.
19. R.E. Weyers, W. Pyc, and M.M. Sprinkel, "Estimating the service life of epoxy-coated reinforcing steel", ACI Mater. J. 95 (5) (1998) 546–557.
20. B.B. Hope, A.K. Ip and D.G. Manning. Cem. Conc. Res. 15 (1985) 525.
21. P.G.Cavalier and P.R.Vassie, Institution of Civil Engineers Vol.70, Part 1 August 1981 p.461-480.
22. R.D.Browne, "Durability of Building Materials", 1(1982).
23. Ha-Won Song1 and Velu Saraswathy," Corrosion Monitoring of Reinforced Concrete Structures", international journal of science 2007.
24. K.C. Clear," Assess the corrosion activity of steel reinforced concrete structures", Transport Res Record 1211 (1989) 28.
25. Koichi Kobayashi and Yuta Kojima," Effect of fine crack width and water cement ratio of SHCC on chloride ingress and rebar corrosion", Cement and Concrete Composites 80 (2017) 235e244.
26. Yue Li, Xiaohan Chen, Liu Jin, and Renbo Zhang," Experimental and numerical study on chloride transmission in cracked concrete", Construction and Building Materials 127 (2016) 425–435.
27. Hailong Ye, Ye Tian, Nanguo Jin, Xianyu Jin, and Chuanqing Fu," Influence of cracking on chloride diffusivity and moisture influential depth in concrete subjected to simulated environmental conditions", Construction and Building Materials 47 (2013) 66–79.

28. Junjie Wang, P.A. Muhammed Basheer, Sreejith V. Nanukuttan, Adrian E. Long, and Yun Bai," Influence of service loading and the resulting micro-cracks on chloride resistance of concrete", Construction and Building Materials 108 (2016) 56–66.
29. Zdenek P. Bazant," physical model for steel corrosion in concrete sea structures theory", journal of the Structural division, 14651, June 1979.
30. M. Stern and A.L. Geary. J," Electrochemical Polarization, a Theoretical Analysis of the Shape of Polarization Curves", Journal of the Electrochemical Society, 104 (1957) 56.
31. C. Andrade, M. C. Alonso, J. A. Gonzalez," an initial effort to use the corrosion rate measurements for estimating rebar durability", ASTM STP., corrosion rates of steel in concrete, Philadelphia. 29-37,1990.
32. M.A. Pech-Canul and P. Castro," Corrosion measurements of steel reinforcement in concrete exposed to a tropical marine atmosphere", cement and concrete research 32 491, 2002.
33. B.Elsener," Ageing of Passive Films on Stainless Steels in Sulfate Solutions - XPS Analysis", Material Science Forum, 192-194, 1995.
34. ACI 222R-01, Protection of Metals in Concrete Against Corrosion, American Concrete Institute, Michigan, USA, 2001, p. 25.
35. E.L. Portela and T.N. Bitterncourt," Time-dependent probabilistic modeling of corrosion propagation for service life prediction in RC structures", University of São Paulo, São Paulo, Brazil, 2011.
36. P.C. Searson and J.L. Dawson. J.," Analysis of Electrochemical Noise Generated by Corroding Electrodes under Open-Circuit Conditions", Electrochem. Soc. 135, 1988.
37. AASHTO T 277," Electrical Indication of Concrete's Ability to Resist Chloride Ion Penetration".
38. D. Sato," Measurement technique of acquiring sodium chloride concentration by using near-infrared spectrum", Proceedings of JSCE annual conference, Vol.56, pp.844-845, 2001.
39. David Trejo and Ceki Halmen," corrosion performance tests for reinforcing steel in concrete: test procedures", report FHWA/TX-09/0-4825-P1.,2009.

40. Brent M. Phares, Fouad S. Fanous, Terry J. Wipf, Yoon-Si Lee, Milan J. Jolley, 2006, “Evaluation of Corrosion Resistance of Different Steel Reinforcement Types”, report CTRE Project 02-103.
41. Carmen ANDRADE, Isabel MARTÍNEZ, 2009, “Embedded sensors for the monitoring of corrosion parameters in concrete structures”, NDTCE’09, Non-Destructive Testing in Civil Engineering Nantes, France.
42. Tamer Almmddawy, Khaled soudki, and timothy topper, 2005, “Long term performance of corrosion-damaged reinforced concrete beams”, ACI Structural Journal, vol 102, No 5, title no 102-S66.
43. Hyoung seok So and Stephen Geoffrey Millard, 2007, “on site measurement on corrosion rate of steel in reinforced concrete”, ACI-material journal, vol 104, No 6, November-December, title no 104-M70.
44. Wiss, Janney, Elstner Associates, Inc, “Comparative Corrosion Testing and Analysis of MMFX 2 Rebars for Reinforced Concrete Applications”, final report 19 Feb 2008, WJE No 20, 3.0707.0.
45. Wenjun Zhu, Raoul François, Dario Coronelli , and David Cleland, “Effect of corrosion of reinforcement on the mechanical behavior of highly corroded RC beams”, Engineering Structures 56 (2013) 544–554.
46. A. Poursaee1, “Corrosion Measurement Techniques in Steel Reinforced Concrete”, Journal of ASTM International, Vol. 8, No. 5, Paper ID JAI103283, 2011.
47. T. Vidal, A. Castel, R. François, “Corrosion process and structural performance of a 17 year old reinforced concrete beam stored in chloride environment”, Cement and Concrete Research 37 (2007) 1551–1561, 13 August 2007.
48. Gustavo S. Duffó and Silvia B. Farina, “Development of an embeddable sensor to monitor the corrosion process of new and existing reinforced concrete structures”, Construction and Building Materials, 23 (2009) 2746–2751.
49. Paul D. Goodwin, Gregory C. Frantz, Jack E. Stephens, “Protection of Reinforcement with Corrosion Inhibitors, Phase II”, Final Report, No. JHR 00-279 N/A, December 2000.
50. Liam Holloway, “concrete reinforcement corrosion: Understanding amino carboxylate Base inhibitor mitigation and Galvanostatic electrochemical Monitoring”, A thesis

submitted to the Faculty of Engineering at Monash University for the degree of Doctor of philosophy, November 2005 Melbourne, Australia.

51. Youping Liu, "Modeling the Time-to-Corrosion Cracking of the Cover Concrete in Chloride Contaminated Reinforced Concrete Structures", Dissertation submitted to the Faculty of the Virginia Polytechnic Institute and State University in partial fulfillment of the requirements for the degree of Doctor of Philosophy in Civil Engineering, October 21, 1996, Blacksburg, Virginia.
52. E. V. Pereira1, R. B. Figueir, M. M. Salta1, I. T. E. Fonseca, "Embedded Sensors for Corrosion Monitoring of Existing Reinforced Concrete Structures", Materials Science Forum Vols. 587-588 (2008) pp 677-681.
53. John S. Popovicsa, Gonzalo E. Galloa, Melanie Sheltonb, and Patrick L. Chapman, "A magnetic sensing approach to characterize corrosion in reinforced concrete", Downloaded From: http://proceedings.spiedigitallibrary.org/ on 07/21/201.
54. Mauricio Mancio, Cruz Carlos Jr., Jieying Zhang, John T. Harvey, and Paulo J. M. Monteiro, "Laboratory Evaluation of Corrosion Resistance of Steel Dowels in Concrete Pavement", Research Report: UCPRC-RR-2005-10, January 2007.
55. Brian M. Pailes, "Statistical Correlation Method to Identify Half-Cell Potential and Electrical Resistivity Threshold Values", Rutgers, The state university of New Jersey, Center of advance infrastructure and transportation, 2014.
56. Matt O'Reilly," Comparison of ASTM A955 Corrosion Testing Methods with Field Performance of Reinforcement", ACI Convention-Phoenix, AZ. 2013
57. Carolyn Hansson, 2013, "The Case for Cyclic Corrosion Testing", ACI Convention-Phoenix, AZ.
58. Chungwook Sim and Robert J. Frosch, 2013," Evaluating corrosion protection systems for bridge decks with modified macrocell specimens", ACI 2013 Fall Convention, Phoenix, AZ.
59. M.P. Papadopoulos, C.A. Apostolopoulos, A.D. Zervaki, G.N. Haidemenopoulos, 2011," Corrosion of exposed rebars, associated mechanical degradation and correlation with accelerated corrosion tests", Construction and Building Materials 25 (2011) 3367–3374.

60. Chuen-Chang Lin and Chi-Xiang Wang,” Correlation between accelerated corrosion tests and atmospheric corrosion tests on steel”, Journal of Applied Electrochemistry (2005) 35:837–843. 2005
61. ASTM C1202, Standard Test Method for Electrical Indication of Concrete's Ability to Resist Chloride Ion Penetration”, West Conshohocken, PA. 2007.
62. https://www.nace.org/uploadedFiles/Publications/ccsupp.pdf.
63. Richard E. Weyers, Brian D. Prowell, Michael M. Sprinkel, and Michael Vorster,” concrete bridge protection, repair, and rehabilitation relative to reinforcement corrosion”, Strategic Highway Research Program, National Research Council, Washington, DC, 1993.
64. Gaal, G.C.M., van der Veen, C., and Djorai, M.H.,” Deterioration of concrete bridges, in the Netherlands”, Proceedings of Structural Faults & Repair (Forde, M. ed.), London, 2001.
65. http://www.cement.org/images/defaultsource/contech/corrosion_water_graphic.jpg?sfvrsn=2.
66. http://www.esgroundingsolutions.com.
67. M. B. Otieno, M. G. Alexander and H.-D. Beushausen,”. Corrosion in cracked and uncracked concrete –influence of crack width, concrete quality and crack reopening”, Magazine of Concrete Research 62, No. 6, June 2010, 393–404
68. ACI 222.3R,” Guide to Design and Construction Practices to Mitigate Corrosion of Reinforcement in Concrete Structures, 2011.
69. Kim, Yun-Yong, Lee, Byung-Jae, and Seung-Jun, “Evaluation Technique of Chloride Penetration Using Apparent Diffusion Coefficient and Neural Network Algorithm”, Sep. 2014.
70. “Corrosion of steel reinforcement in 12 years old concrete: Inspection, evaluation and electrochemical repair of corrosion”, July 2010.
71. Aimin Xu and Ahmad Shayan,” Relationship between Reinforcing Bar Corrosion and Concrete Cracking”, ACI Materials Journal, Volume: 113, Issue: 1, Pages 3-12, Jan. 2016.

72. Mark G Stewart, Ali Al-Harthy," Pitting corrosion and structural reliability of corroding RC structures: Experimental data and probabilistic analysis", Reliability Engineering & System Safety, 2008.
73. Subramaniam, Kolluru, and, Mingdong Bi," Investigation of steel corrosion in cracked concrete: Evaluation of macrocell and microcell rates using Tafel polarization response", SP - 2725–2735, corrosion science, Aug. 2010.
74. ASTM C39," Standard Test Method for Compressive Strength of Cylindrical Concrete Specimens", West Conshohocken, PA. 2007.
75. Tensile strength-ASTM C496," Standard Test Method for Splitting Tensile Strength of Cylindrical Concrete Specimens", West Conshohocken, PA. 2007.
76. Flexural strength- ASTM C78," Standard Test Method for Flexural Strength of Concrete (Using Simple Beam with Third-Point Loading)", West Conshohocken, PA. 2017.
77. Static Modulus of Elasticity- ASTM C469-469 M," Standard Test Method for Static Modulus of Elasticity and Poisson's Ratio of Concrete in Compression", West Conshohocken, PA. 2007.
78. Free Shrinkage- ASTM C157," Standard Test Method for Length Change of Hardened Hydraulic-Cement Mortar and Concrete", West Conshohocken, PA. 2017.
79. Rapid Chloride Permeability- AASHTO T 277," Standard Method of Test for Electrical Indication of Concrete's Ability to Resist Chloride Ion Penetration", 2015.
80. Surface resistivity- AASHTO T 358," Standard Method of Test for Surface Resistivity Indication of Concrete's Ability to Resist Chloride Ion Penetration", 2017.
81. http://www.corrosion service.com.
82. Sang-Soon Park, Seung-Jun Kwon, Sang Hwa Jung," Analysis technique for chloride penetration in cracked concrete using equivalent diffusion and permeation", Construction and Building Materials 29 (2012) 183–192.
83. Hai-Long Wanga, Jian-Guo Dai, Xiao-Yan Sun , Xiao-Long Zhang," Characteristics of concrete cracks and their influence on chloride penetration", Construction and Building Materials 107 (2016) 216–225.

84. Seung Yup Jang, Bo Sung Kim, Byung Hwan, “Effect of crack width on chloride diffusion coefficients of concrete by steady-state migration tests”, Cement and Concrete Research 41 (2011) 9–19.
85. Koichi Kobayashi, Yuta Kojima,” Effect of fine crack width and water cement ratio of SHCC on chloride ingress and rebar corrosion”, Cement and Concrete Composites 80 (2017) 235e244.
86. Yue Li, Xiaohan Chen, Liu Jin, Renbo Zhang,” Experimental and numerical study on chloride transmission in cracked concrete”, Construction and Building Materials 127 (2016) 425–435.
87. Hailong Ye, Ye Tian, Nanguo Jin, Xianyu Jin, Chuanqing Fu,” Influence of cracking on chloride diffusivity and moisture influential depth in concrete subjected to simulated environmental conditions”, Construction and Building Materials 47 (2013) 66–79.
88. Junjie Wanga, P.A. Muhammed Basheer, Sreejith V. Nanukuttan , Adrian E. Long, Yun Bai,” Influence of service loading and the resulting micro-cracks on chloride resistance of concrete”, Construction and Building Materials 108 (2016) 56–66.
89. Jin-xia XU, Lin-hua JIANG2, Qi WANG,” Finite element model of reinforcement corrosion in concrete, Water Science and Engineering, 2009, 2(2): 71-78.
90. Tomasz Krykowskia, Adam Zybura,” Modelling of Reinforced Concrete Element Damage as a Result of Reinforcement Corrosion”, 11th International Conference on Modern Building Materials, Structures and Techniques, MBMST 2013, Procedia Engineering 57 (2013) 614 – 623.
91. Di QIAO,” experimental and numerical study on corrosion-induced damages on reinforced concrete structures, A Dissertation Submitted to Nagoya University in Partial Fulfillment of the Requirements for the degree of Doctoral of Engineering Department of Civil Engineering Graduate School of Engineering, Nagoya University Nagoya, JAPAN.
92. ASTM C 1152/C 1152M – 03, “Standard Test Method for Acid-Soluble Chloride in Mortar and Concrete”, West Conshohocken, PA. 2007.
93. E.L. Portela and T.N. Bittencourt,” sBtrauycetsuiraens inference for the assessment of the carbonation front in RC”, Bakker, Frangopol & van Breugel (Eds) © 2017 Taylor & Francis Group, London, ISBN 978-1-138-02847.

94. ASTM C 1556 – 03, “Standard Test Method for Determining the Apparent Chloride Diffusion Coefficient of Cementitious Mixtures by Bulk Diffusion, West Conshohocken, PA. 2007.
95. P. Ghods, K. Karadakis1, O. B. Isgor, G. McRae1,” Modeling the chloride-induced corrosion initiation of steel rebar in concrete”, Excerpt from the Proceedings of the COMSOL Conference 2009 Boston.
96. Life-365™ Service Life Prediction Model,” Computer Program for Predicting the Service Life and Life-Cycle Cost of Reinforced Concrete Exposed to Chlorides, Version 2.2.1, January 15, 2018.
97. Raja Rizwan Hussain,” Modeling of Corrosion; Steel, Concrete and Environment”, Civil Engineering Department, College of Engineering at King Saud University, Riyadh, Saudi Arabia.
98. E.L. Portela and T.N. Bitterncourt,” Time-dependent probabilistic modeling of corrosion propagation for service life prediction in RC structures”, University of São Paulo, São Carlos, Brazil.
99. S. Altoubat, M. Maalej, and F. U. A. Shaikh,” Laboratory Simulation of Corrosion Damage in Reinforced Concrete”, International Journal of Concrete Structures and Materials, Vol.10, No.3, pp.383–391, September 2016.
100. Modelling of reinforcement corrosion in concrete - State of the art, COIN Project report 7– 2008.
101. Ne´stor F. Ortega, Sandra I. Robles.” Assessment of Residual Life of concrete structures affected by reinforcement corrosion”, Housing and Building National Research Center-HBRC Journal, Nov.2014.
102. Gregory S. Williamson, Richard E. Weyers, Michael M. Sprinkel, and Michael C. Brown,” Concrete and Steel Type Influence on Probabilistic Corrosion Service Life”, ACI Materials Journal/January-February 2009.
103. D. Cusson, Z. Lounis & L. Daigle,” Durability Monitoring for Improved Service Life Predictions of Concrete Bridge Decks in Corrosive Environments”, Computer-Aided Civil and Infrastructure Engineering 26 (2011) 524–541.

104. Ranjith, K. Balaji Rao, K. Manjunath," Evaluating the effect of corrosion on service life prediction of RC structures – A parametric study", International Journal of Sustainable Built Environment (2016) 5, 587–603.

105. AMEC Earth and Environmental, a division of AMCE Americas Limited," Comparative performance of MMFX Microcomposite Reinforcing Steel and other types of steel with respect to corrosion resistance and service life prediction in reinforced concrete structures", MMFX Technologies Corporation, Irvine, California, USA, 20 February 2006.

106. Materials properties and design consideration," a report of MMFX Steel corporation of America, Irvine, California, USA, 2012.

107. Lien Gong, David Drawn, and JoAnn Locker, Jr, "evaluation of mechanical and corrosion properties of MMFX reinforcing steel for concrete", Kensas department of transportation, division of operation, Bureau of materials and research, University of Kansas, 2004.

108. Trevor J. Kirkpatricka, Richard E. Weyersa, Michael M. Sprinkel, Christine M. Anderson-Cook," Impact of specification changes on chloride-induced corrosion service life of bridge decks", Cement and Concrete Research 32 (2002) 1189–1197.

109. R.E. Weyers, M.G. Fitch, E.P. Larsen, I.L. Al Qadi, W.P. Chamberlin, P.C. Hoffman, Concrete bridge protection and rehabilitation: chemical physical techniques, service life estimates, SHRP-S-668, Strategic Highway Research Program, Washington, DC, 1994.

110. T.J. Kirkpatrick, R.E. Weyers, C.M. Anderson-Cook, M.M. Sprinkel, Stochastic model for the chloride induced corrosion service life of bridge decks, Cement and Concrete Research, 2001.

111. P.D. Cady, R.E. Weyers, Deterioration rates of concrete bridge decks, Journal of Transportation Engineering 110 (1) (1984) 35– 44.

112. Sonjoy Deb,"Critical Chloride Content in Reinforced Concrete", August 2012,www.masterbuilder.co.in.

113. S. Erdogdu, T.W. Bremner, I.L. Kondratova, Accelerated testing of plain and epoxy-coated reinforcement in simulated seawater and chloride solutions, Cement and Concrete Research 31 (2001) 861–867.

114. L. Bertolini, B. Elsener, P. Pedeferri, R. Polder, Corrosion of Steel in Concrete, WILEY VCH, 2004.

115. Saleh A. Al-Saleh," Analysis of total chloride content in concrete", Case Studies in Construction Materials 3 (2015) 78–82.

116. Tareq Salih AL-ATTAR and Mustafa Sameer ABDUL-KAREEM," effect of chloride ions source on corrosion of reinforced concrete", Buletinul AGIR nr. aprilie-iunie, Feb. 2011.

117. Hooton R.D, Stanish, K.D., and Thomas, M.D.A,"Testing the Chloride Penetration Resistance of Concrete", University of Toronto, FHWA Contract DTFH61-97-R-00022, 1997.

118. NELSON SILVA," Chloride Induced Corrosion of Reinforcement Steel in Concrete, Threshold Values and Ion Distributions at the Concrete-Steel Interface", Department of Civil and Environmental Engineering, thesis for the degree of Doctor of Philosophy, chalmers university of technology, Gothenburg, Sweden, 2013.

119. Gerhardus H. Koch, Michiel P.H., Brongers, and Neil G. Thompson, "Corrosion Costs and Preventive Strategies in the United States", PUBLICATION NO. FHWA-RD-01-156.

120. Reza Madanipour and Chanakya Arya," Chloride Threshold Value for Corrosion of Steel in Concrete", UCL Department of Civil, Environmental and Geomatic Engineering, Gower St, London, WC1E 6BT.

121. Terry Hholand," Chloride limits in the ACI 318 building code requirements", Publication #J980869, Copyright© 1998, The Aberdeen Group.

122. Muhammad Umar Khan, Shamsad Ahmad, and Husain Jubran Al-Gahtani," Chloride-Induced Corrosion of Steel in Concrete: An Overview on Chloride Diffusion and Prediction of Corrosion Initiation Time", Civil and Environmental Engineering Department, King Fahd University of Petroleum & Minerals, Dhahran 31261, Saudi Arabia, International Journal of Corrosion, Article ID 5819202, 2017.

123. L.-Y. Li, J. Xia, and S.-S. Lin, "A multi-phase model for predicting the effective diffusion coefficient of chlorides in concrete," Construction and Building Materials, vol. 26, no. 1, pp. 295–301, 2012.

124. D. P. Bentz, E. J. Garboczi, Y. Lu, N. Martys, A. R. Sakulich, and W. J. Weiss, “Modeling of the influence of transverse cracking on chloride penetration into concrete,” Cement and Concrete Composites, vol. 38, pp. 65–74, 2013.

125. Thoft-Christensen, P.,” Modeling of the deterioration of reinforced concrete structures”, Proceedings of IFIP Conference on Reliability and Optimization of Structural Systems, Ann Arbor, Michigan, USA, p.15-16, 2000.

126. J. C. M. Maage and S. Helland, “Practical non-steady state chloride transport as a part of a model for predicting the initiation period,” in Proceedings of the 1st International RILEM Workshop, pp. 398–406, 1995.

127. N. S. Que,“History and development of prediction models of time-to-initiate-corrosion in reinforced concrete structures in marine environment”, Philippine Engineering Journal, vol. 28, pp. 29–44, 2007.

128. B.S. Covino Jr., S.D. Cramer, G.R. Holcomb, J.H. Russell, S.J. Bullard, C. Dahlin, J.S. Tinnea, Performance of epoxy-coated steel reinforcement in the deck of the perley bridge, Ministry of Transportation, Toronto, 2000.

129. Trevor J. Kirkpatrick, Richard E. Weyersa, Christine M. Anderson-Cook, and Michael M. Sprinkel,” Probabilistic model for the chloride-induced corrosion service life of bridge decks”, Cement and Concrete Research 32 (2002) 1943–1960.

130. J. Crank,” The Mathematics of Diffusion”, second edition, Oxford University, Great Britain, 1975.

131. K.C. Clear, Effectiveness of epoxy-coated reinforcing steel, Final Report, Canadian Strategic Highway Research Program, 1998.

Appendix

Concrete sealant technical data

i- T-70

CASTEK® A TRANSPO INDUSTRIES COMPANY INC.

Technical Data Sheet

High Molecular Weight Methacrylate (HMWM) Crack Sealer Sealate® (T-70-10 and T-70 MX-30)

Sealate® is a specially formulated, high molecular weight methacrylate resin system that is highly effective for sealing and filling cracks in concrete structures.

Application Procedure

Surface Preparation: It is strongly recommended that all concrete surfaces that are to receive Sealate® be thoroughly clean and sound. Remove all surface dirt, grease, paint, rust, and other contaminates by sand blasting or shot blasting. Applications on LMC overlays do not require blasting or mechanical abrasion, the surface can be high pressure washed to remove contamination. Before application of Sealate® the surface must be dry for 24 hours and just prior to application cracks should be cleaned with dry high pressure compressed air. The concrete surface should be visibly dry and the moisture content in the concrete should be tested according to ASTM D4263. The temperature of the deck and air should be between 50°F and 100°F prior to resin application.

Mixing: Table 1 lists the mixing ratios of the two curing agents. Add the appropriate amount of Cobalt Napthenate promoter to Sealate® resin and stir well. Then add the corresponding amount of CHP initiator, stir again for 1-2 minutes. If machine applied, the resin should be mixed utilizing a two component resin system using promoted resin for one part and initiated resin for the other part. Mixing ratio of promoted/initiated resin should be 1:1. The mixed resin should be applied to the concrete surface within 5 minutes of complete mixing.

Table 1: Mixing Instructions for Sealate®, Cobalt Napthenate and CHP

Sealate® (gal)	Cobalt Napthenate (mL)	CHP (mL)
1	75	150
5	375	750

CAUTION: Never mix CHP initiator with Cobalt promoter. Violent reaction will result!

Application: The rate of application of promoted/initiated resin should be approximately 100-150 square feet per gallon. However, this will vary depending on the surface, porosity, size, and quantity of cracks present in the area being treated.

Spray equipment, if used, should be airless, generating sufficient pressure to atomize mixed resins. If hand applied, the concrete surface should be flooded with the resin, allowing sufficient time for penetration into the surface and complete filling of all cracks. Excess material should be redistributed using squeegees or brooms within 15 minutes after application. The quantity of initiated/promoted resin mixed at one time should be limited to 5 gallons for manual application.

Broadcasting of Aggregate: Broadcast sand should be applied to the entire treated area prior to cure, typically at 1-2 pounds per square yard. The sand used should be 12 x 16 mesh, #1 or #2 blasting sand, and should have a maximum moisture content no greater than 0.5%. It should be placed within 15-20 minutes of the resin application and before any setting of monomer occurs. Traffic can be restored once the concrete surface is cured tack-free. Refer to Table 2 for temperature restrictions and cure times.

Table 2: Cure Times for Sealate®

Ambient Temperature	Approximate Cure Time	
	T-70-10	T-70 MX-30
50°F – 70°F	7 – 12 hr	8 – 16 hr
70°F – 100°F	4 – 7 hr	5 – 8 hr

*Cure times are approximate and will vary with ambient and deck temperature, humidity, and sunlight. Structures can be opened to traffic only after complete cure is achieved.

TRANSPO

Table 3: Properties* of Sealate®

Property	Results		Test Method
	T-70-10	T-70 MX-30	
Appearance	Amber Liquid	Amber Liquid	
Viscosity	15 – 25 cps (MPa-sec)	10 – 25 cps (MPa-sec)	ASTM D2395
Density	8.4 – 8.6 lb/gal (1.01 – 1.03 g/mL)	8.1 – 8.5 lb/gal (0.97 – 1.02 g/mL)	ASTM D1425
Gel Time/Pot Life @ 70°F	35 – 40 min	50 – 60 min	AASHTO T237
Tack Free Time @ 70°F	4 – 7 hr	6 – 8 hr	AASHTO T237
Flash Point	>210°F (>99°C)	>200°F (>93°C)	ASTM D1310/ASTM D93/ASTM 3278
Solids Content	100%	100%	ASTM D1644
Tensile Strength	1,600 psi (>11.0 MPa)	>500 psi (>3.4 MPa)	ASTM D638 Type I
PCC-SSD Bond Strength	>615 psi (>4.2 MPa)	>615 psi (>4.2 MPa)	CA Test 551
Tensile Elongation	1 – 5%	>30%	ASTM D638 Type I
Compressive Strength (24 hr)**	>8,150 psi (56.2 MPa)	>3,500 psi (>24.1 MPa)	ASTM C579 Method B
Volatile Content	30% max	40 – 45%	ASTM D2369
Slant Shear Bond Strength	>1,500 psi (>10.3 MPa)	>1,500 psi (>10.3 MPa)	ASTM C882
Vapor Pressure @ 77°F	0.62 mm Hg	0.52 mm Hg	ASTM D323 Reid Method

*To be used as general guidelines only

**Samples should be made using 2.75 volume parts 20-30 sand per ASTM C778, No. 20 to No. 30 sieve to one volume part of mixed epoxy

Packaging

Sealate® comes in 1, 5 and 55- gallon containers. The initiator, Cumene Hydroperoxide (CHP) and the Cobalt Napthenate promoter are provided in separate labeled containers and in pre-measured quantities to make scale mixes of Sealate®.

Storage

Sealate® should be stored in tightly sealed containers in a dry location and at normal room temperatures (50°F - 85°F). The initiator, Cumene Hydroperoxide (CHP) and the Cobalt Napthenate promoter are provided in separate labeled containers, and should be stored in a cool shaded area separately from each other and away from the monomer.

Caution

Direct contact with Sealate® may produce minor skin irritations to persons prone to such reactions. It is recommended that all persons involved in mixing and application wear protective clothing such as goggles, rubber boots, and rubber gloves. As with all chemicals, read MSDS prior to use.

Warranty

The following warranty is made in lieu of all other warranties, either expressed or implied. This product is manufactured of selected raw materials by skilled technicians. Neither seller nor manufacturer has any knowledge or control concerning the purchaser's use of product and no warranty is made as to the results of any use. The only obligation of either seller or manufacturer shall be to replace any quantity of this product that proves to be defective. Neither seller nor manufacturer assumes any liability for injury, loss or damage resulting from use of this product.

10/2014

20 Jones Street, New Rochelle, NY 10801

Tel: 914-636-1000
Web: http://www.transpo.com

Fax: 914-636-1282
Email: info@transpo.com

ii- Seal Krete-SK

SEAL KRETE

CLEAR-SEAL

CONCRETE PROTECTIVE SEALER

PRODUCT DATA SHEET

DESCRIPTION: Clear protective finish for painted, stained or bare concrete & masonry surfaces; premium water-based urethane-fortified acrylic. Available in Satin & Gloss sheens.

Typical Uses:

- ✓ Pool Decks
- ✓ Patios & Porches
- ✓ Brick & Stone
- ✓ Driveways & Garages
- ✓ Exposed Aggregate
- ✓ Slate & Saltillo
- ✓ Pavers & Stamped Concrete

Important: *Read all directions thoroughly. Recommended: Wear gloves and safety glasses.*

SURFACE PREP*: Note: *The surface should be clean and dry. You may need an oil stain remover such as SEAL-KRETE® Oil Stain Remover to lift stubborn oil stains. Pressure-washing is recommended.*

Bare Concrete: Concrete must have cured for a minimum of 30 days. Etch smooth-finished concrete (such as basement or garage floors) with a concrete etching solution like SEAL-KRETE Clean-N-Etch. ***Note:*** *If etching with muriatic acid the area must be neutralized before proceeding. For more information visit www.seal-krete.com.*

Painted Surfaces: For use over one-part water-based coatings only; not recommended over acid-based stains or oil-based coatings. Freshly painted surfaces must have cured for a minimum of 72 hours. Paint must be sound (not blistering or peeling). Existing painted surfaces should be cleaned with a solution of Trisodium Phosphate (TSP) and water. Rinse well and allow to dry.

APPLICATION: Read "LIMITATIONS" section before use. This product is ready to use; do not dilute. Stir gently; do not shake. Apply in light, even coats. One coat is recommended; however, over porous surfaces (like saltillo tile) or when a higher sheen is desired, apply a second coat. ***Note:*** *Sealer goes on milky white but dries clear.*

Roller: Dampen roller, remove excess water, then saturate roller with product. Keep a wet edge while rolling. Do not allow to puddle, foam or run. (Use a 5 mm nap for smooth surfaces, 10 mm nap for rough or porous surfaces.)

Pump Sprayer: Set at a fine spray and apply using a circular motion. To eliminate puddling or to achieve a more uniform finish, backroll immediately after spraying.

COVERAGE: 13–27 m² per 3.78, depending on surface porosity.

DRY TIME: Dry to touch in 1 hour at 25°C 50% RH. Recoat in 2 hours. Dry to foot traffic in 24 hours. Will accept vehicular traffic in 72 hours. Dry times should be extended in colder climates.

CLEAN-UP & STORAGE: Clean tools with soap and water immediately after use. Store in a dry area. KEEP FROM FREEZING.

MAINTENANCE: Clean with a mild soap and water solution. Do not use solvent-based cleaners.

LIMITATIONS: Temperatures should be 10° to 32°C and should not fall below 10°C within 24 hours of application. Do not apply if rain is expected within 12 hours. Do not use over acid-based stains, 2-part epoxies or oil-based paints. Do not use on glazed tile. Do not use in areas subject to hydrostatic pressure. Smooth-finished concrete may be slippery when wet; consider using an anti-skid additive like SEAL-KRETE Clear Grip on high foot traffic areas.

**Sanding or removing paint containing lead may be hazardous. For information contact the National Lead Information Center at 1-800-424-LEAD or www.epa.gov/lead.*

CAUTION: EYE IRRITANT. Contains Dipropylene Glycol N-Propyl Ether. Avoid contact with eyes and prolonged contact with skin. Do not ingest.

FIRST AID: In case of eye contact, flush with water for 15 minutes. If irritation persists, get medical attention. In case of skin contact, wash thoroughly with soap and water. If swallowed, drink 1–2 glasses of water and immediately contact medical services regarding any instructions to induce vomiting. **KEEP OUT OF REACH OF CHILDREN – DO NOT TAKE INTERNALLY.**

Product	No.	Unit	UPC Code	Carton Bar Code	Carton Size (W x D x H)	Cube / Wt. (cubic ft / lbs)	Carton Qty	Pallet Qty
Clear-Seal Satin Protective Sealer	604801	3.78 L	0 15944 60481 8	1 00 15944 60481 5	36.5 cm x 36.5 cm x 22 cm	.028 m³ / 16.63 kg	4	45 cs
Clear-Seal Satin Protective Sealer	604805	18.9 L	0 15944 60485 6	—	—	.038 m³ / 20.48 kg	1	36 ea
Clear-Seal Gloss Protective Sealer	607801	3.78 L	0 15944 60781 9	1 00 15944 60781 6	36.5 cm x 36.5 cm x 22 cm	.028 m³ / 16.63 kg	4	45 cs
Clear-Seal Gloss Protective Sealer	607805	18.9 L	0 15944 60785 7	—	—	.038 m³ / 20.48 kg	1	36 ea

SEAL KRETE

CLEAR-SEAL

CONCRETE PROTECTIVE SEALER

- EXCELLENT DURABILITY
- INTERIOR/EXTERIOR USE
- FOR COATED & UNCOATED HORIZONTAL SURFACES

TECHNICAL INFORMATION

- Clean-up: soap and water
- Shelf life: 2 years min. (closed container)
- Visual appearance: milky white (wet); dries clear
- Gloss: 25 (1 coat)
- Gloss retention: excellent
- Tire marking: resistant to most tires
- Proprietary urethane-acrylic blend
- ASTM G-53 ultraviolet resistance: excellent
- ASTM D-1640: dry-to-touch 15 min; dry to recoat 2 hours; dry to light foot traffic 24 hours; dry to vehicular traffic 72 hours
- ASTM D-3359B intercoat adhesion: excellent

	Satin	Gloss
• ASTM D-3363 Konig hardness:	70	60
• VOC – EPA Method 24 – Waterproofing Sealer Category	< 100 g/L	< 100 g/L

CHEMICAL/SOLVENT RESISTANCE - ASTM D-1308
(One hour spot test)

- Gasoline: resistant
- Oil: resistant
- Water: resistant
- Salt: resistant
- Chlorine: resistant

FEATURES

- Seals and protects painted, stained or bare concrete
- Seals in color
- Reduces pockmarking and cracking
- Clear finish, will not yellow
- Premium, urethane-fortified acrylic formula

LIQUID PROPERTIES

- Water-Based
- Odor: Low

LIMITED WARRANTY: Manufacturer/Seller makes no warranty of any kind except that this product is free from defect and is of merchantable quality. Buyer remedy for breach of warranty is limited to replacement of SEAL-KRETE product or refund of purchase price. Convenience Products will not be responsible for labor or the cost of labor for removal or application of any product.

TECHNICAL SUPPORT: For more information on surface prep or application guidelines, or to obtain a Material Safety Data Sheet, call 1-800-323-7357, M–F (8:00 am–5:00 pm EST) or visit our website at www.seal-krete.com.

WATERPROOFS & SEALS PAINTED, STAINED, TEXTURED & BARE CONCRETE SURFACES

RESISTANT TO MOISTURE, SALT, CHLORINE, OIL & HOT TIRE PICKUP

HIGHLY DURABLE NON-YELLOWING ACRYLIC

WATERPROOFS CONCRETE SURFACES

RESISTS HOT TIRE PICKUP

PROVIDES A DURABLE, NON-YELLOWING FINISH

Convenience Products
306 Candy Rd., Ashendale, FL 33823 USA
www.seal-krete.com
Questions or comments? e-mail: tech@seal-krete.com
or call 1-800-323-7357

PREMIUM PROTECTIVE SEALER

64017-1-060314-SK